Circum-Pacific Council
for Energy and Mineral Resources
Earth Science Series

Volume 15

Basin Formation, Ridge Crest Processes, and Metallogenesis in the North Fiji Basin

Circum-Pacific Council
for Energy and Mineral Resources
Earth Science Series

H. Gary Greene, Editor-in-Chief
Florence L. Wong, Executive Editor

Volume 1
Tectonostratigraphic Terranes of the Circum-Pacific Region
Edited by D.G. Howell

Volume 2
Geology and Offshore Resources of Pacific Island Arcs—Tonga Region
Edited and Compiled by D.W. Scholl and T.L. Vallier

Volume 3
Investigations of the Northern Melanesian Borderland
Edited by T.M. Brocher

Volume 4
Geology and Offshore Resources of Pacific Island Arcs—Central and Western Solomon Islands
Edited by J.G. Vedder, K.S. Pound, and S.Q. Boundy

Volume 5A
The Antarctic Continental Margin: Geology and Geophysics of Offshore Wilkes Land
Edited by S.L. Eittreim and M.A. Hampton

Volume 5B
The Antarctic Continental Margin: Geology and Geophysics of the Western Ross Sea
Edited by A.K. Cooper and F.J. Davey

Volume 6
Geology and Resource Potential of the Continental Margin of Western North America and Adjacent Ocean Basins—Beaufort Sea to Baja California
Edited by D.W. Scholl, A. Grantz, and J.G. Vedder

Volume 7
Marine Geology, Geophysics, and Geochemistry of the Woodlark Basin—Solomon Islands
Edited by B. Taylor and N.F. Exon

Volume 8
Geology and Offshore Resources of Pacific Island Arcs—Vanuatu Region
Edited by H.G. Greene and F.L. Wong

Volume 9
Geology and Offshore Resources of Pacific Island Arcs—New Ireland and Manus Region, Papua New Guinea
Edited by M.S. Marlow, S.V. Dadisman, and N.F. Exon

Volume 10
Petroleum Resources of China and Related Subjects
Edited by H.C. Wagner, L.C. Wagner, F.F.H. Wang, and F.L. Wong

Volume 11
Geology of the Andes and Its Relation to Hydrocarbon and Mineral Resources
Edited by G.E. Ericksen, M.T. Cañas Pinochet, and J.A. Reinemund

Volume 12
Geology and Offshore Resources of Pacific Island Arcs—Solomon Islands and Bougainville, Papua New Guinea Regions
Edited by J.G. Vedder and T.R. Bruns

Volume 13
Terrane Analysis of China and the Pacific Rim
Edited by T.J. Wiley, D.G. Howell, and F.L. Wong

Volume 14
Geology and Offshore Mineral Resources of the Central Pacific Basin
Edited by B.H. Keating and B.R. Bolton

Volume 15
Basin Formation, Ridge Crest Processes, and Metallogenesis in the North Fiji Basin
Edited by L.W. Kroenke and J.V. Eade

Volumes 1, 3, and 5A through 13 available from AAPG, P.O. Box 979, Tulsa, OK 74101-0979.

Loren W. Kroenke
James V. Eade
Editors

Basin Formation, Ridge Crest Processes, and Metallogenesis in the North Fiji Basin

Circum-Pacific Council
for Energy and Mineral Resources
Earth Science Series, Volume 15

With 107 Figures and 31 Tables

Springer-Verlag
Berlin Heidelberg New York London Paris
Tokyo Hong Kong Barcelona Budapest

Loren W. Kroenke
Hawaii Institute of Geophysics
School of Ocean and Earth Science and Technology
University of Hawaii
Honolulu, HI 96822-3188, USA

James V. Eade
Technical Secretariat
South Pacific Applied Geoscience Commission
Private Mail Bag
GPO, Suva, Fiji

Cover Illustration: Fresh pillow lava lobes photographed with a bottom camera at Station 25.

ISBN-13:978-3-540-57372-2 e-ISBN-13:978-3-642-85043-1
DOI: 10.1007/978-3-642-85043-1

CIP data applied for

Typesetting: Camera ready by editors
32/3145 - 5 4 3 2 1 0 – Printed on acid-free paper

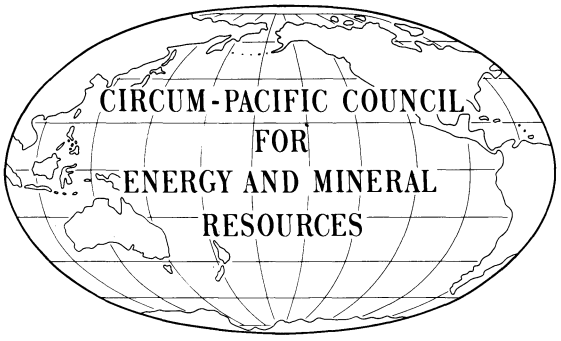

Foreword

The Earth Science Series of the Circum-Pacific Council for Energy and Mineral Resources (CPCEMR) is designed to convey the results of geologic research in and around the Pacific Basin. Topics of interest include framework geology, petroleum geology, hard minerals, geothermal energy, environmental geology, volcanology, oceanography, tectonics, geophysics, geochemistry, and applications of renewable energy. The CPCEMR supports and publishes results of scientific research that will advance the knowledge of energy and mineral resource potential in the circum-Pacific region. The Earth Science Series is specifically designed to publish papers that include new data and new maps, report on CPCEMR-sponsored symposia and workshops, and describe the results of onshore and marine geological and geophysical explorations.

This volume reports the results of one of fourteen internationally sponsored surveys to investigate the energy and mineral resources in the Southwest Pacific. The 1982, 1984 and 1986-1987 surveys were fostered by the Australia-New Zealand-United States Tripartite Agreement. Geophysical and geological data were collected aboard the U.S. Geological Survey's (USGS) R/V *S.P. Lee* and the Hawaii Institute of Geophysics' (HIG) R/V *Kana Keoki* and R/V *Moana Wave* in the waters of Fiji, Kiribati, Papua New Guinea, Solomon Islands, Tonga, Western Samoa, and Vanuatu.

Funding for ship time was made available through the U.S. Agency for International Development, the USGS, the U.S. Office of Naval Research (for HIG's 1982 work), the Australian Development Assistance Bureau, the Australian Bureau of Mineral Resources (BMR), the New Zealand Ministry of Foreign Affairs, the New Zealand Department of Scientific and Industrial Research (DSIR), the New Zealand Geological Survey, and the New Zealand Oceanographic Institute (NZOI). Coordination of the program was provided by the U.S. Department of State and the South Pacific Applied Geoscience Commission (SOPAC, formerly the United Nations-sponsored Committee for the Coordination of Joint Prospecting for Mineral Resources in South Pacific Offshore Areas CCOP/SOPAC) in Fiji. Over 150 scientists and technicians participated in the cruises and represented the South Pacific island nations and funding countries mentioned above, as well as SOPAC, New Caledonia, the United Kingdom and France.

Michel T. Halbouty

Chairman

Preface

This volume summarizes the scientific results of one of six investigations conducted in the southwest Pacific under the terms of the 1982 Tripartite Agreement among Austraia, New Zealand, and the United States in association with the United Nations-sponsored Committee for the Coordination of Joint Prospecting for Mineral Resources in South Pacific Offshore Areas (CCOP/SOPAC). Major funding for this part of the investigations was provided by the U.S. Office of Naval Research and by the governments of Australia and New Zealand. Eight shipboard scientists from four nations participated in the program, which was coordinated by CCOP/SOPAC in Fiji.

Loren W. Kroenke, Co-Chief Scientist	Hawaii Institute of Geophysics School of Ocean and Earth Science and Technology University of Hawaii
James V. Eade, Co-Chief Scientist*	New Zealand Oceanographic Institute
Alan Carter	University of New South Wales
Norman Cherkis	Naval Research Laboratory
Murray Gregory	Auckland University
Walter Jahns	Naval Ocean Research Development Agency
Gary McMurtry	Hawaii Institute of Geophysics School of Ocean and Earth Science and Technology University of Hawaii
Robert Smith	Mineral Resources Department, Suva

Captain R. Hayes, his crew and the scientific technicians on the R/V Kana Keoki, together with F. Campbell, Captain W. Harkness, and C. Matos, who provided shore-based logistical support, made first-order contributions to the success of this program. We thank the governments of Fiji and Vanuatu for waiving all port charges and their geological surveys for logistical support.

We acknowledge support from the Australian Bureau of Mineral Resources and the Hawaii Institute of Geophysics for the production of this volume. We are grateful to those who critically reviewed chapters and to SOEST Publication Services for production.

Loren Kroenke and Jim Eade*

*Now at South Pacific Applied Geoscience Commission (SOPAC)

Contents

List of Contributors

John Brozena
Sun Park Lane
Huntingtown, MD 20639, USA

Norman Cherkis
Naval Research Laboratory, Code 5110
Washington, DC 20375, USA

Patricia Cooper
Hawaii Institute of Geophysics, SOEST*
University of Hawaii
Honolulu, HI 96822, USA

Eric H. DeCarlo
Department of Oceanography, SOEST*
University of Hawaii
Honolulu, HI 96822, USA

James V. Eade
South Pacific Applied Geoscience Commission
(SOPAC)
Technical Secretariat
Suva, Fiji

Murray R. Gregory
Geology Department
University of Auckland, New Zealand

Michael W. Hamburger
Department of Geology
Indiana University
Bloomington, IN 47405, USA

Bryan L. Isacks
Department of Geological Sciences
Cornell University
Ithaca, NY 14853, USA

Kevin T.M. Johnson
University of Tokyo
Geological Institute
Bunkyo-ku, Tokyo 113 Japan

Dibya R. Kansakar
Department of Mines and Geology
Kathmandu, Kingdom of Nepal

James N. Kellogg
Department of Geological Sciences
University of South Carolina
Columbia, SC 29208, USA

Kee Hyun Kim
Department of Oceanography
Chungnam National University
Taejeong, Korea

Loren W. Kroenke
Hawaii Institute of Geophysics, SOEST*
University of Hawaii
Honolulu, HI 96822, USA

Alexander Malahoff
Department of Oceanography, SOEST*
University of Hawaii
Honolulu, HI 96822, USA

Gary M. McMurtry
Department of Oceanography, SOEST*
University of Hawaii
Honolulu, HI 96822, USA

Kenji Nemoto
Faculty of Marine Science and Technology
Tokai University
Shizuoka, Japan

Richard C. Price
Department of Geology
LaTrobe University
Bundoora, Victoria 3083, Australia

Diane Seward
Institute of Nuclear Sciences, DSIR
Lower Ilutt, New Zealand

John M. Sinton
Department of Geology and Geophysics, SOEST*
University of Hawaii
Honolulu, HI 96822, USA

Robert Smith
Mineral Resources Department
Private Mail Bag
Suva, Fiji

Hubert Staudigel
Scripps Institution of Oceanography
La Jolla, CA 94093, USA

Chung Yeung Yan
Geodynamics Research Institute
Texas A & M University
College, Station, TX 77843, USA

Alan Zindler
Lamont-Doherty Earth Observatory
Palisades, NY 10964, USA

* School of Ocean and Earth Science and Technology

Kroenke, L.W., and J.V. Eade, editors, 1993, Basin Formation, Ridge Crest Processes, and Metallogenesis in the North Fiji Basin: Houston, TX, Circum-Pacific Council for Energy and Mineral Resources, Earth Science Series, Vol. 15, Springer-Verlag, New York.

OVERVIEW AND PRINCIPAL RESULTS OF THE SECOND LEG OF THE FIRST JOINT CCOP/SOPAC-TRIPARTITE[1] CRUISE OF THE R/V KANA KEOKI: NORTH FIJI BASIN SURVEY (KK820316 LEG 03)

LOREN W. KROENKE
Hawaii Institute of Geophysics, School of Ocean and Earth Science and Technology, University of Hawaii, Honolulu, Hawaii 96822

JAMES V. EADE
New Zealand Oceanographic Institute, Wellington, New Zealand[2]

and

SCIENTIFIC PARTY[3]

INTRODUCTION

The North Fiji Basin (Figure 1) is an active dilational backarc basin bordered by the Vitiaz Trench to the north, the Lau basin to the east, the Hunter Fracture zone to the south, and the New Hebrides arc and trench to the west. It is the site of a complex accretionary plate boundary that includes at least one R-R-R triple junction. The geological framework of the North Fiji Basin, the configuration of its bounding arcs and trenches, and its relationship to the Fiji Islands have engendered considerable interest for almost two decades. Early workers speculated on the significance of the anomalous heat flow in the North Fiji Basin (Sclater and Menard, 1967), the geotectonic position of Fiji (Dickinson, 1967), the regional seismicity (Isacks et al., 1969), and the petrologic variations across Fiji (Gill, 1970).

Chase (1971), who described the North Fiji Basin (Fiji Plateau) as wonderfully complex, was the first to identify tectonic elements in the basin (Figure 2) and attempt to unravel the tectonic history. Since then the magnetic investigations of Luyendyk et al. (1974) and Malahoff et al. (1982a) have added definition to the fabric of the basin. Tectonic reconstructions have been attempted, based on island geology and geochemistry (Green and Cullen, 1973; Gill and Gorton, 1973; Gill, 1976; Carney and Macfarlane, 1978; Colley and Hindle, 1984), magnetic anomaly lineations (Falvey, 1975), paleo-magnetic analyses (James and Falvey, 1978; Falvey, 1978; Malahoff et al., 1982b), and heat flow (Halunen, 1979). Other investigations that bear on the tectonic configuration of the North Fiji Basin include arc morphology studies of Karig and Mammerickx (1972), seismicity studies of Pascal et al. (1973), Dubois et al. (1973), Nagumo et al. (1975), and Eguchi (1984); seismic refraction studies of Shor et al. (1971) and Sutton et al. (1971); heat flow studies of Sclater et al. (1972) and MacDonald et al. (1973); sediment distribution studies of Luyendyk et al. (1974), Neprochnov et al. (1974), Jezek (1976), and Brocher et al., (1985); petrologic studies of Fryer (1974) and Dunkley (1983); and a regional tectonic synthesis by Kroenke (1984). This volume is primarily concerned with the tectonic, sedimentological, and geochemical setting of the North Fiji Basin.

BACKGROUND

In 1975 the Committee for Coordination of Joint Prospecting for Mineral Resources in South Pacific

[1] Australia, New Zealand, and the United States
[2] Now with CCOP Technical Secretariat, Suva, Fiji
[3] A. Carter, N. Cherkis, M. Gregory, W. Jahns, G. McMurtry, and R. Smith

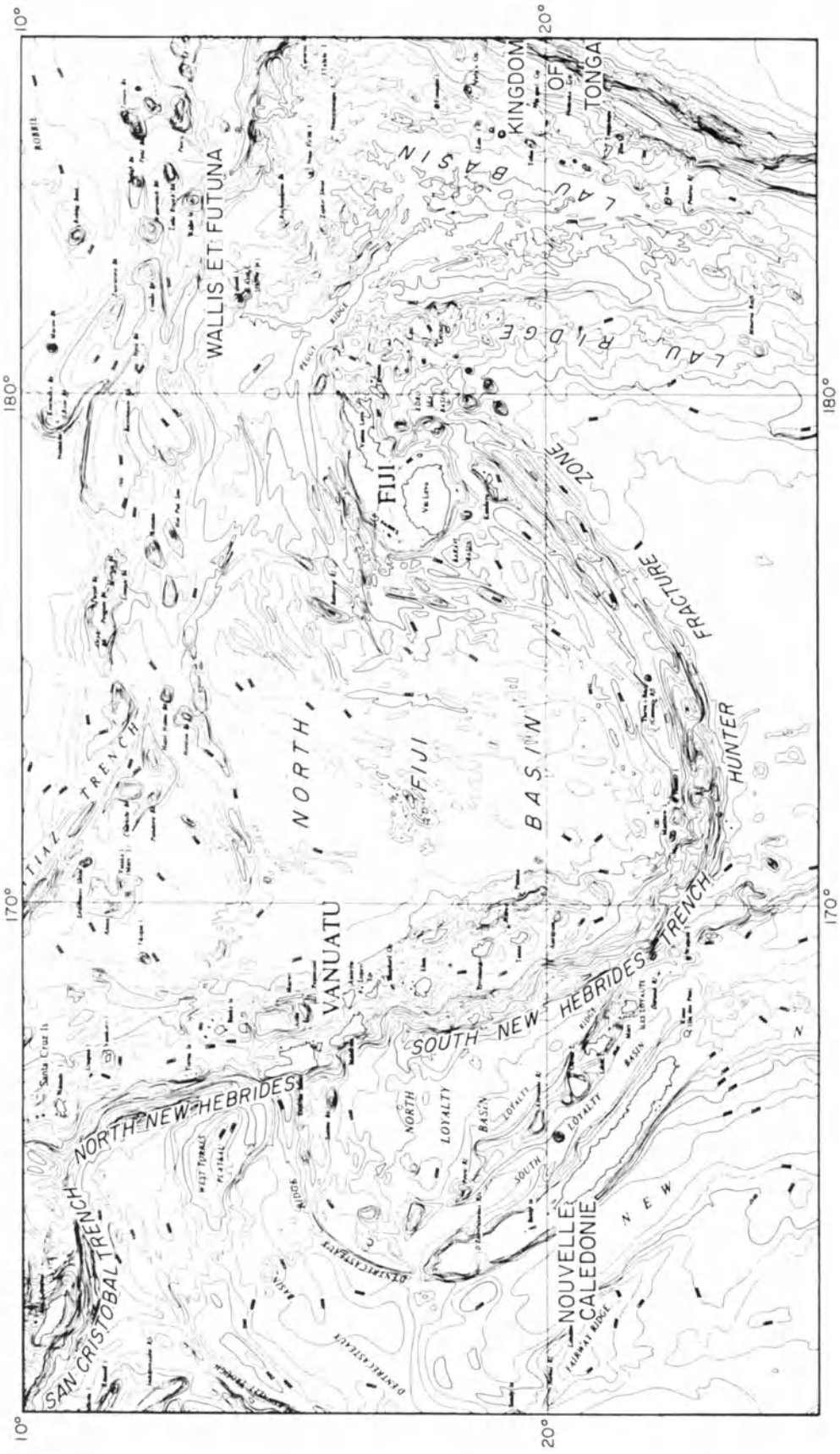

Figure 1. Regional framework of the North Fiji Basin (from Kroenke et al., 1983).

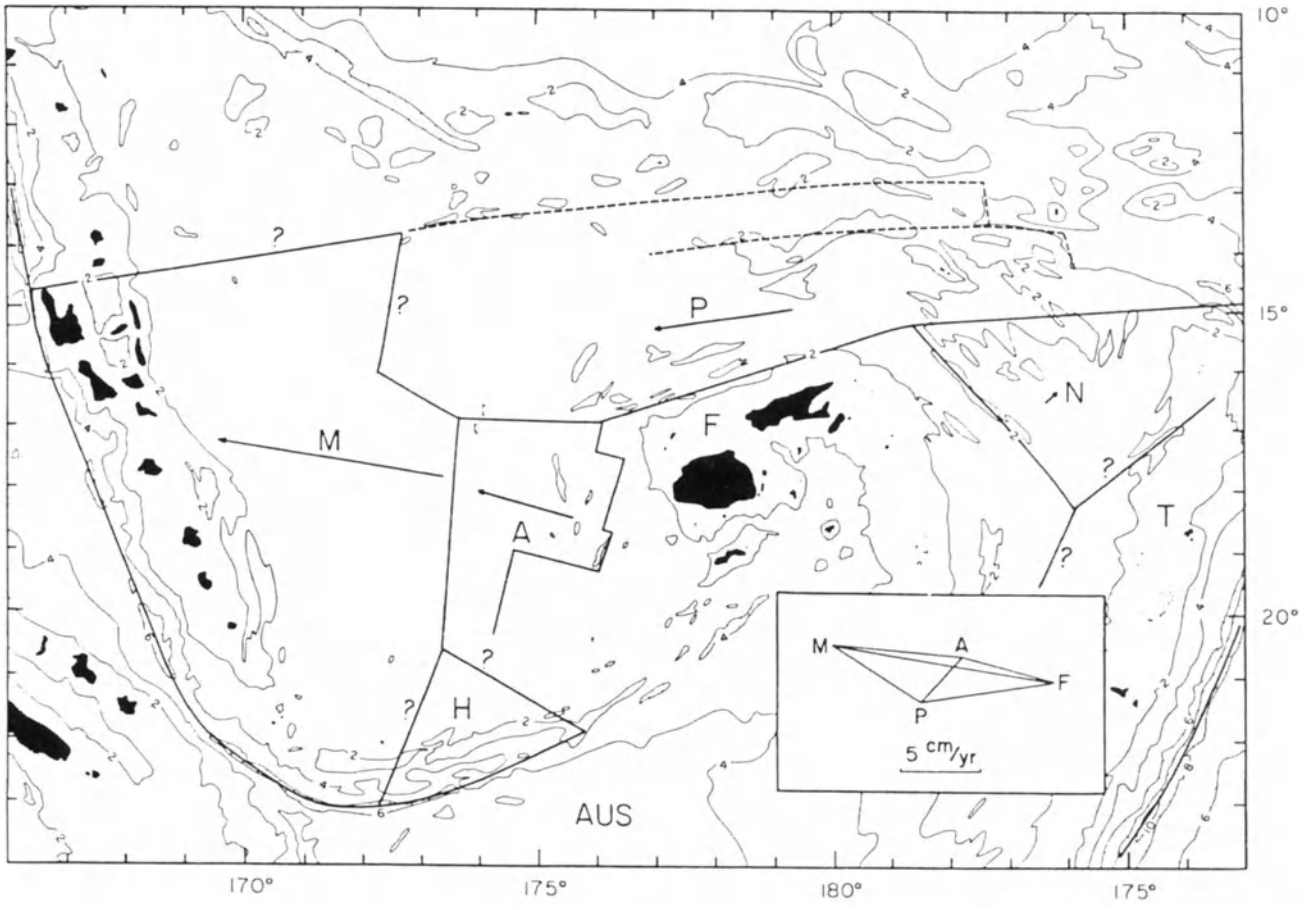

Figure 2. Late Cenozoic tectonics of the Fiji Plateau (from Chase, 1971). Known and speculative block boundaries are shown by heavy solid lines, fossil boundaries by heavy dashed lines. Arrows show motion of plates relative to Fiji to the same scale as resultants in inset sector diagram. Contour interval 2 km. Large plates are labeled P for Pacific and AUS for Australian. Small blocks are F for Fiji, N, T, M , A, and the smallest and most speculative, H, or Hunter block. The South Pandora Ridge (Hazel Holme Fracture Zone) is shown as a transform fault (?) extending westward from the Pacific Plate.

Offshore Areas (CCOP/SOPAC) and the Intergovernmental Oceanographic Commission (IOC), in convening an international workshop on the geology, mineral resources, and geophysics of the South Pacific, had mandated the development of a scientific work program to focus on

> (a) the regional geology and tectonic framework of the oceanic–island arc–continental margins of the Southwest Pacific; and
>
> (b) the occurrence, mode of formation and environmental factors of manganese nodule deposits, hot brines, and metalliferous sediments in the Southwest Pacific.

It was the express purpose of this workshop to develop a program of scientific research and to define research goals, formulate research projects, and make recommendations for their implementation and coordination. The program was intended to lead to a regional synthesis and to a greatly increased knowledge of the resource potential of the South Pacific region (UNESCO, 1975).

In 1980, at a second international workshop convened by CCOP/SOPAC and IOC, this mandate was reaffirmed, past work was reviewed, and new areas of basic research were targeted (UNESCO, 1980). That same year, at the ninth session of CCOP/SOPAC, elements of the workshop research programs were adopted by the committee as part of its own work program. Included were projects relating to the Vitiaz Trench, North Fiji Basin, and the New Hebrides and Solomon Islands Arcs, among others.

Recognizing that CCOP/SOPAC, at the request of its member governments, has sought multilateral assistance in funding and implementing marine research projects and offshore surveys, the governments of Australia, New Zealand, and the United States agreed at Suva in 1982

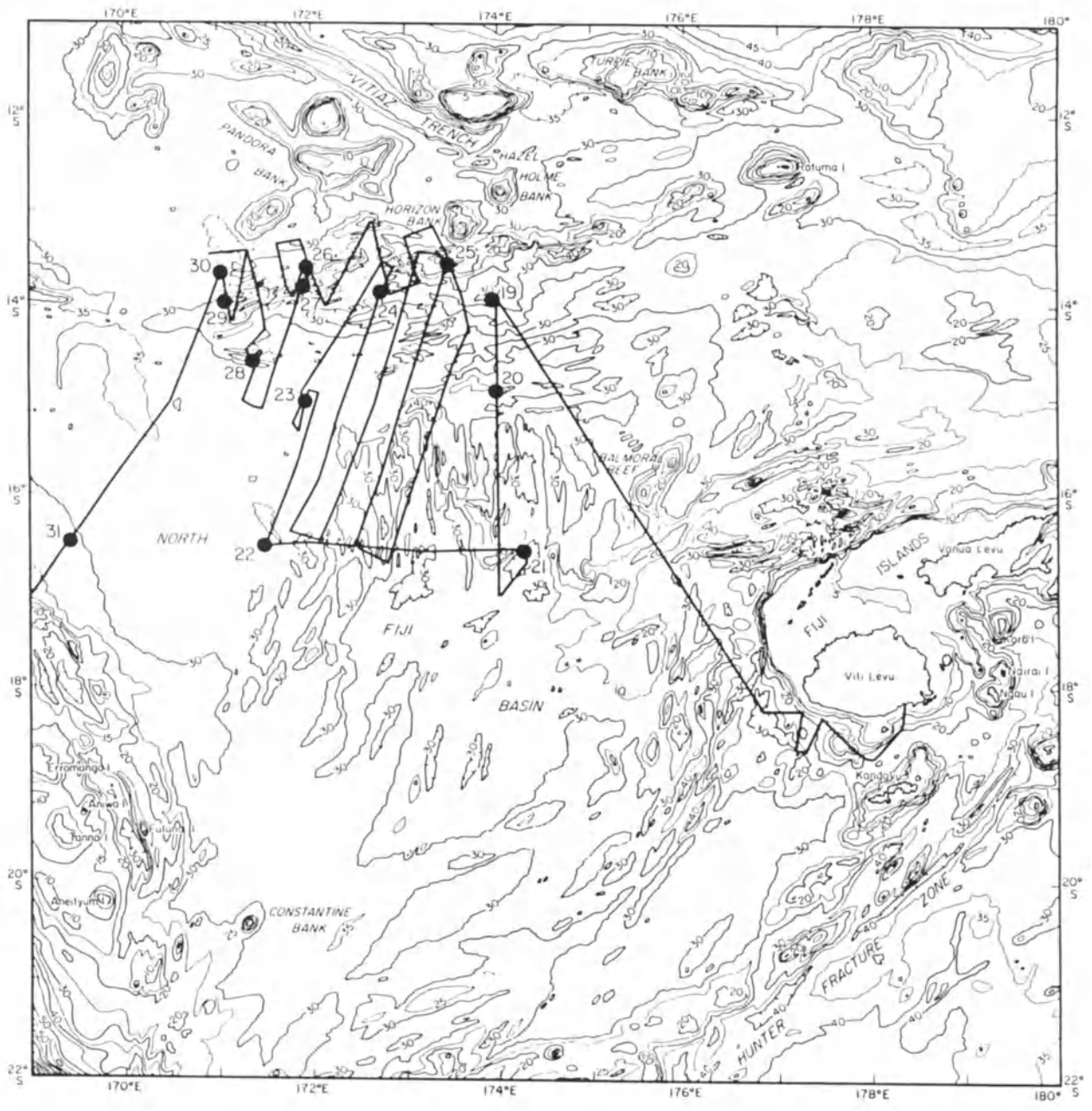

Figure 3. Generalized bathymetry of the North Fiji Basin after Chase et al. (1987) showing the primary study area and KK820316 Leg 3 survey tracks and station locations.

(the "Tripartite" Agreement), in cooperation with CCOP/SOPAC, to conduct a joint program of marine geoscientific research and mineral resource studies of the South Pacific.

Accordingly, as part of that agreement, a marine geophysical/geological survey was conducted across the central North Fiji Basin between 23 April and 12 May 1982, on board the University of Hawaii's research vessel, the R/V KANA KEOKI. This cruise (KK820316 Leg 03) was the second leg jointly undertaken by CCOP/SOPAC and the tripartite countries as part of the CCOP/SOPAC Work Programme: CCSP/REG.4 (Geological and geophysical investigations of the North Fiji Basin) and CCSP/REG.10 (Search for metalliferous muds and hot brines in enclosed oceanic basins). Scientists on board included representatives from the CCOP/SOPAC Technical Secretariat, Australia, Fiji, New Zealand, and the United States.

Focusing on the North Fiji Basin Triple Junction, the second leg had as its specific objectives

> (1) to locate and define the structure of the North Fiji Basin triple junction and that of its northwest limb,

(2) to identify and investigate possible zones of hydrothermal activity along active rifts using underway geophysics, bottom photography, and coring and dredging techniques,

(3) to determine the existence of and examine the distribution of any metalliferous deposits which may occur along the active rift zones.

The area believed to contain the triple junction based on the results of an aeromagnetic survey (Malahoff et al., 1982a) and Cherkis and Malahoff (pers. comm.) was designated as the primary survey area. During the survey, geophysical data were acquired along more than 5000 km of track between Suva, Fiji, and Vila, Vanuatu (Figure 3). Underway, 3.5-kHz echo sounding, seismic reflection profiling (airgun and/or water gun), gravity, and magnetic data were continuously recorded and five ASPER lines were successfully completed. At 13 station locations (Figure 3), five oriented piston cores (with trigger cores) were taken, seven rock dredge lowerings were made, six free-fall corers were dropped, and three bottom camera tows were made. Bottom samples were obtained at all stations.

PRINCIPAL RESULTS

Baravi Basin Survey

Enroute from Suva to the primary survey area, a reconnaissance survey of the Baravi Basin was undertaken. The actual survey track made good is shown in Figure 3. The results of this survey are described by Brocher and Holmes (1985). The basin contains up to 2.0 seconds (two-way time) of sediment (probably in excess of 2500 meters thick) accumulated along the curvilinear axis of the basin, varying in strike from WNW to NNW (roughly paralleling the southwest coast of Viti Levu). A V-shaped trough more than 3100 m deep and containing ponded sediment marks the western limit of the Baravi Basin (see Figure 3 in Brocher and Holmes, 1985).

North Fiji Basin Triple Junction

The location of the survey area in the North Fiji Basin is shown in the rectangle on the regional bathymetry in Figure 4. Magnetic anomaly lineations within the survey area (Malahoff et al., this volume) are shown as solid

Table 1. Sampling station locations KK820316 Leg 03.

Sta No.	Sample type	Latitude °S	Longitude °E	Depth (m)	Time (Z)	Date
19	PCOD-5,TC-5	13°58.4′	173°57.5′	3400	1115	25 April
20	FFC-5,-6	14°50.3′	174°00.0′	2545-2580	0210-0345	26 April
	RD-15 (no sample)					
21	RD-16	16°30′	174°16.6′	3445-2690	0519-0715	26 April
22	PCOD-6,TC-6	16°30.4′	171°32.3′	3165	0546	28 April
23	RD-17	15°00.4′	171°57.4′	3200	0543-0833	29 April
	BC-1	15°02.2′	171°56.5′	3200	1053-1352	29 April
24	PCOD-7, TC-7	13°49.7′	172°46.1′	3150	0906	30 April
25	BC-2	13°32.0′	173°28.2′	2200	0244-0527	5 May
	RD-19	13°32.2′	173°28.2′	2130-2200	0722-0927	5 May
	FFC-7 (no sample)					
	RD-18 (no sample)					
26	PCOD-8, TC-8	13°31.3′	171°58.2′	3020	0830	7 May
27	RD-20	13°46.0′	172°00.5′	4300	1248-1433	7 May
28	RD-21	14°34.6′	171°25.0′	3200	1131-1311	8 May
	BC-3 (no photos)					
29	FFC-8	13°58.5′	171°09.3′	2680	2049	9 May
30	FFC-9	13°35.8′	171°03.9′	3350	0033	10 May
31	PCOD-9,TC-9	16°28.8′	169°30.6′	3040	0243	11 May

Key: BC bottom camera; FFC free-fall corer; PCOD piston core orienting device; RD rock dredge; TC trigger corer

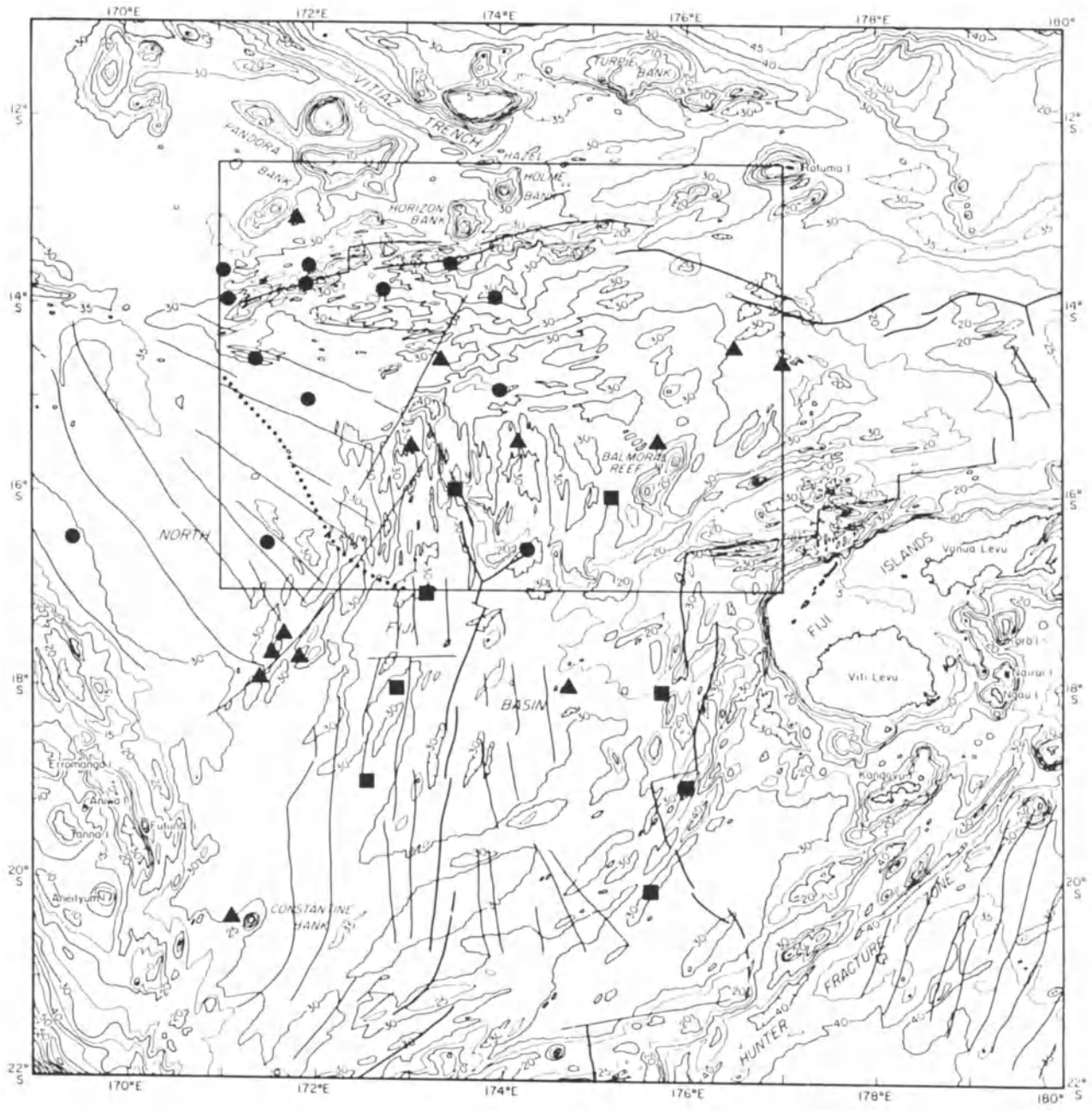

Figure 4. Regional bathymetry of the North Fiji Basin (after Chase et al., 1987) showing the location of the primary survey area enclosed by a bold rectangle. Solid dots and triangles are HIG piston core locations. Solid squares are NZOI core locations. Dotted line indicates boundary between New Hebrides archipelagic apron sediments and pelagic sediments of the North Fiji Basin. Solid lines are magnetic lineations identified by Malahoff et al. (this volume).

lines striking WNW in the western part of the area, south of the South Pandora (Hazel Holme) Ridge. The locations of bottom sampling stations, listed in Table 1, are shown in Figure 3. The locations of all bottom samples analyzed and described in the following chapters are shown in Figure 4.

Our results indicate that the tectonic history has been complex. The new bathymetric and sediment isopach charts (Kroenke et al., a and b, this volume) reveal the presence of both the old triple junction configuration and a possible incipient or newly formed propagating rift system. The ENE-trending South Pandora Ridge, a slightly older but still active spreading center, may connect with the Rotuma Ridge and extend as far east as Rotuma.

The South Pandora Ridge is characterized by the presence of an elongate series of deep troughs (rift valleys) flanked by ridges surmounted by peaks that, on Horizon Bank (Figure 5), shoal to within 40 m of sea level (Kroenke et al., a, this volume). Seismicity studies (Hamburger and Isacks, this volume) indicate that the ridge is seismically active and is undergoing extension.

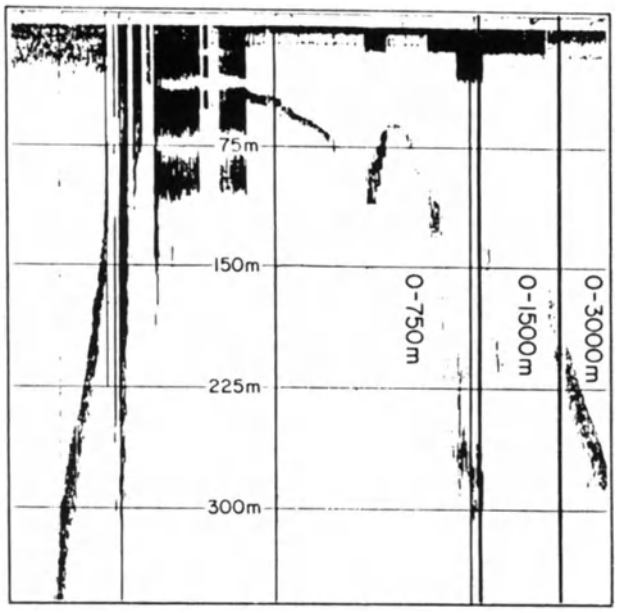

Figure 5. R/V TANGAROA echogram across the 40-m shoal end of Horizon Bank. Note scale changes indicated on the record (profile provided by D. Cullen).

Reflection profiles and 3.5-kHz echograms (Kroenke et al., b, this volume) indicate that the South Pandora Ridge is essentially devoid of sediment, whereas a thin, somewhat variable veneer of sediment between 0.05 to 0.15 seconds blankets most of the remaining part of the region. Lack of sediment cover, photographic evidence of recent pillow basalt flows, and the petrology of the rocks dredged (see below), support our presumption that the South Pandora Ridge is presently active. The spreading center is further defined by a high amplitude pair of magnetic anomalies associated with the rift valleys (Malahoff et al., this volume).

Reflection profiles and 3.5-kHz echograms (Kroenke et al., b, this volume) also reveal a narrow, elevated, sediment-free or thinly veneered zone extending north from the well-defined rift graben terrain that forms the northern end of a N-S aligned spreading center in the southern half of the North Fiji Basin, the central North Fiji Basin Ridge (CNFBR). This narrow zone of sediment-free terrain is believed to comprise a newly activated or incipient spreading segment of the CNFBR that has propagated northward toward the South Pandora Ridge. Reflection profiles also suggest that, far to the southeast of the South Pandora Ridge, another N-S aligned spreading segment may have jumped approximately 300 km to the east of the CNFBR (near 176°E) and is now actively spreading in an E-W direction off Viti Levu.

Results from sedimentological analyses (Eade and Gregory, this volume) reveal that, where present, the sediment blanketing the central part of the North Fiji Basin (northeast of the dotted line in Figure 4) is predominantly pelagic ooze that is heavily bioturbated and contains only minor ash. Several ash-rich horizons and one distinct ash layer are present in cores which span the last 0.7 m.y. In the western part of the basin (southwest of the dotted line in Figure 4), the sediment is dominated by graded beds of dark ash and interbedded ash-rich pelagic ooze with little bioturbation. The graded beds are turbidites transported from the New Hebrides Arc into the North Fiji Basin. The interbedded sequence is part of a broad archipelagic apron, the New Hebrides Apron (west of the dashed line in Figure 4), which onlaps the western part of the North Fiji Basin. In this area any bathymetric fabric related to the northwest-trending anomaly pattern would be hidden beneath this thick wedge of sediment (Kroenke et al., b, this volume).

The sediment geochemistry (McMurtry et al., this volume) indicates that, within the survey area, the noncarbonate fraction of the pelagic sediments is predominantly composed of volcanic ash, amorphous iron and manganese oxides, and an Fe-rich montmorillonite, a phase assemblage similar to those found on other active ridge crests. Iron and manganese oxide concentrations reach values of up to 22 and 4 wt %, respectively, in the < 2-μm fraction of these sediments. These concentrations are well in excess of the limits defined by Cronan (1983) for hydrothermal metalliferous sediments in the Southwest Pacific (Figure 6). Copper and zinc concentrations are also generally in excess of the regional values, and approach the concentrations reported by the East Pacific Rise metalliferous sediments (Figure 7). The presence of metalliferous sediments, which are of no economic consequence in themselves, is indicative of the potential for the presence of more highly enriched deposits, such as massive polymetallic sulfides.

Volcanic pillow fragments were recovered in each of the dredges 16, 17, 19, 20, and 21 (Table 1, Figure 3). As the pillow fragments recovered from dredge 16 (Station 21) are fairly weathered and somewhat encrusted with manganese oxide, they appear to be the oldest volcanic rocks dredged. Pillow fragments from dredge 17 (Station 23) have a thin brown weathering rind. Those from dredge 19 (Station 25) and especially dredge 20 (Station 27) are quite fresh and according to fission track dating (Seward, this volume) are very young. Rock dredge 20 contained extremely fresh glassy pillow basalts and sheet flow fragments typical of active spreading centers. This observation is borne out by the presence of fresh pillow lobes in photographs taken with the bottom camera at Station 25 (Frontispiece).

Petrologic data (Sinton et al., this volume) indicate that dredge 16 recovered fairly normal, low-potassium

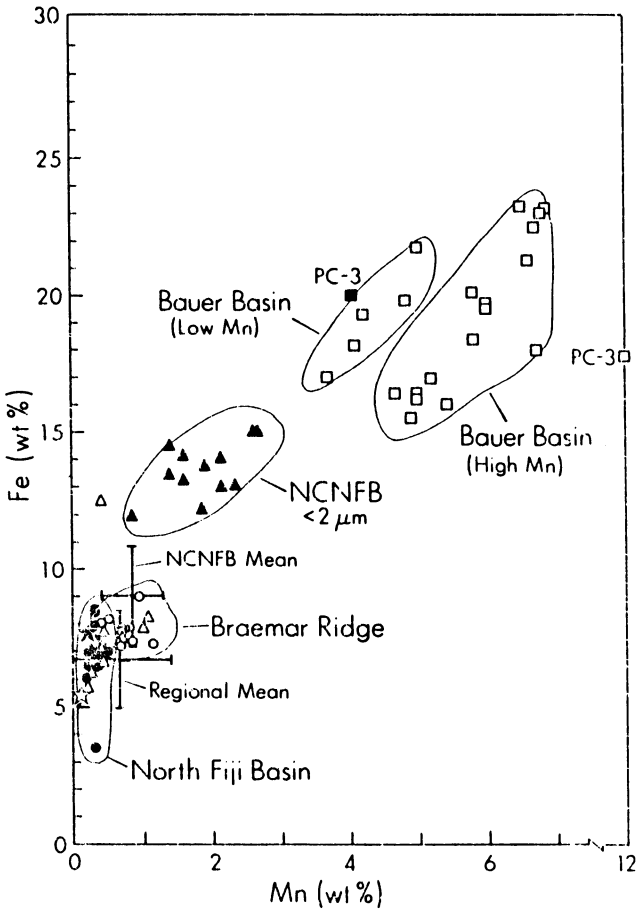

Figure 6. Fe versus Mn plots for the North Fiji Basin sediments. Regional mean from Cronan and Thompson (1978); Braemar Ridge data from Cronan et al. (1981); North Fiji Basin data from Cronan (1983); Bauer Basin data from McMurtry (1979); North Central North Fiji Basin (NCNFB) data from McMurtry et al. (this volume).

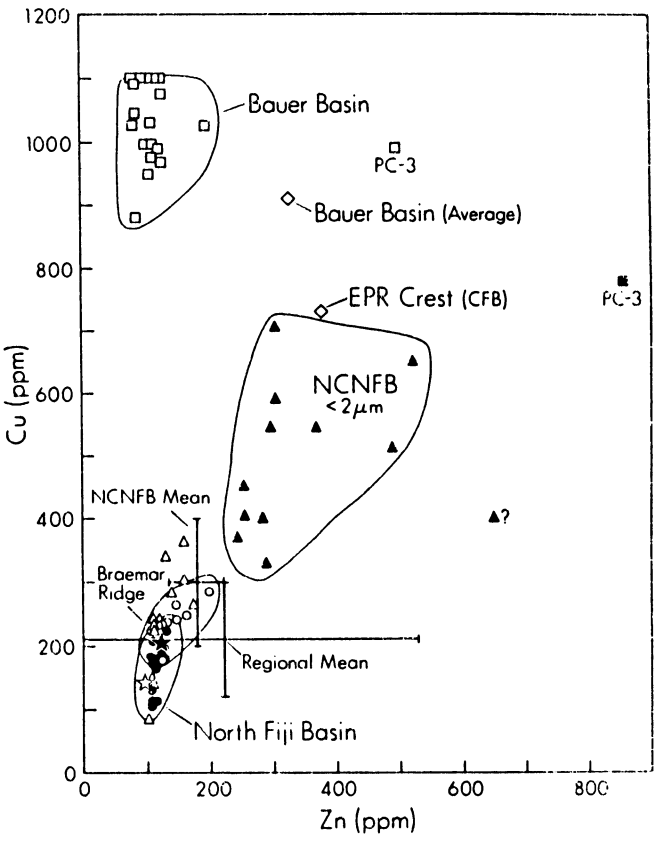

Figure 7. Cu versus Zn plots for North Fiji Basin sediments. Regional mean from Cronan and Thompson (1978); Braemar Ridge data from Cronan et al. (1981); North Fiji Basin data from Cronan (1983); Bauer Basin data from McMurtry (1979); North Central North Fiji Basin (NCNFB) data from McMurtry et al. (this volume); East Pacific Rise and Bauer Basin averages from Dymond et al. (1973).

basalts, typical of spreading center lavas, from midocean ridges and backarc basins. However, those from dredges 19 and 20 (South Pandora Ridge) are decidedly different. They are not easy to classify and seem to be transitional between tholeiitic and alkalic basalts. The characteristics of note are elevated concentrations of Na_2O, K_2O, and P_2O_5 relative to those samples from dredge 16. Yet the basalts from dredges 19 and 20 are hypersthene-normative, so they are not strongly alkalic. As they barely plot on the tholeiitic side of the Macdonald and Katsura (1964) line separating tholeiitic from alkalic lavas in Hawaii, they are probably most accurately described as "transitional." The data are consistent with formation at rather lower degrees of melting of mantle source material relative to "normal" spreading center lavas. Thus we may be seeing a recently or poorly developed extensional regime along the South Pandora Ridge. Samples from dredges 19 and especially 20 are extremely fresh, suggesting a presently active feature regardless of what they represent compositionally.

In summary, evidence of rift valleys associated with large magnetic anomalies, the lack of sediment cover and the presence of youthful, fresh, unaltered pillow and sheet flows, together with the presence of metal- enriched sediments in the adjacent surrounding area, combine to indicate that seafloor spreading and associated hydrothermal activity are presently occurring along the South Pandora Ridge. Evidence is also presented for the existence of a northward propagating rift system south of the South Pandora Ridge and for a recently formed N-S aligned spreading center just west of the Fiji Platform. This is SOEST Contribution no. 1750.

REFERENCES

Brocher, T.M., and R. Holmes, 1985, The marine geology of sedimentary basins south of Viti Levu, Fiji, in T.M. Brocher, ed., Geological Investigations of the Northern Melanesian Borderland: Earth Science Series, v. 3; Houston, Texas, Circum-Pacific Council for Energy and Mineral Resources, p. 123-138.

Brocher, T.M., S. Wirasantosa, F. Theyer, and C. Mato, 1985, Regional sedimentation patterns along the Northern Melanesian Borderland, in T.M. Brocher, ed., Geological Investigations of the Northern Melanesian Borderland: Earth Science Series, v. 3; Houston, Texas, Circum-Pacific Council for Energy and Mineral Resources, p. 77-102.

Carney, J.N., and A. Macfarlane, 1978, Lower to Middle Miocene sediments on Maewo, New Hebrides, and their relevance to the development of the outer Melanesian arc system: Australian Society of Exploration Geophysicists Bulletin, v. 9, p. 123-130.

Chase, C.G., 1971, Tectonic history of the Fiji Plateau, GSA Bulletin, v. 82, p. 3087-3110.

Chase, T.C., B.A. Seekins, J.D. Young, L.W. Kroenke, and V. von Stackelberg, 1987, Marine Topography of the Fiji Region: USGS-CCOP/SOPAC Pacific Project, unpublished.

Colley, B., and W.H. Hindle, 1984, Volcano-tectonic evolution of Fiji and adjoining marginal basins, in B.P. Kokelaar and M.F. Howells, eds., Marginal Basin Geology: Volcanic and Associated Sedimentary and Tectonic Processes in Modern and Ancient Marginal Basins: The Geological Society Special Publication No. 16, p. 151-162.

Cronan, D.S., 1983, Metalliferous sediments in the CCOP/SOPAC region of the Southwest Pacific, with particular reference to geochemical exploration for the deposits: UN ESCAP, CCOP/SOPAC Technical Bulletin no. 4, 55 p.

Cronan, D.S., and B. Thompson, 1978, Regional geochemical reconnaissance survey for submarine metalliferous sediments in the southwestern Pacific Ocean - a preliminary note: Applied Earth Science, v. 87, p. B87-B89.

Cronan, D.S., G.P. Glasby, J. Halunen, J.D. Collen, K.E. Knedler, J.H. Johnston, J. Cooper, C.W. Landmesser, and R.T. Wingfield, 1981, Sediments from the Braemar Ridge and Yasawa Trough, northwest of Fiji: South Pacific Marine Geological Notes, v. 2, no. 2, p. 25-35.

Dickinson, W.R., 1967, Tectonic development of Fiji: Tectonophysics, v. 4, p. 543-553.

Dubois, J., G. Pascal, M. Barazangi, B. Isacks, and J. Oliver, 1973, Travel times of seismic waves between the New Hebrides and Fiji Islands: a zone of low velocity beneath the Fiji Plateau: Journal of Geophysical Research, v. 78, p. 3431-3436.

Dunkley, P.N., 1983, Volcanism and the evolution of the ensimatic Solomon Islands arc, in D. Shimozuru and I. Yokoyama, eds., Arc Volcanism: Physics and Tectonics: Terra Publishing Co., Tokyo, p. 225-241.

Dymond, J., J.B. Corliss, C.W. Field, E.J. Dash, and H.H. Veeh, 1973. Origin of metalliferous sediments from the Pacific Ocean: GSA Bulletin, v. 84, p. 3355-3372.

Eade, J.V., and M.R. Gregory, Sediments of the North Fiji Basin, this volume.

Eguchi, T., 1984, Seismotectonics of the Fiji Plateau and Lau Basin, in R.L. Carlson and K. Kobayashi, eds., Geodynamics of Back-arc Regions: Tectonophysics, v. 102, p. 17-32.

Falvey, D., 1975, Arc reversals and a tectonic model for the North Fiji Basin: Australian Society of Exploration Geophysicists Bulletin, v. 6, p. 47-49.

Falvey, D., 1978, Analysis of paleomagnetic data from the New Hebrides: Australian Society of Exploration Geophysicists Bulletin, v. 9, p. 117-123.

Fryer, P., 1974, Petrology of some volcanic rocks from the northern Fiji Plateau: GSA Bulletin, v. 85, p. 1717-1720.

Gill, J.B., 1970, Geochemistry of Viti Levu, Fiji, and its evolution as an island arc: Contributions to Mineralogy and Petrology, v. 27, p. 179-203.

Gill, J.B., 1976, Composition and age of Lau Ridge and Basin volcanic rocks: Implications for evolution of inter-arc basins: GSA Bulletin, v. 80, p. 1443-1470.

Gill, J.B., and M.P. Gorton, 1973, A proposed geological and geochemical history of eastern Melanesia, in P.J. Coleman, ed., The Western Pacific: Island Arcs, Marginal Seas, Geochemistry: University of Western Australia Press, Nedlands, p. 543-566.

Green, D., and D.J. Cullen, 1973, The tectonic evolution of the Fiji region, in P.J. Coleman, ed., The Western Pacific: Island arcs, Marginal Seas, Geochemistry: University of Western Australia Press, Nedlands, p. 127-145.

Halunen, A.J., 1979, Tectonic history of the Fiji Plateau: Ph.D. Dissertation, University of Hawaii, Honolulu, Hawaii, 127 p.

Hamburger, M.W., and B.L. Isacks, Shallow seismicity in the North Fiji Basin, this volume.

Isacks, B., L.R. Sykes, and J. Oliver, 1969, Focal mechanisms of deep and shallow earthquakes in the Tonga-Kermadec region and the tectonics of island arcs: GSA Bulletin, v. 80, p. 1443-1470.

James, A., and Falvey, D.A., 1978, Analysis of paleomagnetic data from Viti Levu, Fiji: Australian Society of Exploration Geophysicists Bulletin, v. 9, p. 115-117.

Jezek, P.A., 1976, Compositional variations within and among volcanic ash layers in the Fiji Plateau area: Journal of Geology, v. 84, no. 5, p. 595-616.

Karig, D., and J. Mammerickx, 1972, Tectonic framework of the New Hebrides island arc: Marine Geology, v. 12, p. 187-205.

Kroenke, L.W., C. Jouannic, and P. Woodward (compilers), 1983, Bathymetry of the Southwest Pacific, Chart 1 (2 sheets) of the Geophysical Atlas of the Southwest Pacific: CCOP/SOPAC, Suva, Fiji.

Kroenke, L.W., 1984, Cenozoic tectonic development of the southwest Pacific: UN ESCAP, CCOP/SOPAC Technical Bulletin No. 6, 127 p.

Kroenke, L.W., R. Smith, and K. Nemoto, Morphology and structure of the seafloor in the northern part of the North Fiji Basin, this volume.

Kroenke, L.W., J.V. Eade, C.Y. Yan, and R. Smith, Sediment distribution of the North Fiji Basin and Lau Basin, this volume.

Luyendyk, B.P., W.B. Bryan, and P.A. Jezek, 1974, Shallow structure of the New Hebrides island arc: GSA Bulletin, v. 85, p. 1287-1300.

Macdonald, G.A., and T. Katsura, 1964, Chemical composition of Hawaiian lavas; Journal of Petrology, v. 5, p. 84-133.

Macdonald, K.C., B.P. Luyendyk, and R. von Herzen, 1973, Heat flow and plate boundaries in Melanesia: Journal of Geophysical Research, v. 78, p. 2537-2546.

Malahoff, A., R.H. Feden, and H.F. Fleming, 1982a, Magnetic anomalies and tectonic fabric of marginal basins north of New Zealand: Journal of Geophysical Research, v. 87, p. 4109-4125.

Malahoff, A., S.R. Hammond, J.J. Naughton, D.L. Keeling, and R.N. Richmond, 1982b, Geophysical evidence for post-Miocene rotation of the island Viti Levu, Fiji, and its relationship to the tectonic development of the North Fiji Basin: Earth and Planetary Science Letters, v. 57, p. 398-414.

Malahoff, A., L.W. Kroenke, N. Cherkis, and J. Brozena, Magnetic and tectonic fabric of the North Fiji Basin and Lau Basin, this volume.

McMurtry, G.M., 1979, Rates of sediment accumulation and their bearing on metallogenesis on the Nazca Plate, Southeast Pacific: Ph.D. Dissertation, University of Hawaii, Honolulu, Hawaii, 232 p.

McMurtry, G.M., E.H. De Carlo, and K.H. Kim, Geochemistry of the north central North Fiji Basin sediments, this volume.

Nagumo, S., J. Kasahara, and T. Ouchi, 1975, Active seismicity in the Fiji Plateau observed by ocean bottom seismograph: Journal of the Physics of the Earth, v. 23, p. 279-287.

Neprochnov, Yu.P., I.M. Belousov, V.P. Goncharov, A.A. Shreyder, V.N. Moskalenko, N.A. Marova, I.N. Yel'nikov, G.M. Valyashko, and N.A. Shishkina, 1974, Detailed geophysical investigations in the North-Central Fiji Basin: Doklady Akademii Nauk SSSR, v. 218, p. 688-691.

Pascal, G., J. Dubois, M. Barazangi, B.L. Isacks, and J. Oliver, 1973, Seismic velocity anomalies beneath the New Hebrides island arc: Evidence for a detached slab in the upper mantle: Journal of Geophysical Research, v. 78, p. 6998-7004.

Sclater, J.G., and H.W. Menard, 1967, Topography and heat flow of the Fiji Plateau: Nature, v. 216, p. 991-993.

Sclater, J.G., U.G. Ritter and F.S. Dixon, 1972, Heat flow in the southwestern Pacific: Journal of Geophysical Research, v. 77, p. 5697- 5704.

Seward, D., Fission track dates of basalts from the North Fiji Basin, this volume.

Shor, G.G. Jr., H.K. Kirk, and H.W. Menard, 1971, Crustal structure of the Melanesian area: Journal of Geophysical Research, v. 76, p. 2562-2568.

Sinton, J.M., R.C. Price, K.T.M. Johnson, H. Staudigel, and A. Zindler, Petrology and geochemistry of submarine lavas from the Lau and North Fiji Backarc Basins, this volume.

Sutton, G.H., G.L. Maynard, and D.M. Hussong, 1971, Widespread occurrence of a high-velocity basal layer in the Pacific crust found with repetitive sources and sonobuoys, in J.G. Heacock, ed., The structure and physical properties of the earth's crust: Geophysical Monograph 14, Washington, D.C., American Geophysical Union, p. 193-209.

UNESCO, 1975, Report of the CCOP/SOPAC-IOC IDOE International Workshop on Geology, Mineral Resources and Geophysics of the South Pacific, Suva, Fiji, 1-6 September 1975: IOC Workshop Report No. 6, 30 p.

UNESCO, 1980, CCOP/SOPAC-IOC Second International Workshop on Geology, Mineral Resources and Geophysics of the South Pacific, Noumea, New Caledonia, 9-15 October 1980: IOC Workshop Report No. 27, 63 p.

Kroenke, L.W., and J.V. Eade, editors, 1993, Basin Formation, Ridge Crest Processes, and Metallogenesis in the North Fiji Basin: Houston, TX, Circum-Pacific Council for Energy and Mineral Resources, Earth Science Series, Vol. 15, Springer-Verlag, New York.

MORPHOLOGY AND STRUCTURE OF THE SEAFLOOR IN THE NORTHERN PART OF THE NORTH FIJI BASIN

LOREN W. KROENKE
Hawaii Institute of Geophysics, School of Ocean and Earth Science and Technology
University of Hawaii, Honolulu, Hawaii 96822

ROBERT SMITH[1]
Mineral Resources Department, Private Mail Bag, Suva, Fiji

KENJI NEMOTO
Faculty of Marine Science and Technology, Tokai University, Shizuoka, Japan

ABSTRACT

A geophysical survey of the north central North Fiji Basin provides a high density data base for accurately charting seafloor morphology and defining major structural trends. The resulting bathymetric chart is believed to reliably portray the tectonic fabric of the basin and provide insight into the formation of the seafloor and development of associated structural features. The South Pandora Ridge (Hazel Holme Fracture Zone) appears to be a young or recently formed spreading ridge that bifurcates at its eastern end into the ENE-trending Rotuma Ridge and ESE-trending Tripartite Ridge. Southwest of South Pandora Ridge lies Pentecost Basin, interpreted to be originally formed along the western limb of the extinct central North Fiji Basin (CNFB) triple junction and now inundated, at its southwestern end, by sediment of the New Hebrides archipelagic apron. Southeast of the ridge lies Balmoral Basin, interpreted to be originally formed along the eastern limb of the old CNFB triple junction. Between the two basins lies a wedge of sediment-free ridge and trough terrain believed to be formed by a propagating rift. To the east, in the southern part of Balmoral Basin, Balmoral Ridge is interpreted to be the upraised leading edge of an overthrust block of North Fiji Basin crust, to the south of which lies the eastern end of the Fiji Fracture Zone, a presently active transform fault.

INTRODUCTION

The profusion of marginal basins in the Southwest Pacific appears as a puzzling array to most readers. The North Fiji Basin (Figure 1) is, perhaps, the most enigmatic basin in the region. The first bathymetric chart of the North Fiji Basin (Pandora Basin) was included in a bathymetric map of the Melanesian Borderland (Melanesian Border Plateau) produced by Fairbridge and Stewart (1960); the generalized description (which accompanied that map) of the various submarine features within and around the basin provides the basis for nomenclature in the region (see Table 1). Fairbridge and Stewart remark that "the name Melanesian Border Plateau was proposed to designate the partially raised 'rim' of the Melanesian region. It forms the northern limit of the Pandora Basin (or the 'North Fiji Basin' of Wiseman and Ovey, 1955) and is separated from the Fiji Plateau (of Sir John Murray, 1895)" (or 'Fiji Platform' of Coulson et al., 1975) "by the Balmoral Ridge and the Yasawa Trough."

The first detailed bathymetric chart of the North Fiji Basin (Fiji Plateau [sic]) was published by Chase (1971) after an unpublished Scripps Institution of Oceanography chart. Shortly thereafter, more detailed bathymetric charts were published by Green and Cullen (1973) and Cullen (1974), who identified additional major seafloor features while renaming others (Table 1).

[1]Now with SOPAC Technical Secretariat, Suva, Fiji

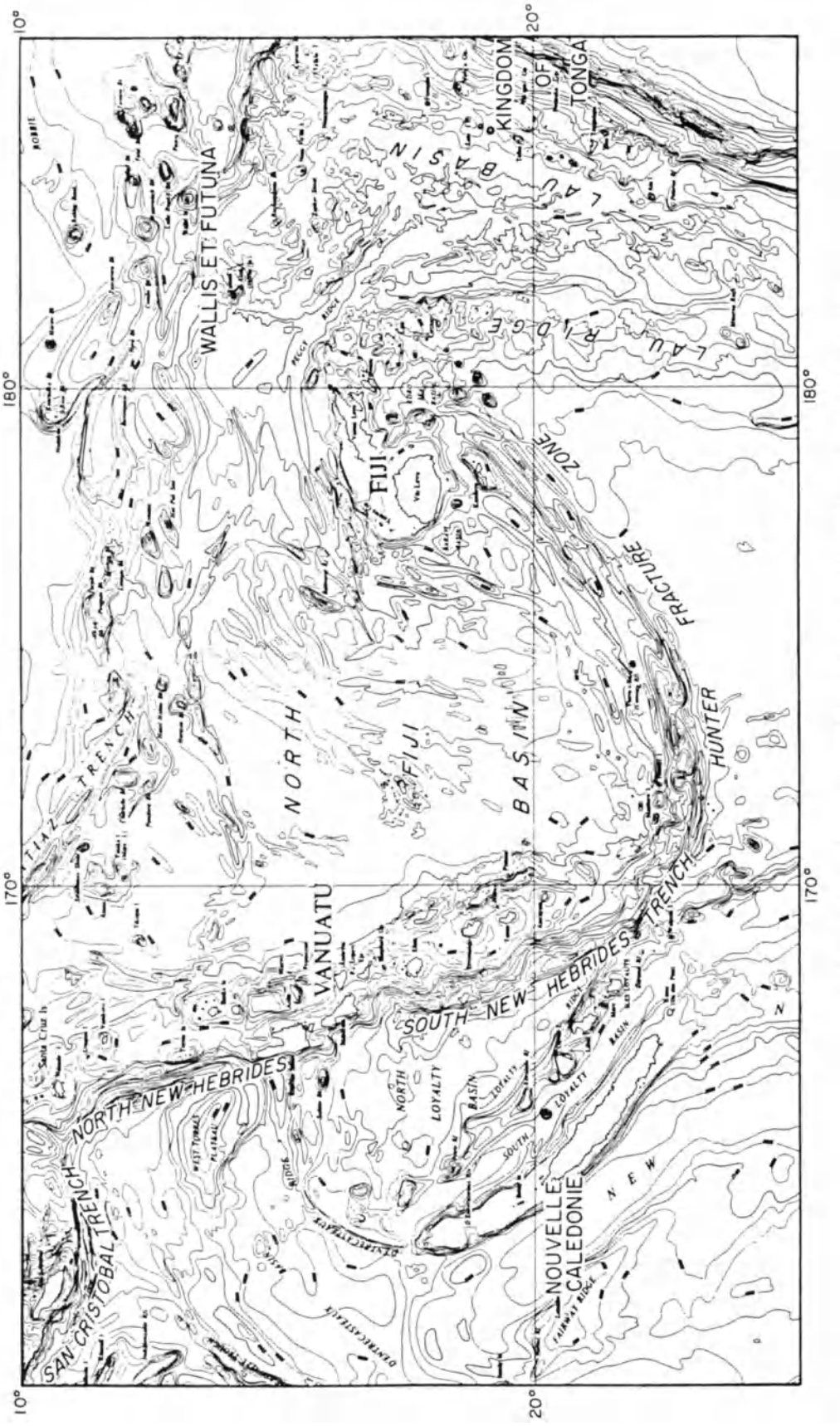

Figure 1. Regional framework of the North Fiji Basin (bathymetry after Kroenke et al., 1983).

Table 1. North Fiji Basin comparative submarine nomenclature.

Fairbridge & Stewart (1960)	Chase (1971)	Green & Cullen (1973)	Cullen (1974)	This paper
Pandora Basin (North Fiji Basin)	Fiji Plateau	Fiji Plateau	unnamed (NZOI Rotuma sheet)	North Fiji Basin
Melanesian Border Plateau	Melanesian Border Plateau	unnamed	unnamed	Melanesian Borderland
Pandora Ridge	unnamed	North Pandora Ridge	North Pandora Ridge	North Pandora Ridge
	unnamed	West Rotuma Trough	Horizon Trough	Horizon Trough
Rotuma Ridge (incorrectly aligned)	unnamed	Rotuma Ridge	Rotuma Ridge	Rotuma Ridge
	Hazel Holme Fracture Zone	South Pandora Ridge	South Pandora Ridge	South Pandora Ridge
unnamed	unnamed	unnamed	unnamed	Techsec Seamount*
unnamed	unnamed	unnamed	unnamed	Sopac Seamount*
Hazel Holme Ridge (incorrectly delimited)	unnamed	unnamed	unnamed	Tripartite Ridge
unnamed	unnamed	Pandora Basin	Pentecost Basin	Pentecost Basin
unnamed	unnamed	unnamed	Balmoral Basin	Balmoral Basin
Balmoral Ridge	unnamed	Balmoral Ridge	Balmoral Ridge	Balmoral Ridge
	unnamed	Yalewa Ridge	Braemar Ridge	Braemar Ridge
Yasawa Trough	unnamed	Yasawa-Yandua Troughs (Fiji Fracture Zone)	Yasawa-Yandua Troughs	Fiji Fracture Zone (Yasawa-Yandua Troughs)
Fiji Plateau	(Fiji Islands)	(Fiji Shelf)	unnamed	Fiji Platform
	Hunter Fracture Zone	Hunter Island Ridge	Hunter Island -Kandavu Ridge	Hunter Fracture Zone

* New name proposed this paper.

Since then, refinements have been added, mainly around the perimeter of the basin (Neprochnov et al., 1974; Hawkins, 1974; Cullen, 1975; Halunen, 1979; Daniel, 1982; Launay, 1982; Brocher, 1985). A regional bathymetric chart of the Southwest Pacific incorporating most of these additions was published by Kroenke et al. (1983).

A detailed survey of the north central part of the North Fiji Basin (Figure 2) was undertaken jointly by Australia, New Zealand, and the United States (Tripartite Agreement) in cooperation with the Committee for Co-ordination of Joint Prospecting for Mineral Resources in South Pacific Offshore Areas (CCOP/SOPAC) in 1982 (see Kroenke and Eade et al., this volume). This survey (KK820316 Leg 3) complemented an earlier survey of the area (KK721108 Leg 2), providing a high-density data base (Figure 3) for more accurately charting seafloor morphology.

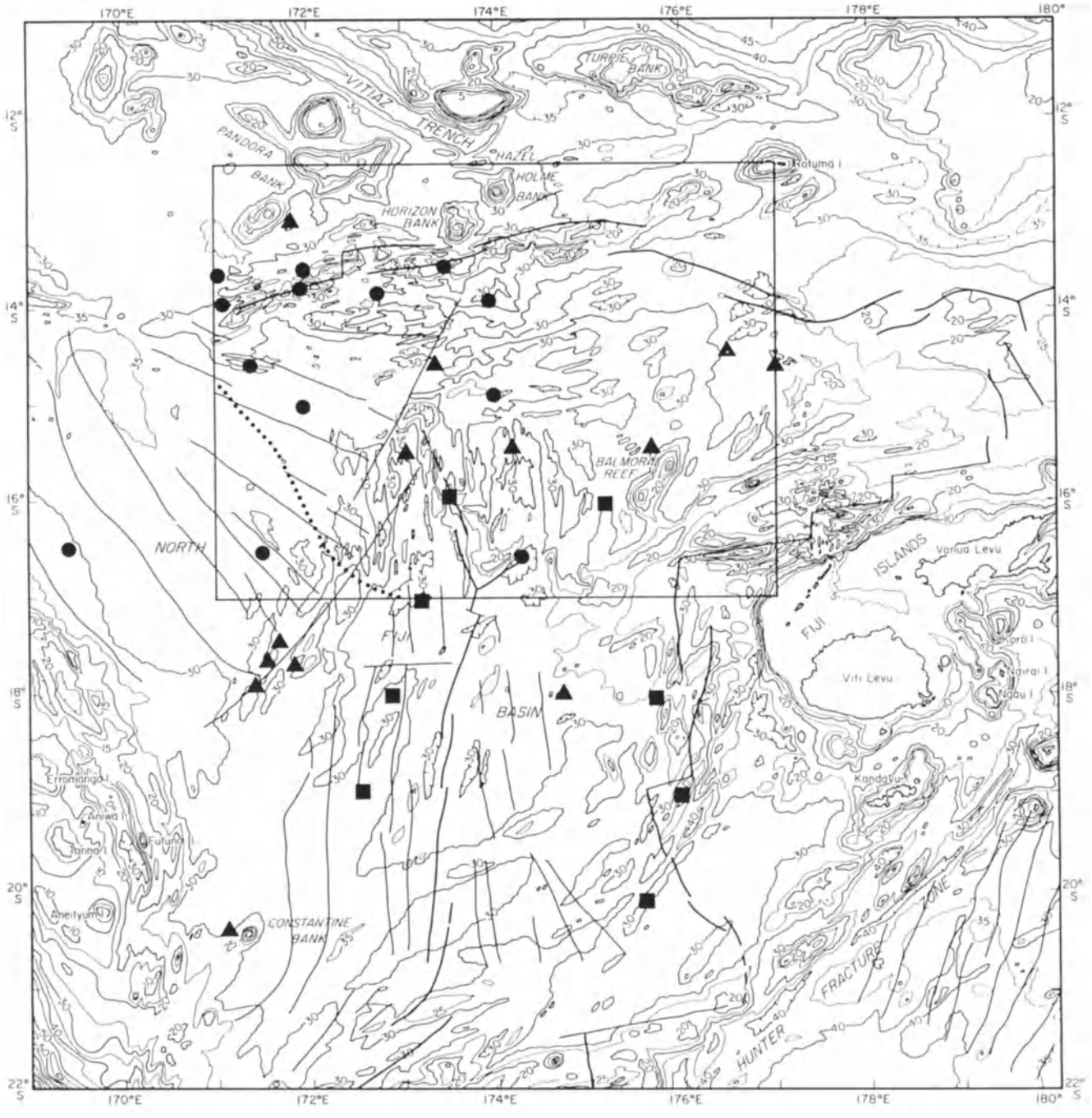

Figure 2. Regional bathymetry of the North Fiji Basin (after Chase et al., 1987) showing location of the primary survey area enclosed by a bold rectangle. Solid dots and triangles are HIG piston core locations. Solid squares are NZOI core locations. Dotted line indicates boundary between New Hebrides archipelagic apron sediments and pelagic sediments of the North Fiji Basin. Solid lines are magnetic lineations identified by Malahoff et al. (this volume).

Since both of these surveys were controlled by satellite navigation and were in good agreement at track intersections, track crossings with earlier cruises could also be evaluated and the older bathymetry merged with the new data to form a common data set. The resulting bathymetric chart is shown in Figure 4. Although some of the contouring is highly subjective, with minor low-relief trends being controlled by the known trends of magnetic anomaly lineations (Malahoff et al., this volume), the chart fairly accurately portrays certain aspects of the tectonic fabric, particularly that of the major structural trends, which are shown in Figure 5.

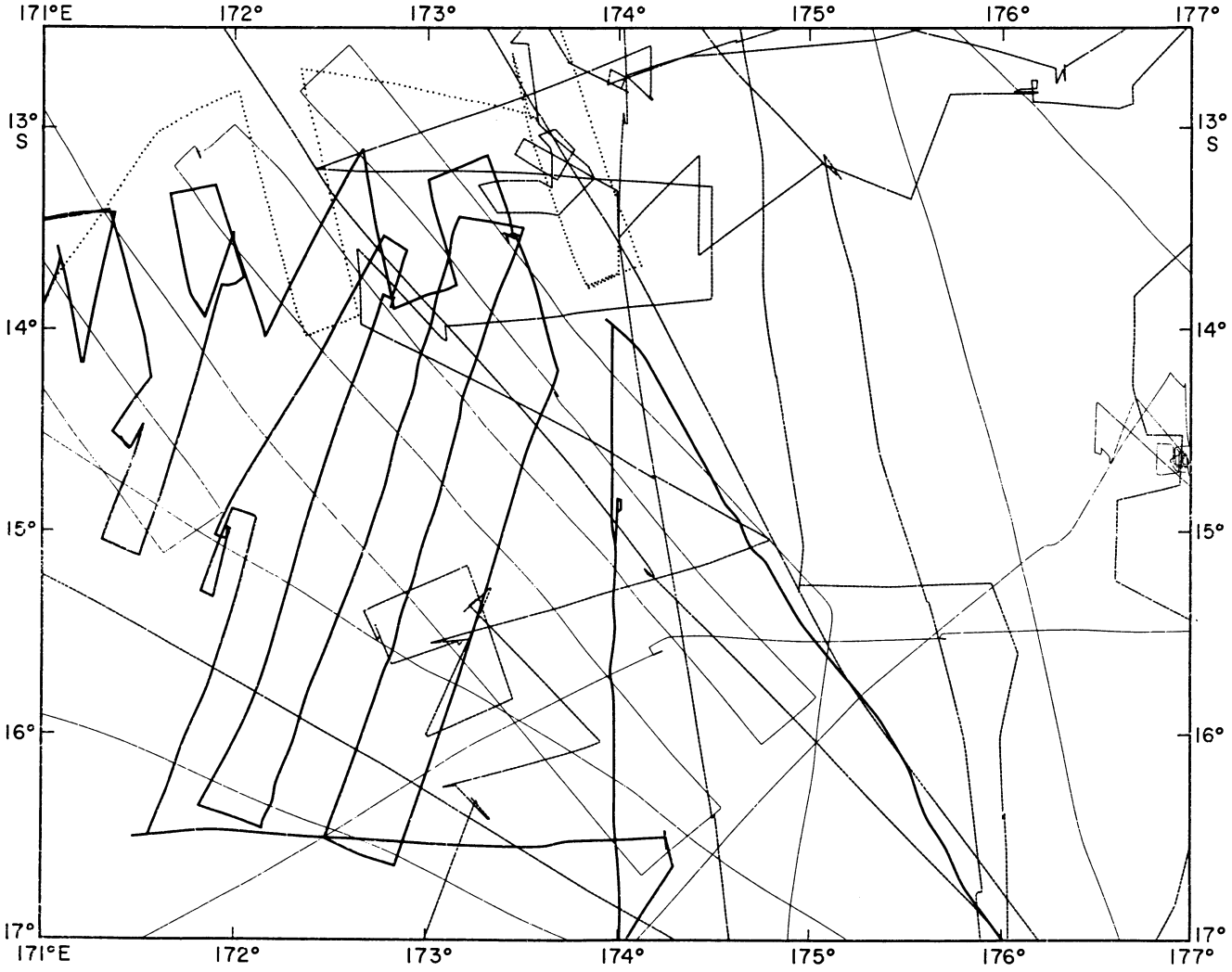

Figure 3. Track control for Figure 4. Heavy solid lines are KK820316 Leg 3 tracks; light solid lines are previous HIG survey tracks; medium dashed lines show locations of earlier survey tracks; dotted line shows the lcoation of the subsequent R/V TANGAROA survey.

SOUTH PANDORA RIDGE

The South Pandora Ridge (part of the Hazel Holme Fracture Zone of Chase, 1971) along the northern margin of the North Fiji Basin, is readily discernible in Figure 4 as a pair of ridges flanking a central or axial trough, all of which are clearly offset in several places. The largest single offset may occur near Horizon Bank at about 173°50'E where the trough appears to terminate and the ridge axis is shifted over 25 km to the north. Other offsets occur at 172°10'E and at 171°20'E. In some places, large seamounts such as Horizon Bank flank the South Pandora Ridge. In other places, small but prominent seamounts occur along the ridge crest (at 174°05'E and 173°20'E). Farther westward, a small volcano appears to fill and obliterate the axial trough (at about 171°50'E). Eastward, outside of the primary survey area, the South Pandora Ridge bifurcates forming two branches: the Rotuma Ridge (northern branch) and the Tripartite Ridge (southern branch). Several seamounts also occur to the east along Rotuma Ridge (Figure 4) but are not as well charted as those on South Pandora Ridge.

The South Pandora Ridge system seems to have all the attributes of a young or recently formed spreading center. Its axial trough and elevated flanking ridges, for example, resemble rift graben terrain. Thus the name "South Pandora Ridge" (Green and Cullen, 1973) is preferred in place of Hazel Holme Fracture Zone (Chase, 1971). The ridges and troughs, for the most part, are sediment free (Kroenke et al., b, this volume). Holocene basalts, pillow lavas, and sheet flow fragments were dredged from small volcanoes within the trough (Sinton et al., this volume) and fresh pillow lobes were

Figure 4. Detailed bathymetry in the primary survey area. Location is shown in Figure 2. Track control is shown in Figure 3. Note the ENE-trending South Pandora Ridge extending from the lefthand side of the figure near 14°00'S to the righthand side of the figure at about 13°15'S.

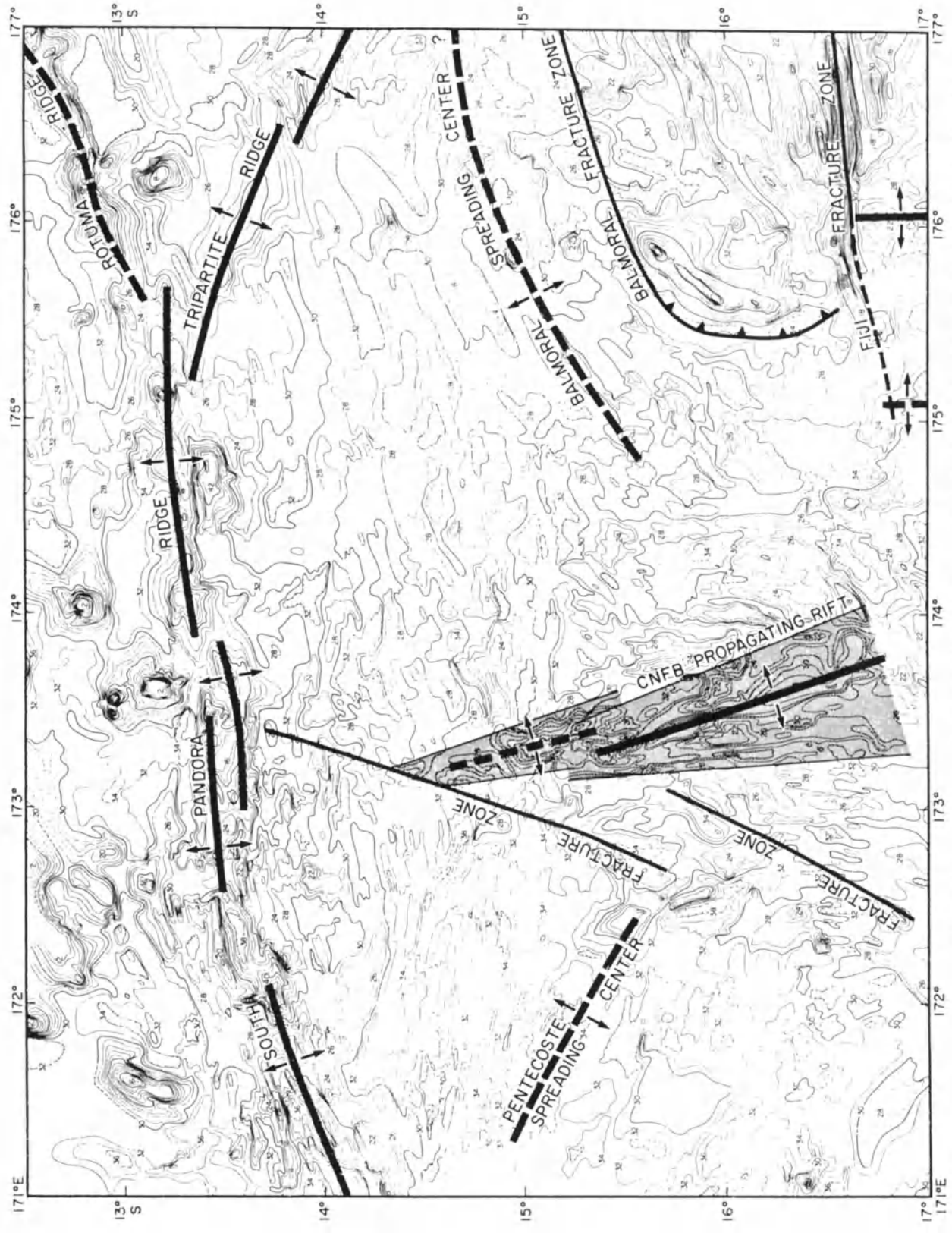

Figure 5. Structural elements within the primary survey area, superimposed on bathymetry. Double solid and dashed lines represent active spreading ridge. Single solid and dotted lines represent active and inactive transform faults, respectively. Dot pattern indicates triple junction, and cross-hatched pattern represents the region formed by propagating rift.

photographed on the trough floor (Kroenke et al., a, this volume).

PENTECOST BASIN

Southwest of the South Pandora Ridge, across the west central part of the survey area within Pentecost Basin (Cullen, 1974), seafloor relief (Figure 4) is believed to reveal the seafloor spreading fabric formed around the locus and along the limb of a presently inactive triple junction, i.e., the site of the old CNFB triple junction formerly located at approximately 14°45'S, 173°E (Figure 5). It should be noted, however, that this seafloor relief is very low amplitude, and considering the subjective nature of the contouring, these trends should be viewed as somewhat hypothetical. The approximate WNW alignment of the seafloor fabric in the northwestern part of Pentecost Basin, however, is substantiated by the trends of the ridges and depressions in that same area as sketched by Neprochnov et al. (1974). Seafloor fabric in the southwestern part of the Basin, in contrast, is considerably more subdued with the trends of basement relief progressively obscured by the archipelagic apron of the New Hebrides Arc (Kroenke et al., b, this volume).

BALMORAL BASIN

Southeast of the South Pandora Ridge, south of Tripartite Ridge, within Balmoral Basin (Cullen, 1974), in the east central part of the survey area, the ENE-trending seafloor relief (Figure 4) evidences the fabric formed by the ENE-trending limb of the older triple junction. In general the seafloor is about 400 m shallower in the Balmoral Basin (2800-3000 m) than in the Pentecost Basin (3200-3400 m).

Dominating the southern half of the survey area is a wedge-shaped area of N-S-trending ridges and troughs. Much of this area is sediment-free (Kroenke et al., b, this volume) and is associated with minor earthquake activity (Hamburger and Isacks, this volume). The overall shape of this ridge and trough terrain suggests that it may have been formed by a propagating rift that has intersected and partially obliterated the locus of the old CNFB triple junction.

East of the hypothetical propagating rift, in the southern part of Balmoral Basin, lies Balmoral Ridge (Figure 4), which has the appearance of an upraised or overthrust block of oceanic crust (see also Kroenke et al., b, this volume). This ridge is bounded to the north by an old transform fault (Balmoral Fracture Zone), which may have connected the thrust fault to a N-S aligned spreading ridge separating the North Fiji and Lau Basins (see Malahoff et al., this volume). Although neither the thrust fault nor the transform fault are active today, the presence of seismicity to the east is interpreted as indicating the presence of shear faulting north of the Fiji Fracture Zone (Hamburger and Isacks, this volume) oblique to Balmoral Ridge.

FIJI FRACTURE ZONE

South of Balmoral and Braemar ridges and north of the Fiji platform lies the ENE-trending Fiji Fracture Zone. Attaining depths of more than 5000 m north of Viti Levu, the fracture zone extends eastward past Vanua Levu from what appears to be a currently active spreading center aligned along longitude 174°E due west of the Fiji Platform (Chase, 1971; Kroenke et al., b, this volume; Malahoff et al., this volume). Originally contoured as an irregular sinuous feature comprising the Yasawa and Yadua troughs (Smith and Raicebe, 1984), the FFZ (when navigational constraints of the various survey cruises are taken into consideration) in reality becomes a remarkably collinear feature, offset by one or more short spreading-ridge segments or relay zones east of the detailed bathymetry shown in Figure 4 (von Stackelberg et al., 1985; Malahoff et al., this volume). Seismicity along the FFZ is intense (Hamburger and Isacks, this volume), indicating its present status as an active transform fault.

CONCLUSIONS

The new bathymetric chart of the northern part of the North Fiji Basin reveals previously unrecognized aspects of basin morphology that, in turn, provide clues to the origin of many of the major structural features that exist within the confines of the basin. The South Pandora Ridge, characterized by the presence of an elongate series of deep troughs (rift valleys) flanked by elevated ridges, is interpreted to be part of an active spreading center, which may connect with the Rotuma Ridge and extend as far east as Rotuma. The WNW-trending seafloor fabric of Pentecost Basin and the ENE-trending fabric of Balmoral Basin collectively are interpreted to indicate the site of an extinct ridge-ridge-ridge triple junction: the old central North Fiji Basin triple junction. The wedge-shaped area of north-trending ridge and trough terrain, located between Pentecost and Balmoral basins, may be an incipient or newly formed propagating rift system. Lying east of this hypothetical propagating rift, the asymmetric profile of Balmoral Ridge resembles that of the upraised leading edge of an overthrust block of North Fiji Basin ocean crust. The western end of the east-trending Fiji Fracture Zone, an active transform fault, is shown to be a much more collinear feature than previously depicted. This is SOEST Contribution no. 1751.

REFERENCES

Brocher, T.M., 1985, On the formation of the Vitiaz Trench Lineament and North Fiji Basin: in T.M. Brocher, ed., Investigations of the Northern Melanesian Borderland, Earth Science Series, v.3: Houston, TX, Circum-Pacific Council for Energy and Mineral Resources, p. 13-33.

Chase, C.G., 1971, Tectonic history of the Fiji Plateau: Geological Society of America Bulletin, v. 82, p. 3087-3110.

Chase, T.E., B.A. Seekins, J.D. Young, L.W. Kroenke, and V. von Stackelberg, 1987, Marine Topography of the Fiji Region, USGS-CCOOP/SOPAC South Pacific Project (unpublished).

Coulson, F.I.E., R.N. Richmond, P. Rodda, and L.W. Kroenke, 1975, Structure of the Fiji Platform: Mineral Resources Department, Fiji, unpublished report.

Cullen, D.J., 1974, Rotuma Bathymetry: N.Z. Oceanographic Institute Chart, Oceanic Series, 1:1,000,000.

Cullen, D.J., 1975, Kandavu Bathymetry: N.Z. Oceanographic Institute Chart, Oceanic Series, 1:1,000,000.

Daniel, J., 1982, Morphologie et structures superficielles de la portie sud de la zone de subduction des Nouvelles-Hebrides: in Equipe Geologie-Geophysique ORSTOM Noumea, Contribution a l'etude geodynamique du Sud-Ouest Pacifique, Travaux et Documents de l'ORSTOM, No. 147, p. 39-60.

Fairbridge, R.W., and H.B. Stewart, 1960, Alexa Bank, a drowned atoll on the Melanesian Border Plateau: Deep-Sea Research, v. 7, p. 100-116.

Green, D., and D.J. Cullen, 1973, The tectonic evolution of the Fiji region: in P.J. Coleman, ed., The Western Pacific: Island Arcs, Marginal Seas, Geochemistry, University of Western Australia Press, Nedlands, p. 127-145.

Halunen, A.J., 1979, Tectonic history of the Fiji Plateau: Ph.D. Dissertation, University of Hawaii, Honolulu, Hawaii, 127 p.

Hamburger, M.W., and B.L. Isacks, Shallow seismicity in the North Fiji Basin, this volume.

Hawkins, J.W., 1974, Geology of the Lau Basin, a marginal sea behind the Tonga Arc: in C.A. Burk and C.L. Drake, eds., The Geology of Continental Margins, Springer-Verlag, New York, p. 505-520.

Kroenke, L.W., C. Jouannic, and P. Woodward, compilers, 1983, Bathymetry of the Southwest Pacific: Chart 1 of the Geophysical Atlas of the Southwest Pacific, CCOP/SOPAC.

Kroenke, L.W., J.V. Eade, and Scientific Party, Overview and principal results of the first joint CCOP/SOPAC tripartite cruise of the R/V KANA KEOKI, North Fiji Basin Survey (KK820316, Leg 03), this volume,a.

Kroenke, L.W., J.V. Eade, C.Y. Yan, and R. Smith, Sediment distribution in the north central North Fiji Basin, this volume,b.

Launay, J., 1982, Morphologie et structure de l'arc insulaire des Nouvelles Hebrides dans sa terminaison sud: in Equipe Geologie-Geophysique ORSTOM Noumea, Contribution a l'etude geodynamique du Sud-Ouest Pacifique, Travaux et Documents de l'ORSTOM, No. 147, p. 163-178.

McMurtry, G.M., E.H. DeCarlo, and K.H. Kim, 1990, Geochemistry of north-central North Fiji Basin sediment, this volume.

Murray, J., 1895, A summary of the scientific results (in two parts): Report of the Scientific Results of the Exploring Voyage of H.M.S. Challenger 1872-1876, (London).

Neprochnov, Yu. P., I.M. Belousiv, V.P. Goncharov, A.A. Shreyder, V.N. Moskalelnko, N.A. Marova, I.N. Yel'niko, G.M. Valysshko, and N.A. Shiskina, 1974, Detailed geophysical investigations in the North Central Fiji Basin: Doklady Akademii Nauk SSSR, v. 218, no. 3, p. 688-691.

Sinton, J.M., R.C. Price, K.T.M. Johnson, H. Staudigel, and A. Zindler, Petrology and geochemistry of submarine lavas from the Lau and North Fiji backarc basin, this volume.

Smith, R., and T. Raicebe, compilers, 1984, Bathymetric map of Fiji, Mineral Resources department, Suva.

Von Stackelberg, V., and Shipboard Scientific Party, 1985, Hydrothermal Sulfide Deposits in Back-Arc Spreading Centers in the Southwest Pacific: BGR Circular.

Wiseman, J.D.H. and C.D. Ovey, 1955, Proposed names of features on the deep-sea floor. 1. The Pacific Ocean: Deep-Sea Research, v. 2, p. 93-106.

Kroenke, L.W., and J.V. Eade, editors, 1993, Basin Formation, Ridge Crest Processes, and Metallogenesis in the North Fiji Basin: Houston, TX, Circum-Pacific Council for Energy and Mineral Resources, Earth Science Series, Vol. 15, Springer-Verlag, New York.

SHALLOW SEISMICITY IN THE NORTH FIJI BASIN

MICHAEL W. HAMBURGER[1] and BRYAN L. ISACKS
Department of Geological Sciences, Cornell University, Ithaca, New York 14853

ABSTRACT

This paper presents a new compilation of shallow seismicity and focal mechanism data that help constrain the model of extension in the North Fiji Basin. Earthquakes are broadly distributed throughout the basin, in marked contrast to the narrow earthquake zones observed near mid-ocean ridge spreading centers. Areas of relatively high activity include the Fiji Fracture Zone, the Hazel Holme Ridge, the western Hunter Fracture Zone, and the proposed spreading center immediately west of Fiji. Areas of deep water in the northern and western North Fiji Basin are notably aseismic and may represent older, presently undeforming portions of the basin. Twenty-three focal mechanism solutions for the basin indicate that the region is dominated by strike-slip deformation. We observe no simple basin-wide system of stress distribution, but consistent stress orientations for groups of mechanisms provide evidence for (1) transcurrent faulting along the Fiji Fracture Zone; (2) hinge faulting of the Indo-Australian Plate near the Hunter Fracture Zone; (3) strike-slip faulting near the Hazel Holme Ridge; (4) strike-slip faulting within the central North Fiji Basin; and (5) normal faulting in the western North Fiji Basin. The orientations of the normal faulting events' tension axe, and the strike-slip events' fault planes are at odds with the configuration of the major spreading centers proposed by previous investigators. A model of "diffuse extension" in the North Fiji Basin provides an explanation for the broadly distributed shallow seismicity, the paucity of normal faulting mechanisms, the obliquity of earthquake fault planes to the strike of proposed spreading centers, and the lack of a uniform basin-wide pattern of stress orientation.

INTRODUCTION

The North Fiji Basin is a prominent example of back-arc extension associated with the tectonics of convergent plate boundaries. Among the world's marginal basins, it stands out as one of the only sites where multiple back-arc basin spreading centers have been directly identified. Compared to the world's other marginal basins, the North Fiji Basin is characterized by a significantly high level of shallow seismic activity. This crustal seismic activity presents us with a unique opportunity to observe the processes of active crustal deformation in a tectonically complex area of back-arc extension. This paper reviews the seismological evidence for deformation within this marginal basin, and presents a new, updated compilation of shallow seismicity and focal mechanism data that bear on the existence of and possible sense of motion along the North Fiji Basin's active spreading centers.

We must bear in mind that the North Fiji Basin is by no means a textbook version of the ideal back-arc basin. The basin is located in a strange position, sandwiched between two subduction zones of opposite polarity at the Tonga and New Hebrides Trenches (Figure 1). It is unusual in its geometry: where most back-arc basins form narrow, elongate troughs separating a single active arc from its relict island arc or continental mainland (e.g., Marianas, Lau Basin, Sea of Japan and others), the

[1]Present address:
Department of Geology
Indiana University
Bloomington, IN 47405

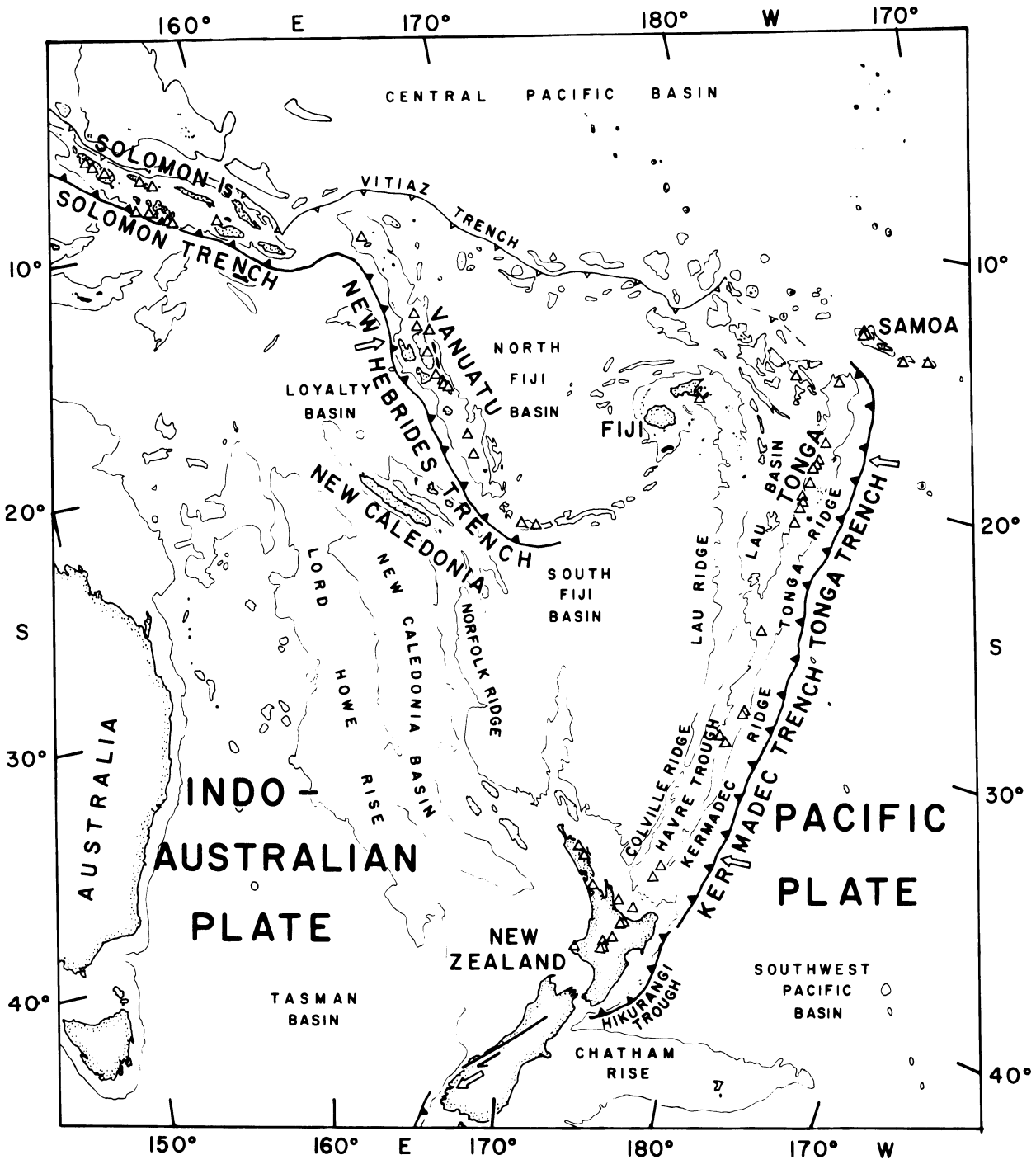

Figure 1. Tectonic setting of the North Fiji Basin. Large arrows indicate direction of relative plate convergence. Contour line shows 2-km isobath. Holocene volcanoes are indicated by open triangles. Data are taken from the Circum-Pacific Council for Energy and Mineral Resources (1981) map.

North Fiji Basin is a broad, trapezoid-shaped basin, bounded on two sides by inactive trenches and on two sides by island-arc platforms. Furthermore, the North Fiji Basin exhibits profuse internal complexity that reflects the complex tectonic histories of the arcs bounding the basin. Lastly, the North Fiji Basin is unique among the world's active back-arc basins in the position of its active spreading centers: in contrast to most basins, where the spreading centers are located within 150 km of the active volcanic arcs (Taylor and Karner, 1983), the North Fiji Basin's spreading centers appear to be distributed up to 800 km from the nearest convergent plate boundary at the New Hebrides Trench.

PREVIOUS SEISMICITY STUDIES

Earthquakes located between the Tonga and New Hebrides arcs have long been an enigma to seismologists. Gutenberg and Richter (1954) first noted the existence of these isolated shallow earthquakes outside the main Tonga and New Hebrides seismic zones, particularly northeast and west of Fiji. Sykes (1966), using computer-relocated epicenters, was able to resolve several discrete zones of seismicity between the Tonga and New Hebrides arcs: one extending from the northern end of the Tonga Trench toward Fiji, a second within the Lau Basin, and a third extending northeastward from the southern New Hebrides into the North Fiji Basin.

Isacks et al. (1969) first placed these interarc earthquakes in a plate tectonic context. They showed that many of the large, shallow earthquakes occurring at the northern end of the Tonga Trench are produced by tearing of the Pacific Plate. The southern portion of the plate subducts beneath the trench, while its northern portion remains at the earth's surface and moves westward relative to the Indo-Australian Plate. A single focal mechanism for an earthquake at the northern edge of the Lau Basin confirmed left-lateral strike-slip motion consistent with this proposed transcurrent motion of the Pacific Plate.

Sykes et al., (1969) presented the first detailed analysis of seismicity of the interarc region. They added to the teleseismic data collected by Sykes (1966) and showed that "the distribution of shallow earthquakes ... indicates that a series of major seismic zones forms a connecting link in a chain of nearly unbroken seismic activity that extends along eastern and northern Melanesia from New Zealand to New Guinea." They showed further that the model of a single arc-arc transform fault connecting the Tonga and New Hebrides zones is unacceptable due to the complexity of the observed seismicity in this region. They suggested that the shallow seismicity delineates two triangular-shaped microplates: one located between Fiji and the New Hebrides Arc (i.e., the North Fiji Basin), and a second between Fiji and the Tonga Arc (i.e., the Lau Basin). In addition, they identified discrete zones of earthquake activity immediately north, west, and south of the Fiji Islands platform.

Chase (1971) extended this tectonic analysis by proposing the existence of five or more microplates between the Tonga and New Hebrides Arcs. On the basis of seismicity, as well as bathymetric and marine geophysical data, he was able to define spreading centers and transform faults along which relative motion between these microplates takes place.

Studies of seismic wave propagation showed striking anomalies in wave velocity and attenuation associated with the back-arc basins between Tonga and the New Hebrides. Dubois (1971), Aggarwal et al. (1972), and Dubois et al. (1973) showed anomalous upper mantle velocities (in the range 7.1-7.7 km/sec) for much of the interarc region. Barazangi and Isacks (1971) and Barazangi et al. (1974) showed further that these zones of low velocity were associated with unusually high attentuation of seismic waves. These seismological observations provided important supporting evidence for active spreading in the Lau and North Fiji basins. Still, the spreading centers themselves remained to be identified directly. The analysis by Chase (1971) had defined areas of crustal generation largely on inference from the distribution of shallow earthquakes and the poorly defined marine magnetic anomalies.

In fact, the new focal mechanism solutions added by Johnson and Molnar (1972) did not verify the tectonic scheme proposed by Chase. Johnson and Molnar proposed an alternative hypothesis, whereby the diffuse seismicity of the interarc region might be explained by thin, weak lithosphere in the North Fiji and Lau basins, unable to support rigid microplate interactions.

Additional attempts to identify the North Fiji Basin spreading centers were based on marine geophysical data, rather than seismological observations. Cherkis (1980), Malahoff et al. (1982a) and Kroenke et al. (this volume) cite magnetic and bathymetric evidence for a major north-trending spreading center in the central portion of the North Fiji Basin, while Brocher and Holmes (1985) offer additional evidence for a younger north-trending spreading center immediately west of the Fiji Islands. And new observations are presented in this volume (Kroenke et al., this volume; Sinton et al., this volume) that suggest that the Hazel Holme (or South Pandora) Ridge may actually accommodate crustal extension as well. Minor spreading centers with varying positions and orientations have been proposed in the North Fiji Basin by Hawkins and Batiza (1975), Hartzell (1975), Halunen (1979), Cherkis (1980), and von Stackelberg (1985).

DISTRIBUTION OF SHALLOW EARTHQUAKES

Data

We have compiled the best available hypocentral information for the teleseismically recorded shallow earthquakes located between Fiji and Vanuatu. The data sources are the compilations of Gutenberg and Richter (1954), Sykes (1966), Sykes et al. (1969), Rothe (1969), and Everingham (1983) for the period 1928-1960, the International Seismological Centre (ISC) catalogs for 1961-1980, and the U.S. Geological Survey's Preliminary Determination of Epicenters (PDE) catalog for 1981-1984. Epicenters for these earthquakes are presented in Figure 2. The events are classified by

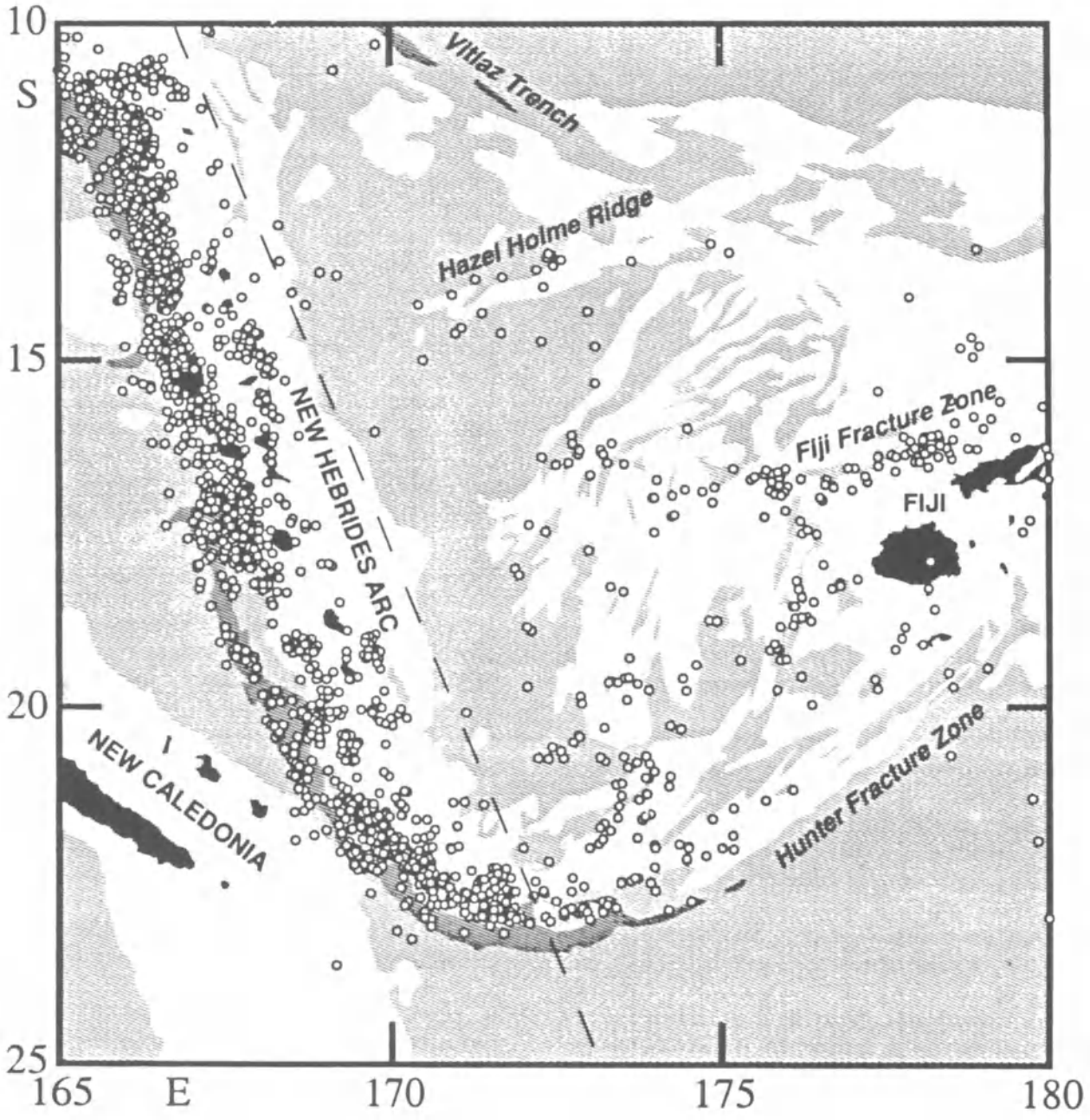

Figure 2. Compilation of shallow earthquakes in the North Fiji Basin (see text for data sources). Earthquakes along the New Hebrides arc (west of the dash line) are from the PDE catalog, 1961-1984. Bathymetric data are from Kroenke et al. (1983); lightly shaded areas have depths >3 km; heavily shaded areas have depths >5 km.

magnitude and by time of occurrence in Figure 3. For comparison, we have also included earthquakes along the New Hebrides plate boundary (west of the dashed line in Figures 2 and 3) located by PDE since 1961.

The location errors for the North Fiji Basin earthquakes vary considerably and are largely a function of the number and azimuthal distribution of recording stations. For the smallest events, recorded by less than 15 stations, gross mislocations of events may occur; these events were thus discarded from consideration. As the number of recording stations increases, the epicentral reliability also increases; earthquakes located by 50 or more stations are expected to be within 10-15 km of the teleseismic location.

In general, the accuracy of earthquake locations has improved with time. The earliest locations, prior to 1950 (Group I in Figure 3), are considered the least reliable. The locations were dependent on a small number of regional seismic stations and manual earthquake location methods, and have in some cases been significantly

modified by macroseismic observations (Everingham, 1983). Between 1950 and 1960 (Group II in Figure 3) the location accuracy steadily improved due to increased timing accuracy at the global seismic stations, the addition of key regional seismic stations, and the introduction of computer location methods. From 1961 to the present (Group III in Figure 3), the global seismic network has provided a relatively uniform, reliable basis for analyzing earthquake distribution. While the depth accuracy may vary considerably for these events, the epicentral accuracy is judged to be ± 15-20 km for most of the earthquakes located after 1961. The data presented in Figures 2 and 3 includes 318 well located events, compared to only 111 earthquakes used in the previous compilation of Sykes et al. (1969). Furthermore, we have discarded from our compilation events located by less than 15 stations and those given "C" quality by Sykes et al. We may thus expect a significant improvement in the resolution of the seismic zones within the North Fiji Basin.

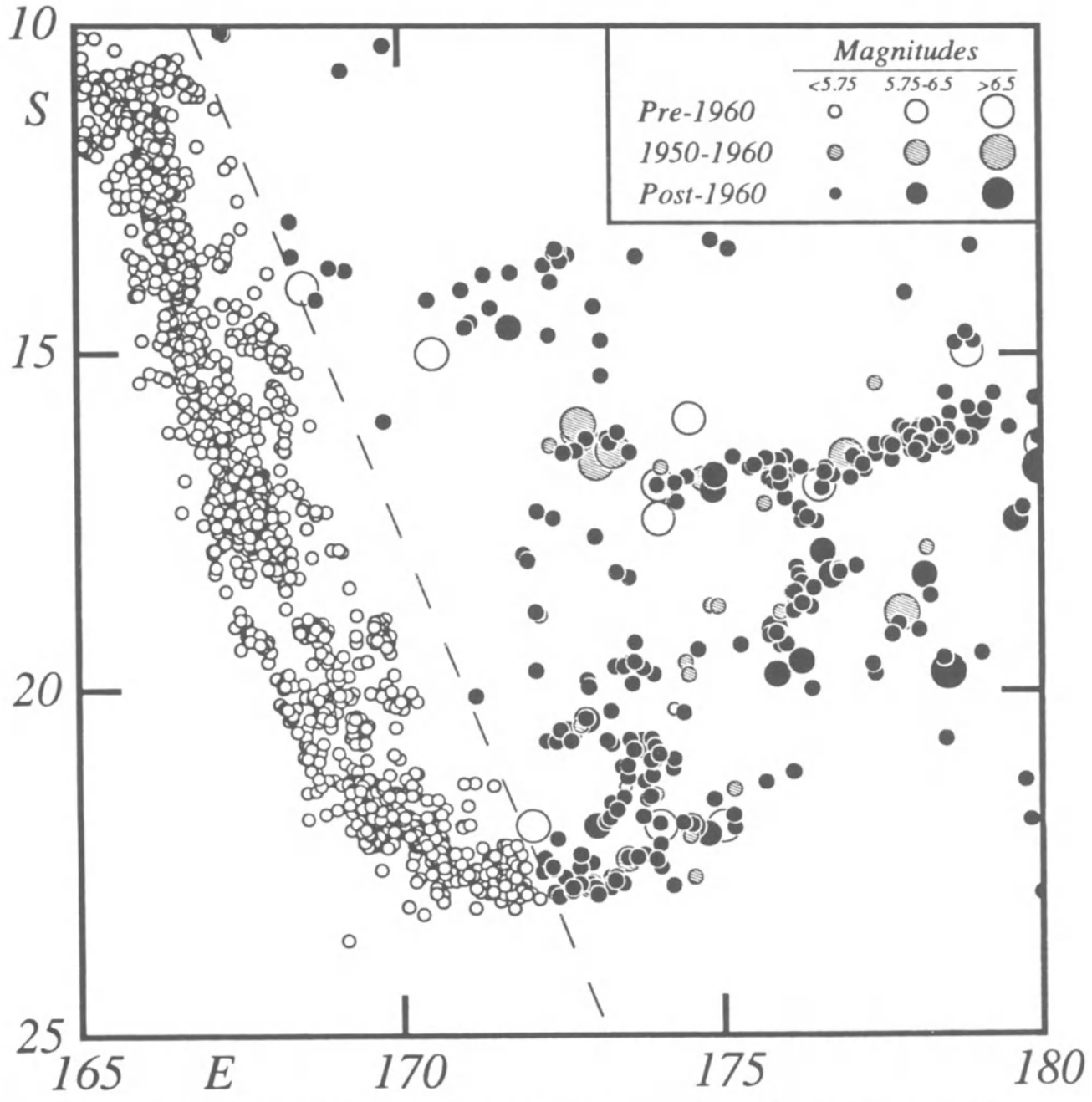

Figure 3. Shallow earthquakes in the North Fiji Basin, graded by magnitude and time of occurrence. Data sources are as in Figure 2.

Results

We note first that earthquakes in the North Fiji Basin are rather widely distributed throughout the basin; clearly they are not limited to two linear seismic belts as Sykes et al. (1969) suggested. On the other hand, the North Fiji Basin is not uniformly active: seismicity does appear to be restricted to areas of relatively shallow water (unshaded portion of Figure 2) that, according to models of thermal subsidence (e.g., Parsons and Sclater, 1977), would also represent the younger portions of the basin.

Seismic energy release within the basin appears to be relatively low, with only 15 earthquakes of magnitude greater than 6.5 occurring there since 1904 (Figure 3). In fact, several of the earlier of these earthquakes may represent New Hebrides events that have been mislocated into the basin. There are no earthquakes in the North Fiji Basin with reported surface-wave magnitudes greater than 7.1. This level of seismicity contrasts sharply with that along the neighboring convergent plate boundaries and suggests that the Indo-Australian/Pacific plate motion is accommodated here through more broadly diffused, more aseismic, plate interaction. In contrast to the distribution of small and moderate-sized events, the largest earthquakes concentrate along the northern and southern edges of the basin, and around the edges of the Fiji Islands platform (Hamburger and Everingham, 1986).

The overall pattern of earthquake occurrence is clearly non-random. While earthquakes occur throughout much of the basin, they do concentrate within discrete areas of the basin. In the following section, we describe each of the areas of seismic activity within the North Fiji Basin.

Fiji Fracture Zone

A notable group of events cluster along an east-trending zone near 16°S. This belt of earthquakes is part of a larger seismogenic feature and extends to the east into an area of rough topography and high seismicity just north of the Fiji Islands. Further east, the belt of seismicity can be traced as a complex but continuous zone which extends to the northern end of the Tonga Trench. As such, it may represent the present southern transcurrent boundary of the Pacific Plate in this area and has been termed the Fiji Fracture Zone (Green and Cullen, 1973; Hamburger and Everingham, 1986). The concentration of large earthquakes along this belt (Figure 3) confirms the contention that a major portion of the interplate deformation is taken up there. The westward extent of the fracture zone is more ambiguous, as its topographic expression is not well preserved west of Fiji. Seismicity extends into the central portion of the basin, but rapidly drops off west of about 174°E.

Hazel Holme Ridge

A second group of earthquakes is located in the northern portion of the basin, near 14°S. This cluster of events, while less clearly defined and less densely populated than the Fiji Fracture Zone, is correlated with an area of rough seafloor topography. The earthquakes coincide with a well-defined northeast-trending ridge variously named Hazel Holme Fracture Zone (Chase, 1971; Halunen, 1979; Eguchi, 1984) and South Pandora Ridge (Kroenke et al., this volume). The ridge has been interpreted by Halunen (1979) and Eguchi (1984) to represent the present southern (transcurrent) boundary of the Pacific Plate in this portion of the basin. Kroenke et al. (this volume) have suggested that the ridge accommodates active crustal extension, evidenced by its thin sediment cover, ridge and trough morphology, and the presence of fresh pillow basalts near its axial valley. Seismicity along this zone extends eastward from the New Hebrides Arc to about 174°E, and then rapidly subsides. It is interesting to note that the seismicity on the Hazel Holme zone appears to drop off at the same longitude where the Fiji Fracture Zone activity picks up; this change in activity might be interpreted as a change in the tectonic activity of both features where they encounter a spreading center near 174°E. Several large earthquakes are also associated with the Hazel Holme Ridge (Figure 3).

Hunter Fracture Zone

A dense cluster of events is associated with the rough topography extending eastward from the southern end of the New Hebrides Trench. The events occur close to and landward of the bathymetric trough (Figure 2) and extend in a diffuse manner into the North Fiji Basin to the north. The density of events associated with the fracture zone appears to drop off rapidly east of 174°E, where it may intersect a major North Fiji Basin spreading center (Chase, 1971), but isolated events, including large historical earthquakes, extend along this zone well into the Fiji Islands Platform (Hamburger and Everingham, 1986).

176°E Spreading Center

A secondary, young spreading center in the eastern North Fiji Basin, was proposed by Sclater and Menard (1967), and supporting observations were presented by Chase (1971) and Brocher and Holmes (1985). This area of rough topography, thin sediment cover, and high-amplitude magnetic and gravity anomalies (Brocher and Holmes, 1985) is associated with a group of earthquakes extending southward from the Fiji Fracture Zone to about 20°S. There, the seismicity drops off, and the tectonic configuration of the spreading center is unknown. The belt of seismicity includes no events with magnitudes greater than 6.5, and only five events with

magnitudes greater than 5.75. It is also populated by smaller magnitude events recorded by local networks in the Fiji Islands (Sykes et al., 1969; Hamburger and Everingham, 1986).

Central North Fiji Basin

Isolated earthquakes also appear to group into a diffuse, north-trending zone between 172° and 174°E. This belt has been linked to extension along the major North Fiji Basin spreading center (Chase, 1971; Cherkis, 1980; Malahoff et al., 1982a) but the breadth and irregularity of the seismic zone are in sharp contrast to the seismicity associated with spreading/transform segments of the mid-ocean ridge system (e.g., Sykes, 1969). Well-located events in this zone are distributed at distances to 100 km from the simple spreading ridge proposed by the previous investigators. A single ocean-bottom seismograph deployed by Nagumo et al. (1975) recorded over 100 microearthquakes in this portion of the North Fiji Basin during a 10-day recording period.

The remaining portions of the North Fiji Basin are remarkably aseismic: the area north of the Hazel Holme Ridge, the area west of 172°E, and the area north of the Fiji Fracture Zone. These areas could represent older and presently undeforming portions of the North Fiji Basin.

EARTHQUAKE FOCAL MECHANISMS

Data

Figure 4 presents a new compilation of focal mechanism solutions for the North Fiji Basin. The compilation represents all the reliably determined mechanisms for shallow earthquakes in the study area. It includes one newly determined mechanism, as well as 14 events obtained by the Harvard/PDE moment tensor inversion method (Dziewonski et al., 1981). The new mechanism (event no. 8 on Figure 4) was obtained using P-wave first motions and S-wave polarization directions read on long-period seismograms from the Worldwide Standard Seismograph Network. The mechanism parameters are summarized in Table 1, and a lower hemisphere stereograph projection of the new mechanism is given in Figure 5.

Several of the published mechanisms have been discarded due to poor readings or to poor constraint on the mechanisms' nodal planes. In an area with relatively few focal mechanisms, a single errant solution can seriously obstruct any reliable tectonic analysis. We have presented only the earthquakes within the basin itself. A large number of mechanisms are available for the region within and surrounding the Fiji Islands Platform and will be the subject of a future paper.

Results

Several first-order observations emerge from Figure 4. Most significantly, this supposedly extensional tectonic regime is wholly dominated by strike-slip deformation. With the exception of two normal faulting events (nos. 14 and 23) and two events along the Hunter Fracture Zone (nos. 2 and 10), all of the larger North Fiji Basin earthquakes occur by strike-slip faulting. Similar results have been obtained for the Lau Basin as well (Eguchi, 1984).

A second important observation is that, while the mechanisms certainly are not randomly oriented, there is no simple regional-scale pattern of stress orientations. There are clear local groupings of earthquakes with similar stress orientations (see discussion below); however, we do not observe a simple dominance of east-west normal faulting or transform faulting earthquakes that are predicted by the tectonic analyses of Chase (1971) and others. Below, we consider each of the groups of focal mechanism solutions individually.

Southern North Fiji Basin

Two events at the southernmost edge of the basin (nos. 2 and 10) can be interpreted as hinge faulting of the Indo-Australian Plate. These events share a nearly vertical east-northeast trending fault plane, along which the north wall is downdropped. This type of faulting, well documented at the northern end of the Tonga Trench (Isacks et al., 1969), is kinematically required if the northern portion of this plate is to be subducted at the New Hebrides Trench and the southern portion is to remain at the earth's surface. Such a faulting mechanism has been proposed for intermediate-depth earthquakes at the southern end of the New Hebrides Arc by Louat (1982).

Western North Fiji Basin

Two recently obtained moment-tensor solutions (nos. 14 and 23) confirm, for the first time, extensional deformation in the North Fiji Basin. The earthquakes are situated within the north-trending belt of seismicity between 172° and 174°E, and directly south of the ridge triple junction proposed by Kroenke et al. (this volume). The stress directions inferred for these two events are virtually identical (see inset in Figure 4), but are strikingly dissimilar from the remainder of the basin. The tension axes are rotated by approximately 55° from the neighboring earthquakes along the Hazel Holme Ridge, and by 60-65° from those observed in the central North Fiji Basin and along the Fiji Fracture Zone. Significantly, the tension axes deviate from the east-west extension direction predicted by the tectonic models of Chase (1971), Malahoff et al. (1982a) and others. These two events are close to the north-trending limb of the ridge

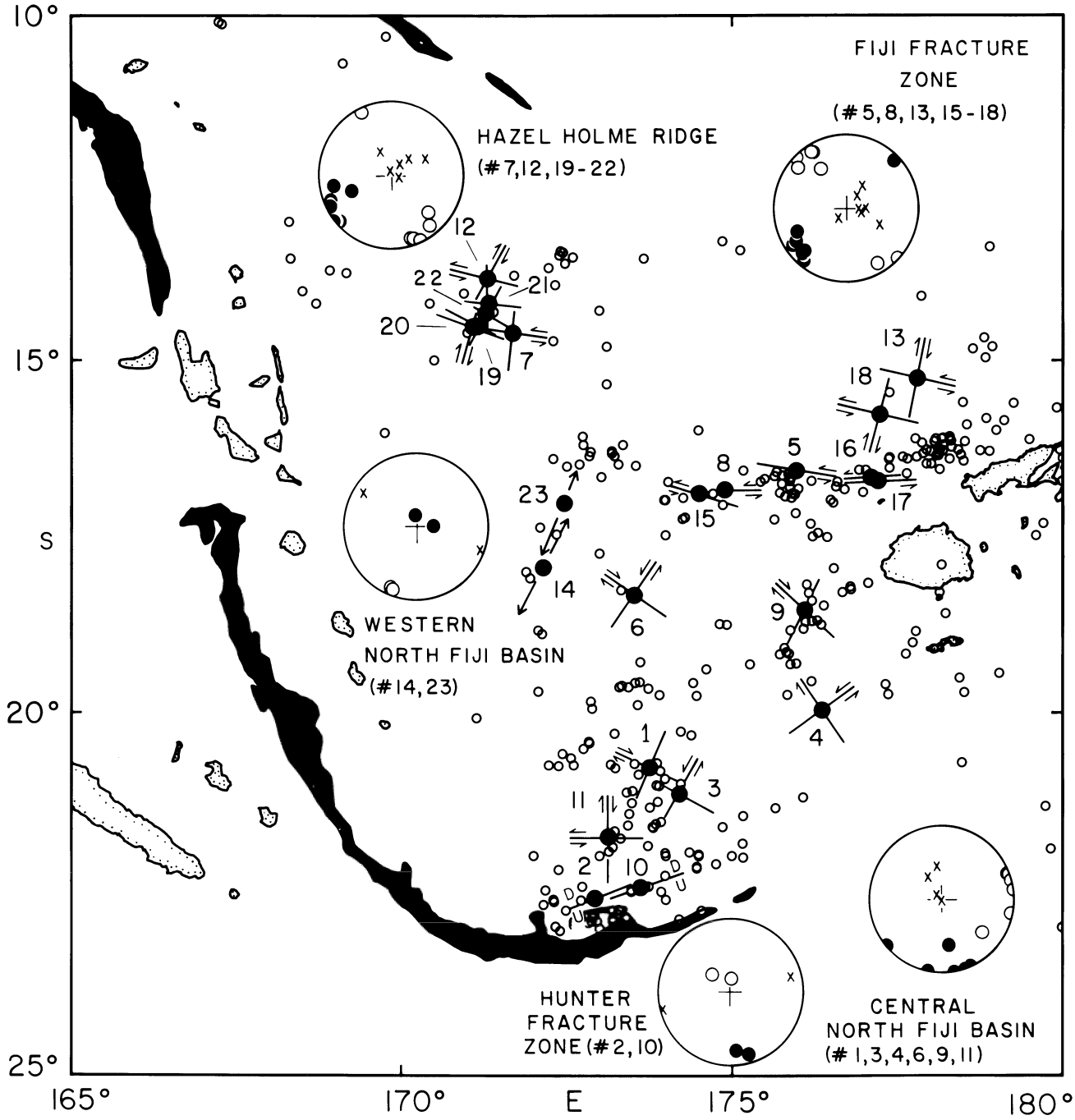

Figure 4. Interpreted focal mechanism solutions for the North Fiji Basin. Mechanism parameters are given in Table 1. Strike of preferred plane of vertical dip-slip mechanisms is shown, with sense of motion given by U (up) and D (down). Single preferred plane or both planes of strike-slip mechanisms are shown with arrows indicating sense of motion. Insets show stress axes for areas of uniform stress distribution: P-axes = filled circles; T-axes = open circles; B-axes = X's. Earthquake locations as in Figure 2.

triple junction proposed by Kroenke et al. (this volume), and to the northeast-trending spreading ridge proposed by Halunen (1979). Again, the north-northeast strike of the T-axes is at odds with the simple tectonic interpretations of the bathymetric data. Nevertheless, these two earthquakes offer the first seismic evidence of normal faulting within the entire interarc region.

Central North Fiji Basin

A second group of earthquakes located south and east of the normal faulting events (nos. 1, 3, 4, 6, 9, and 11) corroborate strike-slip deformation within the North Fiji Basin. With the exception of event no. 11, all these events share a common, east-oriented T-axis (see inset in Figure 4) and may directly result from east-west ex-

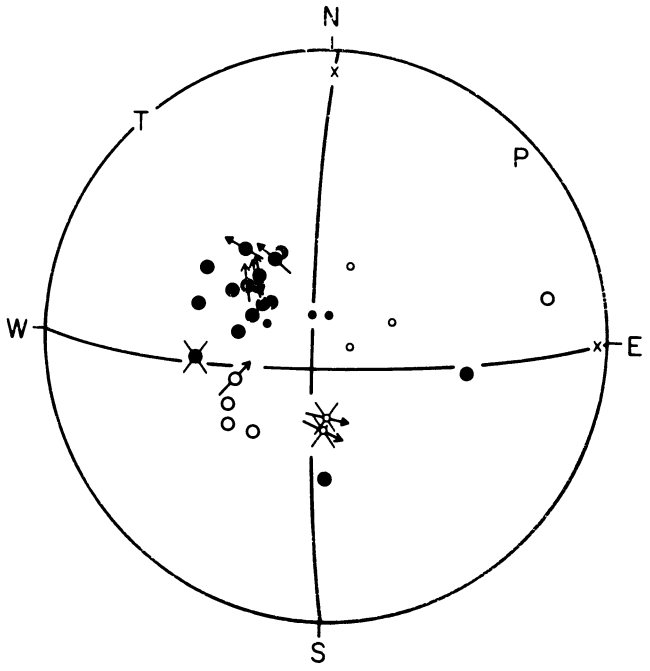

Figure 5. Lower hemisphere projection of the new focal mechanism for the earthquake of 1 January 1972. Mechanism parameters are given in Table 1. Large open and filled circles represent clear dilatational and compressional first motions, respectively. Uncertain first motions are shown as small circles. Large crosses indicate P-wave arrivals that are judged to be near a nodal plane. Arrows with filled and open heads represent clear and uncertain S-wave polarization directions, respectively. X-marks on the nodal planes indicate the poles to the opposite plane. The P (pressure) and T (tension) axes are located at the base of the letters P and T.

tensional stresses within the basin. However, our observations corroborate Eguchi's (1984) finding that the fault planes of these events are oriented obliquely to the proposed strike of both of the north-trending spreading centers proposed in this portion of the basin (Chase, 1971; Malahoff et al., 1982a; Brocher and Holmes, 1985). The earthquakes have a common southeast-trending fault plane accommodating dextral shear and a northwest-trending plane accommodating sinistral shear. By way of exception, event no. 11 has east-west and north-south fault planes. The east-trending plane is close to both the local trend of the southern New Hebrides volcanic arc and to a possible lineation of shallow earthquakes in the same area.

Fiji Fracture Zone

Five mechanisms located in this segment of the Fiji Fracture Zone (nos. 5, 8, 15, 16, and 17) are consistent with sinistral shear along an east-trending fault zone. These east-trending fault planes are close to the regional trend of the seismic zone (Hamburger and Everingham, 1986) as well as to other focal mechanisms along much of its length (Isacks et al., 1969; Sykes et al. 1969; Johnson and Molnar, 1972), and provide a relatively straightforward tectonic interpretation of westward motion of the Pacific Plate relative to the Lau Basin, the Fiji Islands platform, and the North Fiji Basin. This simple interpretation is complicated somewhat by the discovery of fresh basaltic lava dredged from a small north-trending ridge offsetting east-striking segments of the fracture zone north of Fiji (von Stackelberg et al., 1985). The simple transform-fault interpretation is also complicated by the occurrence of earthquakes well to the north of the active seismic zone (Figures 2 and 3). Mechanisms are available for two of these events (nos. 13 and 18). They indicate that the region north of the fracture zone is also dominated by shear faulting and that the stress system is identical to that observed along the fracture zone itself (see inset in Figure 4).

Hazel Holme Ridge

Six focal mechanisms (nos. 7, 12, 19, 20, 21, and 22) are available for this feature, proposed as a site of recent back-arc extension by Kroenke et al., (this volume). The stress axes are remarkably consistent within this group (see inset in Figure 4). Like most of the North Fiji Basin earthquakes, these mechanisms also indicate strike-slip faulting. However, their stress axes (and fault planes) are rotated by 45' from those in the central North Fiji Basin and are close to those observed along the Fiji Fracture Zone (inset in Figure 4). In this case, the T-axes are nearly perpendicular to the strike of the ridge and its axial valley (Figure 2), consistent with the proposed direction of extension. The fault planes, however, are oriented oblique to the strike of the ridge, at odds with a simple ridge/transform interpretation. Furthermore, an important question remains in the interpretation of event no. 7. Chinn and Isacks (1983), using the accurate synthetic seismogram method, showed that this event occurred at an anomalous depth of 48 km. This focal depth would be unusual for old oceanic lithosphere, but is enigmatic in this proposed setting of hot, thin, newly-created lithosphere. The occurrence of subcrustal seismicity beneath the Hazel Holme Ridge might be interpreted in terms of rifting of an older, thicker fragment of island arc lithosphere.

DISCUSSION AND CONCLUSIONS

Independent of any observations within the North Fiji Basin, a clear tectonic requirement for extension has emerged from outside the basin: subduction at the Tonga and New Hebrides trenches is occurring in opposite directions. Because the two trenches are opposite-facing, the trench-trench distance must increase at least as rapidly as the Pacific and Indo-Australian Plates converge. Normally, this would result in the growth of a trench-trench transform fault. However, the latitudinal overlap of the Tonga and New Hebrides

Table 1. Focal mechanism parameters for North Fiji Basin earthquakes.

Event No.	Date	Position* (degrees)	Depth* (km)	Pole 1 AZ	Pole 1 PL	Pole 2 AZ	Pole 2 PL	P Axis AZ	P Axis PL	T Axis AZ	T Axis PL	B Axis AZ	B Axis PL	Reference
1	15 JUN 1965	20.80S 173.73E	33	24	0	114	0	159	0	69	0	0	90	SO6
2	6 JUL 1965	22.54S 172.91E	54	157	58	347	33	163	13	2	76	254	5	SO7
3	13 JUN 1966	21.14S 174.21E	40	30	0	120	0	165	0	75	0	0	90	SO8
4	28 AUG 1968	19.97S 176.37E	40	145	4	55	2	191	2	101	4	304	85	J75
5	16 NOV 1968	16.58S 175.98E	36	270	36	10	14	226	14	326	36	118	51	J77
6	13 MAR 1971	18.35S 173.53E	25	34	0	124	0	169	0	79	0	0	90	E06
7	3 OCT 1971	14.60S 171.69E	48†	96	10	188	10	52	0	142	14	322	76	C84
8	1 JAN 1972	16.85S 174.90E	11	91	4	359	10	46	8	315	2	218	75	**
9	10 SEP 1980	18.56S 176.11E	24	120	22	218	25	170	37	82	0	352	52	EV
10	4 MAR 1982	22.42S 173.69E	53	201	62	341	22	174	21	313	63	77	17	HP
11	17 JUL 1982	21.72S 173.16E	13	91	17	188	21	230	3	139	28	325	62	HP
12	23 MAY 1983	13.81S 171.31E	27	194	28	299	27	247	41	156	1	65	49	HP
13	14 MAY 1984	15.25S 177.81E	33	12	0	282	17	236	12	328	11	101	73	HP
14	31 AUG 1984	17.96S 172.15E	29	42	33	189	52	88	71	208	10	301	16	HP
15	6 SEP 1984	16.91S 174.52E	33	196	28	290	7	246	25	150	14	33	61	HP
16	12 OCT 1984	16.68S 177.11E	13	266	19	357	2	220	12	313	15	91	71	HP
17	12 OCT 1984	16.72S 177.22E	12	178	16	271	12	225	20	134	2	37	70	HP
18	13 OCT 1984	15.77S 177.25E	10	193	4	285	22	237	18	331	12	92	68	HP
19	21 NOV 1984	14.51S 171.16E	23	207	15	297	2	253	12	161	9	36	75	HP
20	21 NOV 1984	14.51S 171.09E	24	19	0	289	8	244	5	335	6	110	82	HP
21	23 NOV 1984	14.31S 171.28E	33	210	24	303	7	259	22	164	12	48	65	HP
22	23 NOV 1984	14.17S 171.33E	33	89	14	185	25	228	7	135	28	332	61	HP
23	19 DEC 1984	17.04S 172.47E	34	17	34	208	56	355	78	2-2	11	111	5	HP

*Hypocentral data through 1982 are from ISC catalog; data for 1983-84 are from PDE catalog.

†Depth from body-wave synthetic seismogram matching (Chinn and Isacks, 1983).

References: C: Chinn and Isacks (1983); E: Eguchi (1984); EV: Everingham (1985); HP: Harvard /PDE Moment Tensor Inversion; J: Johnson and Molnar (1972); S: Sykes et al. (1969); **: This study.

trenches requires that new lithosphere be generated in the intervening area, at a rate comparable to the plate convergence rate. The convergence rate between the Pacific and Indo-Australian plates in this area is approximately 10 cm/yr (Minster and Jordan, 1978). In fact, observations of flexural uplift rates seaward of the two trenches (Dubois et al., 1975, 1977) suggest that the rate of trench divergence may be as high as 20 cm/yr. This 20 cm/yr of divergence demands an equivalent amount of extension within the Lau and North Fiji basins.

Thus, the high topography, high heat flow, thin sediment cover, shallow seismicity, high-amplitude magnetic anomalies and the presence of young basaltic volcanism in the North Fiji Basin have confirmed the existence of active back-arc extension. The high rates of extension predicted for the basin have all strengthened the expectation of a system of lithospheric generation comparable to the mid-ocean ridges. In fact, the array of spreading ridge systems proposed for the North Fiji Basin may result as much from this expectation as from any inescapable requirements of the geological and geophysical data. While we know that extension must be occurring here, simple ridge configurations have not been identified that explain all the observed morphological and geophysical complexity of the basin.

There is little disagreement among investigators as to the existence of back-arc extension within the North Fiji Basin; the major contention is over the manner in which that deformation is distributed. The primary tectonic model, followed by most previous researchers, holds that lithospheric generation in the North Fiji Basin takes place by processes analogous to those observed at mid-ocean ridge spreading centers. Back-arc extension is expected to occur along discrete, well-defined spreading ridges, creating new lithosphere symmetrically distributed about the ridge axes. The morphologic and geophysical signature of the mid-ocean ridges, however, has often been strikingly regular over large distances and relatively straightforward to interpret. The marginal basins' spreading centers, while often identifiable, are generally less clearly defined than the mid-ocean ridges (e.g., Lawver and Hawkins,1978). Weissel (1981) and Taylor and Karner (1983) contended nonetheless that the processes of crustal accretion in the back-arc basins are similar to those observed in the major ocean basins. Chase (1971), Falvey (1978), Cherkis (1980), and Malahoff et al. (1982a) attempted to fit the history of the North Fiji Basin into this mid-ocean ridge tectonic model. The alternate approach, put forth by Lawver and Hawkins (1978), holds that the extension in many marginal basins takes place by a more diffuse system of

back-arc extension. They contend that lithospheric generation in these environments is complicated by the presence of point-source volcanism (seamounts), short-lived spreading ridges, and rapid jumping of ridge crests. An extreme end-member of this tectonic model is the extensional deformation in the Basin and Range province of the western U.S. In this environment, extension occurs through a complex, broadly distributed system of high- and low-angle normal faults and rotational movements of individual blocks by strike-slip faulting (e.g., Stewart, 1978; Smith, 1978).

This model of "diffuse extension" is supported by several aspects of the North Fiji Basin seismicity. First, the broadly distributed shallow seismicity and seismic attenuation indicate that deformation is not limited to narrow belts of activity associated with spreading centers and transform faults. Second, the observed diversity in stress orientations (see insets in Figure 4) contradicts the notion of a simple basin-wide system of crustal extension. Rather, it suggests that seismic deformation is concentrated along several discrete zones, whose stress orientations are determined by the regional interaction of crustal blocks. The rapidly changing geometry of the basin may require that faulting take place along inherited zones of weakness with widely varying orientations. Third, varying orientations of faulting in the central portion of the North Fiji Basin have been proposed based on marine geophysical observations. These must be reconciled with the new seismological observations. The magnetic anomaly data examined by Chase (1971), Cherkis (1980), Malahoff et al. (1982a), and Brocher and Holmes (1985) have been interpreted to indicate northerly striking spreading centers and thus imply east-trending transforms. The bathymetric data for this region have met with more widely varying interpretation. Kroenke et al. (this volume) have interpreted new bathymetric data between 15° and 17°S to support this north-trending ridge morphology. On the other hand, the regional bathymetric fabric (Kroenke et al., 1983) as well as the detailed bathymetry from two proposed spreading ridges in the central North Fiji Basin (Hartzell, 1975; Halunen, 1979) are suggestive of northwest-trending ridges and thus northeast-trending transforms.

The focal mechanisms observed in the central portion of the basin (Figure 4) are dominated by northwest- and northeast-trending fault planes. These fault plane orientations, if they represent transform faulting associated with active spreading ridges, would support the latter interpretation. However, the model of diffuse extension allows for the existence of irregular spreading ridges with oblique transform faults (i.e., "leaky transform" faulting).

Last, the observed dominance of strike-slip faulting must be accounted for. If crustal generation occurs along short, en echelon spreading segments, as the diffuse extension model implies, we might expect shear deformation to dominate. Along most mid-ocean ridges, however, normal faulting as well as strike-slip deformation is usually observed (e.g., Sykes, 1967). If the mid-ocean ridge-type spreading model is correct, the paucity of normal faulting focal mechanisms would demand that the marginal basin lithosphere be even thinner, weaker, and less able to support large stresses than the young oceanic lithosphere near the mid-ocean ridges.

In any event, the rapid rotation of the Fiji and New Hebrides Arcs (Falvey, 1978; Malahoff et al. 1982b) requires a continuously changing geometry of the North Fiji Basin, and a continuously evolving configuration of spreading centers. This situation does not seem compatible with the kind of long-lived, linear spreading configurations such as those proposed by Cherkis (1980) and Malahoff et al. (1982a).

While our observations support the model of diffuse extension in the North Fiji Basin, we do not contend that the seismic activity is uniformly distributed throughout the basin, nor that the earthquake stress axes are randomly oriented. Seismic deformation and, in all likelihood, lithospheric generation are concentrated along the belts of shallow earthquake activity within the North Fiji Basin. But the earthquake focal mechanisms do not demonstrate any simple system of regular spreading centers responsible for present-day extension in the basin. Rather, they indicate a system that is more spatially variable and more shear-dominated then previous researchers have postulated.

ACKNOWLEDGMENTS

The authors wish to thank Loren Kroenke for providing bathymetric data for the central North Fiji Basin. Tom Brocher, Roger Bowman, and Muawia Barazangi provided useful comments on an earlier version of the manuscript. E. Farkas, J. Chatelain, and C. Bass assisted in preparation of the figures, and the manuscript was typed by T. Alt. This research was supported by U.S. Office of Foreign Disaster Assistance Grant No. PDC-0000-G-SS-2134-00. This is Cornell contribution No. 825.

REFERENCES

Aggarwal, Y.P., M. Barazangi, and B. Isacks, 1972, P and S travel times in the Tonga-Fiji region: A zone of low velocity in the uppermost mantle behind the Tonga island arc: Journal of Geophysical Research, v. 77, p. 6427-6434.

Barazangi, M., and B.L. Isacks, 1971, Lateral variations of seismic wave attenuation in the upper mantle above the inclined zone of the Tonga island arc: Deep anomaly in the upper mantle: Journal of Geophysical Research, v. 76, p. 8493-8516.

Barazangi, M., B. Isacks, J. Dubois, and J. Pascal, 1974, Seismic wave attenuation in the upper mantle beneath the Southwest Pacific: Tectonophysics, v. 24, p. 1-12.

Brocher, T.M., and R. Holmes, 1985, The marine geology of sedimentary basins south of Viti Levu, Fiji, in T.M. Brocher, ed., Geological Investigations of the Northern Melanesian Borderland, Earth Science Series, v. 3: Houston, TX, Circum-Pacific Council for Energy and Mineral Resources, p. 122-137.

Chase, C.G., 1971, Tectonic history of the Fiji Plateau: GSA Bulletin, v. 82, p. 3087-3110.

Cherkis, N.Z., 1980, Aeromagnetic investigations and seafloor spreading history in the Lau Basin and northern Fiji Plateau, in Symposium on Petroleum Potential in Island Arcs, Small Ocean Basins, Submerged Margins and Related Areas: UN ESCAP, CCOP/SOPAC Technical Bulletin, No. 3, p. 3746.

Chinn, D.S., and B.L. Isacks, 1983, Accurate source depths and focal mechanisms of shallow earthquakes in western South America and in the New Hebrides island arc. Tectonica, v. 2, p. 529-563.

Circum-Pacific Council for Energy and Mineral Resources, 1981, Plate tectonic map of the circum-Pacific region, Southwest quadrant, 1:10,000. American Association of Petroleum Geologists, Tulsa, OK.

Dubois, J., 1971, Propagation of P waves and Rayleigh waves in Melanesia: Structural implications: Journal of Geophysical Research, v. 76, p. 7217-7240.

Dubois, J., G. Pascal, M. Barazangi, B.L. Isacks, and J. Oliver, 1973, Travel times of seismic waves between the New Hebrides and Fiji islands: A zone of low velocity beneath the Fiji Plateau: Journal of Geophysical Research, v. 78, p. 3431-3436.

Dubois, F., J. Launay, and J. Recy, 1975, Some new evidence on lithospheric bulges close to island arcs: Tectonophysics, v. 26, p. 189-196.

Dubois, J., J. Launay, J. Recy, and J. Marshall, 1977, New Hebrides Trench: Subduction rate from associated lithospheric bulge: Canadian Journal of Earth Science, v. 14, p. 250-255.

Dziewonski, A.M., T.A. Chou, and J.H. Woodhouse, 1981, Determination of earthquake source parameters from waveform data for studies of global and regional seismicity: Journal of Geophysical Research, v. 86, p. 2825-2852.

Eguchi, T., 1984, Seismotectonics of the Fiji Plateau and Lau Basin: Tectonophysics, v. 102, p. 17-32.

Everingham, I.B., 1983, Reports of eathquakes felt in Fiji, 1850-1940: Mineral Resources Department of Fiji, Report 48, 54 p.

Everingham, I.B., 1985, Focal mechanisms of earthquakes near Fiji: Mineral Resources Department of Fiji, Note.

Falvey, D.A., 1978, Analysis of palaeomagnetic data from the New Hebrides: Bulletin of the Australian Society for Exploration Geophysicists, v. 9, p. 117-123.

Green, D., and D.J. Cullen, 1973, The tectonic evolution of the Fiji region, in P.J. Coleman, ed., The Western Pacific: Island Arcs, Marginal Seas, Geochemistry: University of Western Australia Press, Nedlands, p. 127-145.

Gutenberg, B., and C.F. Richter, 1954, Seismicity of the Earth, 2nd ed.: Princeton University Press, Princeton, New Jersey, 310 p.

Halunen, A.J., 1979, Tectonic history of the Fiji Plateau: Unpublished Ph.D. thesis, University of Hawaii, Honolulu, 127 p.

Hamburger, M.W., and I.B. Everingham, 1986, Seismic and aseismic zones in the Fiji region: Royal Society of New Zealand, Bulletin, v. 24, p. 439-454.

Hartzell, S.H., 1975, Geophysical study of the Fiji Plateau near 15°30'S, 173°30'E (abstract): Eos, Transactions of the American Geophysical Union, v. 56, p. 1063.

Hawkins, J.W., and R. Batiza, 1975, Tholeiitic basalt from an active spreading center on the North Fiji Plateau near 15°30'S, 173°30'E (abstract): Eos, Transactions of the American Geophysical Union, v. 56, p. 1078.

Isacks, B.L., L.R. Sykes, and J. Oliver, 1969, Focal mechanisms of deep and shallow earthquakes in the Tonga-Kermadec region and the tectonics of island arcs: GSA Bulletin, v. 80, p. 1443-1470.

Johnson, T., and P. Molnar, 1972, Focal mechanisms and plate tectonics of the Southwest Pacific: Journal of Geophysical Research, v. 77, p. 5000-5032.

Kroenke, L.W., C. Jouannic, and P. Woodward, 1983, Bathymetry of the Southwest Pacific: Chart 1 of the Geophysical Atlas of the Pacific, CCOP/SOPAC

Kroenke, L.W., R. Smith, and K. Nemoto, 1990, Morphology and structure of the seafloor in the north central North Fiji Basin: this volume.

Lawver, L.A., and J.W. Hawkins, 1978, Diffuse magnetic anomalies in marginal basins: Their possible tectonic and petrologic significance: Tectonophysics, v. 45, p. 323-339.

Louat, R., 1982, Seismicite et subduction de la terminaison sud de l'arc insulaire des Nouvelles Hebrides, in Equipe de Geologie-Geophysique du Centre ORSTOM de Noumea: Contribution a l'Etude Geodynamique du Sud-Ouest Pacifique. Travaux et Documents de l'ORSTOM, No. 147, p. 179-185.

Malahoff, A., R.H. Feden, and H.S. Fleming, 1982a, Magnetic anomalies and tectonic fabric of marginal basins north of New Zealand: Journal of Geophysical Research, v. 87, p. 4109-4125.

Malahoff, A., S.R. Hammond, J.J. Naughton, D.L. Keeling, and R.N. Richmond, 1982b, Geophysical evidence for post-Miocene rotation of the island of Viti Levu, Fiji, and its relationship to tectonic development of the North Fiji Basin: Earth and Planetary Science Letters, v. 57, p. 398-414.

Minster, J.B., and T.H. Jordan, 1978, Present-day plate motions: Journal of Geophysical Research, v. 83, p. 5331-5354.

Nagumo, S., J. Kasahara, and T. Ouchi, 1975, Active aseismicity in the Fiji Plateau observed by ocean-bottom seismograph: Journal of Physics of the Earth, v. 23, p. 279-287.

Parsons, B., and J.G. Sclater, 1977, An analysis of the variation of ocean floor bathymetry and heat flow with age: Journal of Geophysical Research, v. 82, p. 803-827.

Rothe, J.P., 1969, The Seismicity of the Earth, 1953-1965: UNESCO, Paris. 336 p.

Sclater, J.G., and H.W. Menard, 1967, Topography and heat flow of the Fiji Plateau: Nature, v. 216, p. 991-993.

Sinton, J.M., R.C. Price, and K.T.M. Johnson, 1990, Petrology and geochemistry of submarine lavas from the Lau and North Fiji back-arc basins: this volume.

Smith, R.B., 1978, Seismicity, crustal structure and Cenozoic tectonics of the western Cordillera, in R.B. Smith and G.P. Eaton, eds., Cenozoic Tectonics and Regional Geophysics of the Western Cordillera: GSA Memoir 152, p. 111-144.

Stewart, J.H., 1978, Basin-range structure in western North America: A review, in R.B. Smith and G.P. Eaton, eds., Cenozoic Tectonics and Regional Geophysics of the Western Cordillera: GSA Memoir 152, p. 132.

Sykes, L.R., 1966, The seismicity and deep structure of island arcs: Journal of Geophysical Research, v. 71, p. 2981-3006.

Sykes, L.R., 1967, Mechanism of earthquakes and nature of faulting on the mid-ocean ridges: Journal of Geophysical Research, v. 72, p. 2131-2153.

Sykes, L.R., B.L. Isacks, and J. Oliver, 1969, Spatial distribution of deep and shallow earthquakes of small magnitude in the Fiji-Tonga region: Bulletin of the Seismological Society of America, v. 59, p. 1093-1113.

Taylor, B., and G.D. Karner, 1983, On the evolution of marginal basins: Reviews of Geophysics and Space Physics, v. 21, p. 1727-1741.

von Stackelberg, U., and Shipboard Scientific Party, 1985, Hydrothermal sulfide deposits in back-arc spreading centers in the Southwest Pacific: Bundesanstalt fur Geowissenschaften und Rohstoffe Circular 2, p. 3-14.

Weissel, J.K., 1981, Magnetic lineations in marginal basins of the western Pacific: Philosophical Transactions of the Royal Society of London, v. A300, p. 223-247.

Kroenke, L.W., and J.V. Eade, editors, 1993, Basin Formation, Ridge Crest Processes, and Metallogenesis in the North Fiji Basin: Houston, TX, Circum-Pacific Council for Energy and Mineral Resources, Earth Science Series, Vol. 15, Springer-Verlag, New York.

DEEP SEISMICITY IN THE NORTH FIJI BASIN

PATRICIA COOPER and LOREN W. KROENKE
Hawaii Institute of Geophysics, School of Ocean and Earth Science and Technology, University of Hawaii
Honolulu, Hawaii 96822

ABSTRACT

Seismological evidence based on the spatial distribution and focal mechanisms of deep earthquakes in the North Fiji Basin supports a model in which Indo-Australian oceanic lithosphere, subducted at a former (11–8 Ma) position of the New Hebrides Trench, was detached as the trench migrated clockwise to its present position. A careful selection of well-determined hypocenters in the region, for the years 1964–1984, defines two segments of a deep Wadati-Benioff zone within the upper mantle at a depth of 545–655 km. The dips vary gently, the deep segments constituting an effectively flat zone of seismicity. The thin, slablike distribution of these hypocenters is similar to that in regions of active subduction. The horizontal extent of the relict slab segments is defined. It is apparent that lithosphere at this depth possesses enough strength to support earthquake generating stresses and to cause severe deformation of Pacific lithosphere subducted at the Tonga Trench. The slab segments have settled above the 700-km level and may represent a physical boundary which would preclude whole-mantle convection, at least in this area.

INTRODUCTION

A fundamental concept of plate tectonics associates deep earthquakes with active subduction of oceanic lithosphere into the upper mantle. Although this assumption is generally valid, the deep (545–665 km) earthquakes of the North Fiji Basin are not clearly related to either of the well-defined Wadati-Benioff (W-B) zones associated with the active subduction zones of the Tonga-Kermadec or New Hebrides Trenches (Figure 1). Studies of the regional seismicity (Chase, 1971; Isacks and Molnar, 1971; Johnson and Molnar, 1972; Dubois et al., 1973; Pascal et al., 1973; Pascal et al., 1978; Billington, 1980) and of the deep earthquakes of the central part of the basin in particular (Sykes, 1964; Hanus and Vanek, 1981, 1983; Hamburger and Isacks, 1985) have yielded inconclusive results regarding the site of subduction for the lithosphere in which these deep earthquakes originate. Pascal et al. (1973) imply that all of the deep earthquakes originate in lithosphere subducted at the New Hebrides Trench. Others regard the deep earthquakes as originating in two separate pieces of lithosphere (Pascal et al., 1978; Hanus and Vanek, 1981, 1983; Hamburger and Isacks, 1985). Those occurring in the northern part of the North Fiji Basin with a west-northwest trend are described as originating in Pacific lithosphere subducted at the Vitiaz Trench whereas those located near Fiji and the New Hebrides are described as originating in Indo-Australian lithosphere subducted at the New Hebrides Trench.

This study investigates the geometry of the deep seismicity and considers its origin in light of recent advances in understanding the tectonic evolution of the Northern Melanesian Borderlands.

TECTONIC SETTING

The North Fiji Basin is situated south of an inactive subduction zone located along the Vitiaz Trench and between two active subduction zones located along the New Hebrides and Tonga Trenches, within the present convergence zone between the Pacific and Indo-Australian Plates (Figure 1). The region has long been recognized as an extensional marginal basin (Packham and Falvey, 1971; Karig, 1971), the northern part of which is considered to be a part of the Pacific Plate

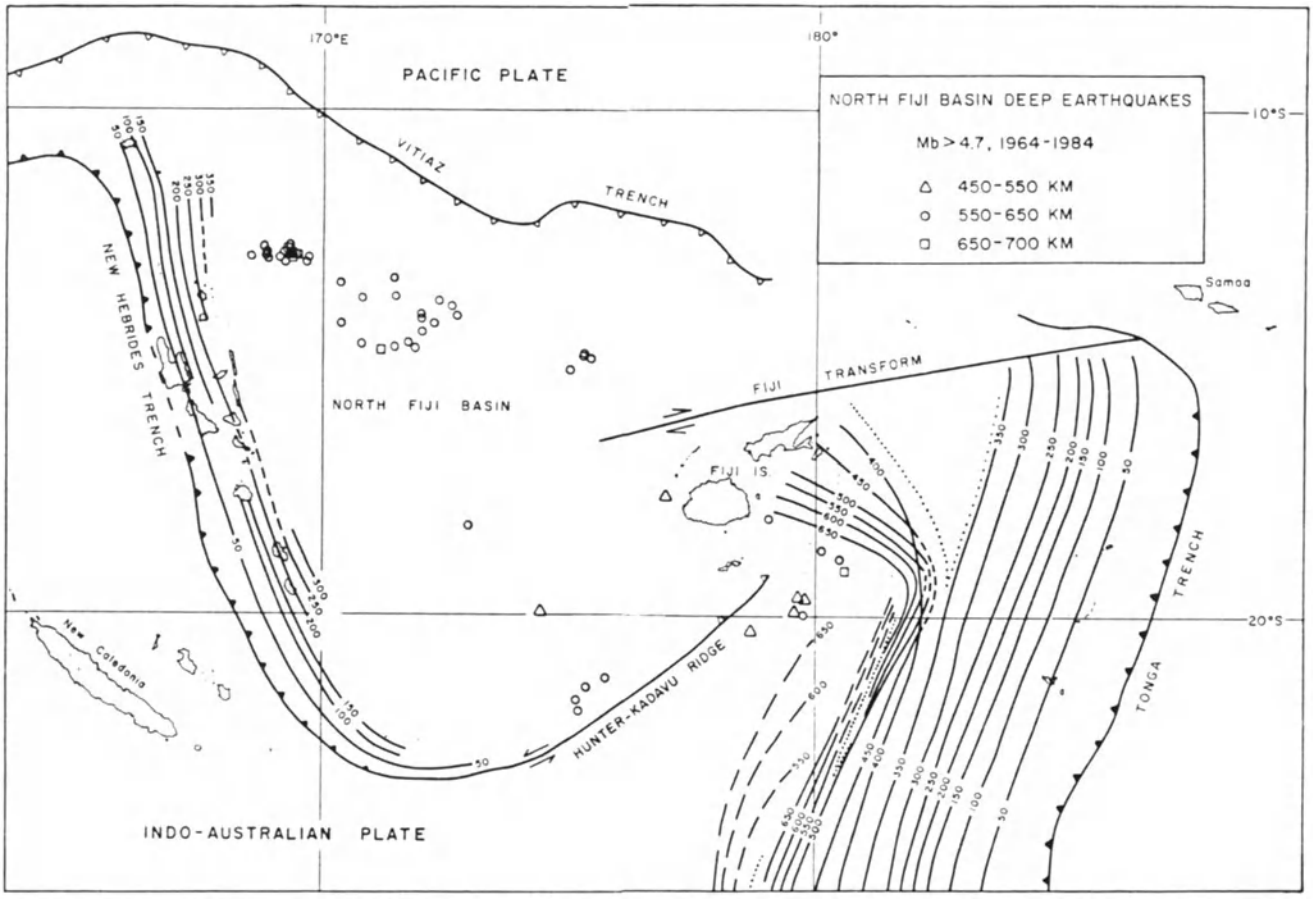

Figure 1. Deep earthquakes of the North Fiji Basin. Deep earthquakes are shown relative to the Wadati-Benioff zones of the New Hebrides and Tonga arcs. The Wadati-Benioff zones are contoured in 50-km intervals. Topographic trench axes are indicated by sawtooth lines; sawteeth point in the direction of subduction. The trench axis is dashed where its location is uncertain.

(Chase, 1971). Whereas no one feature clearly extends from the New Hebrides to the Tonga Trench, the boundary between the North and South Fiji basins is usually defined by the Matthew Hunter Ridge and the Hunter-Kadavu Ridge.

In general, the North Fiji Basin is characterized by shallow water depth (Karig, 1970; Chase, 1971), high heat flow (Sclater et al., 1972; MacDonald et al., 1973; Halunen, 1979), large positive free air anomalies (Watts et al., 1983; Kellogg and Kansakar, this volume), thin crustal and sedimentary sections (Solomon and Biehler, 1969), and, in some parts of the basin, exposed fresh pillow basalts (Sinton et al., this volume). Shallow earthquake epicenters are aligned along the Fiji Fracture Zone (north of Fiji) and the Hunter Fracture Zone (southwest of Fiji) (Hamburger and Isacks, this volume). Relative motion along these two features is indicated in their Figure 1. Sparse shallow seismicity also occurs in the central part of the North Fiji Basin and is believed to originate within transform fault offsets of the intrabasin spreading ridge segments (Hamburger and Isacks, this volume). Combined divergence of the North Fiji and Lau Basins is estimated by Dubois et al. (1977) to be about 110 mm/yr.

Structural and stratigraphic relationships of the lithologic units exposed on the land areas surrounding the North Fiji Basin provide evidence for at least three distinct periods of convergence (Kroenke, 1984; Rodda and Kroenke, 1984): southwestward subduction in the Oligocene along the West Melanesian Trench (including the Manus, North Solomon, and Vitiaz trenches) that ceased by early Miocene time (about 25 Ma); westward subduction in the early Miocene along the Lau Trench (predecessor to the Tonga Trench) that ceased in late Miocene time (about 10 Ma); and northwestward subduction along the then collinear New Britain-San Cristobal-New Hebrides trenches in the late Miocene (prior to translation and rotation into their present configuration).

Petrological, geochronological, and paleomagnetic data from the New Hebrides, Vitiaz, and Tonga arcs suggest that from late Eocene/early Oligocene until early Miocene, the North Solomon-Vitiaz-Fiji arcs formed a single, collinear, ENE-facing volcanic arc on the Indo-Australian Plate beneath which the Pacific Plate was

subducted to the southwest (Gill, 1970, 1976; Chase, 1971; Karig and Mammerickx, 1972; Gill and Gorton, 1973; Packham and Andrews, 1975; Falvey, 1975, 1978; Coleman and Packham, 1976; Carney and Macfarlane, 1982; Colley and Hindle, 1984). Collision of the Ontong Java Plateau with the North Solomon Trench in the latest Oligocene or earliest Miocene is believed to have precipitated the shift of the convergence zone elsewhere (Kroenke, 1984; Kroenke et al., 1986).

East-northeast subduction beneath the WSW-facing New Britain-San Cristobal-New Hebrides arcs was sufficiently well established by mid-late Miocene to produce arc volcanism (Carney and Macfarlane, 1982; Neef, 1982; Packham, 1982). Dilatation of the North Fiji Basin began about 8 Ma (Malahoff et al., 1982), and clockwise rotation of the New Hebrides Arc began about 6 Ma in response to this back-arc basin formation (Falvey, 1978; Brocher and Holmes, 1985).

The New Hebrides Trench, the site of eastward subduction of the Indo-Australian Plate, now consists of two main segments, the North New Hebrides, or Torres Trench, and the South New Hebrides, or Vanuatu Trench. The segments of deep trench are separated by a zone of abnormal trench morphology (Carney and Macfarlane, 1982), shown by a dashed line in Figure 1, and the forearc is uplifted and deformed, probably the result of subduction of D'-Entrecasteaux Ridge (Carney and Macfarlane, 1982; Burne et al., 1985). The trench strikes NNW and marks the surface trace of a W-B zone dipping steeply to the northeast. The convergence direction is roughly N75°E (Pascal et al., 1978); the convergence rate is about 120 mm/yr. For most of the length of the arc, the W-B zone is continuous and dips at about 70 degrees (Pascal et al., 1978; Louat et al., 1982). Observations of attenuation and velocity structure in this region (Barazangi et al., 1973; Oliver et al., 1973; Pascal et al., 1973, 1978) indicate that the present depth extent of subduction along the New Hebrides Trench is only about 350 km. The deeper earthquakes, which extend across much of the basin (Figure 1), occur in lithosphere that is spatially separated from the New Hebrides slab.

The Tonga-Kermadec Trench, currently the site of westward subduction of the Pacific Plate, also consists of two segments, the northern Tonga Trench and the southern Kermadec Trench, separated by the Louisville Ridge. The Tonga-Kermadec subduction zone, which has one of the deepest (>650 km) and most active W-B zones, exhibits extreme variability in morphology, the subducted slab being either highly contorted (Billington, 1980) or torn and segmented (Louat and Dupont, 1982) or both. Subducted Pacific Plate now underlies part of the North Fiji Basin.

DEEP FOCUS EVENTS

The data set consists of 50 deep events (Mb > 4.7; > 15 observations) located by ISC in the area between about 12 and 23°S. The spatial extent of the deep earthquakes in the North Fiji Basin for the period 1964–1984 is indicated by the stippled area in Figure 2. The relative location of the deep seismicity is shown with respect to the New Hebrides and Vitiaz trenches and the volcanic line of the New Hebrides Arc. The northernmost trend is subparallel to the strike of the Vitiaz Trench; the southernmost trend is subparallel to the strike of the New Hebrides Trench. The seismicity does not necessarily outline a triangular slab; if it does, then the interior portion of the slab is aseismic. The events seem to be distributed within two horizontal slab segments. The northernmost segment (A-A' in Figure 3b) appears to dip to the north-northeast. Focal depth also increases from southeast to northwest. Isacks and Molnar (1971) obtained three focal mechanisms (one normal event and two normal with large strike-slip components) within this area, and concluded that they orignated in a nearly horizontal slab. The northernmost events at their eastern end appear to terminate in a recurvature in the intensely deformed Pacific Plate of the Tonga-Kermadec subduction zone. The southernmost events at their eastern end lie near or beneath the Hunter Fracture Zone. Seismicity from the two segments appears to converge in the northern New Hebrides (Figure 1). The northeastern end, nearest New Hebrides, is more active and possesses the more pronounced dip. The angle sub-

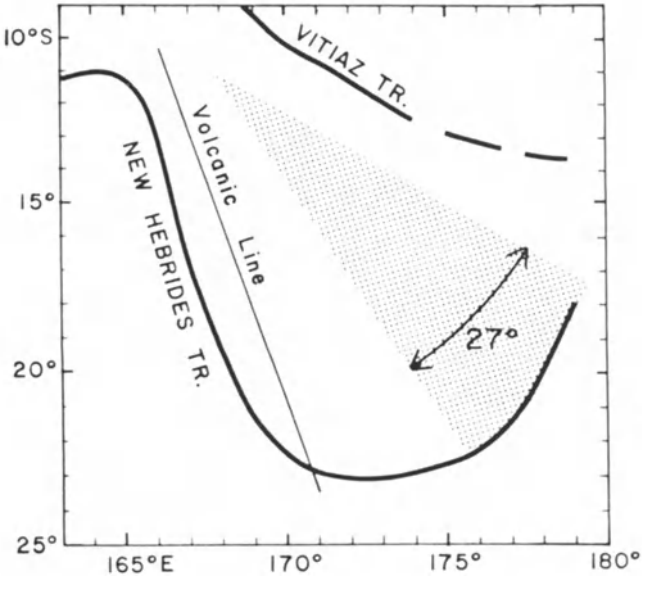

Figure 2. Schematic diagram of the areal extent of deep North Fiji Basin earthquakes (stippled area). Heavy lines show axes of (top) the Vitiaz trench and (bottom) the New Hebrides trench and the Hunter-Kadavu Ridge. A "volcanic line" has been fitted through the active volcanoes of the New Hebrides Arc.

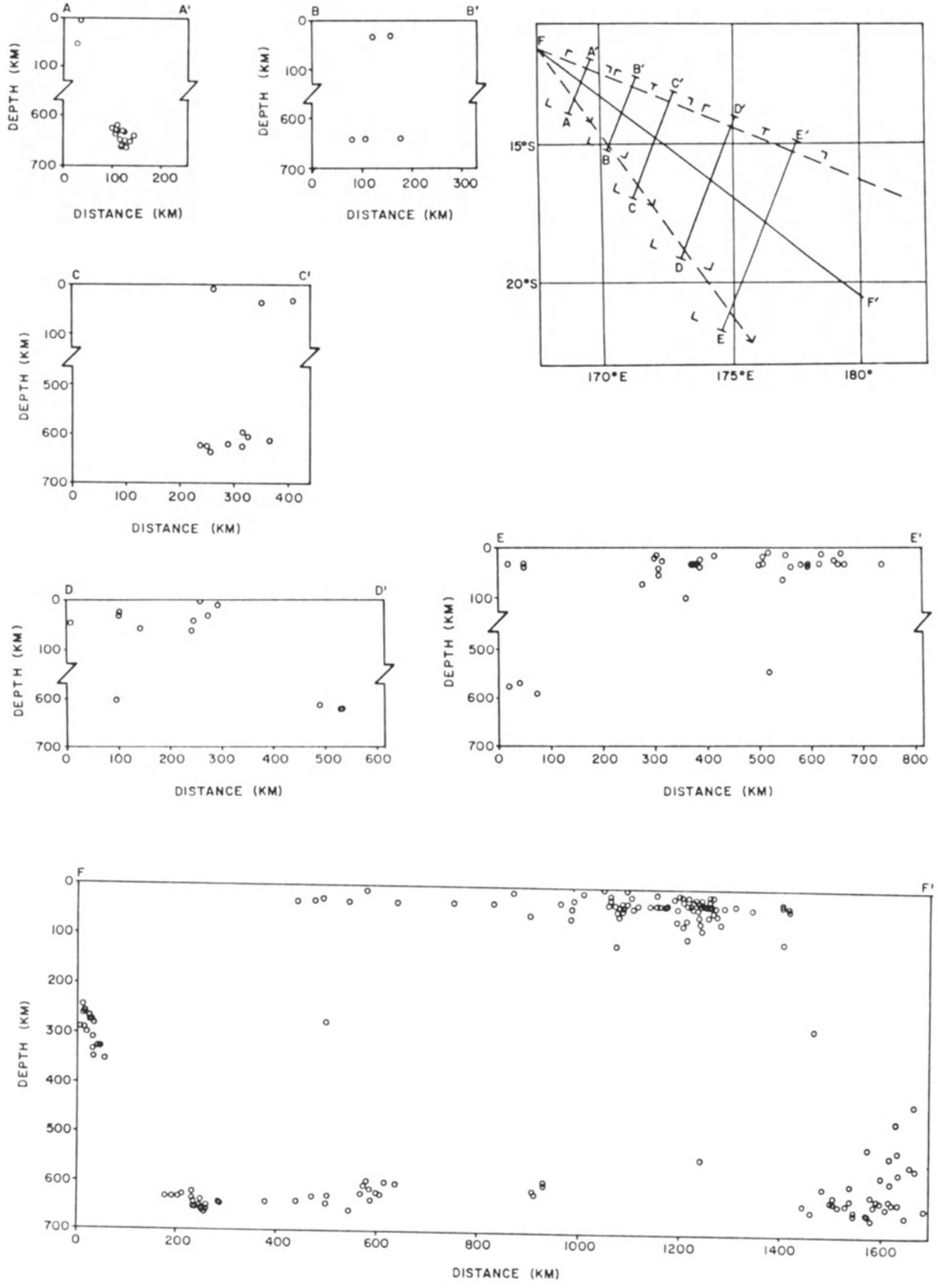

Figure 3. Seismic cross sections; locations are shown in figure upper right.

tended by the entire deep earthquake set is about 27° (Figure 2). This is very close to the total amount of clockwise rotation of the New Hebrides Arc, 30° (Falvey, 1978).

The slab segments have settled above the 670-km discontinuity. All relict slab seismicity (within the specified magnitude and observational bounds) is confined to the depth interval 545–665 km. This range may be due in part to undulations in the slab caused by deep collision with the Tonga slab. The distribution of hypocenters with depth is shown in greater detail in vertical cross sections (Figure 3b–g). The locations and widths of these sections are shown in Figure 3a. The three-dimensional distribution of subducted lithosphere in the North Fiji basin is depicted in Figure 4 and is based on observed seismicity.

CONCLUSIONS AND DISCUSSION

Deep earthquakes in the North Fiji Basin probably are not related to subduction of Pacific Plate lithosphere along the Vitiaz Trench. Rather, they more likely are the result of an early phase of subduction of Indo-Australian Plate along initial strike of the New Hebrides Trench. As the New Hebrides subduction zone migrated to its present location, pieces of slab detached and sank. The evidence supporting this interpretation:

(1) The arc has rotated clockwise about 30° (Falvey, 1978) and the angle subtended by the triangular distribution of deep earthquakes is about 27°.

(2) The deep seismicity extends across the entire basin, yet few events extend south of the Hunter-Kadavu Ridge (formed during the rotation).

(3) The total length of the New Hebrides slab is too small when the time span and rate of convergence are considered, i.e., a large portion of the slab is missing. However, the combined lengths of the presently subducting slab and the two horizontal deep segments are roughly equivalent to that expected at the present rate of convergence since initiation of subduction in earliest late Miocene time.

(4) Although there is a slight increase in depth to the northwest, the slab segments are effectively flat, only the northwest corner has a slight north-eastward dip.

Subduction at the New Hebrides Trench appears to have continued uninterrupted throughout the dilatation of the North Fiji Basin. Commencing in earliest late Miocene, the New Hebrides arc/trench system migrated clockwise about its northern terminus (San Cristobal) through 30 degrees of arc (Packham, 1973;

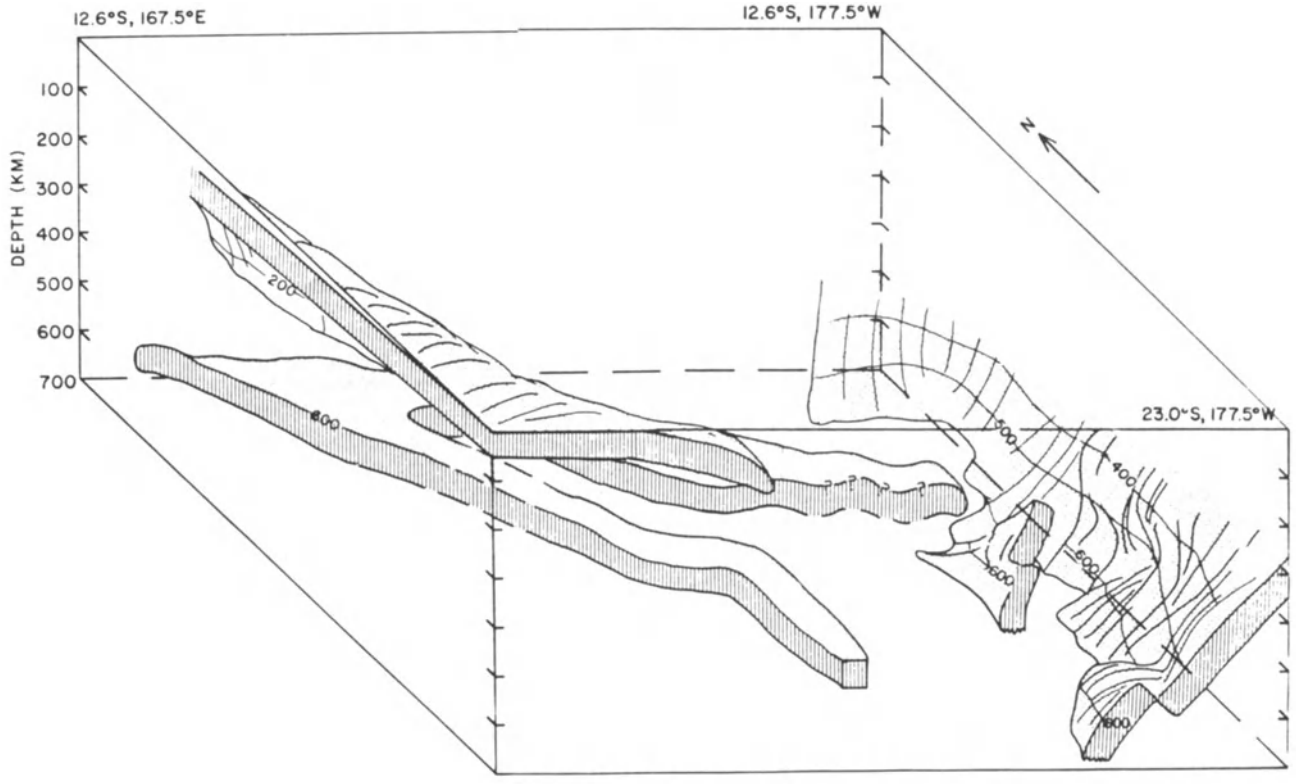

Figure 4. Three-dimensional representation of subducted lithosphere in the North Fiji Basin as viewed from the south, looking north. The relative positions of the slabs are based on observed seismicity; slab thicknesses are arbitrary. The deformation of the deep Tonga slab has been simplified (smoothed); it was not possible to include all of the very small lateral offsets in the slab.

Falvey, 1978). The subducting slab may have been effectively anchored in the upper mantle (Tullis, 1972) and hence broke off—unable to halt the migration of the trench southward and unable to move laterally fast enough to keep pace with the rotation of the trench axis.

The presence of the deep slab has some further implications for the region in general. The presence of both south-southwest and west-dipping Wadati-Benioff zones in northern Tonga (Figure 1) is evidence of a change in subduction direction in the 350-700 km depth region (Figure 1). Dupont (1982) suggested that the apparent change in dip direction is a result of the subduction of the Louisville Ridge. However, as Billington points out, the bend in the deep lithosphere formed in material which was subducted no earlier than 5 Ma. Hence, the major impact of the Louisville Ridge on subduction appears to be limited to shoaling of the trench axis and production of a relatively aseismic region. If the change in subduction direction did not coincide with a change in the direction of convergence between the Pacific and Indo-Australian Plates and is not due to subduction of the Louisville Ridge, what did produce the bend in the lithosphere at depth? Billington (1980, figure 17a) found that several epicenters located within the concave side of the bend, in the deep contours (see Figure 1) at about 19°S and about 150 km away from the Tonga deep seismicity, do not fit the pattern of seismicity described by the Wadati-Benioff zone contours. It is possible that these earthquakes originate in Indo-Australian lithosphere, subducted earlier at the New Hebrides Trench, and that deep Pacific lithosphere, subducted later at the Tonga Trench, has collided with the deep detached segment and has deformed around it. Figure 4 illustrates this possibility.

The deep slab segments may act as a physical barrier per se, or their position in the upper mantle may represent a depth limit to sinking slabs. Either situation is consistent with observations of seismic phases in the region. Observations of deep reflected phases in the Tonga area (Mitronovas and Isacks, 1971; Sondergeld et al., 1977; Frolich and Barazangi, 1980; Bock, 1981; and Fischer et al., 1986) provide conflicting evidence for lithosphere which has penetrated below 670 km. That the deepest parts of the Tonga slab appear to be partly deformed and/or detached and displaced laterally suggests difficulty in penetrating the mantle beyond the "670-km discontinuity" (Giardini and Woodhouse, 1984). Tomography studies (Dziewonski and Anderson, 1984), although controversial, show a very cool upper mantle (about 500 km) above a relatively hot lower mantle (about 2500 km), implying that there is some barrier in this region both to whole-mantle convection and to thermal diffusion. Further, because there are active spreading segments directly above the relict slab segments, back-arc spreading in this region must necessarily be the result of very shallow convection, possibly initiated by the relative movement of the plates themselves.

REFERENCES

Barazangi, M., B. Isacks, J. Oliver, J. Dubois, and G. Pascal, 1973, Descent of lithosphere beneath New Hebrides, Tonga-Fiji and New Zealand: Evidence for detached slabs: Nature, v. 242, p. 98-101.

Billington, S., 1980, The morphology and tectonics of the subducted lithosphere in the Tonga-Fiji-Kermadec region from seismicity and focal mechanism solutions. Unpublished Ph.D. Dissertation, Cornell University, Ithaca, New York, 128 p.

Bock, G., 1981, The effect of the descending lithosphere beneath Tonga island arc on P-wave travel-time residuals at the Warramunga Seismic Array: Physics of the Earth and Planetary Interiors, v. 25, p. 360-370.

Brocher, T., and R. Holmes, 1985, Tectonic and geochemical framework of the Northern Melanesian Borderland: An overview of the KK820316 Leg 2 objectives and results, in T.M. Brocher, ed., Geological Investigations of the Northern Melanesian Borderland, Earth Science Series, v. 3: Houston, TX, Circum-Pacific Council for Energy and Mineral Resources, p. 1-12.

Carney, J.N., and A. Macfarlane, 1982, Geological evidence bearing on the Miocene to Recent structural evolution of the New Hebrides Arc: Tectonophysics, v. 87, p. 147-175.

Chase, C.G., 1971, Tectonic history of the Fiji Plateau: GSA Bulletin, v. 82, p. 3087-3110.

Coleman, P.J., and G.H. Packham, 1976, The Melanesian Borderlands and Indian-Pacific plates boundary, Earth-Science Reviews, v. 12, p. 197-233.

Colley, B., and W.H. Hindle, 1984, Volcano-tectonic evolution of Fiji and adjoining marginal basins, in B.P. Kokelaar and M.F. Howells, eds., Marginal Basin Geology: Volcanic and associated sedimentary and tectonic processes in modern and ancient marginal basins: The Geological Society Special Publication No. 16,

Dubois, J., G. Pascal, M. Barazangi, B. Isacks, and J. Oliver, 1973, Travel times of seismic waves between New Hebrides and Fiji Islands: A zone of low velocity beneath the Fiji Plateau: Journal of Geophysical Research, v. 78, p. 3431-3436.

Dubois, J., J. Launay, J. Recy, and J. Marshall, 1977, New Hebrides Trench: Subduction rate from associated lithospheric bulge: Canadian Journal of Earth Science, v. 14, p. 250-255.

Dupont, J., 1982, Morphologie et structures superficielles de l'arc insulaire des Tonga-Kermadec: In Equipe Geologie-Geophysique ORSTOM Noumea, Contribution a l'etude geodynamique du Sud-Ouest Pacifique: Travaux et Documents ORSTOM, v. 147, p. 262-283.

Dziewonski, A.M., and D.L. Anderson, 1984, Seismic tomography of the earth's interior: American Scientist, v. 72, p. 4983-494.

Falvey, D., 1975, Arc reversals and a tectonic model for the North Fiji Basin: Australian Society of Exploration Geophysicists Bulletin, v. 6, p. 47-49.

Falvey, D., 1978, Analysis of palaeomagnetic data from the New Hebrides: Australian Society of Exploration Geophysicists Bulletin, v. 9, p. 117-123.

Fischer, K.M., K.C. Creager, and T.H. Jordan, 1986, Mapping the Tonga slab: Eos, Transactions American Geophysical Union, v. 67, p. 381.

Frolich, C., and M. Barazangi, 1980, A regional study of mantle velocity variations beneath eastern Australian and the southwestern Pacific using short-period recordings of P, S, PcP, ScP and ScS waves produced by Tonga deep earthquakes: Physics of the Earth and Planetary Interiors, v. 21, p. 1-14.

Gill, J.B., 1970, Geochemistry of Viti Levu, Fiji and its evolution as an island arc: Contributions to Mineralogy and Petrology, v. 27, p. 179-203.
Gill, J.B., 1976, From island arc to oceanic islands; Fiji, southwestern Pacific: Geology, v. 4, p. 123–126.
Gill, J.B., and M. Gorton, 1973, A proposed geological and geochemical history of eastern Melanesia, in P.J. Coleman, ed., The Western Pacific: Island Arcs, Marginal Seas, Geochemistry: University of Western Australia Press, Nedlands, p. 543-566.
Halunen, A.J., 1979, Tectonic history of the Fiji Plateau: Ph.D. Dissertation, University of Hawaii, Honolulu, Hawaii, 127 p.
Hamburger, M., and B. Isacks, 1985, Deep earthquakes in the Southwest Pacific: Morphology and tectonic history: Earthquake Notes, v. 55, p. 32.
Hamburger, M.W., and B.L. Isacks, Shallow seismicity in the North Fiji Basin: this volume.
Hanus, V., and J. Vanek, 1981, Plate tectonic interpretation of deep earthquakes between the Tonga- Lau and New Hebrides subduction zones: Tectonophysics, v. 75, p. T19–T28.
Hanus, V., and J. Vanek, 1983, Deep structure of the Vanuatu (New Hebrides) island arc: Intermediate depth collision of subducted lithospheric plates: New Zealand Journal of Geology and Geophysics, v. 26, p. 133–154.
Isacks, B., and P. Molnar, 1971, Distribution of stresses in the descending lithosphere from a global survey of focal mechanism solutions of mantle earthquakes: Reviews of Geophysics and Space Physics, v. 9, p. 103–174.
Isacks, B., L. Sykes, and J. Oliver, 1967, Spatial and temporal clustering of deep and shallow earthquakes in the Fiji-Tonga-Kermadec region: Bulletin of the Seismological Society of America, v. 57, p. 935–958.
Johnson, T., and P. Molnar, 1972, Focal mechanisms and plate tectonics of the Southwest Pacific: Journal of Geophysical Research, v. 77, p. 5000–5032.
Karig, D.E., 1970, Ridges and basins of the Tonga-Kermadec island arc system: Journal of Geophysical Research, v. 75, p. 239–254.
Karig, D.E., 1971, Origin and development of marginal basins in the Western Pacific: Journal of Geophysical Research, v. 76, p. 2542–2562.
Karig, D., and J. Mammerickx, 1972, Tectonic framework of the New Hebrides island arc: Marine Geology, v. 12, p. 187–205.
Kellogg, J.N., and D.R. Kansakar, Gravity field of the North Fiji Basin: this volume.
Kroenke, L.W., 1984, Cenozoic Tectonic Development of the Southwest Pacific: U.N. ESCAP, CCOP/SOPAC Technical Bulletin No. 6, 126 p.
Kroenke, L.W., J.M. Resig, and P. Cooper, 1986, Tectonics of the Southeastern Solomon Islands: Formation of the Malaita Anticlinorium, in J.G. Vedder, K.S. Pound, and S.Q. Boundy, eds., Geology and Offshore Resources of Pacific Island Arc—Central and Western Solomon Islands, Earth Science Series, v. 4: Houston, TX, Circum-Pacific Council for Energy and Mineral Resources, p. 109–116.
Louat, R., J. Daniel, and B. Isacks, 1982, Sismicite de l'arc des Nouvelles Hebrides: In Equipe Geologie-Geophysique ORSTOM Noumea, Contribution a l'etude geodynamique du Sud-Ouest Pacifique: Travaux et Documents ORSTOM, v. 147, p. 111–148.
Louat, R., and J. Dupont, 1982, Sismicite de l'arc des Tonga-Kermadec: In Equipe Geologie-Geophysique ORSTOM Noumea, Contribution a l'etude geodynamique du Sud-Ouest Pacifique: Travaux et Documents ORSTOM, v. 147, p. 299–318.
MacDonald, K.C, B.P. Luyendyk, and R.P. von Herzen, 1973, Heat flow and plate boundaries in Melanesia: Journal of Geophysical Research, v. 78, p. 2537–2546.
Malahoff, A., S.R. Hammond, J.J. Naughton, D.L. Keeling, and R.N. Richmond, 1982, Geophysical evidence for post-Miocene rotation of the island of Viti Levu, Fiji, and its relationship to the tectonic development of the North Fiji Basin: Earth and Planetary Science Letters, v. 57, p. 398–414.
Mitronovas, W., and B.L. Isacks, 1971, Seismic velocity anomalies in the upper mantle beneath the Tonga-Kermadec island arc: Journal of Geophysical Research, v. 76, p. 7154–7180.
Neef, H., 1982, Plate tectonic significance of late Oligocene/early Miocene deep sea sedimentation at Maewo, Vanuatu (New Hebrides): Tectonophysics, v. 87, p. 177–183.
Oliver, J., B. Isacks, M. Barazangi, and W. Mitronovas, 1973, Dynamics of the downgoing lithosphere: Tectonophysics, v. 19, p. 133–147.
Packham, G.H., 1973, A speculative Phanerozoic history of the Southwest Pacific, in P.J. Coleman, ed., The Western Pacific: Island Arcs, Marginal Seas, Geochemistry: University of Western Australia Press, Nedlands, p. 369–388.
Packham, G.H., 1982, Foreword to paper on Tectonics of the Southwest Pacific region, in The Evolution of the India-Pacific Plate Boundaries: Tectonophysics, v. 87, p. 1–10.
Packham, G.H., and J.E. Andrews, 1975, Results of Leg 30 and the geologic history of the Southwest Pacific Arc and marginal sea complex: Initial Reports of the Deep Sea Drilling Project: v. 30, p. 691–705.
Packham, G.H., and D. Falvey, 1971, An hypothesis for the formation of marginal seas in the Western Pacific: Tectonophysics, v. 11, p. 79–109.
Pascal, G., J. Dubois, M. Barazangi, B. Isacks, and J. Oliver, 1973, Seismic velocity anomalies beneath the New Hebrides Island Arc: Evidence for a detached slab in the upper mantle: Journal of Geophysical Research, v. 78, p. 6998–7004.
Pascal, G., B.L. Isacks, M. Barazangi, and J. Dubois, 1978, Precise locations of earthquakes and seismotectonics of the New Hebrides island arc: Journal of Geophysical Research, v. 83, p. 4957–4973.
Rodda, P., and L.W. Kroenke, 1984, Fiji: A fragmented arc: in L.W. Kroenke, Cenozoic Tectonic Development of the Southwest Pacific: U.N. ESCAP, CCOP/SOPAC Technical Bulletin, No. 6, p. 87–109.
Sclater, J.G., U.G. Ritter, and F.S. Dixon, 1972, Heat flow in the southwestern Pacific: Journal of Geophysical Research, v. 77, p. 5697–5704.
Sinton, J.M., R.C. Price, K.T.M. Johnson, H. Staudigel, and A. Zindler, Petrology and geochemistry of submarine lavas from the Lau and North Fiji basins: this volume.
Solomon, S., and S. Biehler, 1969, Crustal structure from gravity anomalies in the Southwest Pacific: Journal of Geophysical Research, v. 74, p. 6696–6701.
Sondergeld, C.B., B.L. Isacks, M. Barazangi, and S. Billington, 1977, A search for velocity anomalies near the deep portions of the inclined seismic zone of Tonga island arc: Bulletin of the Seismological Society of America, v. 67, p. 537–541.
Sykes, L.R., 1964, Deep focus earthquakes in the New Hebrides region: Journal of Geophysical Research, v. 69, p. 5353–5355.
Tullis, T.E., 1972, Evidence that lithosphere slabs act as anchors (Abstract): Eos, Transactions of the American Geophysical Union, v. 53, p. 522.
Watts, A.N., M.G. Kogan, J. Mutter, G.D. Karner, and F.J. Davey, 1981, Free-air gravity field of the Southwest Pacific Ocean, Geological Society of America map, MC-42.

This is SOEST Contribution no. 1752.

Kroenke, L.W., and J.V. Eade, editors, 1993, Basin Formation, Ridge Crest Processes, and Metallogenesis in the North Fiji Basin: Houston, TX, Circum-Pacific Council for Energy and Mineral Resources, Earth Science Series, Vol. 15, Springer-Verlag, New York.

GRAVITY FIELD OF THE NORTH FIJI BASIN

JAMES N. KELLOGG[1]
Hawaii Institute of Geophysics, School of Ocean and Earth Science and Technology
University of Hawaii, Honolulu, Hawaii 96822

and

DIBYA R. KANSAKAR
Department of Mines and Geology, Kathmandu, Kingdom of Nepal

ABSTRACT

New computer-contoured free-air and Bouguer gravity anomaly maps have been prepared for the North Fiji Basin. The regional gravity gradient is associated with a long wavelength gravity bulge probably caused by the downgoing dense lithosphere at the New Hebrides Trench. The South Pandora (Hazel Holme) Ridge is characterized by an axial valley 1-2 km deep and 10-20 km wide. The free-air gravity anomalies reflect the bathymetry with 40-90 mgal lows over the axial valleys. Low relative Bouguer anomalies indicate that three seamounts on the South Pandora Ridge were erupted at or near a ridge crest. The axial valley and symmetrical gravity and bathymetry suggest that slow spreading may have formed the South Pandora Ridge. Active spreading is indicated by extensional earthquake focal mechanisms, the lack of sediments, and the discovery of fresh pillow basalts in the axial valley. If this interpretation is correct, some spreading is occurring normal to the arc, raising questions about the basic processes involved in back-arc spreading.

INTRODUCTION

The North Fiji Basin (Plateau) is a back-arc basin located between the New Hebrides Arc and Fiji (Figure 1). Active spreading in the basin is indicated by high seismicity, low sediment cover, and high heat flow (Isacks et al., 1969; Chase, 1971; Sclater et al., 1972; Macdonald et al., 1973; Barazangi et al., 1974; Halunen, 1979; Hamburger and Isacks, this volume). Active spreading is also inferred from magnetic anomalies and fresh basalts associated with the ridges (Chase, 1971; Cherkis, 1980; Malahoff et al., 1982; Malahoff et al., this volume; Kroenke et al., this volume). Seismic waves that originate in or cross the central North Fiji Basin are also highly attenuated (Barazangi and Isacks, 1971; Dubois et al., 1973). Most tectonic interpretations of the basin are based on magnetic data and involve back-arc spreading at ridges aligned approximately parallel to the New Hebrides Arc (Falvey, 1978; Halunen, 1979; Cherkis, 1980; Malahoff et al., 1982). The axis of the South Pandora (Hazel Holme) Ridge (Figure 1) is approximately normal to the New Hebrides Arc, and the ridge has generally been interpreted as a fracture zone (Chase, 1971; Macdonald et al. 1973). However, underway geophysical data collected aboard the Hawaii Institute of Geophysics R/V KANA KEOKI in 1982 prompted us to re-examine the tectonics of the North Fiji Basin and re-interpret the origin of the South Pandora Ridge.

[1]Now at Department of Geological Sciences, University of South Carolina, Columbia, SC 29208

Figure 1. Location map of the study area. Bathymetry from Kroenke et al. (1983).

GRAVITY FIELD

No detailed map of the gravity field of the North Fiji Basin has been published prior to this study. Some of the earlier gravity data have been included in regional compilations by Watts et al., (1981) and Bowin et al., (1982). The South Pandora Ridge and the area 300 km south of the ridge were surveyed by the R/V KANA KEOKI in 1971, 1972, and 1982. Gravity measurements were made with a Lacoste-Romberg gravity meter mounted on a gyrostabilized platform. The estimated accuracy of the measurements is ±3.0 mgal. The measurements were corrected for instrument drift and reduced to free-air anomalies (Figure 2) using the 1967/71 International Gravity formula (IAG, 1971). Simple Bouguer anomalies were also calculated with a density of 2.0 g/cm^3 for the mass correction (Figure 3). By removing topographic effects, Bouguer anomalies reveal lateral density variations in the crust and upper mantle. To calculate simple marine Bouguer anomalies, at each observation point add the gravitational attraction of an infinite horizontal slab (with density equal to that of rock minus water, and thickness equal to the water depth beneath the point) to the free-air anomaly at the point. The rock density used for Figure 3 (2.0 g/cm^3) is appropriate for marine sediments but is lower than the densities of most submarine volcanic features, such as seamounts (2.6 ± 0.3 g/cm^3, Kellogg and Ogujiofor, 1985). By underestimating the rock density, excessive Bouguer corrections and overestimates of lateral density variations were precluded. The free-air and Bouguer gravity anomalies were interpolated to 2500 and 8100 rectangular grid points located approximately 10 and 6 km apart, respectively. The relative degree of spline versus Laplacian interpolation was adjusted to smooth the data while minimizing spurious peaks. The Bouguer data were more heavily smoothed than the free-air data. Finally the gridded data were digitally contoured at 5-mgal contour intervals (Figures 2 and 3). It should be noted that the computer contouring tended to close the isogals, resulting in a less linear pattern than hand contouring would have achieved.

Interesting features of the free-air anomaly map (Figure 2) include

(1) A regional gradient. Average free-air anomaly values decrease 30 to 35 mgal from the western border of the map area to the eastern border.

(2) Clearly defined en echelon ENE-trending relative gravity lows flanked by symmetrical gravity highs are located in the northwestern part of the map area from 13.5 to 14.0°S. The symmetrical anomalies coincide with the position of the South Pandora Ridge.

(3) A relative gravity low in the center of the map at 15.0°S is flanked by poorly defined relative highs.

The Bouguer anomaly map (Figure 3) shows features similar to the free-air maps, including

(1) A regional gradient with values decreasing 35 to 40 mgal from west to east.

(2) A relative Bouguer gravity low trends ENE between latitudes 13.5 and 14.0°S. The low values coincide with seamounts on the South Pandora Ridge. However, there are no Bouguer anomaly patterns associated with the ridge itself.

Regional Gravity Field

Although the seafloor is approximately 400 m shallower on the eastern border of the map area (175°E) than on the western border (171°E) (Kroenke et al., this volume), the free-air gravity anomalies to the east are 30-35 mgal lower than the anomalies to the west. As a result, the average Bouguer anomalies to the east are 35-40 mgal lower than those to the west. The regional gravity gradient is approximately 0.06-0.08 mgal/km. The free-air gravity gradient corresponds to a gradient observed in the geoid based on GEOS 3 satellite altimetry data (Collot and Malahoff, 1982). The geoid anomaly expresses the amplitude of deformation of the equipotential surface of the oceans with respect to a reference ellipsoid. The geoid anomalies, like the free-air anomalies, are caused by heterogeneous distribution of mass within the earth. A strong positive bulge of the geoid (+71 m) is located at the southwest corner of the map area (Figures 2 and 3) east of the islands of Vate', Erromango, and Tanna. The geoid anomaly decreases to +60 m at the northeast corner of the map area.

Collot and Malahoff (1982) attributed the long wavelength gravity bulge to the gravimetric effect of the slab subducted at the New Hebrides Trench. Hatherton (1970), Grow (1973), Grow and Bowin (1975), and Sager (1980) analyzed the gravity effect of the subducted lithosphere at the Hikurangi, Aleutian, Chile, and Mariana trenches respectively. Collot and Malahoff (1982) calculated that a downgoing dense slab with a density contrast of 0.06 g/cm^3 would produce a gravity anomaly of about 80 mgal with a wavelength of 1000 km. The difference between the predicted gradient of about 0.16 mgal/km and the observed gradient of 0.06-0.08 mgal/km in the map area may be caused by crustal thinning to the east (Solomon and Biehler, 1969).

SOUTH PANDORA RIDGE

The South Pandora (Hazel Holme) Ridge has been commonly interpreted as a fracture zone (Chase, 1971; Macdonald et al., 1973). To investigate this interpretation, we examined the gravity and bathymetric data col-

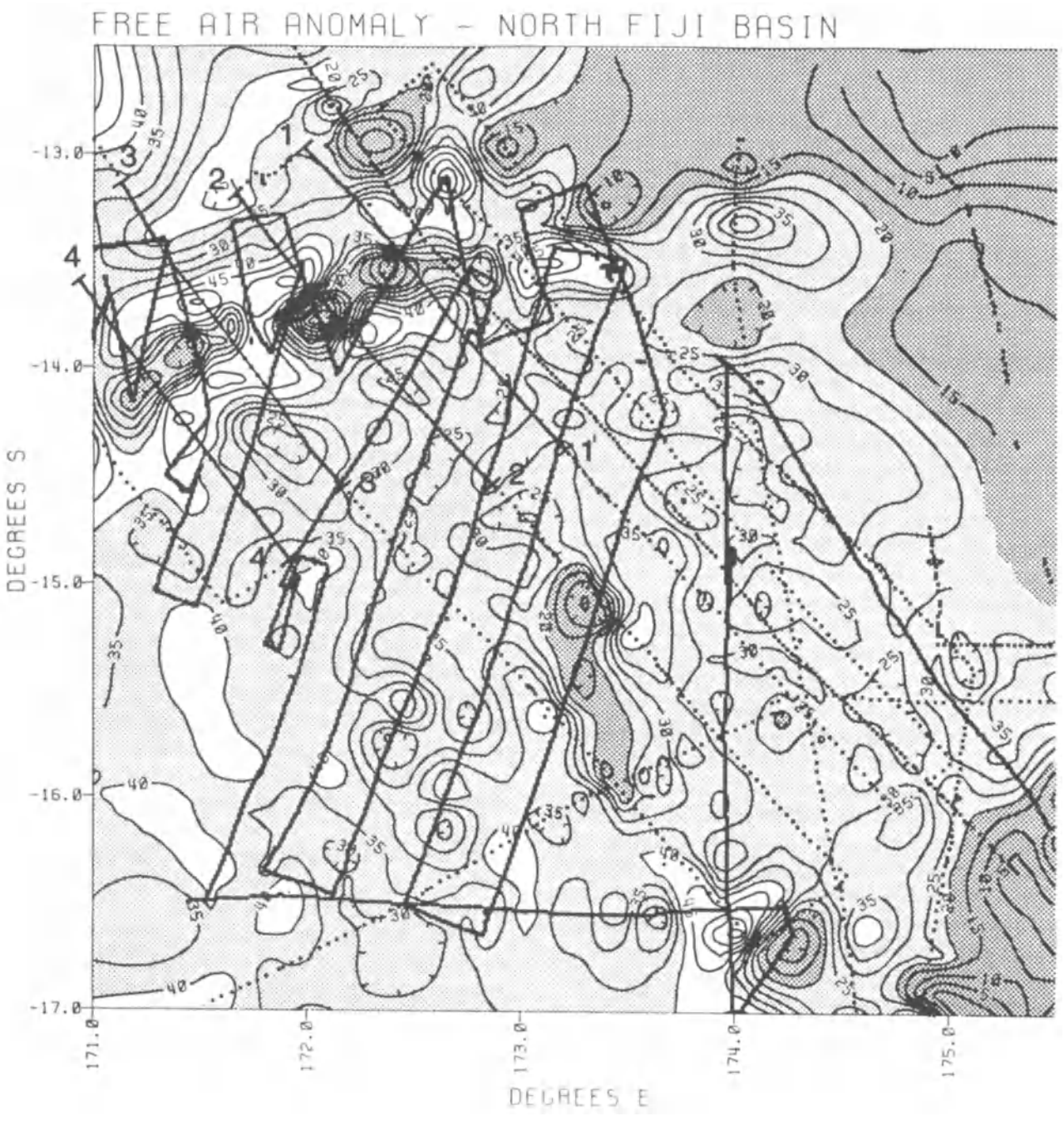

Figure 2. Free-air gravity anomaly map of the North Fiji Basin. Contour interval = 5 mgal. Dark pattern: < 20 mgal; light pattern: 20–40 mgal; white: > 40 mgal. Dots show station locations. Numbers indicate location of four profiles shown in Figure 4.

lected aboard the Hawaii Institute of Geophysics R/V KANA KEOKI in 1971 and 1982. Free-air gravity anomaly and bathymetric profiles from four traverses of the South Pandora Ridge are shown in Figure 4. All the bathymetric profiles are characterized by axial valleys 1-2 km deep and 10-20 km wide (Figure 4). The valleys are flanked by symmetrical ridges that slope away from the axis, dropping about 1000 m in 100 km. The free-air gravity profiles reflect the bathymetry directly. The relative gravity lows over the axial valleys vary from 40 to 90 mgal.

While it does not preclude strike-slip faulting, the symmetry of the gravimetric and bathymetric profiles prompted us to compare them to profiles of known spreading ridges. Figure 5 shows typical profiles of the East Pacific Rise and the Mid-Atlantic Ridge. The free-air gravity anomaly and bathymetric profile for the East Pacific Rise were projected normal to the rise axis at about 6°S (Madsen et al., 1984). The profile for the Mid-Atlantic Ridge is the average symmetric component of five profiles between 14°10'N and 14°40'N (Parmentier and Forsyth, 1985; Collette et al., 1980).

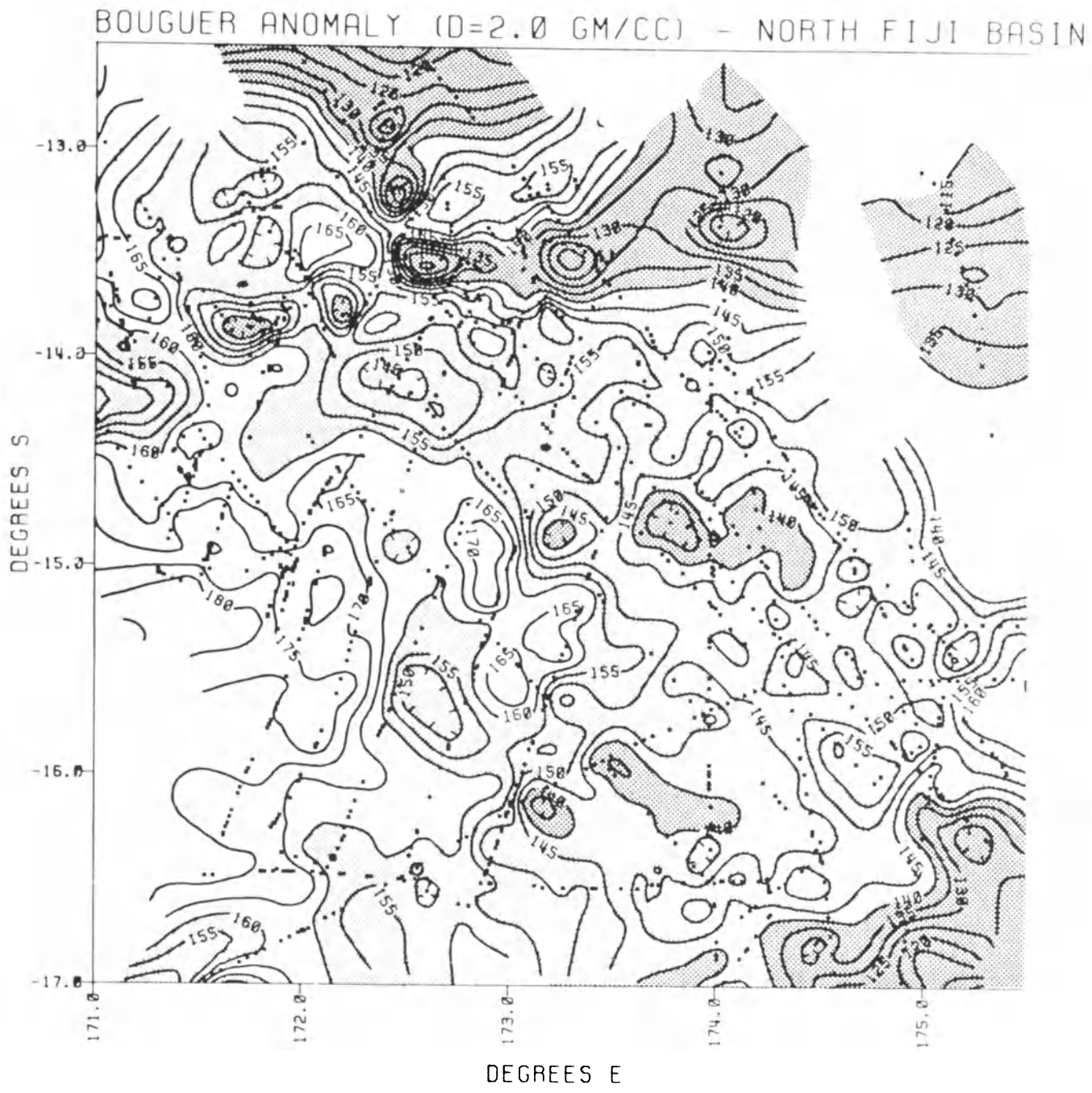

Figure 3. Bouguer gravity anomaly map of the North Fiji Basin (density = 2.0 g/cm^3). Contour interval = 5 mgal. Dark pattern: < 140 mgal; light pattern: 140–160 mgal; white: > 160 mgal. Dots show station locations.

Slow spreading ridges (10-20 mm/yr), such as the Mid-Atlantic Ridge, are characterized by an axial valley 10-15 km wide and 1-3 km deep, which is absent on faster spreading ridges such as the East Pacific Rise (Macdonald, 1982). The general similarity between the profiles for the South Pandora and the Mid-Atlantic ridges is evident. Both ridges have similar axial valleys and gravity anomalies of the same shape and magnitude.

Evidence for recent spreading on South Pandora Ridge is the lack of sediment on the ridges and valley and fresh pillow lobes that were photographed on the valley floor (Kroenke et al., this volume). In addition, earthquake focal mechanism solutions indicate extension normal to the South Pandora (Hazel Holme) Ridge (Hamburger and Isacks, this volume). Bouguer gravity coverage is available for three seamounts on the South Pandora Ridge. One is located at 171°48'E in the axial valley; the others are located at 173°20'E and at 174°5'E (Kroenke et al., this volume). All three seamounts are characterized by relative free-air anomaly highs, but by relative Bouguer anomaly (density = 2.0 g/cm^3) lows. Thus, there is a mass deficit associated with the

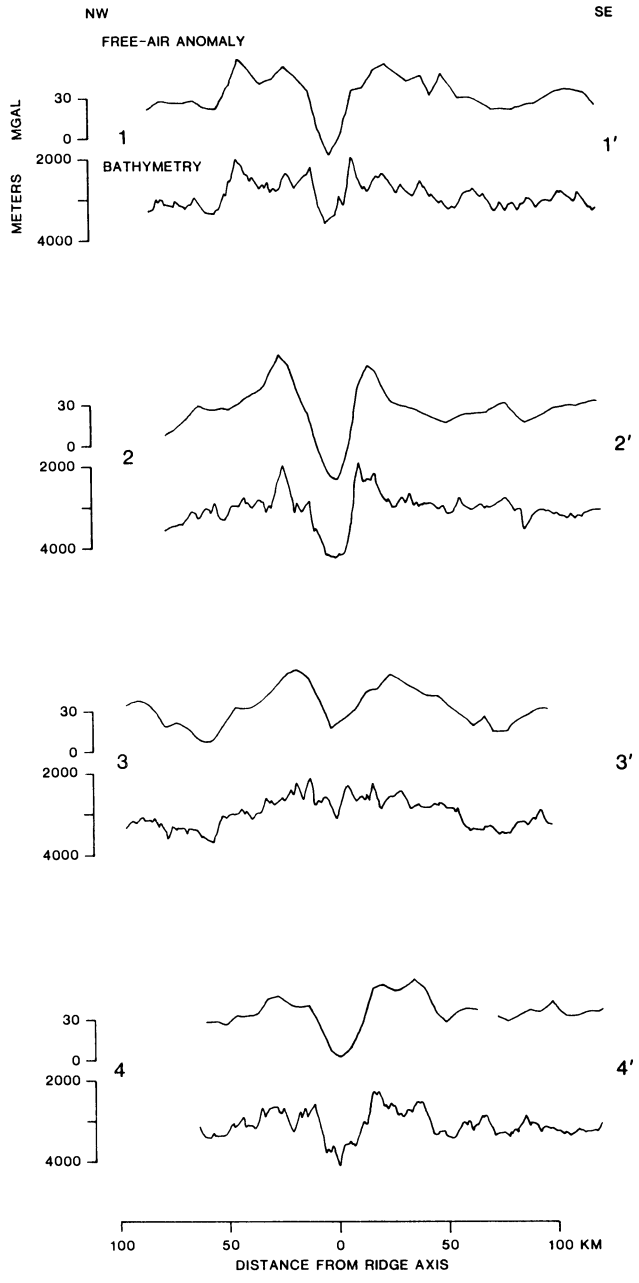

Figure 4. Gravity and bathymetry profiles across South Pandora Ridge. Locations are shown in Figure 2.

seamounts, suggesting that they are to a large extent locally isostatically compensated. As oceanic lithosphere moves away from a ridge crest, it cools and thickens so that its effective elastic thickness is increased. Seamounts formed on young seafloor near ridge crests are often associated with short wavelength, low amplitude gravity anomalies, local isostatic compensation, and thin effective elastic lithosphere thicknesses (Kellogg and Ogujiofor, 1985). Thus, we conclude that the three seamounts surveyed on South Pandora Ridge were formed on a thin elastic plate near a ridge crest. Furthermore, Holocene basalts, pillow lavas, and sheet flow fragments were dredged from the small volcano within the axial valley at 171°148'E (Sinton et al., this volume).

DISCUSSION

The long wavelength gravity field in the North Fiji Basin is dominated by the effect of the rapidly subducting dense lithosphere at the New Hebrides Trench.

The most prominent short wavelength features of the gravity field are associated with the South Pandora Ridge where the axial valley, the bathymetric symmetry, the lack of sediment, and earthquake focal mechanism solutions suggest slow spreading. Unlike most back-arc ridges, however, the South Pandora Ridge is almost perpendicular to the arc. Models to explain back-arc basin formation include mantle diapirism, induced asthenospheric convection, and global plate kinematics (Taylor and Karner, 1983). Because the proposed driving mechanism for the first two models is the subducting slab, these models do not explain spreading parallel to the arc such as the formation of new crust at the South Pandora Ridge.

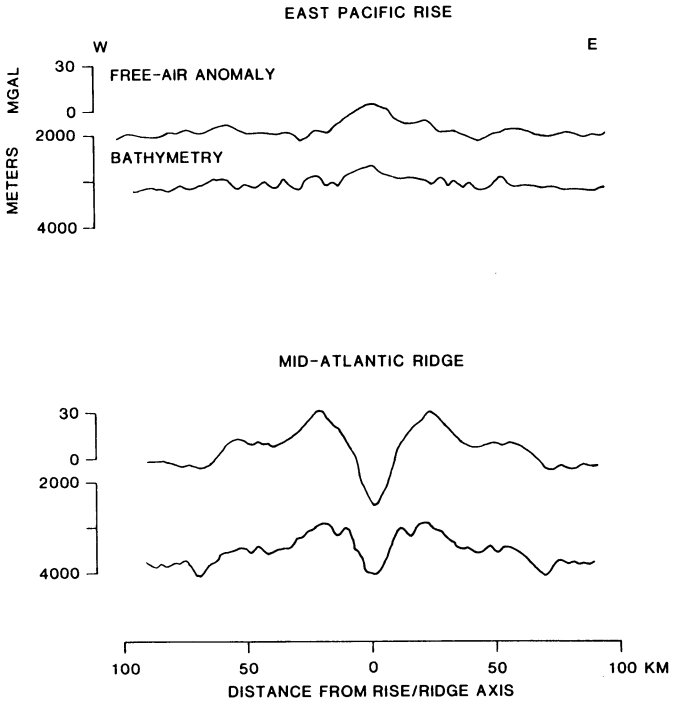

Figure 5. Typical gravity and bathymetry profiles from the East Pacific Rise and the Mid-Atlantic Ridge. The profile for the East Pacific Rise was projected normal to the rise axis at about 6°S (Madsen et al., 1984). The profile for the Mid-Atlantic Ridge is the average symmetric component of five profiles between 14°10'N and 14°40'N (Parmentier and Forsyth, 1985).

On the southeastern border of the map area (Figures 2 and 3) at 17°S, 174°E, the Fiji transform fault intersects a south-trending spreading ridge (Brocher, 1985). Earthquake focal mechanisms indicate that the Fiji transform is accommodating rapid spreading on the ridge with left-lateral movement (Hamburger and Isacks, this volume). Malahoff et al. (1982) estimated a full spreading rate of 7 cm/yr on the ridge south of the Fiji transform at the time of magnetic anomaly 4.

Between the Fiji transform fault and South Pandora Ridge, the basin kinematics are not well established, however. A relative free-air gravity low has been noted at 15°S in the center of the map area (Figure 2). The low is flanked by two relative highs and may continue to 17°S although the computer contouring closed the feature at 16°S. The gravity low at 15°S corresponds to a 4-km-deep basin where three structural trends intersect (Kroenke et al., this volume) and may represent the tip of a northward propagating rift. The kinematics of the North Fiji Basin are probably in a period of active reorientation. Further shipboard studies, particularly utilizing side-looking sonar, will be needed to determine the present tectonic configuration of the basin.

ACKNOWLEDGMENTS

The authors wish to thank L. Kroenke, B. Taylor, and J.Y. Collot for providing many insights into the tectonic interpretation of the data. The manuscript was improved after helpful reviews by B. Davy and L. Kroenke. R. Lukas and D. Hills supplied the revised program used to grid and contour the gravity data. O. Athens provided considerable help with the computations and prepared Figures 4 and 5. R. Rhodes assisted in preparation of the figures, and the manuscript was typed by A. Leong. SOEST Contribution No. 1753.

REFERENCES

Barazangi, M., and B.L. Isacks, 1971, Lateral variations of seismic wave attenuation in the upper mantle above the inclined zone of the Tonga island arc: Deep anomaly in the upper mantle: Journal of Geophysical Research v. 76, p. 8493- 8516.

Barazangi, M., B. Isacks, J. Dubois, and G. Pascal, 1974, Seismic wave attenuation in the upper mantle beneath the Southwest Pacific: Tectonophysics, v. 24, p. 1- 12.

Bowin, C., W. Warsi, and J. Milligan, 1982, Free-air gravity anomaly atlas of the world: GSA Map andChart, Series MC-46.

Brocher, T.M., 1985, On the formation of the Vitiaz Trench lineament and North Fiji Basin, in T.M. Brocher, ed., Geological Investigations of the Northern Melanesian Borderland, Earth Sciences Series, v. 3: Houston, TX, Circum-Pacific Council for Energy and Mineral Resources, p. 13-34.

Chase, C.G., 1971, Tectonic history of the Fiji Plateau: GSA Bulletin, v. 82, p. 3087-3110.

Cherkis, N.Z., 1980, Aeromagnetic investigations and sea floor spreading history in the Lau Basin and northern Fiji Plateau, in Symposium on Petroleum Potential in Island Arcs, Small Ocean Basins, Submerged Margins and Related Areas, Suva, Fiji, September 1979: U.N. ESCAP, CCOP/SOPAC Technical Bulletin, No. 3, p. 37-45.

Collette, B. J., J. Verhoef, and A. F. J. de Mulder, 1980, Gravity and a model of the median valley: Journal of Geophysics, v. 47, p. 91-98.

Collot, J.Y, and A. Malahoff, 1982, Gravimetric anomalies and structure of the New Hebrides subduction zone, In Equipe Geologie–eophysique ORSTOM Noumea, Contribution a l'etude geodynamique du Sud-Ouest Pacifique: Travaux et Documents de l'ORSTOM, v. 147, p. 91-109.

Dubois, J., G. Pascal, M. Barazangi, B.L. Isacks, and J. Oliver, 1973, Travel times of seismic waves between the New Hebrides and Fiji Islands: A zone of low velocity beneath the Fiji Plateau: Journal of Geophysical Research, v. 78, p. 3431-3436.

Falvey, D.A., 1978, Analysis of paleomagnetic data from the New Hebrides: Australian Society of Exploration Geophysicists Bulletin, v. 9, p. 117-123.

Grow, J.A., 1973, Crustal and upper mantle structure of the central Aleutian arc: GSA Bulletin, v. 84, p. 2169-2192.

Grow, J. A., and C.O. Bowin, 1975, Evidence for high-density crust and mantle beneath the Chile Trench due to the descending lithosphere: Journal of Geophysical Research, v. 80, p. 1449- 1458.

Halunen, A.J., 1979, Tectonic history of the Fiji Plateau: Unpublished Ph.D. Dissertation, University of Hawaii, Honolulu, Hawaii, 127 p.

Hamburger, M.W., and B.L. Isacks, Shallow seismicity in the North Fiji Basin, this volume.

Hatherton, T., 1970, Upper mantle inhomogeneity beneath New Zealand: Surface manifestations: Journal of Geophysical Research, v. 15, p. 369-384.

International Association of Geodesy, 1971, Geodetic Reference System 1967: Bulletin of Geodesy, Special Publication No. 3, 116 p.

Isacks, B., L.R. Sykes, and J. Oliver, 1969, Focal mechanisms of deep and shallow earthquakes in the Tonga-Kermadec region and the tectonics of island arcs: GSA Bulletin, v. 80, p. 1443-1470.

Kellogg, J.N., and I.J. Ogujiofor, 1985, Gravity field analysis of Sio Guyot: An isostatically compensated seamount in the Mid-Pacific Mountains: Geo-Marine Letters, v. 5, p. 91-97.

Kroenke, L.W., C. Jouannic, and P. Woodward, (comps.) 1983, Bathymetry of the Southwest Pacific, Chart 1 of the Geophysical Atlas of the Southwest Pacific: CCOP/SOPAC, Suva.

Kroenke, L.W., R. Smith, and K. Nemoto, Morphology and structure of the seafloor in the northern part of the North Fiji Basin, this volume.

Macdonald, K.C., 1982, Mid-ocean ridges: Fine scale tectonic, volcanic and hydrothermal processes within the plate boundary zone: Annual Review of Earth and Planetary Sciences, v. 10, p. 155-190.

Macdonald, K.C., B.P. Luyendyk, and R. P. von Herzen, 1973, Heat flow and plate boundaries in Melanesia: Journal of Geophysical Research, v. 78, p. 2537-2546.

Madsen, J. A., D. W. Forsyth, and R. S. Detrick, 1984, A new isostatic model for the East Pacific Rise crest: Journal of Geophysical Research, v. 89, p. 9997-10015.

Malahoff, A., R. H. Feden, and H. F. Fleming, 1982, Magnetic anomalies and tectonic fabric of marginal basins north of New Zealand: Journal of Geophysical Research, v. 87, p. 4109-4125.

Malahoff, A., L.W. Kroenke, N. Cherkis, and J. Brozena, Magnetic and tectonic fabric of the North Fiji Basin and Lau Basin, this volume.

Parmentier, E. M., and D. W. Forsyth, 1985, Three-dimensional flow beneath a slow spreading ridge axis: A dynamic contribution to the deepening of the median valley toward fracture zones: Journal of Geophysical Research, v. 90, p. 678-684.

Sager, W.W., 1980, Mariana arc structure inferred from gravity and seismic data: Journal of Geophysical Research, v. 85, p. 5382-5388.

Sclater, J. G., U. G. Ritter, and F. S. Dixon, 1972, Heat flow in the Southwestern Pacific: Journal of Geophysical Research, v. 77, p. 5697-5704.

Sinton, J.M., R.C. Price, K.T.M. Johnson, H. Staudigel, and A. Zindler, Petrology and geochemistry of submarine lavas from the Lau and North Fiji back-arc basins: this volume.

Solomon, S., and S. Biehler, 1969, Crustal structure from gravity anomalies in the Southwest Pacific: Journal of Geophysical Research, v. 74, p.6696-6701.

Taylor, B., and G.D. Karner, 1983, On the evolution of marginal basins: Reviews of Geophysics and Space Physics, v. 21, p.1727–1741.

Watts, A.B., M.G. Kogan, J. Mutter, G.D. Karner, and F.J. Davey, 1981, Free-air gravity field of the Southwest Pacific Ocean: GSA Map and Chart Series MC-42.

Kroenke, L.W., and J.V. Eade, editors, 1993, Basin Formation, Ridge Crest Processes, and Metallogenesis in the North Fiji Basin: Houston, TX, Circum-Pacific Council for Energy and Mineral Resources, Earth Science Series, Vol. 15, Springer-Verlag, New York.

MAGNETIC AND TECTONIC FABRIC OF THE NORTH FIJI BASIN AND LAU BASIN

ALEXANDER MALAHOFF and LOREN W. KROENKE
Hawaii Institute of Geophysics, School of Ocean and Earth Science and Technology
University of Hawaii, Honolulu, Hawaii 96822

NORMAN CHERKIS and JOHN BROZENA
Naval Research Laboratory, Washington, D.C.

ABSTRACT

Detailed airborne and shipboard magnetic studies conducted over the eastern marginal basins of the southwest Pacific between New Zealand and the Solomon Islands suggest that seafloor spreading in the North Fiji Basin, which began in the latest Miocene, continues today. The North Fiji Basin is marked by at least two triple junctions, located in the central (16°50'S, 173°45'E) and northeastern (14°S, 179°30'E) parts of the basin. Both were apparently formed during the past five million years in response to continuing adjustments in the strike of the active spreading centers in the North Fiji Basin. Two additional contemporary spreading centers appear to have formed within the last one million years to the north and immediately to the west of Viti Levu. Although magnetic anomalies from 1 to 3 (0–5 Ma) are seen to form a clearly defined lineation pattern over the North Fiji Basin, earthquake foci suggest that only portions of the present North Fiji/Lau Basin spreading center system are currently active.

Analysis of the magnetic anomalies suggests that spreading began in the North Fiji Basin about 8 Ma (shortly before anomaly 4). At about 6 Ma (shortly before anomaly 3), the New Hebrides/Fiji island arc began to fragment through the development of an active spreading center (calculated half-spreading rate of 3.5 cm/yr) located between the New Hebrides and Fiji portions of the island arc. Subsequently, portions of the northeastern sector of the South Fiji Basin Plain were subducted beneath the North Fiji Basin. Between 4.5 Ma and 3.5 Ma (anomalies 3 and 2'), spreading in the North Fiji Basin extended into the Lau Basin and Havre Trough, thus separating the Tonga and Lau ridges. As a result, a distinct series of active spreading centers developed southward along the axis of the Havre Trough/Lau Basin.

The continuum of spreading centers from the North Fiji Basin into the Lau Basin and Havre Trough has been accomplished through the formation of triple junctions located in the North Fiji and northern Lau basins and propagating southward rifts in the southern Lau Basin.

INTRODUCTION

A detailed aeromagnetic study was conducted between 1977 and 1980 over an extensive area between New Zealand, Fiji, Tonga, and Vanuatu to investigate the geological age and tectonic processes that are active in the marginal basins of this area north of New Zealand, as described earlier by Karig (1970, 1971). Early studies of the North Fiji (Chase, 1971) and Lau basins (Sclater et al., 1972; Lawver et al., 1976; and Watts et al., 1977a,b) have shown the presence of linear magnetic anomalies striking parallel to the general axial trend of the basin, a trend commonly disrupted by the presence of transform faults. Other studies by Weissel (1977) identified these anomalies as 1 to 2' (0 to 3.2 Ma in age). The youth of the Lau Basin, coupled with its apparent continuous

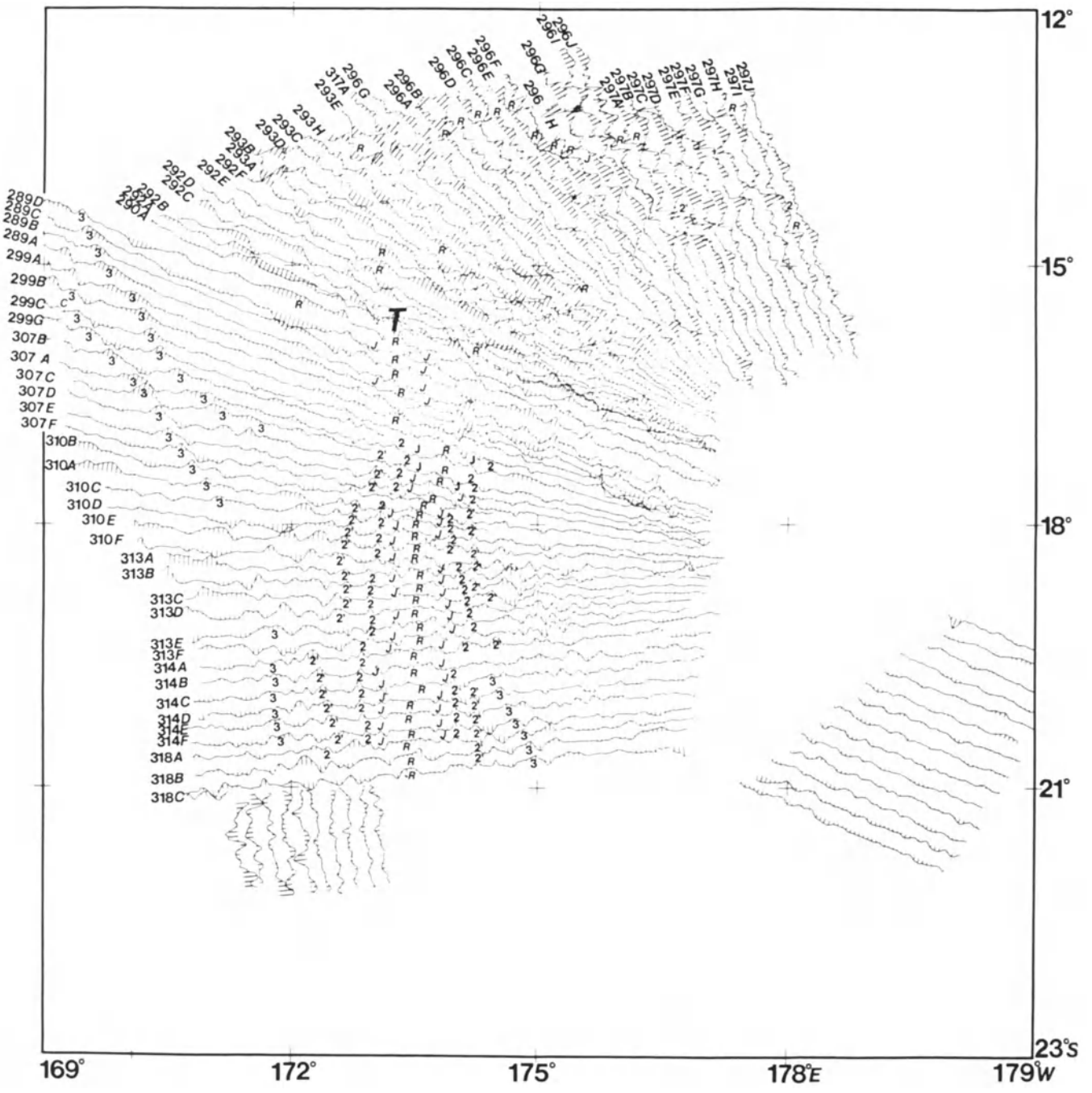

Figure 1. Location and flight number of residual magnetic anomaly profiles over the North Fiji Basin; R = ridge axis; magnetic anomalies identified by numbers. T marks the site of the currently active triple junction.

extension south into the Havre Trough (water depth 2.0-3.5 km), suggests a close geological link with the active central volcanic region of the North Island of New Zealand (Malahoff et al., 1982).

In order to extend these studies to other parts of the region, the authors, using a Naval Research Laboratory P3A Orion aircraft flying at an elevation of 300 m, obtained a sequence of aeromagnetic profiles over the region extending from the North Island of New Zealand to the islands of Fiji and across the North Fiji Basin (Cherkis et al., 1978, 1980; Cherkis, 1980; Malahoff et al., 1982). Tracks were flown radially out from Viti Levu across the Fiji and North Lau basins (Figures 1 and 2).. In other areas, tracks were flown perpendicular to tectonic features. Navigational control was maintained with twin Litton 72 inertial navigation systems. Cumulative errors at the end of the 10-hour flights did not exceed 1.1 km. Therefore, we estimate the average absolute navigation error in the detailed study areas as ± 0.2 km. A Geometrics Model 801/3 proton-precision mag-

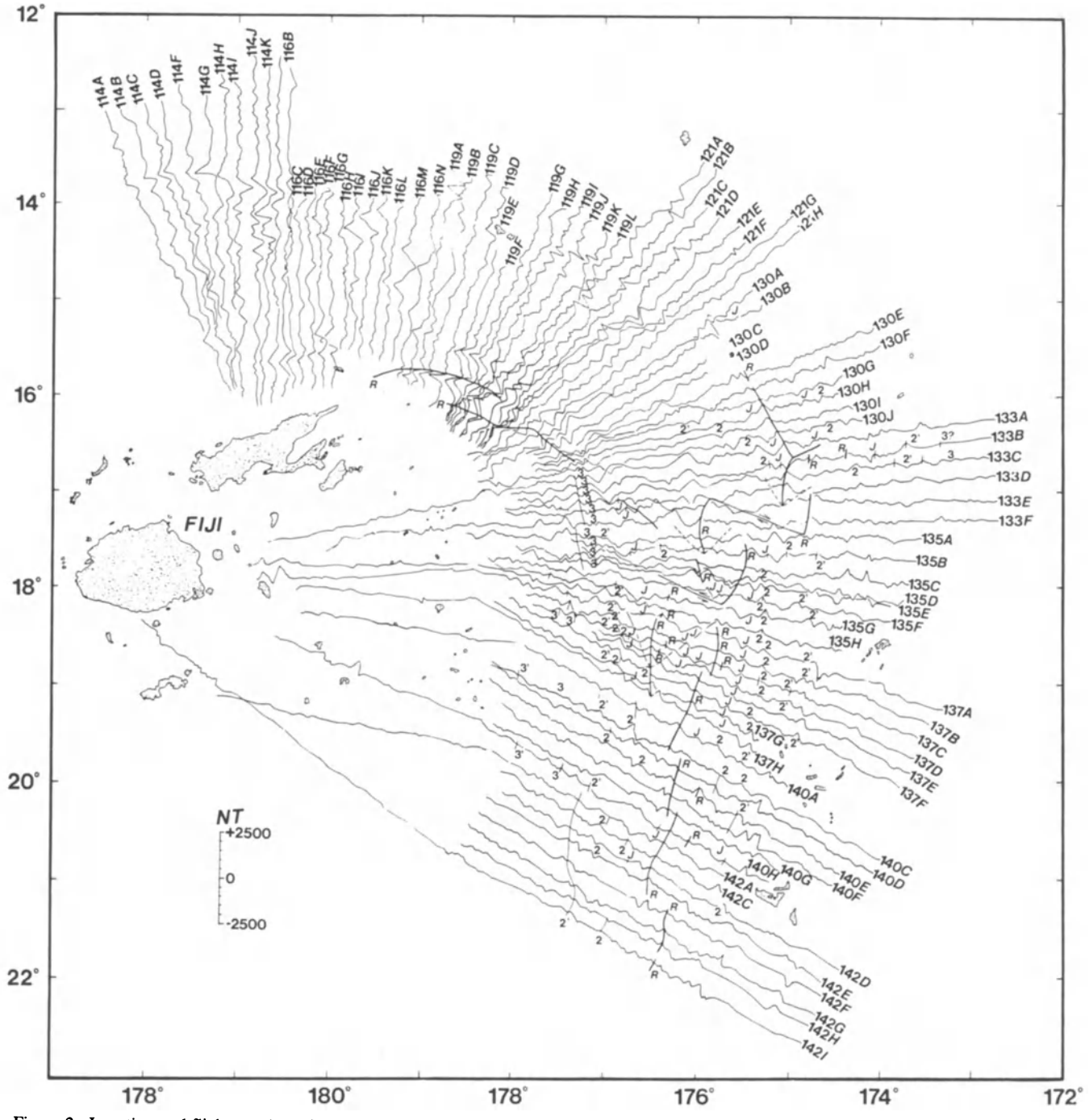

Figure 2. Location and flight number of residual magnetic anomaly profiles over Lau Basin; R = ridge axis; magnetic anomalies identified by numbers.

netometer system was used for magnetic field data acquisition. The inputs of total magnetic field, position and altitude were merged to a common time base with a Hewlett Packard 21 MX mini-computer. In addition, as a result of the accuracy and high reliability of the Litton inertial navigation systems, the International Geomagnetic Reference Field (1975) was removed in real-time and the residual magnetic field data were plotted along track while in flight. Additional shipboard lines were run by Kroenke et al. (this volume).

Magnetic Anomalies Over the North Fiji Basin and Northern Lau Basin

The North Fiji Basin is a currently active marginal basin with a shallower water depth (average depth 3,000 m) than the adjacent Pacific Ocean basin. The basin has been described by Chase (1971) as an area of young oceanic crust with a high heat flow; he also noted that the morphology of the ocean floor on the western side of the basin (Fiji Plateau) resembles that of the Lau

Basin because of its lack of significant sedimentary cover. The youthful appearance of the ocean floor morphology was further substantiated by Chase through the correlation of magnetic anomalies along four incomplete and widely separated magnetic profiles extending across the south-central part of the North Fiji Basin. In tentatively correlating the magnetic anomalies, Chase identified the presence of anomalies 1, 2, and 3, and calculated a half-spreading rate of 3.9 cm/yr and extended the age of the basin to 7 Ma (anomaly 3-4). Falvey (1975) re-examined the data of Chase for the North Fiji Basin and determined the half-spreading rate to be 4.75 cm/yr. Falvey further suggested that the magnetic anomaly sequence extends back to anomaly 4.

Further re-examination by Falvey (1975) and Malahoff et al. (1982) of the magnetic anomaly sequence in the North Fiji Basin, with knowledge of the oldest consistent date for marine volcanic rocks of Viti Levu, suggests that rotation and the realignment of the North Fiji Basin spreading centers occurred as recently as 5 Ma, or at the time of magnetic anomaly 3. In order to confirm the identity of the magnetic anomalies in both the North Fiji Basin and Lau Basin and the location and strike direction of the modern spreading center, a series of closely spaced aeromagnetic lines were flown over the Lau and North Fiji basins. The aeromagnetic coverage of these specific study areas is shown in Figures 1 and 2.

The synthetic anomalies used in this paper were calculated for a half-spreading rate of 3.5 cm/yr based on the magnetic reversal time scale of LeBrecque et al. (1977) using the technique of Schouten and McCamy (1972). The actual spreading rates were determined from a comparison of the observed and calculated rates. In discussing the age of geological events, we have used the LeBrecque et al. (1977) magnetic reversal chronology throughout the paper.

In this paper, we have conducted a detailed and systematic analysis of the complete magnetic anomaly data set in light of current geophysical and tectonic studies of the North Fiji Basin, such as those conducted by Auzende et al. (1988). In a preliminary analysis of our partial magnetic anomaly data set, Auzende et al. (1988) used only trend analyses without the benefit of anomaly identification. In this paper, we present an analytical discussion of the anomaly profiles. Identifications of the anomalies in our data set have placed the positions of the triple junctions and spreading center axes in a pattern different from that published by Auzende et al. (1988).

The composite total force residual magnetic anomaly map is shown in Figure 3. In this presentation of data, the axis of the spreading center of the North Fiji Basin, striking north along 173°30'E, is clearly seen. Locations of the spreading centers and the residual total force magnetic anomalies, as interpreted from the data set shown in Figure 3, are shown in plan in Figure 4. This spreading center has had a stable spreading regime in existence only since the time of anomaly 2 (Figures 3 and 4), at which time the northwestern limb of a triple junction that had been in existence since the time of anomaly 3', or possibly 4, ceased to be active. At the time of anomaly 2', a new spreading regime appears to have formed, marked by a new spreading axis extending through a series of westwardly propagating rifts.

The total force residual magnetic anomalies map shown in Figures 3 and 4 exemplifies the changing spreading patterns in the Lau/North Fiji basin back-arc basin setting. This setting is unusual because of the continuum in the spreading regime over a 180° segment. Figure 4 shows that the strike of the currently active spreading centers is at 005°. Limbs of the Lau Basin and North Fiji Basin triple junctions tend to strike at 305° and 060°. An exception to this pattern is the newly developed east-west striking rift located over Pandora Ridge. This apparent pattern of triple junctions, relocating through time, and overlapping and propagating rifts has made it possible for seafloor spreading to take place west, north, and south of the islands of Fiji.

The data presented in this study confirm the tentative findings (Chase, 1971; Falvey, 1975) of the youthful nature of the North Fiji Basin. The magnetic anomaly data located over the southern half of the North Fiji Basin (Figure 5) suggest that anomalies 1 to 4 (0 to 7.8 Ma) may be present in the North Fiji Basin. The high heat flow of ≥3.0 HFU, observed over the North Fiji Basin by Watanabe et al. (1977), suggests the presence of one of several active spreading centers in the area. A pattern of shallow focus earthquakes was found to be associated with the location of the spreading center proposed by Nagumo et al. (1975). The calculated spreading rate of 7 cm/yr for the North Fiji Basin could be contributing to an earthquake-passive phase of seafloor spreading. Conversely, the earthquake data may indicate a contemporary cessation of spreading activity over most of the length of the spreading system.

Residual Total Force Magnetic Anomaly Map and Seafloor Spreading Patterns in the North Fiji Basin

The magnetic anomaly and magnetic lineations map shown in Figure 3 was constructed from that data in the magnetic profiles shown in Figures 1 and 2. The contoured data show that the structure of the elongate anomalies extends in a semicircular continuous setting around the Fiji islands, extending from the North Fiji Basin west of Viti Levu to the Lau Basin east of Viti Levu. In order to tectonically interpret this observed magnetic lineations pattern, we propose to invoke a series of triple junctions, whose tectonic relationships are described below.

Over the North Fiji Basin, the magnetic lineation pattern north of Hunter Fracture Zone at 21°S, 173°E, reflects the presence of a segmented rift zone whose spreading activity may have persisted since the time of anomaly 3' (Figures 3 and 5). At 18°S, 173°30'E, a discernible change in the strike of magnetic anomaly 3' from north to northwest reflects spreading processes at an R-R-R triple junction. Since the time of anomaly 3', the R-R-R triple junction has apparently migrated northward; because of the northward propagation of the southern rift, the current triple junction is located at about 16°50'S, 173°45'E (Figure 1). The axis of the southern limb of the triple junction is offset by several east-west striking transform faults or rift overlaps between 16°50'S and 21°S at the termination at the Hunter Fracture Zone. The most recent northward propagation of the rift probably took place since the J event, during which time the rift tip propagated from 18°S to its present position at 16°50'S. During very recent times, probably within the last 500,000 years, the currently active spreading center has relocated along several possible overlapping rifts located over the Hazel Holme Fracture Zone, which extends east-west from 14°S, 171°E to 14°S, 180°E where the east-west trending line of spreading centers terminates against a complex triple junction. The axis of this east-west striking rift system is characterized by a -100 to -300 nT discontinuous anomaly.

Shallow seismicity events studied by Hamburger and Isacks (this volume) also suggest the presence of new spreading centers located at 176°E. A positive 400 nT magnetic anomaly located at 16°30'S, 175°30'E could mark the presence of the new spreading center. The magnetic data available in this paper are, however, insufficient to localize the presence of this new spreading center. The North Fiji Basin sector located between Vanua Levu and the Pandora Ridge is characterized by east-west trending continuous magnetic anomalies ranging in amplitude from -300 to + 500 nT. These anomalies are associated with bathymetric features resembling fissures and could mark the presence of "leaky" transform faults or jumped spreading centers. The magnetic anomaly data suggest that spreading activity in this area commenced at about the time of magnetic anomaly 2.

Tectonic Development of the North Fiji Basin

In order to accommodate the evidence from paleomagnetic studies of the rocks from Viti Levu (Malahoff et al., 1982) that the island of Viti Levu had rotated at least by 90° in a counterclockwise direction, a complex set of spreading centers has to be invoked to exist north and west of the island of Viti Levu. The distribution of magnetic anomalies over the North Fiji Basin does indeed suggest the presence of several formerly active triple junctions. Several of the triple junctions appear to have been short-lived. A triple junction, probably located at 16°50'S, 173°45'E, appears to have been active since the time of anomaly 3' or about 5 Ma until the present magnetic epoch. The breakup of the northern east-west striking limb of the triple junction since 2.5 Ma (anomaly 2') is evident from the examination of the magnetic anomaly map in Figure 3. The transformation of the spreading center from the North Fiji Basin to the Lau Basin occurs through a series of R-R-R triple junctions (Figures 3 and 4).

Current magnetic activity may be concentrated along a newly developed spreading center (formed after 2.5 Ma) located along the axis of the South Pandora Ridge (Hazel Holme Fracture Zone) south of Horizon Bank. In order to extend the anomaly identifications over the southern half of the south Fiji Basin shown in Malahoff et al. (1982) to the northern half of the Fiji Basin, a complete set of stacked magnetic profiles extending from the Profile 318C south to Profile 297J was developed as shown in Figure 1. A stack of the residual magnetic anomaly profiles extending from Profile 318C to Profile 310B (Figure 5) shows a proposed identification sequence of the magnetic anomalies for the southern half of the North Fiji Basin. Magnetic anomalies from anomaly 1 out to anomaly 3, and possibly anomaly 4, may be recognized in this pattern. The eastern limb of the magnetic anomaly stack in Figure 5 shows a series of high-amplitude, long wavelength anomalies located east of the anomaly 3' lineations. This sequence is tentatively proposed to represent magnetic anomalies generated by contemporary spreading centers located 100 and 210 km west of Viti Levu, respectively. Seismicity patterns (Hamburger and Isacks, this volume) associated with the proposed spreading center located nearest to Viti Levu suggest that this overlapping pair of centers may be currently active. SeaBeam studies of this area by IFREMER during the 1986 SEAPSO cruise support the magnetic interpretation of the anomaly patterns in terms of a currently active overlapping spreading center.

In plan, the magnetic data suggest that the North Fiji Basin has undergone several stages of seafloor spreading orientation since the time of anomaly 3'. Anomalies 3 and 3' are represented in the magnetic anomaly lineation patterns of Figure 4 by a set of anomalies striking at 320°. The strike direction of 320° is interpreted from the magnetic data to represent the strike of the axis of a spreading center and triple junction that was active five million years ago. At the time of the anomaly 2, or approximately 2 Ma, the R-R-R triple junction moved east from 17°00'S, 172°25'E to its present position at 16°50'S, 173°45'E (Figure 4). During this period, the southern limb of the triple junction rotated clockwise by approximately 25°.

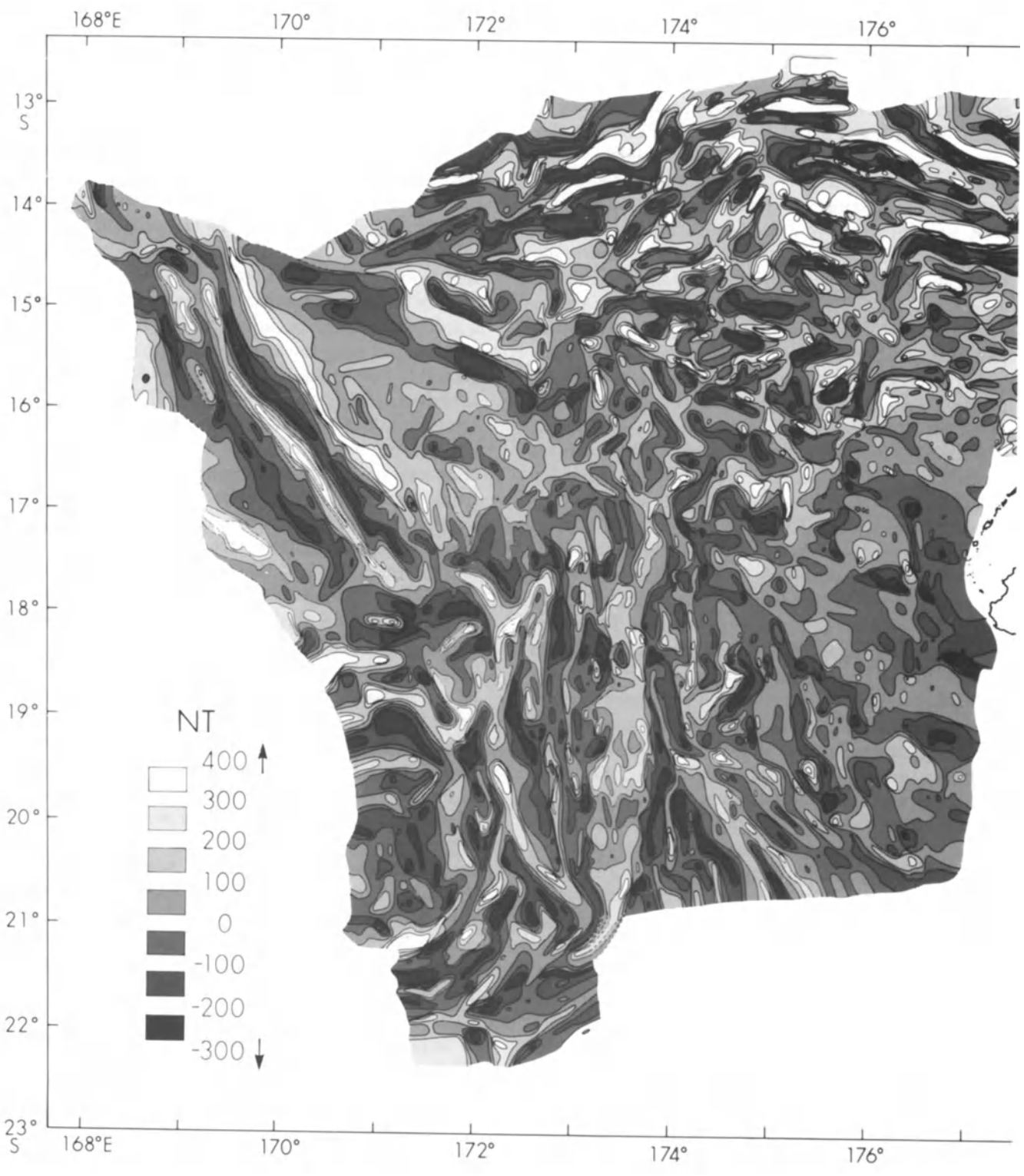

Figure 3. Residual total magnetic force anomaly map of the North Fiji and Lau basins; contour interval 100 nT. Constructed from data shown in Figures 1 and 2.

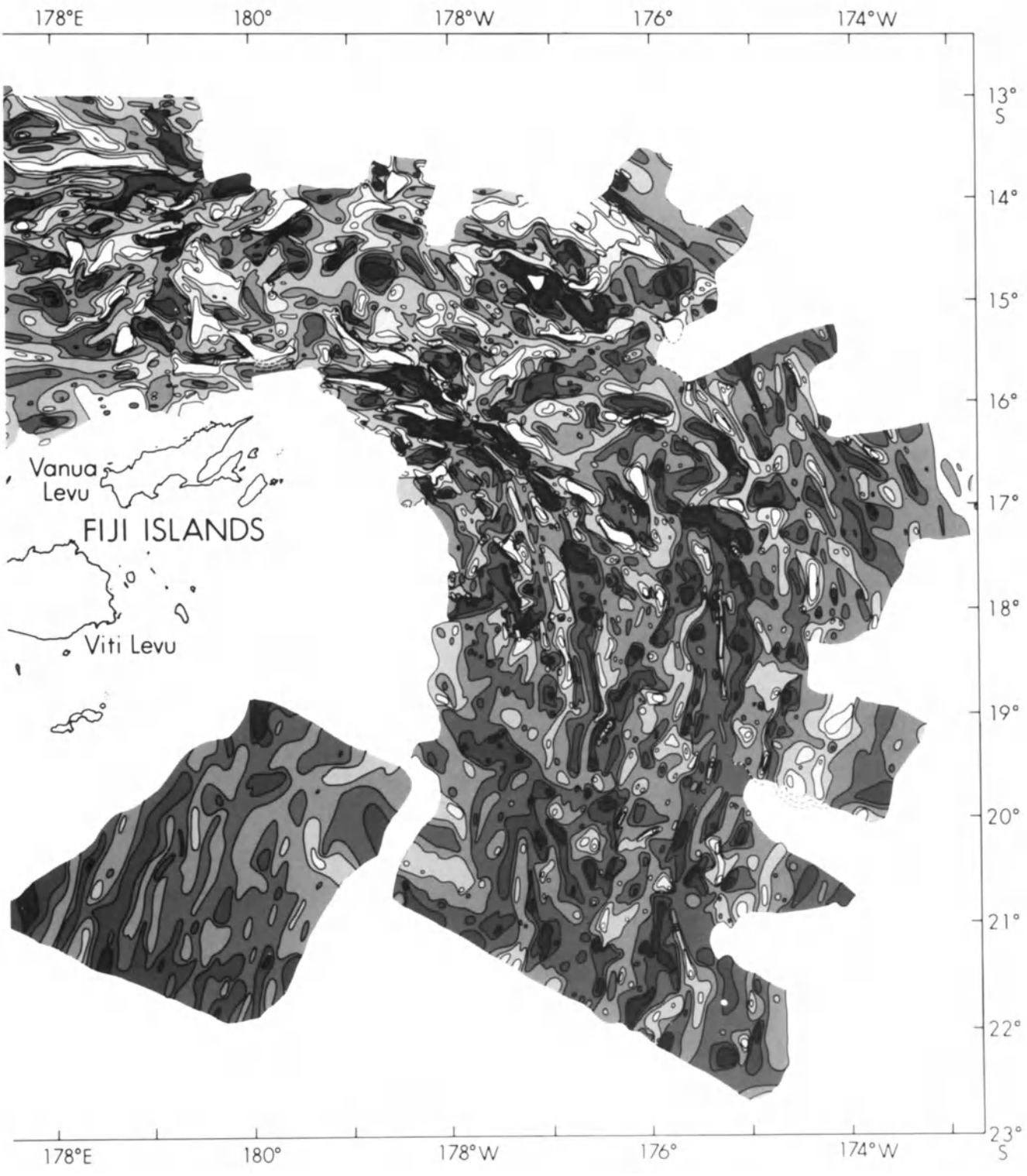
178°E
180°
178°W
176°
174°W
13° S
14°
15°
16°
17°
18°
19°
20°
21°
22°
23° S
Vanua Levu
FIJI ISLANDS
Viti Levu

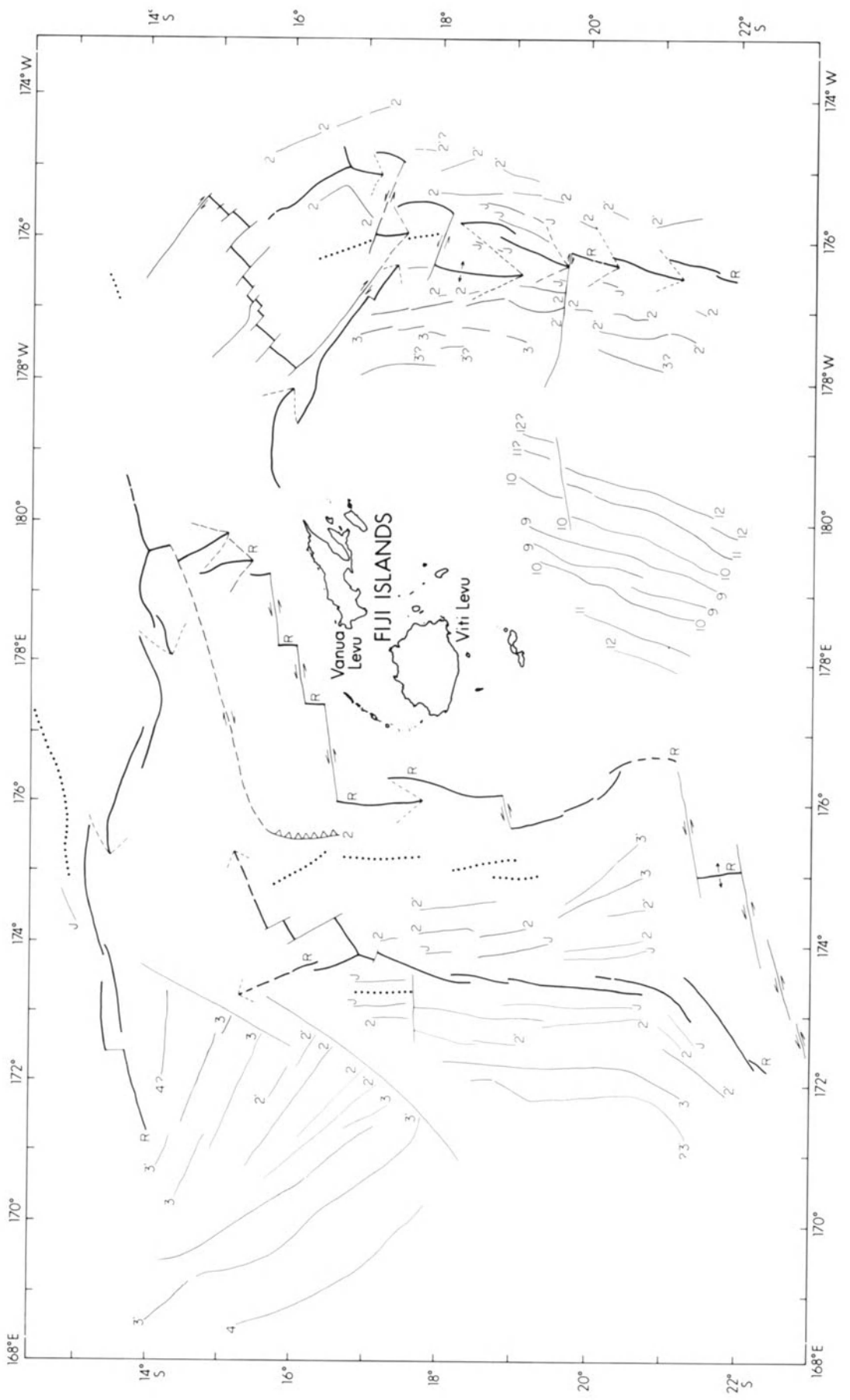

Figure 4. Location of principal magnetic anomaly lineations and spreading ridge segments located over the North Fiji and Lau basins. Anomaly lineations with magnetic anomaly numbers are shown by light lines, the ridge axis by a heavy line, and all interpreted from data shown in Figures 1 through 3.

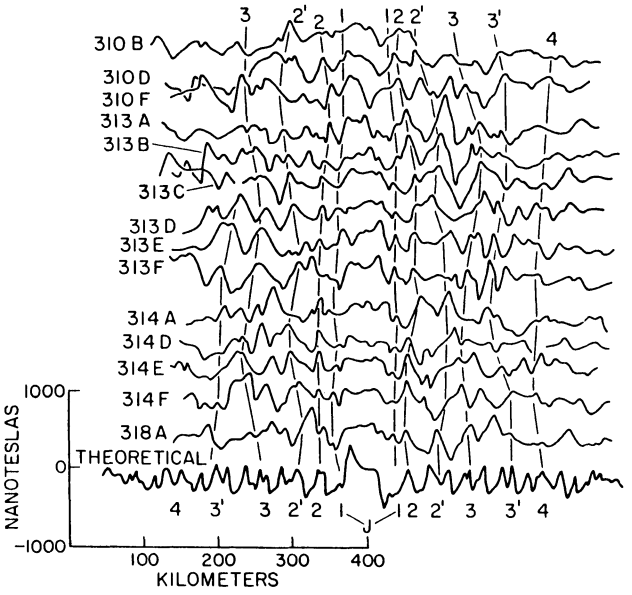

Figure 5. Stacked residual magnetic anomaly profiles over southern half of the North Fiji Basin. (See Figure 1 for location of profiles.)

These changes in the location of the spreading axis and the appearance and disappearance of spreading segments and propagating limbs during the past two million years (Figure 4) represent the surficial manifestations of rapid changes in the convection regimes in the asthenosphere underlying the North Fiji Basin. Undoubtedly, the regime does undergo long-term changes as well, as illustrated by the 90° clockwise rotation of Viti Levu during the past seven million years (Malahoff et al., 1982).

The contemporary setting of the spreading centers of the North Fiji Basin is illustrated in Figure 4 and may be described as follows. The currently active triple junction located at 16°50'S, 173°45'E has been formed off a southern limb consisting of a series of progressively westward displaced ridge segments. The apparent curvature of this ridge axis westward at the southern end of the ridge, where it abuts against the Hunter Fracture Zone, probably represents numerous short rift segments that are progressively displaced by transform motion along elements of the Hunter Fracture Zone. The two northern limbs of the North Fiji Basin triple junction have been interpreted in this paper as youthful propagations with propagation directions of 340° and 070°. SeaBeam studies (Auzende et al., 1988), seismicity studies, and the current magnetic surveys suggest that a new triple R-R-R junction system located north of Vanua Levu Island at 15°40'S, 179°30'E, has been forming within the past one million years. The southern limb of this system has been formed of propagating rift limbs located at 15°00'S, 179°30'E; left laterally offset ridge segments located north of Vanua Levu and Viti Levu; and overlapping rifts located 100 km west of Viti Levu. The northwest limb of this triple junction system is also relatively young, probably one to two million years in age. The location of the proposed north rift spreading center is based upon prominent, continuous and correlatable high amplitude magnetic anomalies (over 1000 nT peak-to-peak) observed in the northern aeromagnetic profiles 297A to 297J (Figure 6). The bathymetry over the proposed rift segments consists of shallow ridges with fresh pillow lavas (Sinton et al., this volume). The identification of the anomaly sequence (Figure 6) suggests that the north rift spreading center coincides with the South Pandora Ridge, which has been formed through volcanism along a number of overlapping spreading centers whose ages do not exceed the age of anomaly 2' (2.5 Ma). One interpretation of the data would have the north rift forming as a consequence of the cessation at 2.5 Ma of spreading activity along the northwest limb of the proto triple junction. Between 2.5 Ma and 1 Ma, the southern rift of the South Fiji Basin would have formed a triple junction with the north rift at about 14°S, 175°E, the site of a currently confusing pattern of magnetic anomalies. The back-arc basin area located northeast of Vanua Levu marks the continuum from the North Fiji Basin into the Lau Basin. Magnetically, this region marks a tectonically disturbed region without an apparent continuous pattern of magnetic anomaly lineations (Figure 3).

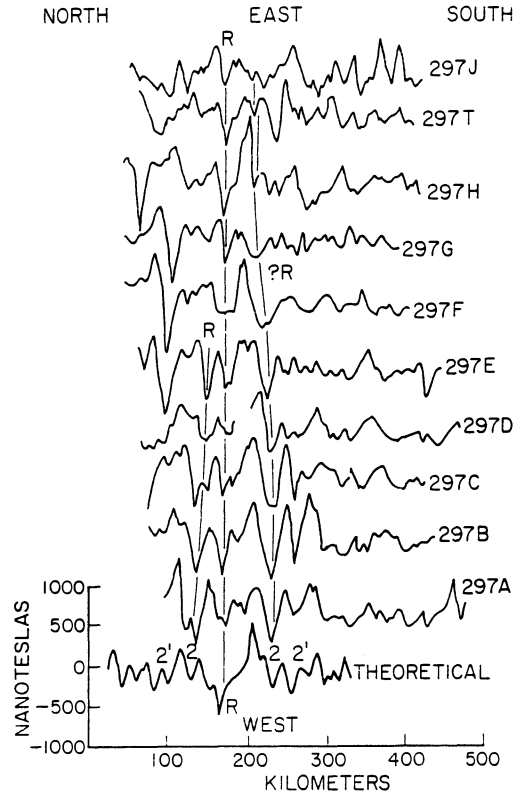

Figure 6. Stacked residual magnetic anomaly profiles over the South Pandora Ridge spreading center in the northern half of the North Fiji Basin show the location of the currently active spreading center. (See Figure 1 for location of profiles.)

Magnetic Lineations and Seafloor Spreading Patterns in the Lau Basin

Magnetic anomaly lineations are readily recognizable in the magnetic profiles (Figures 1 and 2) and in the contoured magnetic anomaly map (Figure 3). Unstable triple junctions and overlapping rifts (Figure 7) characterize the tectonic setting of the northern Lau Basin as interpreted from the magnetic anomalies.

The most complicated feature in the magnetic anomaly map (Figure 3) is the site of the postulated Fiji/Lau triple junction located at 14°S, 179°30'E, north of Vanua Levu. The Fiji/Lau triple junction marks the possible site where continuous readjustment in the tectonic setting of the east-west trending North Fiji rift and north- to west-striking elements of the northern Lau Basin rift have been taking place. A temporal and spatial reconstruction of this triple junction since its initiation at about the time of anomaly 2 is difficult with the available magnetic data and is not conducted in this paper. The northern Lau Basin is characterized by a patchwork setting of northeast- and northwest-striking magnetic anomalies up to 600 nT in amplitude, which probably mark the sites of alternating northwest and northeast striking rift segments. These rift segments in the northern portion of the Fiji-Lau basins are probably not continuously active rifts but represent tectonic lineaments that probably changed from transform faults to leaky transform faults to spreading centers and vice versa during the time from magnetic anomaly 2 until today. Anomaly 2 is tentatively identified as the oldest anomaly for the northern portion of the North Fiji-Lau basin.

Peggy Ridge, located at 16°S, 177°30'W, is a seismically active bathymetric feature and is probably, at the present time, undergoing a change from the site of a transform fault to that of a spreading center (Figure 4). The postulated regime of alternating transform and spreading activity along orthogonally opposed lineaments striking in northeast and northwest directions is probably active from the north to about 17°30'S along the axis of the Lau Basin. The western end of the Peggy Ridge spreading center is marked by an overlapping rift and rift propagation sequence (Figures 3, 7 and 8). The site also represents an unstable triple junction. The northeastern limb of the junction is represented by a spreading ridge consisting of ten ridge segments terminating at the northeastern end against a high lateral

Figure 7. Stacked residual magnetic anomaly profiles over the northern Lau Basin, showing the magnetic configuration of the proposed spreading center located northeast of Vanua Levu, Fiji. (See Figure 2 for location of profiles.)

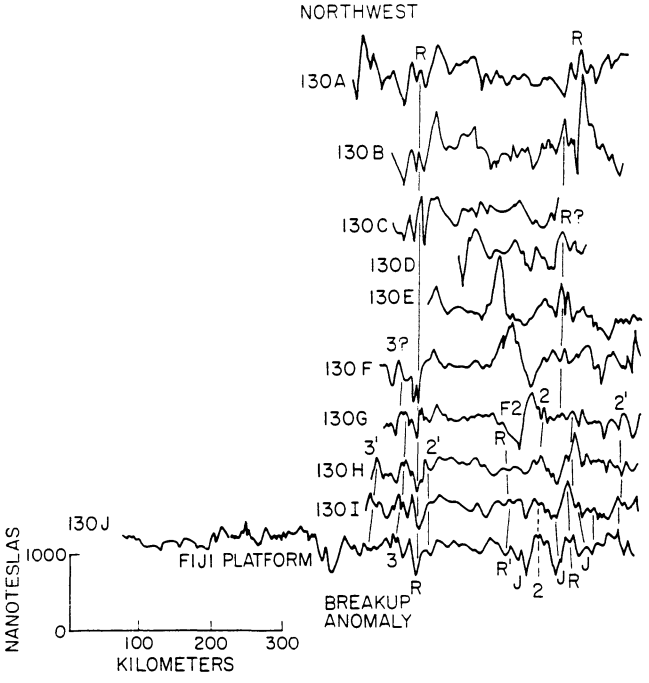

Figure 8. Stacked magnetic anomaly profiles over the northern Lau Basin west of Peggy Ridge where a double ridge spreading setting is proposed for the northern Lau Basin. (See Figure 2 for location of profiles.)

transform fault. An R-R-R triple junction located at 17°30'S, 175°40'W marks the beginning of a relatively steady state back-arc spreading regime that extends from the Lau Basin R-R-R triple junction south through the Lau Basin and Havre Trough, terminating at the central volcanic zone of New Zealand (Malahoff et al., 1982).

A Lau Basin triple junction located at 17°30'S, 175°40'W (Figures 3 and 4) marks the tectonically unstable interaction between the propagating southeast-striking rift limb of Peggy Ridge, a transform fault, and a southwest-striking propagating limb of the Lau Basin spreading segments. Approximately 40 km south of the triple junction, the Lau Basin Ridge is intersected by magnetic anomalies associated with Peggy Ridge. If Peggy Ridge is considered to be currently a new evolving spreading center, then the new R-R-R triple junction is probably located at this site.

The southern Lau Basin ridge segments appear to be southwest propagating, successively overlapping eastward segments that strike at 200°. The principal ridge segments of the Lau Basin ridge south of 17°30'S (Figures 4, 8, 9, 10, and 11) appear to be about 100 km in length between the overlaps. The magnetic data suggest that the overlapping rifts are the probable neotectonic setting for the rift segments of the northern Lau back arc basin. The southernmost rift segment, located at 21°50'S, 176°30'W (Figure 11), is coincident with the volcanically young Vala Fau Ridge.

The northern Lau Basin between 18°S and 14°S (Figures 7 through 12) is marked by a series of displaced ridge segments overlapping ridges and propagating ridges. The two-rift system is readily observed in profiles 130A to 130I in Figure 8. South of the complex triple junction located at 176°W, 17°S the ridge tectonics of the Lau Basin more resemble steady state spreading regimes than those observed to the north. South of the triple

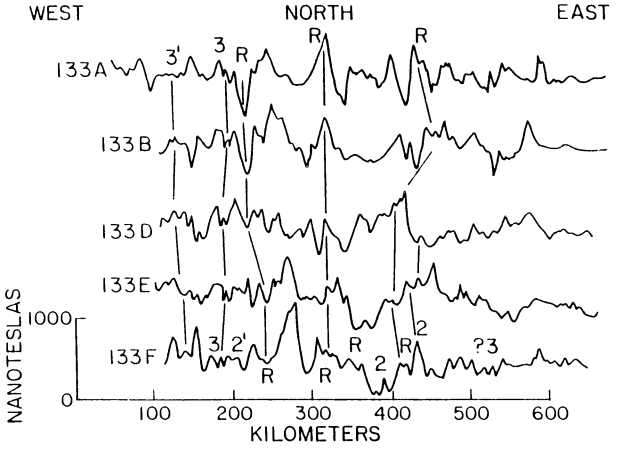

Figure 9. Stacked magnetic anomaly profiles over the Lau Basin showing the site for a proposed three-ridge spreading setting in the northern Lau Basin. (See Figure 2 for location of profiles.)

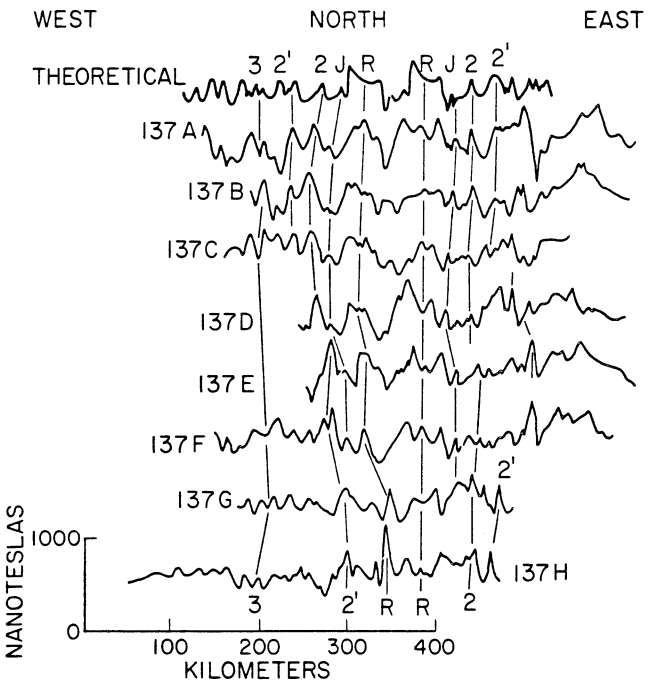

Figure 10. Stacked residual magnetic anomaly profiles over a double rift system in the central Lau Basin. (See Figure 2 for location of profiles.)

junction, a series of progressively westward-displaced, southward-propagating ridge segments form the primary back-arc spreading regime of the Lau Basin. Overlapping rift segments are readily discernible in the magnetic stacks of Figure 10, where an apparent double rift is seen in profile 137A. At the northern end of the data set in Figure 2, the magnetic profiles are erratic in the configuration of the anomalies and the central

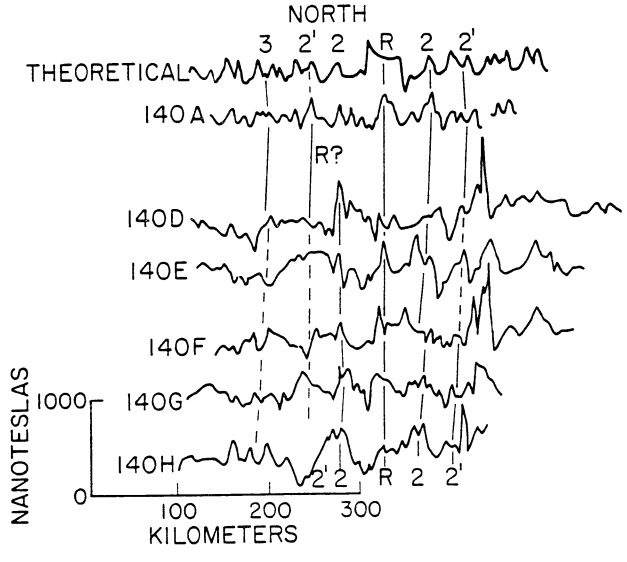

Figure 11. Stacked residual magnetic anomaly profiles over a single rift segment located in the central Lau Basin. (See Figure 2 for location of profiles.)

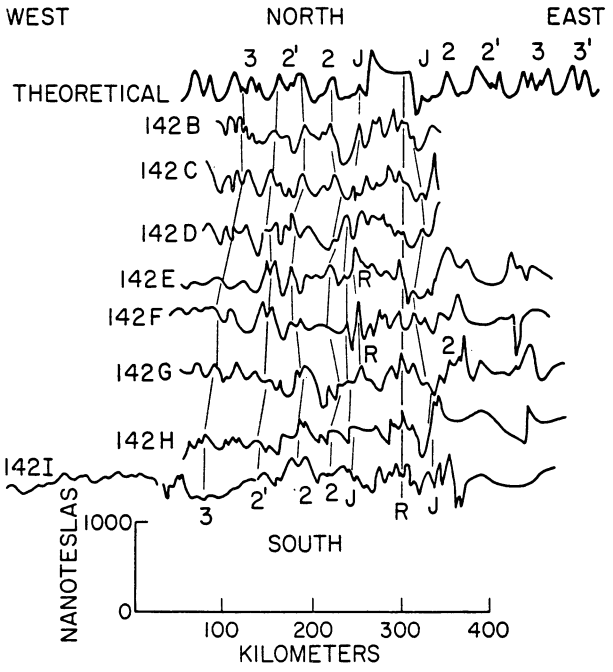

Figure 12. Stacked magnetic anomaly profiles over a single rift segment on the Valu Fa Ridge, located in the central Lau Basin at the southern end of the current data set. (See Figure 2 for location of profiles.)

anomaly is difficult to interpret; thus ambiguities in the interpretation of the data may exist. However, if the currently active spreading center is identified from profile to profile (Figure 2), an overlapping rift sequence appears to be the dominant neotectonic setting for the current spreading regime (Figure 4).

Figure 4 marks the interpretive compilation of the whole magnetic data set discussed in this paper. The locations of the rift axes, as well as the magnetic anomaly lineations, are presented in this figure. The foremost deduction on back-arc spreading regimes from this figure is that the regime is dominated by the presence of unstable (through time) overlapping rifts, propagating rifts and triple junctions. None of these features studied in this paper appear to remain stable for more than about one million years. It is these unstable overlapping rifts, propagating rifts, and triple junctions that reflect the continuous spreading regime surrounding the Fiji Islands platform on three sides.

CONCLUSIONS

Analysis of residual magnetic anomalies collected over the North Fiji Basin and the Lau Basin-Havre Trough region suggest that

1. Spreading was initiated in the North Fiji Basin and later progressively migrated into the Lau Basin and Havre Trough.

2. The ages of the basins, based on the magnetic anomaly data, are as follows:

North Fiji Basin	8 Ma to the present (magnetic anomaly 4-1)
Lau Basin	4.8 Ma to the present (magnetic anomaly 3'-1)
Havre Trough	2.8 Ma to the present (magnetic anomaly 2-1)

3. The North Fiji Basin commenced development during the Late Miocene about 8 Ma, shortly before the time of anomaly 4. During a subsequent stage in the formation of the North Fiji Basin, subduction of the older South Fiji Basin oceanic lithosphere occurred at the site of the New Hebrides-Hunter Fracture Zone.

4. At about 4.8 Ma, shortly before the time of magnetic anomaly 3', spreading migrated into the Lau Basin and at about 2.0 Ma (at the time of magnetic anomaly 2) into the Havre Trough and into the central volcanic zone of New Zealand.

5. The development phases of the marginal basins appear to commence and cease with changes in the directions and rates of spreading from the East Pacific Rise and with changes in the convergence directions between the Indian, Antarctic, and Pacific Plates (Jurdy, 1979). These changes appear to have triggered the development phases of the marginal basins of the Southwest Pacific, while leaving the subduction patterns along major trenches and the geographic location of major trenches such as the Tonga-Kermadec Trench relatively secure.

6. The complex patterns of overlapping ridges, triple junctions, and propagating ridges located over the North Fiji and Lau basins, as interpreted in this paper, appear to be unstable through time and thus would reflect a non-steady state of magmatic convection beneath the ocean floor of the inverted U-shaped North Fiji/Lau basin spreading center complex.

7. On the basis of the Fiji/Lau back-arc basin magnetic studies, we suggest an unstable, spreading regime through time in the development of this back-arc basin.

ACKNOWLEDGMENTS

The authors would like to thank Stephen Kish and Claude Hanson and their officers and flight crew of the P3 Orion from the Naval Research Laboratory's Patuxent River Flight Detachment, who flew the magnetic profiles. The authors are grateful for the many fruitful discussions with Richard Hey and Phil Jarvis

during the preparation of this manuscript and to Phil Jarvis for critically reviewing the manuscript. Our thanks also go to Cheryl Komenaka who prepared the manuscript. The research was supported by funding from the NOAA's National Ocean Survey and the Naval Research Laboratory, Washington, DC. This is SOEST contribution No. 1754.

REFERENCES

Auzende, J.-M., Y. Lafoy, and B. Marsset, 1988, Recent geodynamic evolution of the north Fiji basin, Geology, v. 16, p. 925-929.

Chase, C.G., 1971, Tectonic history of the Fiji Plateau: Geological Society of America Bulletin, v. 82, p. 2087-2110.

Cherkis, N.Z., 1980, Aeromagnetic investigations and seafloor spreading history in the Lau Basin and Northern Fiji Plateau, in Proceedings, Petroleum Potential in Island Arcs, Small Ocean Basins, Submerged Margins and Related Areas Symposium, UN ESCAP, CCOP/SOPAC Technical Bulletin 3, p. 37.

Cherkis, N.Z., A. Malahoff, and J.M. Brozena, 1978, Magnetic lineations over the Fiji Plateau, EOS, Transactions, American Geophysical Union, 59, p. 266 (abstract).

Cherkis, N.Z., Malahoff, A., and Brozena, J.M., 1980, An aeromagnetic investigation of the Lau Basin and the North Fiji Plateau, Abstracts w/ Program 12, Geological Society America, Northeastearn section, 15th Annual Meeting (abstract).

Falvey, D., 1975, Arc reversals and a tectonic model for the North Fiji Basin, Australian Society for Exploration Geophysicists Bulletin, v. 6, p. 47-49.

Hamburger, M.W., and B.L. Isacks, Shallow seismicity in the North Fiji Basin: this volume.

Jurdy, D.M., 1979, Relative Plate Motions and the formation of marginal basins, Journal of Geophysical Research, v. 84, p. 6796-6802.

Karig, D.E., 1970, Ridges and basins of the Tonga-Kermadec island arc systems, Journal of Geophysical Research, v. 75, p. 239-254.

Karig, D.E., 1971, Origin and development of marginal basins in the Western Pacific, Journal of Geophysical Research, v. 76, p. 2542-2562.

Kroenke, L.W., J.V. Eade, C.Y. Yan, and R. Smith, Sediment distribution in the north central North Fiji Basin: this volume.

Lawver, L.A., J.W. Hawkins, and J.G. Sclater, 1976, Magnetic anomalies and crustal dilation in the Lau Basin, Earth and Planetary Science Letters, v. 33, p. 27-35.

LeBrecque, J.L., D.V. Kent, and S.C. Cande, 1977, Revised magnetic polarity time scale for the Late Cretaceous and Cenozoic time, Geology, v. 5, p. 330-335.

Malahoff, A., R.H. Feden, and H.S. Fleming, 1982, Magnetic anomalies and tectonic fabric of marginal basins north of New Zealand, Journal of Geophysical Research, v. 87, p. 4109-4125.

Nagumo, S., J. Kasahara, and T. Ouchi, 1975, Active seismicity in the Fiji Plateau observed by ocean-bottom seismograph, Journal of Physics of the Earth, v. 23, p. 279-287.

Schouten, H. and K. McCamy, 1972, Filtering marine magnetic anomalies, Journal of Geophysical Research, v. 77, p. 7089-7099.

Sclater, J.F., J.M. Hawkins, J. Mammerickx, and C.G. Chase, 1972, Crustal extension between the Tonga and Lau Ridges: Petrological and geophysical evidence, Geological Society of America Bulletin, v. 83, p. 505-518.

Sinton, J.M., R.C. Price, K.M. Johnson, H. Staudigel, and A. Zindler, Petrology and geochemistry of submarine lavas from the Lau and North Fiji back-arc basins: this volume.

Watanabe, T., M.G. Langseth, and R.N. Anderson, 1977, Heat flow in back-arc basins of the western Pacific, in M. Talwani, and W.C. Pitman (eds.), Island Arcs, Deep Sea Trenches, and Back-arc Basins; Maurice Ewing Series, v. 1, p. 137-161, American Geophysical Union.

Watts, A.B., J.K. Weissel, and F.J. Davey, 1977a, Tectonic evolution of the south Fiji marginal basin, in M. Talwani, and W.C. Pitman (eds.), Island Arcs, Deep Sea Trenches, and Back-arc Basins; Maurice Ewing Series, v. 1, p. 419-427, American Geophysical Union.

Watts, A.B., J.K. Weissel, and R.L. Larson, 1977b, Sea-floor spreading in marginal basins of the Western Pacific, Tectonophysics, v. 37, p. 167-181.

Weissel, J.K., 1977, Evolution of the Lau Basin by the growth of small plates, in M. Talwani, and W.C. Pitman (eds.), Island Arcs, Deep Sea Trenches, and Back-arc Basins; Maurice Ewing Series, v. 1, p. 429-436, American Geophysical Union.

Kroenke, L.W., and J.V. Eade, editors, 1993, Basin Formation, Ridge Crest Processes, and Metallogenesis in the North Fiji Basin: Houston, TX, Circum-Pacific Council for Energy and Mineral Resources, Earth Science Series, Vol. 15, Springer-Verlag, New York.

SEDIMENT DISTRIBUTION IN THE NORTH-CENTRAL NORTH FIJI BASIN

LOREN W. KROENKE
Hawaii Institute of Geophysics, School of Ocean and Earth Science and Technology
University of Hawaii, Honolulu, Hawaii 96822

JAMES V. EADE[1]
New Zealand Oceanographic Institute, Wellington, New Zealand

CHUN YEUNG YAN[2]
Hawaii Institute of Geophysics, School of Ocean and Earth Science and Technology
University of Hawaii, Honolulu, Hawaii 96822

ROBERT SMITH[1]
Mineral Resources Department, Private Bag, Suva, Fiji

ABSTRACT

Sediment distribution patterns mapped across the North Fiji Basin are interpreted to be indicative of crustal age relationships within the basin. Elevated, sediment-free areas occurring along the ENE-trending South Pandora Ridge and along a north-trending wedge of ridge and trough terrain that extends northward from the presently active Central North Fiji Basin Ridge (CNFBR) are interpreted as having recently formed, i.e., they are younger than 2 Ma. Abyssal hill terrains formed adjacent to these features within the adjoining Pentecost and Balmoral basins are interpreted as having formed between 2 and 5 Ma, along, respectively, WNW- and ENE-trending limbs of a formerly active triple junction. Older North Fiji Basin crust formed prior to 5 Ma lies beneath the undulating areas on the northern and southern margins of Pentecost and Balmoral basins. Maximum age crust, probably no older than late Miocene in age (< 10 Ma), underlies the smooth or flat regions lying due south of the ancient Vitiaz Arc (adjacent to the South Pandora Ridge) and immediately east of the New Hebrides Arc.

INTRODUCTION

Sediment distribution patterns can provide clues to the tectonic development of a region and signal the potential for the occurrence of economic mineral deposits and hydrocarbon accumulations. The North Fiji Basin (Figure 1), because of the thin veneer of sediment blanketing the basin and the presence of active accretionary plate boundaries, was targeted for investigation of potential deposits of metalliferous sediments (Kroenke et al., a, this volume). Sediment distribution patterns in the North Fiji Basin had previously been investigated on a reconnaissance scale by Chase (1971), who observed that a "sediment fan comes off the New Hebrides complex and spills out onto the Fiji Plateau" (North Fiji Basin) and that the sediment cover in the central North Fiji Basin west of the Fiji Plateau "pinches out against a presumed spreading center aligned along longitude 174°E."

Thus the stage was set for the intensive geological and geophysical investigations of the North Fiji Basin that were to follow. The sediment fan or archipelagic apron east of the New Hebrides Arc, first identified by Karig

[1]Now with SOPAC Technical Secretariat, Suva, Fiji
[2]Now with Texas A&M University, College Station, TX

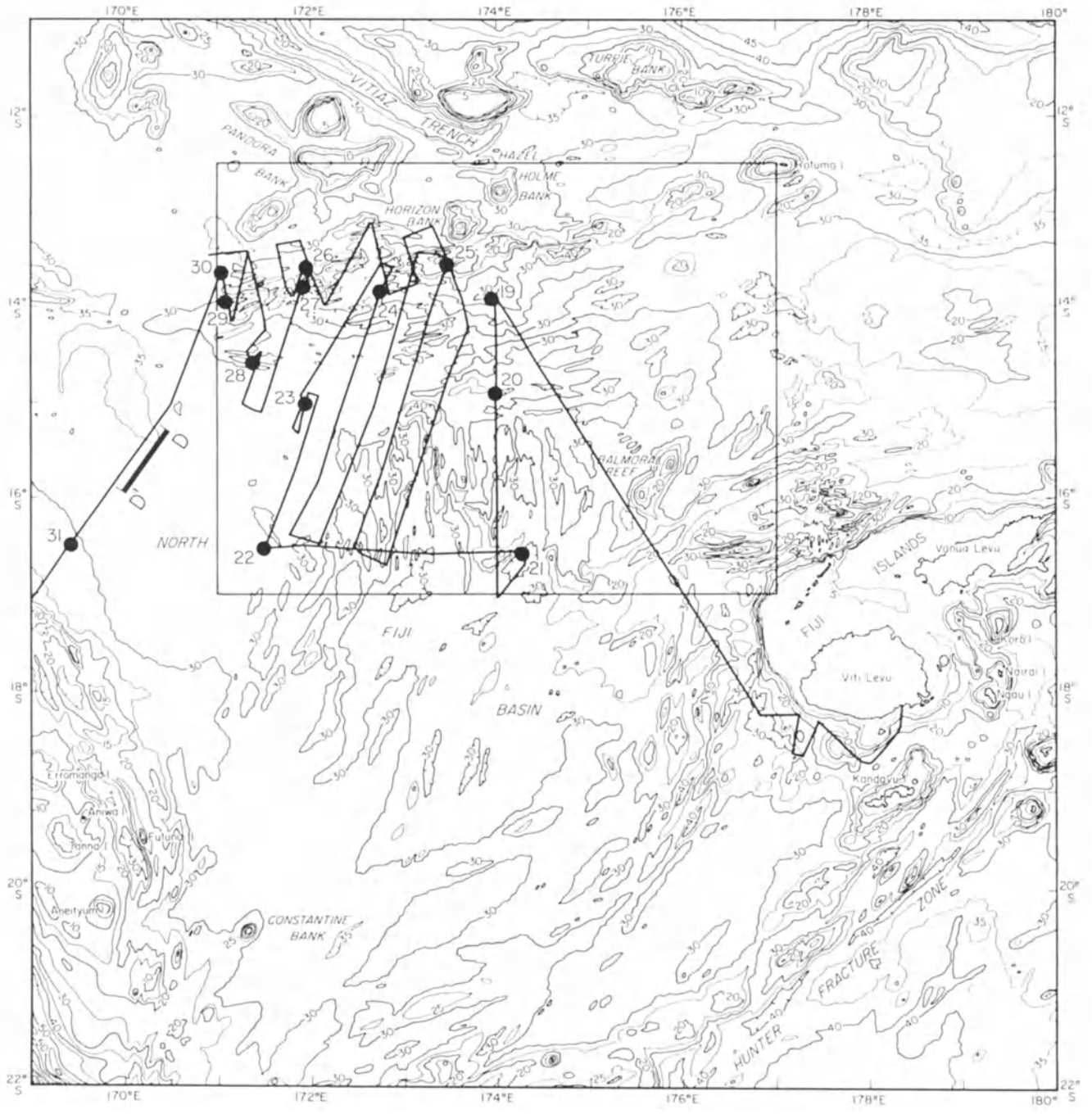

Figure 1. Generalized bathymetry of the North Fiji Basin after Chase et al. (1987) showing the primary study area, KK820316 Leg 3 survey tracks, station location, and location of profile DD' shown in Figure 8.

and Mammerickx (1972) and mapped by Luyendyk et al. (1974), is most recently discussed by Katz (1988) in conjunction with a description of the geology of the intra-arc basins in offshore Vanuatu. Sediment distribution patterns farther east in the North Fiji Basin also were re-examined by Halunen (1979) who, in light of new data, reinterpreted structural lineaments within the basin. This study, based on a considerably expanded data set, delineates the sediment distribution patterns described by Chase (1971) and Halunen (1979) in the north central North Fiji Basin (Figure 2) and identifies previously unrecognized structural elements in that area.

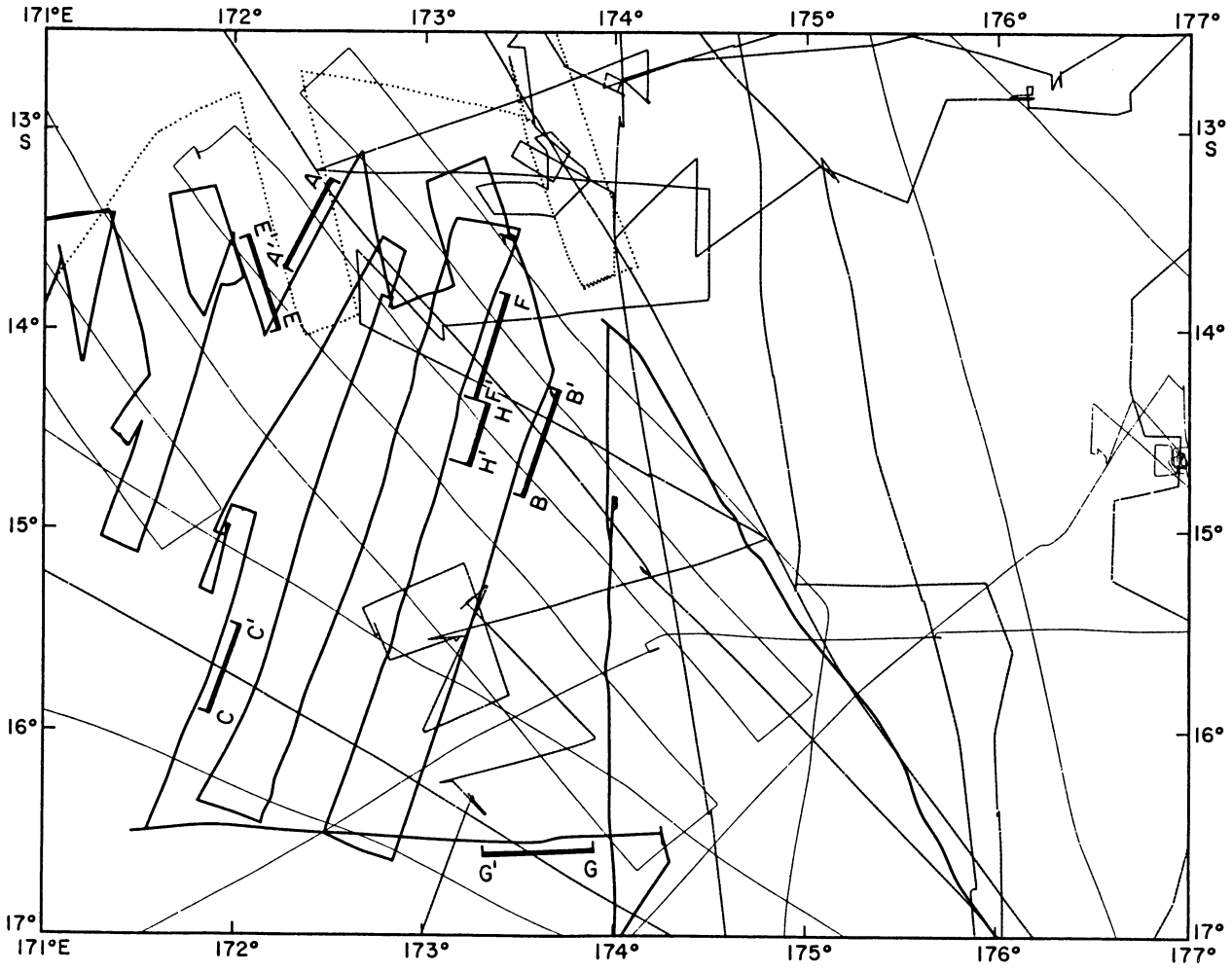

Figure 2. Location of ship tracks in the north central North Fiji Basin along which the reflection profiles and 3.5-kHz echograms used in this study were acquired. Heavy lines indicate the location profiles shown in Figures 4 to 12.

ANALYSIS OF THE REFLECTION PROFILING DATA

In the open ocean environment the thickness of sediment covering oceanic crust is largely a function of age of the crust or crustal residence time; i.e., the older the crust, the longer that crust has been exposed to pelagic sedimentation processes and thus the greater the sediment thickness. In active back-arc regions such as the North Fiji Basin two factors come into play: (1) proximity to or distance from the volcanic arc, and (2) the age/depth of the back-arc basin crust. Close to the arc, volcaniclastic and epiclastic debris shed from the arc predominate. Far from the arc, where the newly formed back-arc basin crust is hot and elevated and the seafloor lies well above the calcium carbonate compensation depth, sediments are dominated by calcareous pelagic organisms.

Piston cores reveal that most sediments of the study area are predominantly calcareous, i.e., being for the most part 60-80% calcium carbonate and have accumulated at an average rate of about 9 m/m.y. during the last 0.7 m.y. (Eade and Gregory, this volume). Departures from this rate are attributed to erosion or non-deposition on scarps and ridges, reworking into troughs and basins, and variations in the influx of airborne volcanogenic detritus. These fluctuations notwithstanding, it is possible to relate variations in sediment thickness across the North Fiji Basin to either proximity to an active island arc or crustal age and seafloor spreading processes.

Reflection profiles and 3.5-kHz echograms obtained during the second leg of the 1982 CCOP/SOPAC Tripartite survey cruise (KK820316, Leg 03) to the North Fiji Basin (Figure 2) and analyzed in conjunction with those collected earlier by Halunen (1979) contain information on both patterns of sediment distribution and the sites of deposition in the north central North Fiji Basin.

Analysis of these data has enabled construction of a sediment thickness chart of the primary survey area

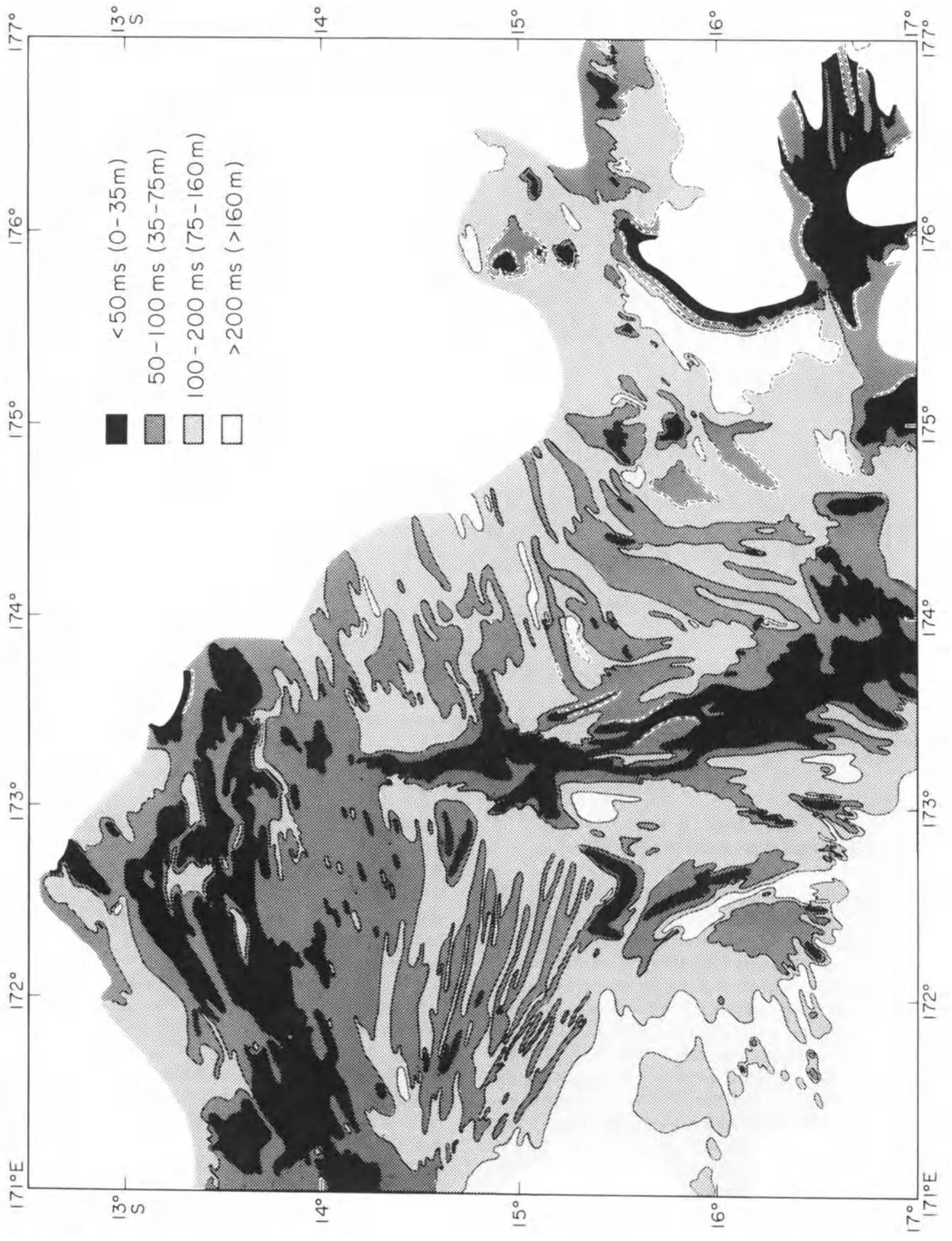

Figure 3. Sedimentary isopach map of the north central North Fiji Basin.

(Figure 3) and allowed classification of the various depositional terrains encountered within that area (Figure 4). Four types of terrains have been recognized:

1. "sediment free" areas (Figure 5), where sediment is not discernible on either high- or low-frequency reflection profiles (< 0.05 seconds thick);

2. "abyssal hill" areas (Figure 6), where sediment is just thick enough to smooth the rough basement topography (0.05-0.10 seconds thick);

3. "gently undulating" areas (Figure 7), where abyssal hills are more thickly blanketed by sediment and ponds of sediment occur in adjoining depressions (0.10-0.20 seconds thick);

4. "flat" areas with large sediment ponds (Figure 8) where abyssal hill topography is almost completely obliterated by thick wedges or deep ponds of sediments (> 0.2 seconds).

The chart shown in Figure 4 was prepared by comparing adjacent reflection profiles, establishing the category to which the profile or parts of the profile belonged, then locating the position of the boundaries between categories along those profile tracks. Sediment cover throughout most of the study area is never very thick (rarely thicker than 0.20 seconds), and differences in thickness are often subtle; the actual thickness values expressed here are approximate only. The thickest sediments (> 0.2 seconds) occur in the western part of the study area where the archipelagic apron of the New Hebrides, here named the New Hebrides Apron, extends east from the New Hebrides Arc into the North Fiji Basin.

DISCUSSION

The sediment thickness map prepared from seismic reflection data collected on the 1982 R/V KANA

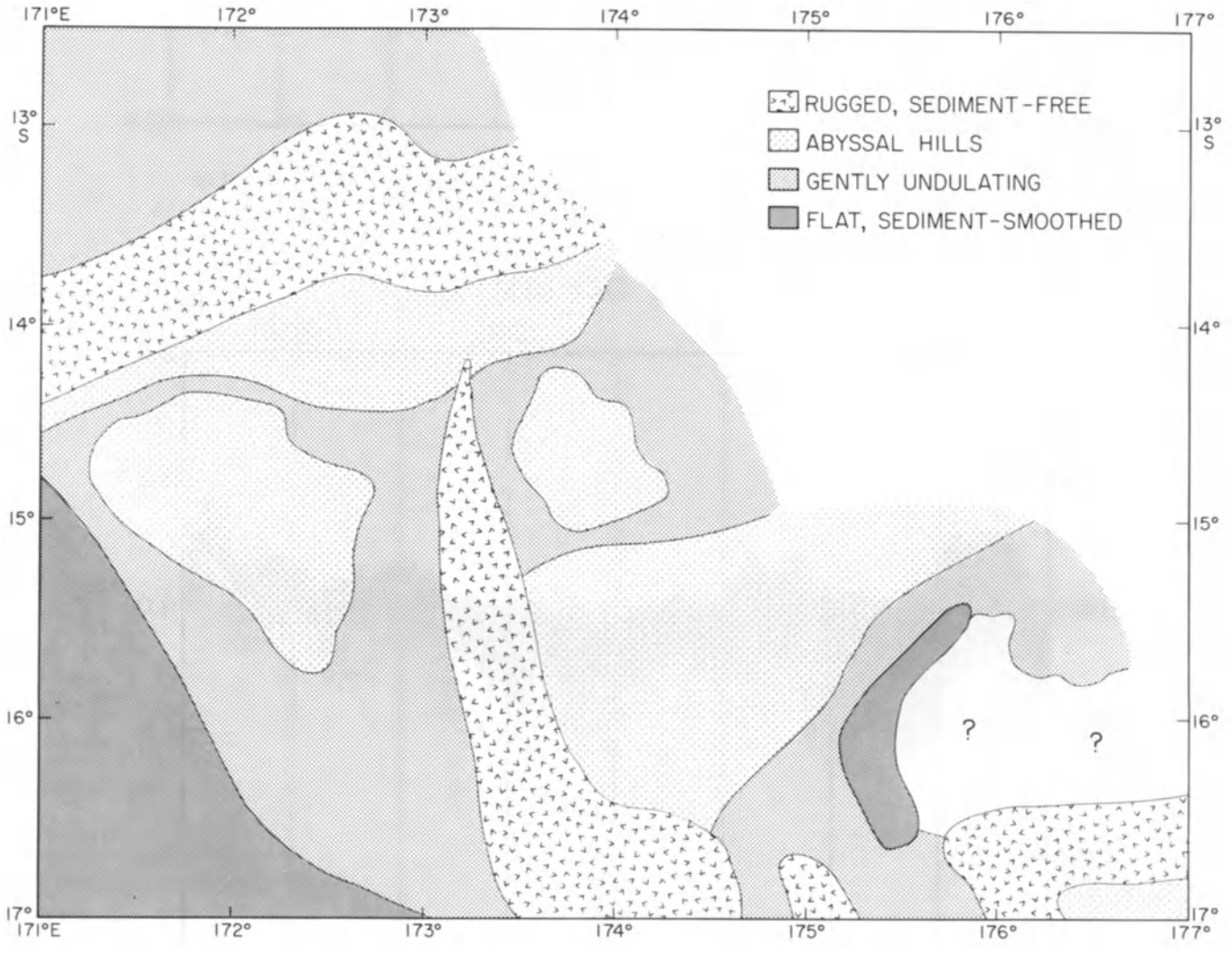

Figure 4. Sedimentary terrains in the north central North Fiji Basin: rugged sediment-free terrain (< 0.05 sec of reflection time); abyssal hill terrain (0.05-0.10 sec of reflection time); gently undulating terrain (0.10-0.20 sec of reflection time); flat, sediment-smoothed terrain (> 0.20 sec of reflection time).

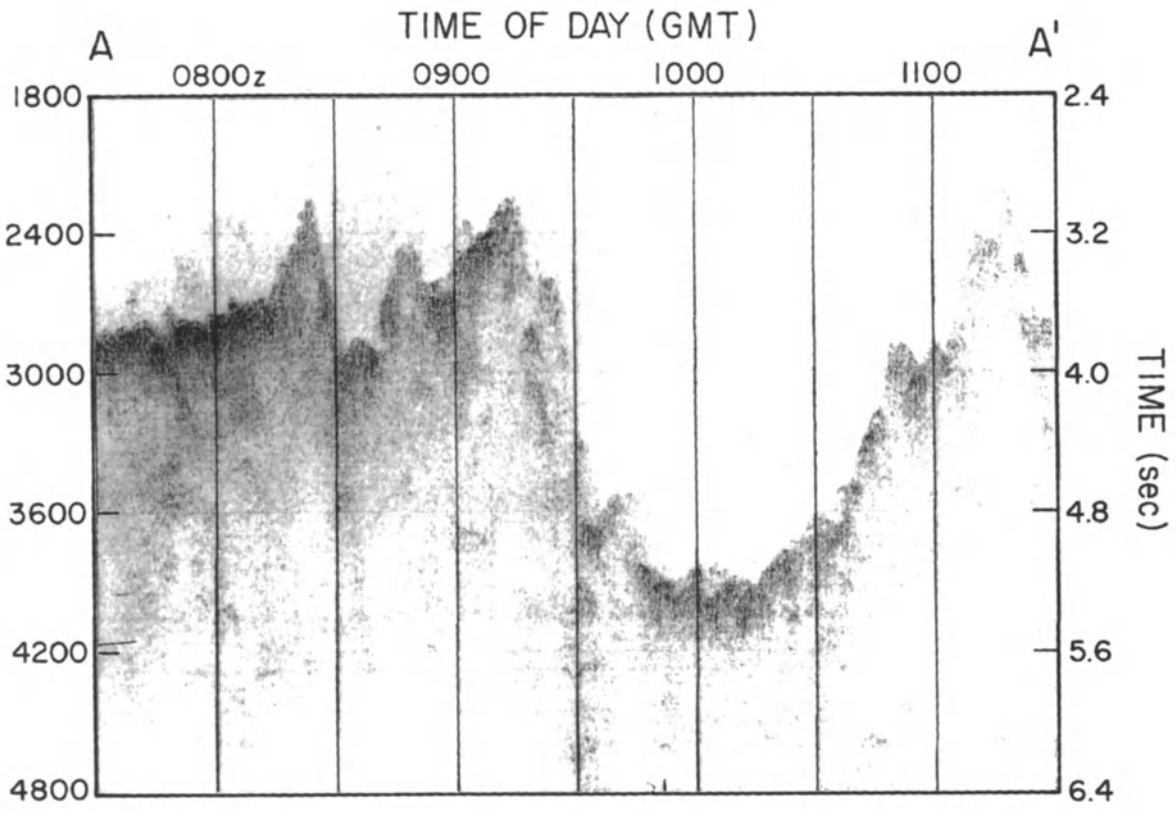

Figure 5. Reflection profile AA' (located in Figure 2) showing sediment-free areas along the South Pandora Ridge.

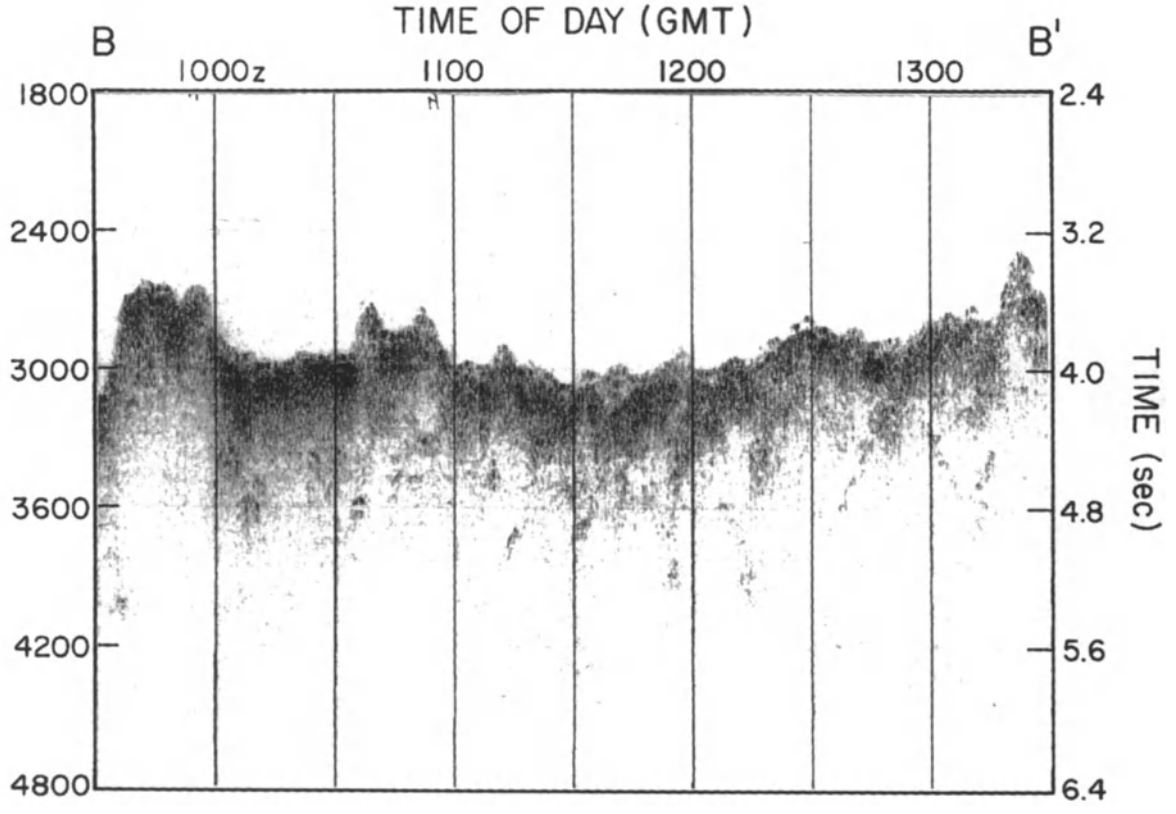

Figure 6. Reflection profile BB' (located in Figure 2) showing smoothed abyssal hill terrain.

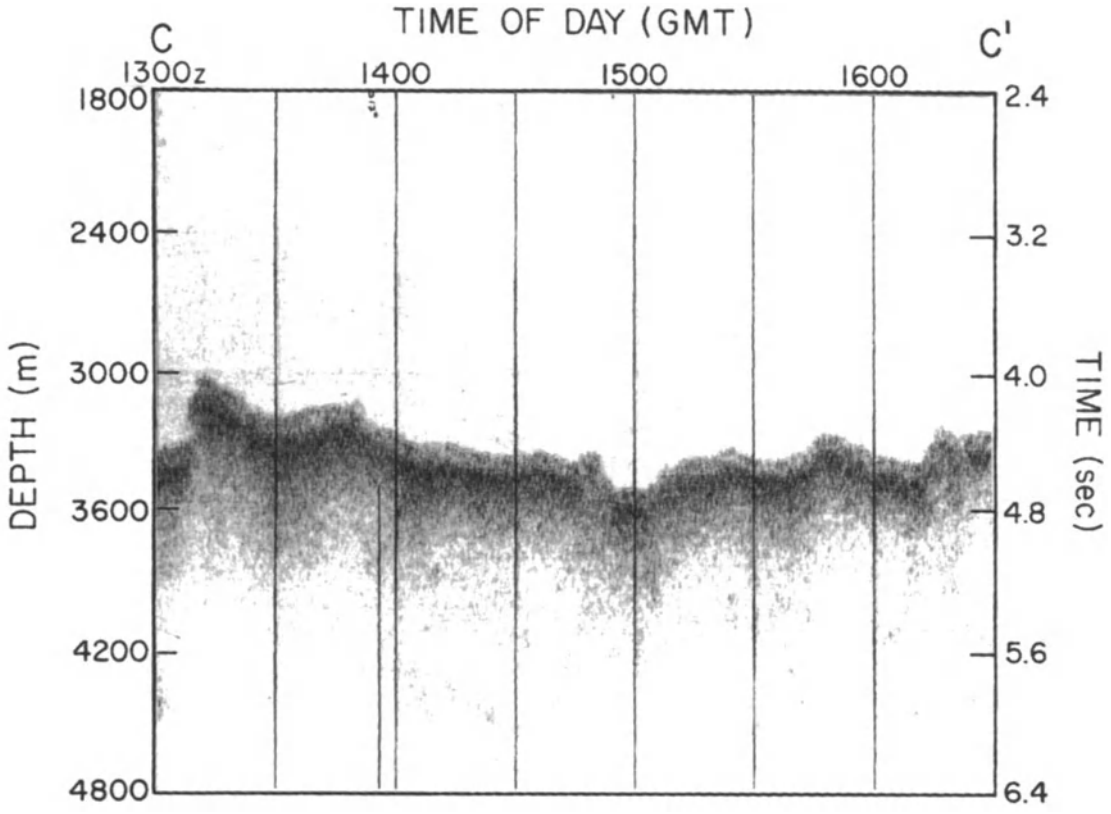

Figure 7. Reflection profile CC' (located in Figure 2) across gently undulating areas.

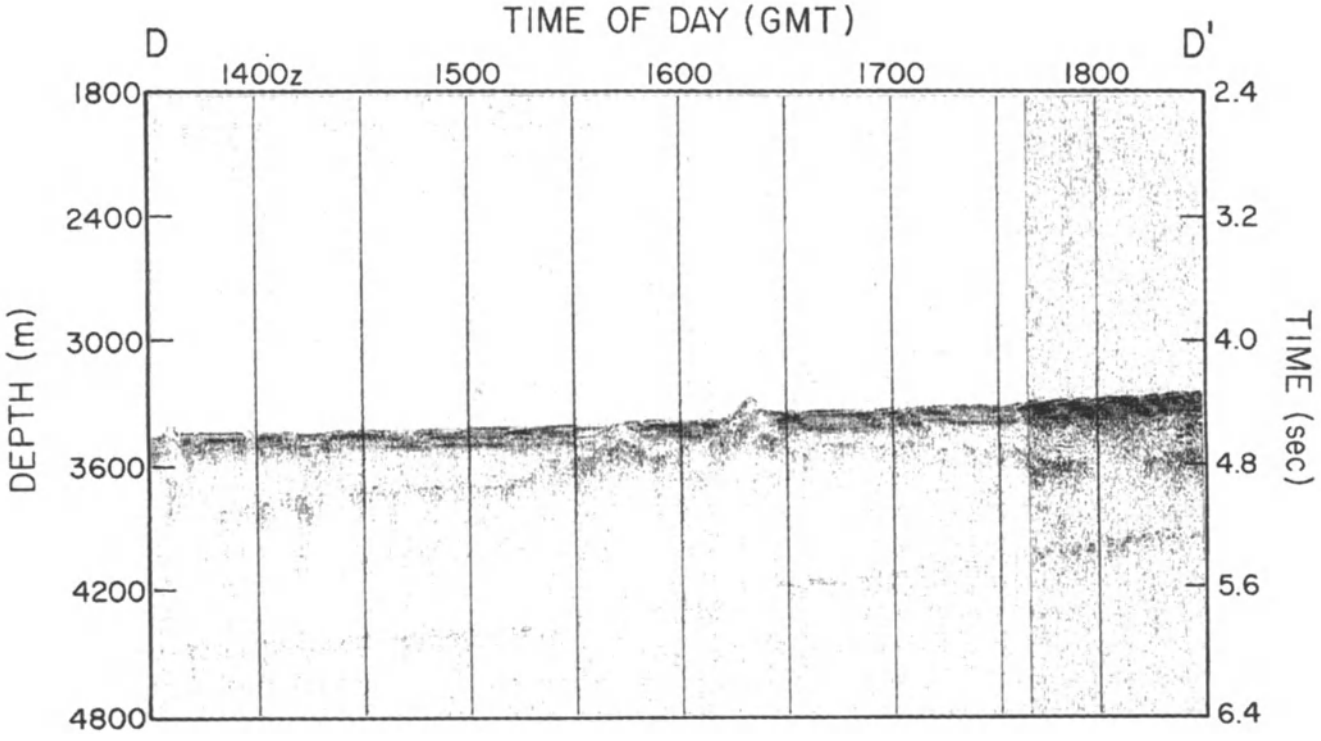

Figure 8. Reflection profile DD' (located in Figure 2) showing thick sediment wedges obscuring burial abyssal hill topography in the New Hebrides Apron east of the New Hebrides Arc.

KEOKI cruise to the North Fiji Basin displays a direct relationship to basin formation and active spreading ridge processes identifiable in other data sets (bathymetry, gravity and magnetic anomalies, sediment and rock analyses, underwater photography, and seismicity).

In the northwestern part of the area studied, the South Pandora Ridge (Hazel Holme Fracture Zone) trends WSW-ENE and consists of an elevated rift valley system essentially free of sediment (Figure 9). The rift zone is ofset at 14°00'S, 171°20'E, at 13°40'S, 172°10'E, and at 13°15'S, 173°50'E, just west of Horizon Bank (Kroenke et al., b, this volume). Between the latter two offsets, near 13°30'S, 173°00'E, the basin floor adjoining the southern flank of the South Pandora Ridge is broadly elevated and the seafloor is very irregular and, for the most part, thinly veneered with sediment as another sediment-free rift system, which trends almost N-S, approaches from the south. This area is heavily fractured and several large scarps are crossed by the cruise tracks through this area (Figure 10). The trends of some of these features are not known, but they are assumed to parallel the nearest rift (see Figure 4, Kroenke et al., b, this volume).

South of the South Pandora Ridge, sediment cover gradually thickens to the SW, away from both rift zones, the thickest cover lying in the southwest corner of the study area. North of the South Pandora Ridge, sediment thickness is controlled by topography. Sediment cover is thinner (<0.1 seconds) on elevated areas and thicker (>0.1 seconds) in adjacent basins.

Extending north from the central North Fiji Basin Ridge (CNFBR), the southern sediment-free rift zone is distinctly developed as a topographic depression between 17°S and 15°S (Figure 11) where it is approximately 20 km wide. Between 15°S and 13°30'S, where it approaches the southern flank of the South Pandora Ridge, the sediment-free area is narrower than that to the south and the topographic expression of the rift zone is more ill-defined and difficult to trace (Figure 12). "Abyssal hills" form narrow bands on either side of the rift zones; the bands are generally not much wider than the adjacent rift zone.

In some parts of the study area, especially the southwestern and southeastern ends, the sediment cover is thicker than 0.15 seconds. In the southwestern corner of the survey area, the sediment cover thickens to more than 0.2 seconds (Figure 3), demarcating the distal end of the New Hebrides Apron. The New Hebrides Apron extends from the New Hebrides Arc east into the North Fiji Basin (Chase, 1971; Luyendyk et al., 1974). It extends southward along the arc from the northern end to about 20°45'S where it ends abruptly (Karig and Mammerickx, 1972) and forms a thick wedge extending eastward from the arc about 350 km into the basin.

Near the arc as much as 1 km depth of sediment is present in the apron (Luyendyk et al., 1974). Away from the arc it thins, spilling into the depressions of the abyssal hill province in the north central part of the North Fiji Basin (Neprochnov et al., 1974; Eade and Gregory, this volume) and forming thin fingers of sedimentary fill. Over much of the apron the thick wedge of sediment totally buries basement relief, masking the tectonic fabric (Figure 11). Sediments in the apron are interbedded ash-rich pelagic ooze and volcaniclastic turbidites with a few air-transported ash layers (Eade and Gregory, this volume).

Luyendyk et al. (1974) state that "seismic reflection data show generally thicker sediment cover in the presumably older Pacific province north of the Hazel Holme Fracture Zone." What they show however is a profile (Figure 6 of Luyendyk et al., 1974) that is, very definitely located within the archipelagic apron east of the New Hebrides. Even though the track (shown in Figure 3 of Luyendyk et al., 1974) crosses a shallow, more or less sediment-free area toward the left side of the profile (shown in their Figure 6) i.e., south of "Hazel Holme Fracture Zone," the thickness of sediment visible at both ends of the profile is about the same.

In the southeastern part of the survey area, a partially filled sediment trough (Balmoral Trough) lies west of and adjacent to the Balmoral Ridge. Although the total thickness of sediment in the trough is unknown, profiles across the flanks of the trough indicate the presence of thicknesses in excess of 0.2 seconds. The presence of this trough adjacent to the steep western escarpment of Balmoral Ridge is suggestive of the depressed basin floor thrust beneath an adjoining upraised crustal block. The depression itself is probably partially filled by debris flows and turbidites.

CONCLUSIONS

Within much of the north central North Fiji Basin east of the New Hebrides Apron, the thickness of sediment overlying basement is directly related to the age of the oceanic crust in the North Fiji Basin. Along the active rift system, within the N-S rift zone, there is little or no sediment cover. Adjacent to the rift zone some ponding occurs. Outside the rift system, sediment thickness generally increases away from the rift zone.

During the last 700,000 years, average sedimentation rates in the study area have been approximately 9 m/m.y. (Eade and Gregory, this volume). Sediment rates, however, apparently were higher in the past. In the Pliocene, productivity – and thus sedimentation rate – was considerably higher than in the Pleistocene (W. Berger, pers. comm.). For example, the maximum Pliocene

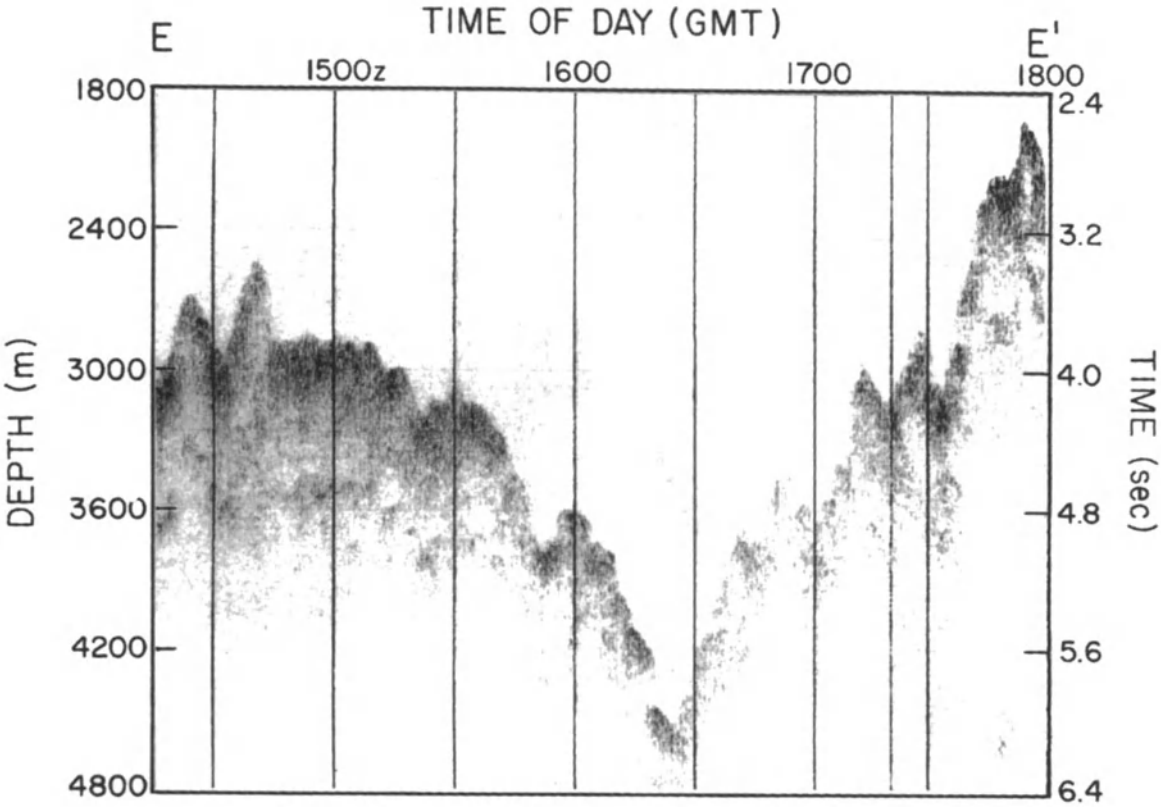

Figure 9. Reflection profile EE' (located in Figure 2) across the rift valley in the South Pandora Ridge.

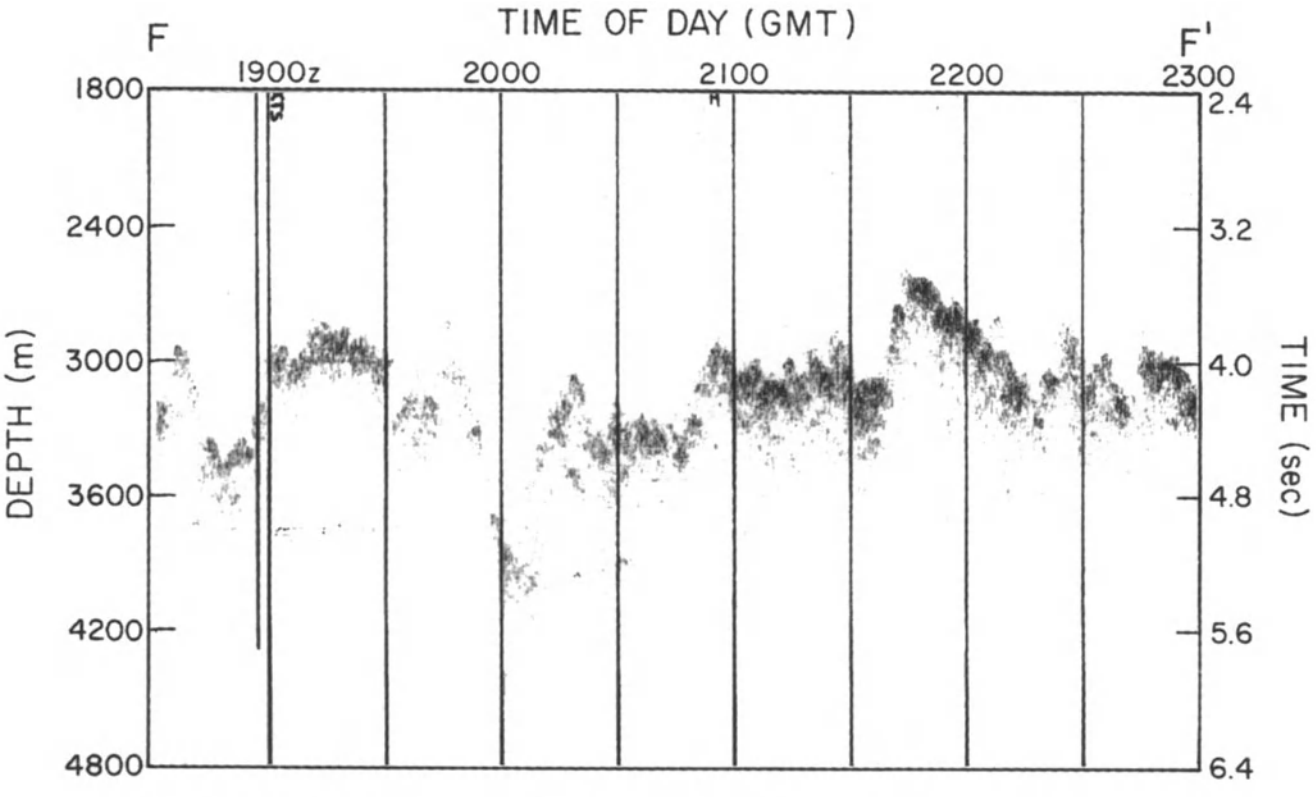

Figure 10. Reflection profile FF' (located in Figure 2) across the fractured area southeast of the triple junction.

Figure 10. Reflection profile FF' (located in Figure 2) across the fractured area southeast of the triple junction.

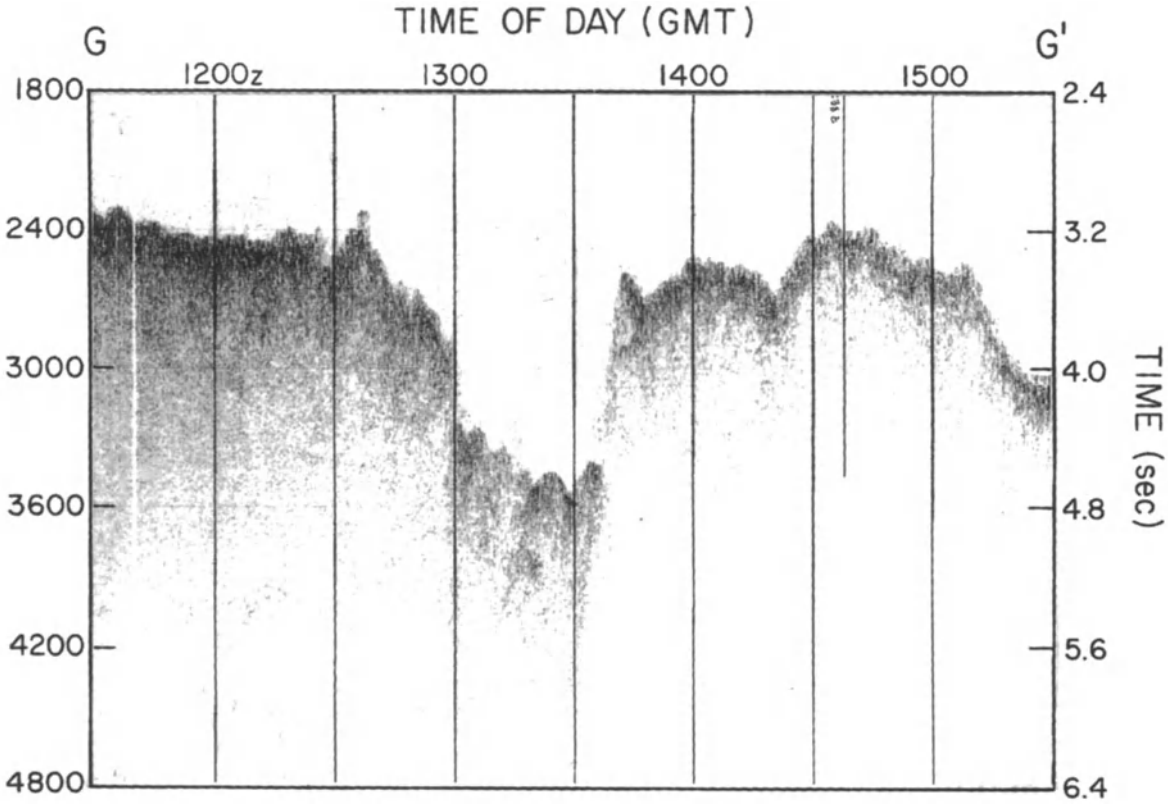

Figure 11. Reflection profile GG' (located in Figure 2) across the southern part of the southern rift system.

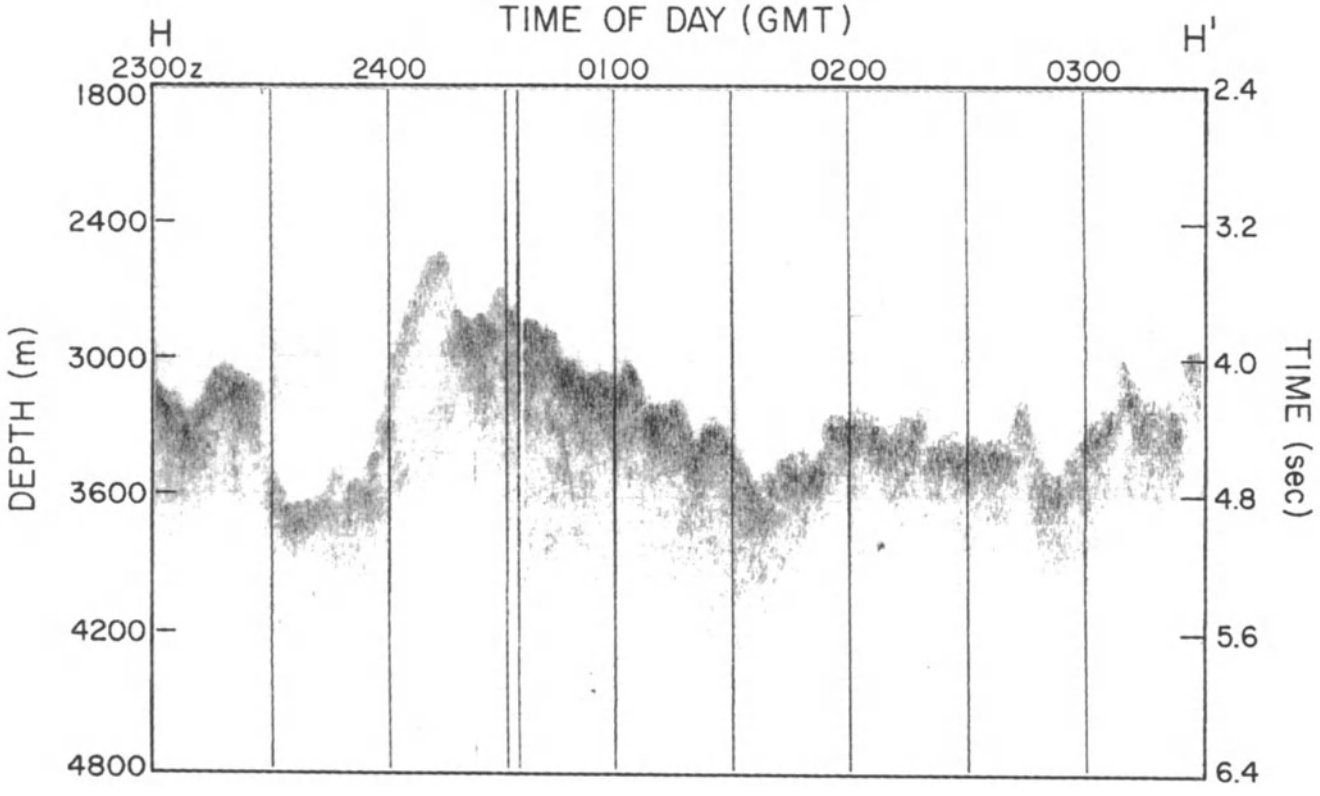

Figure 12. Reflection profile HH' (located in Figure 2) across the northern part of the southern rift system.

sedimentation rate on the Ontong Java Plateau at DSDP site 586 was almost twice as much as the maximum Pleistocene rate (Moberly, Schlanger, et al., 1986). If average (and more moderate) relative differences in sedimentation rates at Site 586 are used to adjust the late Pleistocene North Fiji Basin rate back to the late Miocene, the following rates can be inferred: 0-2.7 Ma = 9 m/m.y.; 2.7-5.1 Ma = 16 m/m.y.; 5.1-8 Ma = 6 m/m.y.; and >8 Ma = 16 m/m.y. Although sediment thickness values are approximate, an indication of age of basement may be deduced from sediment thickness and the average sedimentation rate. Estimated relative ages for each category of sediment thickness are

1. "sediment free": <3.5 Ma;
2. "abyssal hills": 3.5-7 Ma;
3. "gently undulating": >8 Ma;
4. "flat": variable in age, i.e., depending on location.

Maximum age of crust in the study area is probably upper Miocene (<10 Ma) south of the Vitiaz Arc and in the back-arc area immediately east of the New Hebrides volcanic arc. This is SOEST contribution no. 1755.

REFERENCES

Chase, C.G., 1971, Tectonic history of the Fiji Plateau: Geological Society of America Bulletin, v. 82, p. 3087-3110.

Chase, T.E., B.A. Seekins, J.D. Young, L.W. Kroenke, and V. von Stackelberg, 1987, Marine Topography of the Fiji Region, USGS-CCOP/SOPAC Pacific Project (unpublished).

Eade, J.V., and M.R. Gregory, Sediments of the North Fiji Basin, this volume.

Halunen, A.J., 1979, Tectonic history of the Fiji Plateau: Ph.D. Dissertation, University of Hawaii, Honolulu, Hawaii, 127 p.

Karig, D., and J. Mammerickx, 1972, Tectonic framework of the New Hebrides island arc: Marine Geology, v. 12, p. 187-205.

Katz, H.R., 1988, Offshore geology of Vanuatu—previous work, in Greene, H.G., and F.L. Wong (eds.), Geology and Offshore Resources of Pacific Island Arcs - Vanuatu Region, Earth Science Series, v. 8: Houston, Texas, Circum-Pacific Council for Energy and Mineral Resources, p. 93-122.

Kroenke, L.W., C. Jouannic, and P. Woodward (compilers), 1983, Bathymetry of the Southwest Pacific, Chart 1 of the Geophysical Atlas of the Southwest Pacific: CCOP/SOPAC, Suva.

Kroenke, L.W., J.V. Eade, and Scientific Party, Overview and Principal Results of the Second Leg of the First Joint CCOP/SOPAC Tripartite Cruise of the R/V KANA KEOKI, North Fiji Basin Survey (KK820316, Leg 3), this volume.

Kroenke, L.W., R. Smith, and K. Nemoto, Morphology and structure of the seafloor in the northern part of the North Fiji Basin, this volume.

Luyendyk, B.P., W.B. Bryan, and P.A. Jezek, 1974, Shallow structure of the New Hebrides island arc: Geological Society of America Bulletin, v. 85, p. 1287-1300.

Moberly, R., S.O. Schlanger, et al., 1986, Site 586, in Moberly, R., S.O. Schlanger, et al., Initial Reports of the Deep Sea Drilling Project, v. 89: Washington, DC, U.S. Government Printing Office, p. 213-235.

Neprochnov, Yu.P., I.M. Belousiv, V.P. Goncharov, A.A. Shreyder, V.N. Moskalenko, N.A. Marova, I.N. Yel'niko, G.M. Valysshko, and N.A. Shiskina, 1974, Detailed geophysical investigations in the North-Central Fiji Basin: Doklady Akademii Nauk SSSR, v. 218, no. 3, p. 688-691.

Kroenke, L.W., and J.V. Eade, editors, 1993, Basin Formation, Ridge Crest Processes, and Metallogenesis in the North Fiji Basin: Houston, TX, Circum-Pacific Council for Energy and Mineral Resources, Earth Science Series, Vol. 15, Springer-Verlag, New York.

SEDIMENTS OF THE NORTH FIJI BASIN

JAMES V. EADE[1]
New Zealand Oceanographic Institute, Wellington, New Zealand

MURRAY R. GREGORY
Geology Department, University of Auckland, New Zealand

ABSTRACT

Sediments of the North Fiji Basin have been studied as part of a geological and geophysical survey of the central and western parts of the basin. The study is based on a detailed examination of five piston cores that have sampled a continuous sedimentary record of the last 0.8 m.y. Three cores are from the sediment-covered, abyssal hill terrain in the central part of the Basin and two are from an archipelagic apron (New Hebrides apron), which extends east from Vanuatu into the western part of the North Fiji Basin. In the central part of the basin, calcareous pelagic oozes (nannofossil oozes) are the predominant sediment. Volcanic glass is also common, occurring in a single ash bed in each core, in ashy intervals where glass is less than 50%, and in pelagic ooze where it is persistently present as a few percent of the total sediment. From its physical and chemical characteristics the glass appears to be mostly airfall ash, derived from the central chain volcanoes of the New Hebrides arc to the west. A westerly origin is supported by the existence of strong tropospheric westerlies which dominate the structure of the atmosphere. Bioturbation is moderate to intense throughout all the central basin cores, the upper 5-20 cm commonly being continually churned over. Only the thickest ashes (greater than 2 cm) have survived this biological mixing moderately intact. Thinner ashes have either been partially mixed with ooze to form an ashy interval, or completely mixed and lost as recognizable layers. Three stratigraphic units are recognised in the central basin cores. The middle unit, approximately 0.5-0.25 Ma in age, has significantly more ash than the other two units and represents a period of increased volcanic activity in Vanuatu. Sediment accumulation rates are as low as 9 m/m.y. for the ooze and as high as 20 m/m.y. for the middle unit in one core where, in addition to ooze and ash, there has also been some reworking of sediment from an adjacent topographic high. In the western part of the North Fiji Basin, sediments are predominantly alternating ashy pelagic ooze and volcaniclastic graded beds of the New Hebrides Apron. Sediment in the graded beds was derived from shallow water along the eastern side of the New Hebrides arc and transported by turbidity currents eastward into the western part of the North Fiji Basin.

INTRODUCTION

The North Fiji Basin (also called the Fiji Plateau) lies at 2000-3000 meters water depth and is bounded by the New Hebrides Arc to the west, seamounts of the Melanesian Borderland to the north, the Fiji platform to the east, and the Hunter Ridge to the south (Figure 1). The broad geological and geophysical setting is reviewed by Kroenke et al. (this volume,a). Sediments accumulating across the basin are dominated by the remains of pelagic carbonate organisms settling from surface waters and fine volcanic debris from surrounding volcanic centers.

Chase (1971) found the sediments to be calcareous-siliceous oozes with 5-10% volcanic glass and other noncarbonate minerals. He concluded that sediment at the base of the longest core from the northern part of the Balmoral Basin was probably no older than 0.5 Ma, giving a sedimentation rate of approximately 10 m/m.y., and that older microfossils present had been reworked. The sediment covering basement in most of the basin was recognized as being thin (less than 400 m), especially

[1]Now with SOPAC Technical Secretariat, Suva, Fiji

in the central part where it was seen to be less than 100 m. He concluded therefore that the basin was quite young. Chase (1971) also noted the presence of a sediment fan coming off the New Hebrides arc complex to the west and spilling out eastward into the basin. Its thickness decreased from 1200 m at the base of the arc to 400 m at its eastern limit.

Luyendyk et al. (1974) also noted the Quaternary age of several cores from the basin and described them as being rich in ash. They referred to a sediment apron on the western side of the basin, describing it as extending for 200 km along the New Hebrides volcanic chain.

Neprochnov et al. (1974) recognized the extreme morphologic heterogeneity of the North Fiji Basin. They observed that the sediment cover in the northern part of their study area (the South Pandora Ridge) contained ash and was very thin (less than 50 m) if not absent in many places. In the west and southwest they identified an aggradational plain sloping gently eastward from the New Hebrides arc. In this part of the basin, plain sediments were up to 50 m thick, filling depressions on the seafloor. Farther east sediments 100-150 m thick were draped over a hilly terrain.

Jezek (1976) studied three cores from the western side of the North Fiji Basin. Each of these had a high frequency of volcanic ash beds which averaged about two per meter of core. He found wide compositional variations in the glass shards from individual ash beds which made correlation between cores difficult. Glasses typical of both calc-alkaline suites and suites with tholeiitic affinities were recognized. Jezek concluded that these beds were ashes most likely from recent volcanoes of the New Hebrides arc, but noted that prevailing wind and current directions did not support a westerly source. He also concluded that the glasses originated from a stratified magma chamber or from multiple eruptions of a single magma chamber rather than eruptions of two or more unrelated volcanic centers.

Brocher et al. (1985), in a study of the regional sedimentation patterns along the Northern Melanesian Borderland, described sediments in the northeastern part of the North Fiji Basin as calcareous oozes with minor ash that had accumulated at an average rate of 7 m/m.y. This rate was higher near prominent structural highs and volcanic centers. They concluded that a substantial portion of the volcanic glass present in cores in the North Fiji Basin represented abraded pumice fragments originating from Tonga. The results of a magnetostratigraphic survey of a number of cores, including five used in this study, were appendixed to Brocher et al. (1985). Cores PC-5 and PC-7 penetrate the Brunhes-Matuyama Boundary (0.7 Ma). PC-5 has a maximum age of 0.85 Ma indicating an average sediment accumulation rate of about 13.5 m/m.y., and PC-7 has a maximum age of 0.7 Ma indicating an average sediment accumulation rate of about 10.7 m/m.y. These rates were higher than those recorded in most of the other cores that Brocher et al. (1985) studied, which were from localities farther east and north of the cores studied here. The other three cores, PC-6, PC-8, and PC-9, are all magnetically normal and were therefore assumed to be less than 0.7 Ma in age.

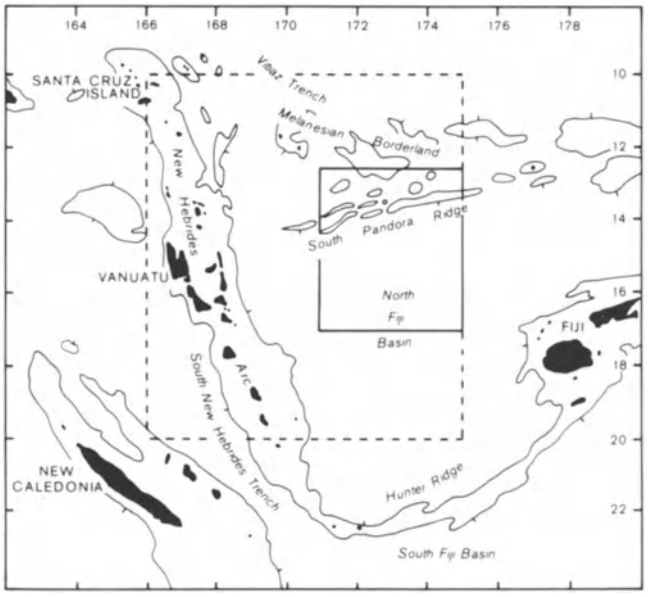

Figure 1. Map of the area surveyed by cruise KK820316 Leg 3 (solid line) and the area discussed in this paper (dashed line).

METHODS

This study is based primarily on five piston cores (Table 1), supplemented by three free-fall gravity cores, collected on cruise KK820316 Leg 3 by the Hawaii Institute of Geophysics (HIG) vessel R/V KANA KEOKI. The area studied during the cruise focused on the central part of the North Fiji Basin including the South Pandora Ridge (Figure 1). Other cores and surface sediment samples in the collection of HIG and New Zealand Oceanographic Institute (NZOI) were examined in passing but not studied in detail.

The five KK820316 cores were examined in detail by both authors. The following were studied: core stratigraphy and bioturbation (visual examination); sediment composition (smear slides study); grain size (sieve and pipette methods); carbonate determination (acid digestion and titration); glass morphology and composition (scanning electron microscope with an attached energy dispersive X-ray microanalyzer).

CORE LOCALITIES

Three distinct sedimentary terrains have been recognized in the study area: (1) rugged, mostly sediment-free areas (e.g., South Pandora Ridge); (2) smoothed, sediment-covered abyssal hill terrain (Pentecost, Balmoral,

Table 1. Station data.

Sta No.	Core No.	Latitude °S	Longitude °E	Depth (m)	Core Length (cm)
19	PC-5	13°58.4'	173°57.5'	3400	1161
22	PC-6	16°30.4'	171°32.3'	3165	962
24	PC-7	13°49.7'	172°46.1'	3150	765
26	PC-8	13°31.3'	171°58.2'	3020	798
31	PC-9	16°28.8	169°30.6'	3040	426

and Pandora basins)[1]; and (3) a flat archipelagic apron (New Hebrides apron).

The five cores studied came from two of these terrains (Figure 2), the abyssal hill terrain and the archipelagic apron. Three of these cores (PC-5, PC-7, PC-8) are from the abyssal hill terrain (Figure 3). Core PC-5 is from a small, narrow trough in the northwestern part of Balmoral Basin approximately 45 km from South Pandora Ridge. The trough is about 7 km wide, and its floor lies at 3400 m, some 600 m below the regional depth of the surrounding seafloor. Sediment in the trough and on the adjacent hills is 0.1-0.2 seconds thick. PC-5 was collected at the edge of the trough at the foot of a steep (approximately 20 degrees) slope. PC-7 is from an area of rugged relief in the northeastern corner of Pentecost Basin less than 25 km from South Pandora Ridge. The maximum relief is about 350 m and there are no steep slopes within the immediate vicinity of PC-7. Sediment distribution is patchy. Topographic highs are either sediment-free or have a very thin cover of sediment. PC-7 is from a small depression, 150 m deep, with sediment no more than 0.1 seconds thick. PC-8 is from the edge of a basin which lies at 3000 m and where sediments are about 0.25 seconds thick. A few kilometers south of PC-8 the seafloor rises steeply 900 m to the crest of the South Pandora Ridge. On parts of the ridge there is some sediment (up to 0.05 seconds) but most slopes appear sediment free.

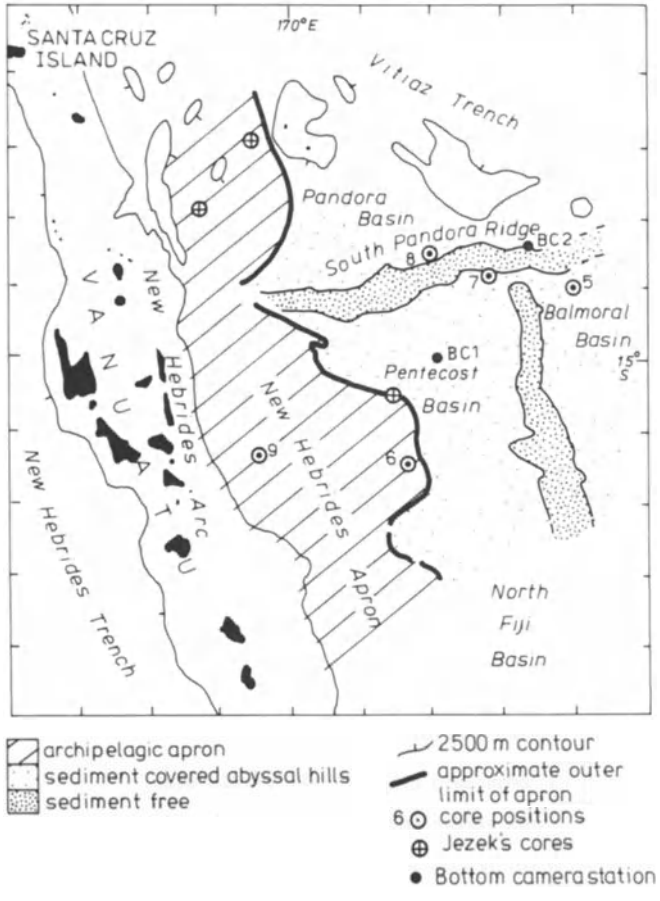

Figure 2. Diagram of sediment terrains in the North Fiji Basin and core sampling locations.

The South Pandora Ridge is an active spreading center (Kroenke et al., this volume,a) and is therefore the closest potential source of pyroclastic material to PC-5, PC-7, and PC-8 core localities. The nearest sources of Quaternary subaerial volcanism to these three core localities are Vanuatu, 500-750 km to the west, and Fiji, 600-800 km to the southeast.

Two cores, PC-6 and PC-9, are from the New Hebrides apron (Figure 2). PC-6 is from a trough at the outer (eastern) edge of the apron. Here the apron extends, as fingers of sedimentary fill up to 0.25 seconds thick, east into the deeper parts of the abyssal hill terrain (Figure 3). PC-9 is from the central part of the apron where the seafloor slopes very gently eastward. Sediments are up to 0.7 seconds thick in the vicinity of PC-9 and completely bury the irregular basement relief (Figure 3). Sediments at both localities on the apron have many highly reflective layers which lie subparallel to the seafloor (Figure 3). PC-9 and PC-6 lie 150 km and 350 km respectively from the New Hebrides arc.

REGIONAL SURFACE SEDIMENT DISTRIBUTION

Surface sediments of the North Fiji Basin (Figure 4) are clay-rich calcareous oozes with varying amounts of volcanic ash (Chase 1971; Jezek, 1976; Brocher et al., 1985; McMurtry et al., this volume). Carbonate content is between 50% and 75% over most of the basin floor. Values are higher (greater than 60%) in the northern part of the basin than in the south. Silt-sized nannofossils make up most of the carbonate fraction and many of them are fragmented to clay-sized grains to form a muddy nannofossil hash. Sand-sized foraminifera may be locally abundant, especially on and around topographic highs where coarser grained sediments are

[1]Kroenke et al. (this volume, b) further divide this category: abyssal hills and gently undulating terrain.

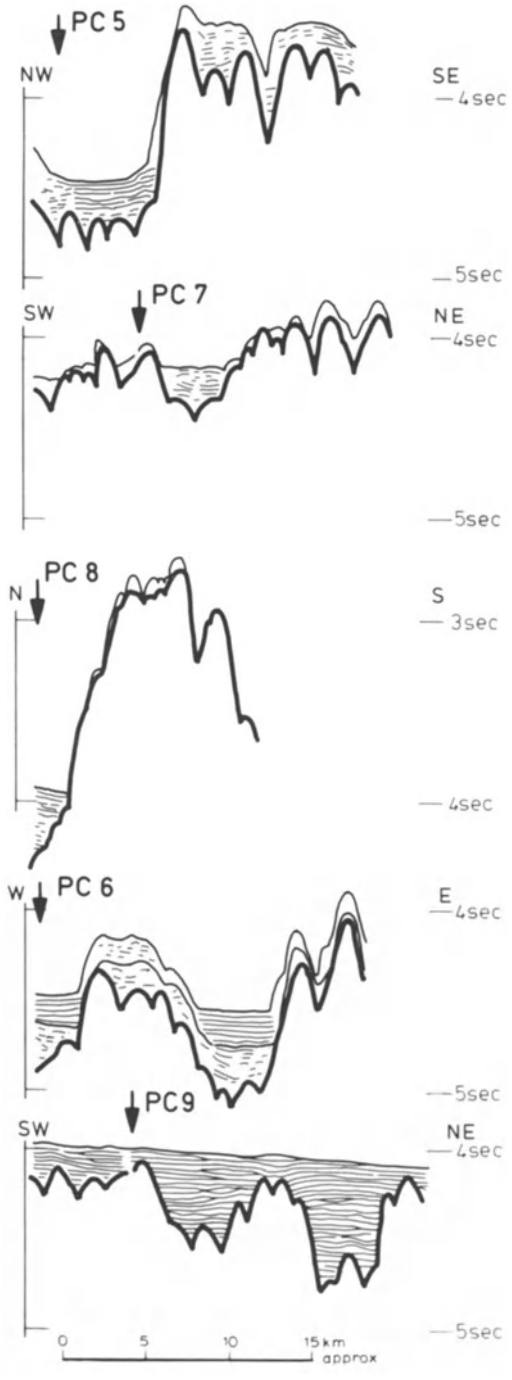

Figure 3. Tracings of seismic reflection profiles taken as R/V KANA KEOKI crossed core positions PC-5, PC-6, PC-7, PC-8, and PC-9.

more common (Brocher et al., 1985). Carbonate values decrease in the west to less than 30% over most of the sediment apron, which extends east from the New Hebrides arc.

Surficial sediments of the North Fiji Basin commonly contain 15-20% volcanic glass sediment. This decreases to less than 10% in the north and northwest (Brocher et al., 1985), and increases to the west, being more than 30% in the sediment apron east of Vanuatu. Also, surficial sediments along the New Hebrides arc are dominated by glass and pumice (Exon and Cronan, 1983).

Clay minerals are present in moderate amounts (10-25%) in all samples. Smectites, probably formed in place by the alteration of volcanic glass (McMurtry et al., this volume), are the most common clays present.

SUBSURFACE SEDIMENTS

Sediments of the two terrains cored are distinctly different and will be discussed separately. Sediments of the abyssal hill terrain of the central part of the North Fiji Basin (cores PC-5, PC-7, and PC-8) consist typically of foram- and clay-rich nannofossil ooze with variable amounts of ash. Sediments of the New Hebrides apron in the western part of the North Fiji Basin are dominated by interbedded ashy nannofossil ooze and graded volcanic silt and sand beds. All cores contain coarse sand- to granule-sized, rotten pumice clasts scattered throughout.

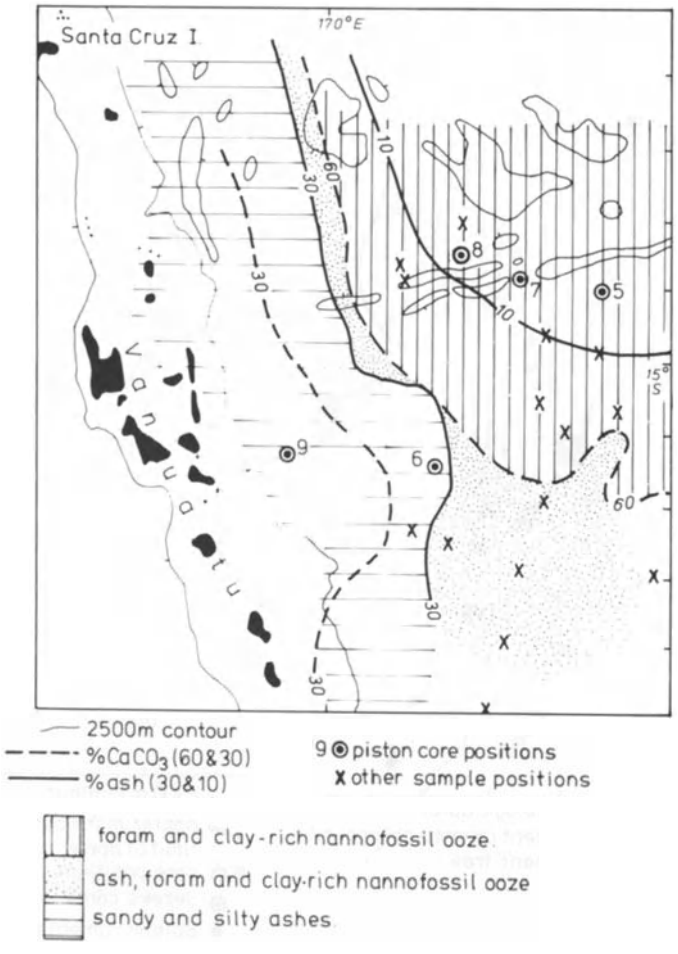

Figure 4. Surface sediments of the central and western North Fiji Basin.

Abyssal Hill Terrain Sediments (Cores PC-5, PC-7, PC-8)

A summary of the physical parameters and composition of abyssal hill terrain sediments is given in Table 2. Results of smear slide analyses are given in Appendix 1.

Most of the sediments in cores PC-5, PC-7, and PC-8 are uniform light yellow brown (10YR 6/4)[1] to yellow brown (10YR 5/4), sandy silty clays (Figure 5) consisting of ash-bearing, foram- and clay-rich nannofossil oozes. Calcium carbonate is dominant (57-89%) and is made up of nannofossils, very fine non-specific carbonate grains (probably nannofossil 'hash'), and foraminifera. Clay minerals are present throughout all cores in moderate (10-25%) amounts. Volcanic glass grains also occur in the oozes of all three cores but only in small quantities (1-13%). Rare individual coarse sand- to granule-sized grains of degraded pumice are also present.

Table 2. Average grain size, carbonate, and volcanic glass for cores PC5, PC-7, and PC-8.

	Grain size			CaCO3	Volcanic Glass
	s	z	c	%	%
Ooze	20	34	46	73	5
Ashy ooze	21	46	33	59	22
Major ash	39	41	20	10	76

In all cores there are several intervals slightly darker (brown - 10YR 5/3 to dark brown - 10YR 4/3) and slightly coarser (sandy clayey silt - Figure 5) than the nannofossil oozes. These intervals differ from the ooze in having less calcium carbonate (60-67%) and more volcanic glass (10-46%) and are referred to here as "ashy intervals". Both upper and lower boundaries of these intervals are diffuse and the darker and coarser ashy ooze grades both up and down into lighter and finer nannofossil ooze. In each core there is one interval which is dominantly volcanic glass. In PC-5 this interval occurs at 690-697 cm sub-bottom and consists of 85% volcanic glass. In PC-7 it lies at 522-534 cm and has 60% glass, and in PC-8 it is found at 760-770 cm and has 82% glass. These intervals are volcanic ashes with very fine sand- to coarse silt-sized glass grains (Figure 5). They have sharp bases and grade upwards into ashy ooze which in turn grade into overlying ooze. Sediment grain size is directly related to the proportion of volcanic glass present (Figure 6).

Volcanic glass grains were found in all smear slides examined from all three cores PC-5, PC-7, and PC-8 (Appendix 1). Most grains are coarse silt-sized (31-63 microns) and range from fine silt to fine sand. Some finer (<31 micron) ash is present in all samples. Glass grains in the single ash layer in each core are dominantly very fine sand- to coarse silt-sized. Both shard and pumice-shaped grains are common (Figures 7a,b). Shards are fragments from the walls of large vesicles and both elongate and equidimensional shard grains are common. Pumice grains are generally elongate and have

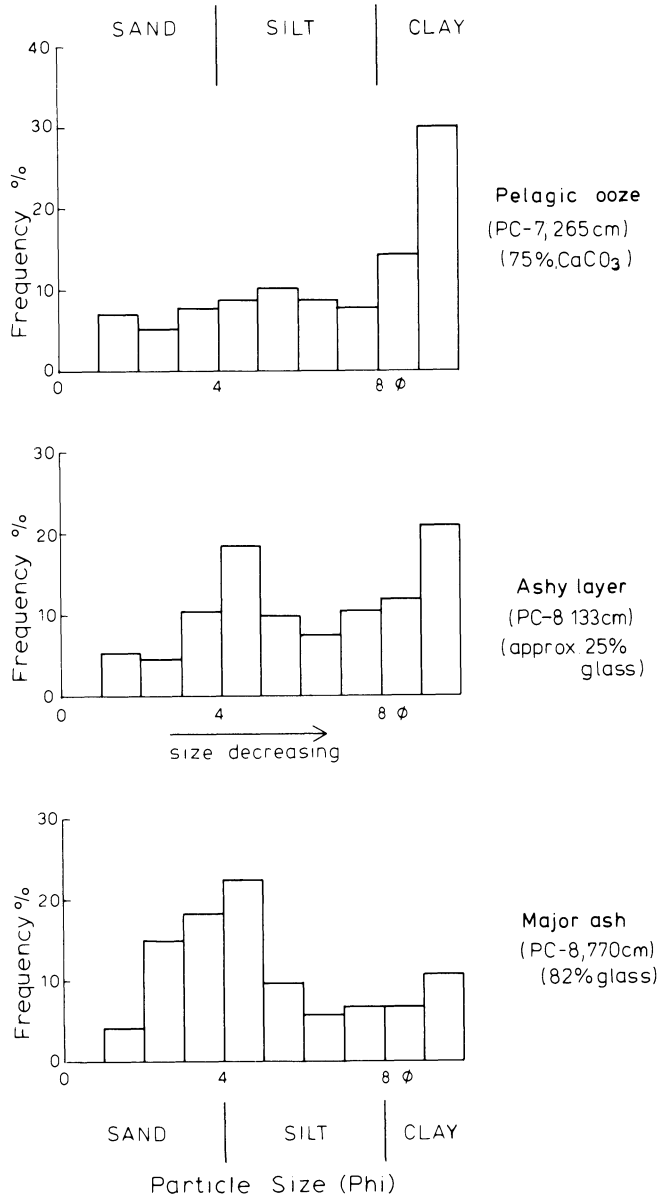

Figure 5. Typical grain size analyses for the major ash, an ashy layer, and pelagic ooze in cores from the central part of the North Fiji Basin.

[1]Munsell color system

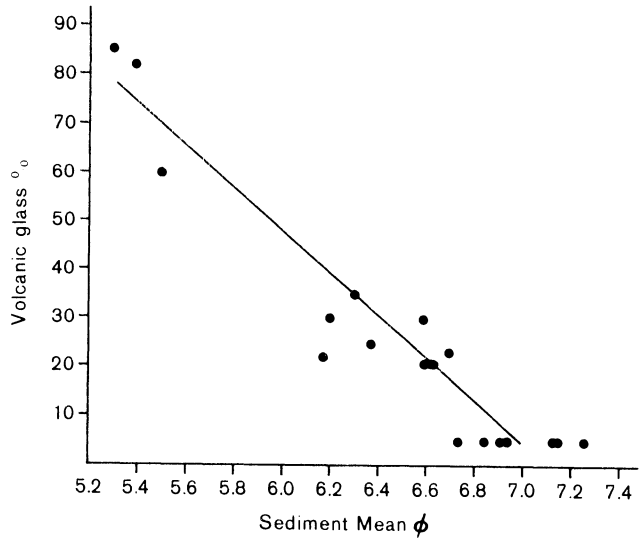

Figure 6. The relationship between grain size (sediment mean) and the percentage volcanic glass in sediments of the central part of the North Fiji basin.

tubular vesicles in subparallel alignment (Figure 7b). Equidimensional pumice grains are also present and have more spherical vesicles and generally thicker walls between vesicles (Figure 7c). All grains are moderately fresh to fresh looking with clean faces and sharp edges. Some have a slightly dirty appearance with clay-sized grains attached to their surfaces. These grains appear to be partly altered. In transmitted light most glass is clear to light brown in color. Clear colorless glass dominates in the single ash layer.

Chemical analyses of individual glass grains indicate that there is as much variability of the chemistry of grains within intervals as between intervals (Appendix 2). The most distinct variable is SiO_2 content which ranges from basaltic (48%) to rhyolitic (73%). The majority of the grains analyzed are either andesitic (58-65% SiO_2) or dacitic (65-70% SiO_2). Although there is considerable variation in other elements, certain distinctive features are apparent. K_2O and $Na_2O + K_2O$ are both high. Some analyses with exceptionally high K_2O values may be suspect but most analyses on a plot of K_2O versus SiO_2 fall within an elongated cluster. On this plot, grains from the single ash layer all lie in a tight cluster at the most silicic end of all analyses. K_2O at SiO_2 57.5 is approximately 3.0. TiO_2 (average 0.7%), Na_2O/K_2O (average 1.0%), and MgO (average 1.5%) are all low.

New Hebrides Apron Sediments (Cores PC-6, PC-9)

A summary of the physical parameters and composition of New Hebrides apron is given in Table 3. Details of the composition from smear slide analyses are given in Appendix 1.

The apron sediments are mostly interbedded ashy pelagic oozes and graded beds of volcanic sand and silt.

Table 3. Average grain size, carbonate and volcanic glass for cores PC-6 and PC-9

		Grain size			$CaCO_3$	Volcanic Glass
		s	z	c	%	%
Pelagic ooze	(PC-6)	22	39	39	50	16
Ashy ooze	(PC-6)	24	49	27	34	41
Ashy ooze	(PC-9)	42	42	16	19	22
Graded bed base	(PC-6)	47	45	8	16	82
Graded bed base	(PC-9)	55	38	7	2	50*
light grey ashes	(PC-9)	4	84	12	0	94

* more opaque minerals, i.e., heavy minerals sorted out of PC-6 (pyroxene/opaques/feldspars)

The mineralogy of these has been described in detail by Jezek (1976) who studied three cores from the apron. Two were located north of South Pandora Ridge (the Hazel Holme Fracture Zone in Jezek, 1976) and one to the south (Figure 2). Both PC-6 and PC-9 are from the apron south of the South Pandora Ridge. PC-6 and Jezek's southern core are from the distal end of the apron and PC-9 is from the inner part of the apron.

The upper part of the sedimentary column cored at both PC-6 and PC-9 consists mostly of yellow brown (10YR 5/4) ooze to very dark brown (10YR 3/2) ashy ooze. The ooze, found only in PC-6, is a silty clay with average contents of 50% $CaCO_3$ and 16% volcanic glass (Table 3). Ashy intervals occur in both cores and are darker (very dark brown, 10YR 3/2), coarser (clayey sandy silts), have less carbonate (average 19% and 34%), and have more volcanic glass (average 22% and 41%) than the ooze of PC-6. In the middle part of PC-6 and the lower part of PC-9, black silty sand beds are common. These beds consist predominantly of volcanic glass (averages of 50% and 52%) but also contain moderate amounts of feldspar and heavy minerals such as pyroxene and opaques which include magnetite. Most of these grains do not look fresh and have a tumbled and abraded appearance (Figures 7d,e). The black silty sands have sharp bases grading up to clayey silt (ashy ooze) in both cores and commonly up to silty clay (pelagic ooze) in PC-6 only. In many of these graded units three parts can be identified. These are a basal massively to faintly laminated part, a middle finely laminated part, and an upper, lighter-in-color, moderate to heavily bioturbated part. The middle laminated part is not always seen and where not present may have been destroyed by bioturbation.

Six glass grains from the base of one graded unit in PC-6 were analyzed and found to vary from basaltic (48% SiO_2) to andesitic (61% SiO_2). This supports the much more detailed observations of Jezek (1976) who analyzed many glasses from these black sandy beds and

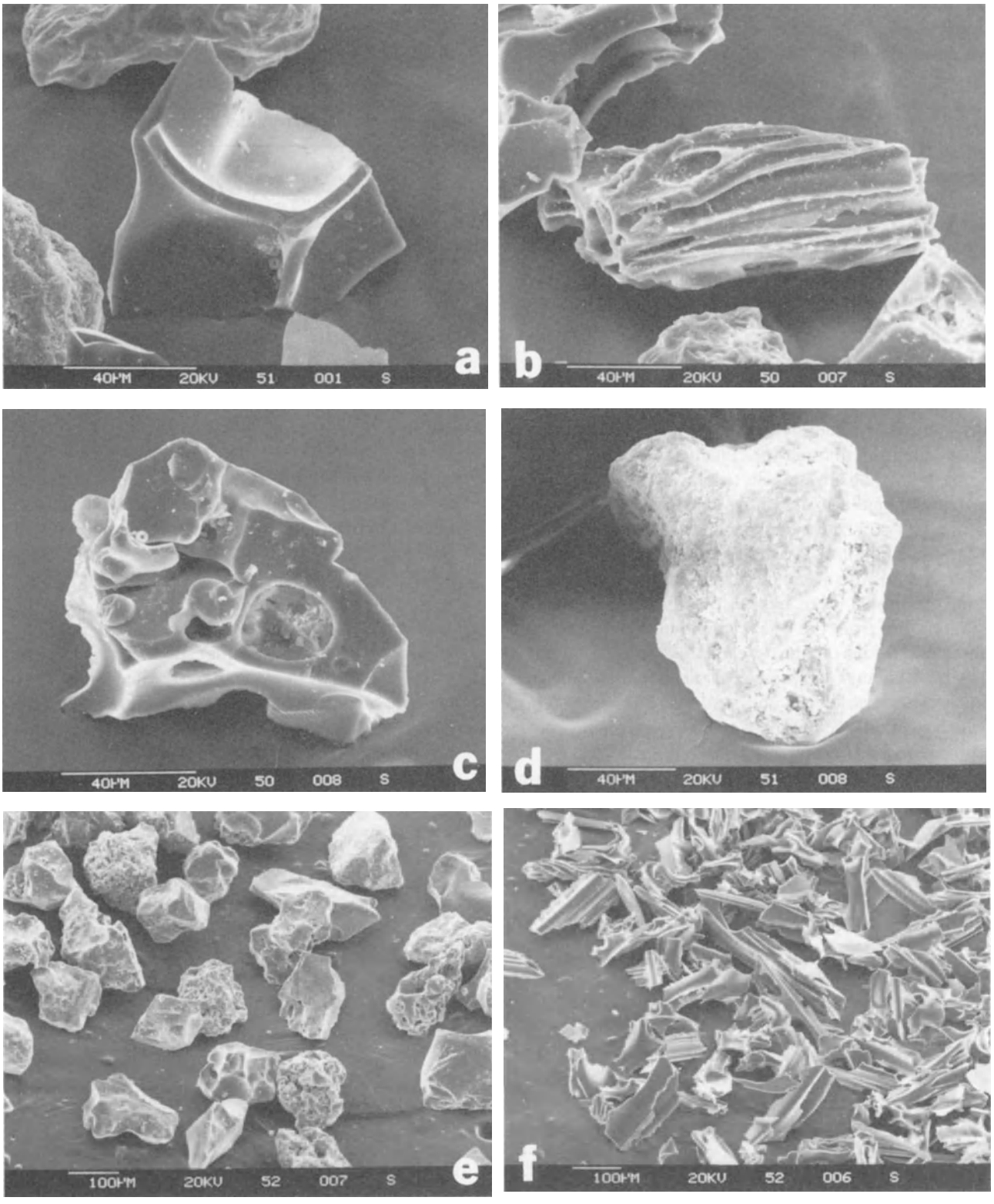

Figure 7. Volcanic glass, North Fiji Basin: (a) bubble-wall shard, PC-5, 694 cm; (b) pumice grain with elongate, tube-like vesicles, PC-5, 394 cm; (c) equidimensional pumice grain with spherical vesicles, PC-5, 394 cm; (d) abraded grain from graded bed, PC-9, 44 cm; (e) abraded grains from graded bed (turbidite), PC-9, 200 cm; (f) fresh-looking shards from ash bed, PC-9, 269 cm.

found wide compositional variations in glass grains from individual layers. The graded nature of these beds, the presence of laminations within many beds, the presence of abraded grains in the coarser basal part, and considerable variation in chemical composition of glass grains, suggest a turbidity current origin for the black graded beds. These grade upwards into lighter colored pelagic sediment.

Also present in both cores are a few light blue-grey (10YR 6/2) well-sorted silts consisting of fresh, clear shards of volcanic glass (Figure 7f). Four grains from one of these beds were chemically analyzed. All four are very similar and lie on the dacite-rhyolite boundary at 68-70% SiO_2.

BIOTURBATION

A seafloor intensely churned by biologic activity is seen in bottom photographs taken at Station 23 (BC-1) in the smoothed abyssal hills terrain (Kroenke et al., this volume,b), and also at Station 25 (BC-2) where pelagic sediment is pocketed amongst the fresh pillow basalts of the South Pandora Ridge (Figures 8-11, also see McMurtry et al., this volume, Figures 8a,b). Very few bottom organisms were captured on film at these two stations, but from the tracks visible in the photographs several different organisms can be identified. In only a few of the almost 90 frames examined is there any sign of ripple marks, scours, and shadows or other evidence which suggests sediment winnowing through bottom current action (Figure 12).

Lebensspuren are identified in the bottom photographs and can be separated into sedentary and mobile functional types (Table 4) using criteria established by Young et al. (1985).

Sedentary

The seafloor is dominated by conical mounds (Figures 8a, 9a,b, and 11b) of varying shape and size (estimated diameters of up to and occasionally exceeding 50 cm and heights of up to 20 cm or so). An apical pit, perhaps the surface expression of an open vertical shaft, is present in several smaller, steeper-sided mounds. At the crests of some mounds there are ill-defined shallow depressions which have been formed by decay and collapse following abandonment by their maker. The progenitors of these mounds are unquestionably several (see Young et al., 1985) although decapod crustaceans are likely to be the dominant taxa. One mound was seen to be partly surrounded by weak rays similar to those described by Young et al. (1985, Figure 6) and for which a xenophyophorian origin is suggested.

Table 4. Functional types of epifaunal and shallow infaunal lebensspuren identified in bottom photographs at Stn 23 (BC-1) and STN 25 (BC-2) (see Figures 8-11).

Sedentary	Mobile
mounds	meandering ridge (=*Scolicia*)
craters	meandering grove (=*Scolicia)*
pits	indeterminate ploughings
tubes	faecal castings
rosettes	"feathery tread" trails
(=*Glockeria*)	hollows (? fish feeding

In many photographs the seafloor is extensively pitted by numerous small holes. The distribution of these appears random and no paired openings or organised patterns of the kinds often recorded from deep-sea pelagic deposits (e.g., Ekdale and Berger, 1978; Young et al., 1985) are recognizable.

Indistinct, tiny tubular structures of possible agglutinated construction, either standing erect and proud from the seafloor or lying on the sediment surface, were noted in several photographs. They were probably common, but recognition was limited by lack of photographic resolution.

Large cratered structures (see McMurtry et al., this volume, Figure 8a) were not uncommon and in an isolated instance housed a solitary, erect-stalked organism tentatively identified as a sea pen. In addition, several rosetted or star-like markings, with numerous, simple shallow grooves radiating from a central (domichnial) hole, and closely comparable to the ichnogenus *Glockeria* (see Ekdale and Berger, 1978, Figure 5; and Young et al., 1985, Figure 9) were identified (Figure 11b).

Mobile

Smoothly rounded, irregularly meandering ridges with estimated widths of 5-10 cm are most common (Figures 10a,b). Several exhibited a faint central furrow (Figure 10b) and some may be weakly bilobed or "broken" along their length (see Ekdale and Berger, 1978, Figures 2 and 3; also Young et al., 1985, Figures 13 and 15). Lebensspuren of this kind, which are analagous to the ichnofossil *Scolicia,* are widely accepted to have been produced by spatangoid echinoids and holothurians although other, unidentified errant organisms must also be responsible for some of them (see Young et al., 1985). Indeterminate plough marks (Fig-

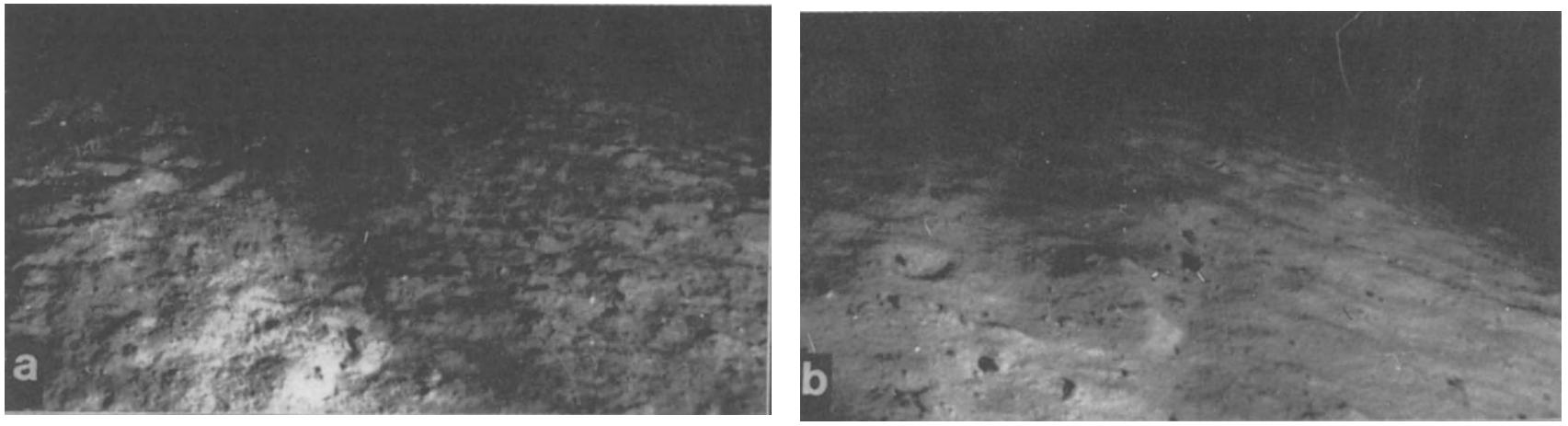

Figure 8. Photos of seafloor biological activity. (a) Churning of surficial seafloor sediments as seen by the presence of numerous mounds and irregular hummocks (position BC-1); (b) Shallow pits or craters and indistinct furrows (position BC-2).

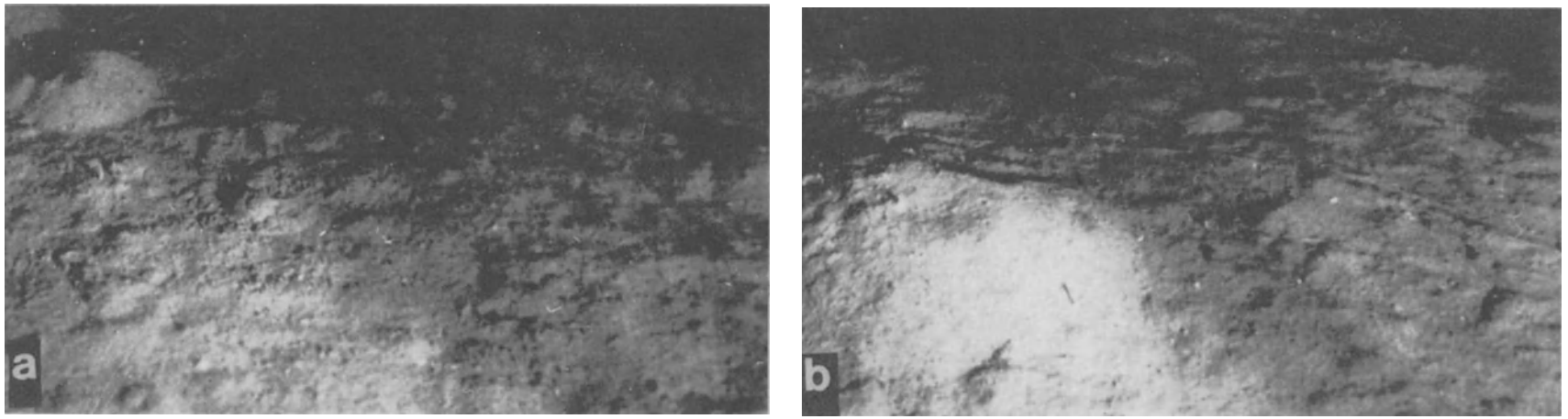

Figure 9. Photos of seafloor biological activity. (a) Larger conical mounds with indistinct apical pit (position BC-1); (b) Apical pit topped by a shallow collapse depression (note the indistinct meandering [? lobed] furrow or plough mark) (position BC-1).

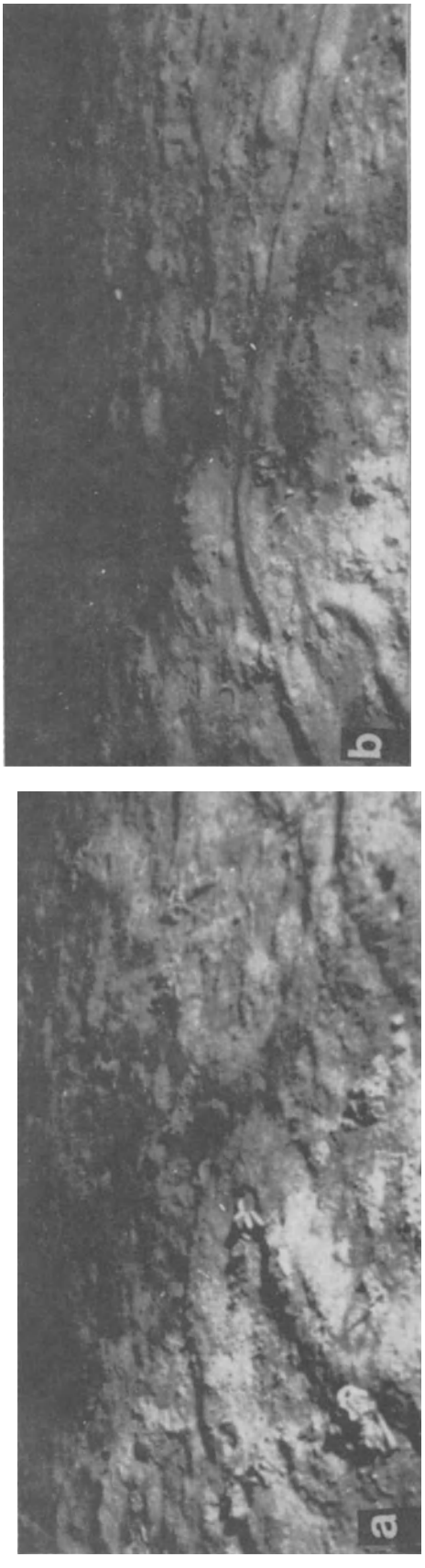

Figure 10. Photos of seafloor biological activity. (a) Meandering ridges of the kind often attributed to spatangoids on a seafloor otherwise dominated by conical mounds--ridges indistinctly bilobed (position BC-1); (b) Meandering ridges with a faint longitudinal grove (position BC-1).

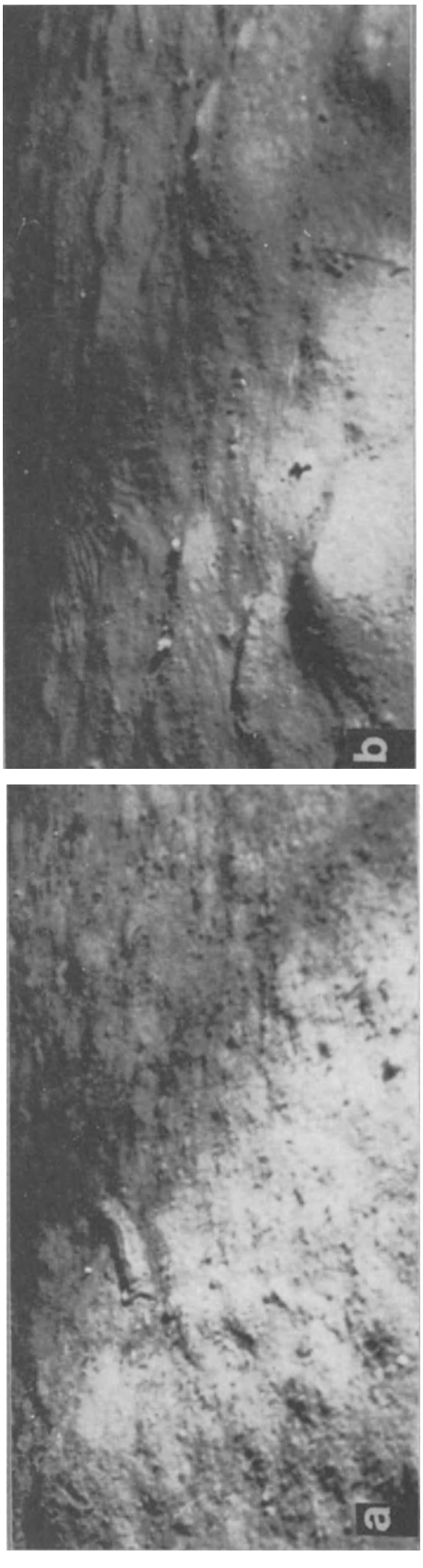

Figure 11. Photos of seafloor biological activity (a) Degrading mounds and pits with fecal castings and a possible holothurian (center) (position BC-1); (b) Abundant conical mounds with rare apical pits and a radiating pattern of simple shallow groves (center) reminiscent of Glockeria (position BC-2).

Figure 12. Photo of seafloor biological activity—muted ripples on a moderately churned seafloor. There is some minor evidence of current scour around the isolated pillows amongst which the sediment is pocketed. Fresh pillow basalts were dredged from this locality (position BC-2).

ure 9a) and meandering grooves, some of which are flanked to either side by indistinct low ridges (Figure 9b), are not common.

Epibenthic holothurians (Figure 11a) were tentatively identified in several photographs from Station 23 (BC-1) and may be responsible for occasional "feathery tread" trails. Fecal castings in the form of strings, tight and loose coils, and minor piles are quite common. These never take on a *Helminthoides*-like aspect. Infrequent shallow depressions (Figure 8b) may reflect the activities of bottom-dwelling fish.

These epifaunal and shallow infaunal traces, tracks, trails, and burrows are closely comparable to those found characteristic of similar depths and substrates of the Ontong Java Plateau by Ekdale and Berger (1978). Detailed descriptions of these and other lebensspuren are also given by Young et al. (1985). While the available bottom photographs are deemed inadequate for their quantitative approach, an empirical assessment suggests sedentary/mobile ratios compatible with those Young et al. (1985) determined for hemipelagic and pelagic substrates at slightly greater depths in the Caribbean Sea. The seafloor micro-relief is maintained if not accentuated by sedentary deposit feeders.

Ichnofossils in the Cores

A complex bioturbate fabric is evident throughout virtually the entire length of all piston and trigger cores examined except PC-9 (Station 3) which is dominated by numerous conspicuous (turbidite) volcanic sand and ashy intervals rather than uniformly monotonous carbonate ooze. Definition of biogenic structures is often subtle, and without recourse to x-radiography more detailed study was not possible. Many of the biogenic structures are nondiagnostic and indeterminate and not readily assignable to generally accepted ichnotaxa. Most of these are of the kind usually and informally recorded in DSDP literature as biodeformational structures, mottles, rinds, haloes, and blobs (e.g., Chamberlain, 1975; Nelson, 1985).

Formal identification of particular ichnotaxa in split cores is fraught with difficulty (Chamberlain, 1978). Of those recognized in this study (see Table 5) three variants of *Planolites* (separated on size; see Wetzel, 1983, 1984) and *Chondrites* would be the most common. Vertical or near vertical tubes assignable to "*Tigillites*" (? = *Skolithos*) together with vaguely meniscate burrows reminiscent of *Scolicia* as well as thin, curving (? branching) tubes similar to "*Mycellia*" and simple subvertical threadlike forms (? *Trichichnus*) are present but never abundant. Fragmentary spreiten burrows suggestive of *Zoophycos* and/or *Teichichnus* were rarely recorded. Some of the smaller traces were pyritized. From the DSDP and other research, this ichnofacies is widely accepted to be characteristic of deep-sea pelagic carbonates accumulating at depths a little above the Carbonate Compensation Depth (CCD) (e.g., Chamberlain, 1975; Ekdale, 1977; Ekdale and Bromley, 1984; Nelson, 1985). Significant numbers of *Planolites* burrows and mottles exhibit smeared-out margins (Figure 13,14) that are not always a response to the coring process and more probably reflect diminished shear strengths to be associated with sediments of moderate clay content (see Berger et al., 1979; Ekdale, 1980).

Preservation and Diversity

An attempt has been made to record vertical variation in trace fossil preservational character (ranked from "poor" to "optimal") and diversity (= number of identified taxa over an arbitrarily chosen core interval) in all five cores studied using criteria and approaches described by Wetzel (1983), Ekdale et al. (1984), and Nelson (1985). The results are summarized in Table 5. Following Ekdale et al. (1984), preservational state was logged as "poor" (little or no bioturbation), "fair" (traces evident but outlines fuzzy and density usually low), "good" (sharp outlines), and "optimal" (sharp textural or

Table 5. Trace fossil identification, distribution and abundance, preservation, and diversity in North Fiji Basin cores.

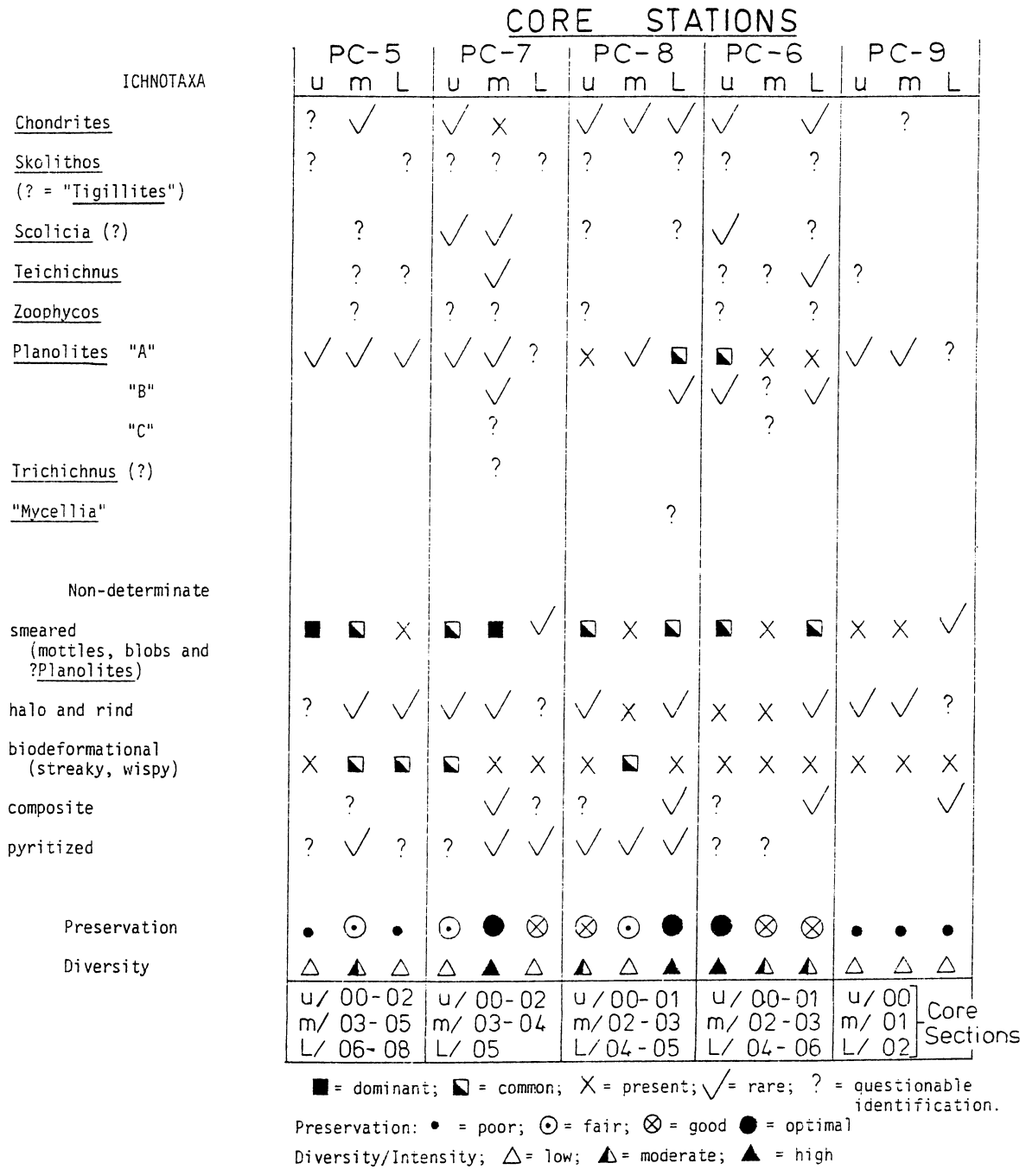

vivid color contrasts between trace and host sediment). These categories approximate those of minor (<30%), moderate (30-60%), and intense (>60%) used to describe apparent degree of bioturbation in DSDP and other cores, and which can be translated into an arbitrary 10-point scale (see Nelson, 1985, Figure 5). It should be noted that very intense bioturbation can lead to sediment homogenization and no visible fossil traces. Optimal preservation or visibility (Figure 13) and highest diversity occur where there are maximum color contrasts, as between dark (10YR 3/2) or light (10YR 6/4) ashes and the pelagic carbonate ooze (10YR 5/4), and also with the selective diagenetic color enhancement seen in many ill-defined darker horizons (10YR 4/3) apparently enriched in Mn and/or Fe (see Swinbanks and Shiryama, 1984). Where definition of trace fossils is subtle, smear slide evidence reveals no textural or mineralogic differences between burrow fill and the background host, except for occasional concentrations of foraminiferal sand in the former. Most thinner (<4 cm) and a few thicker ash horizons have been mixed upwards to a greater or lesser degree with the pelagic carbonate ooze

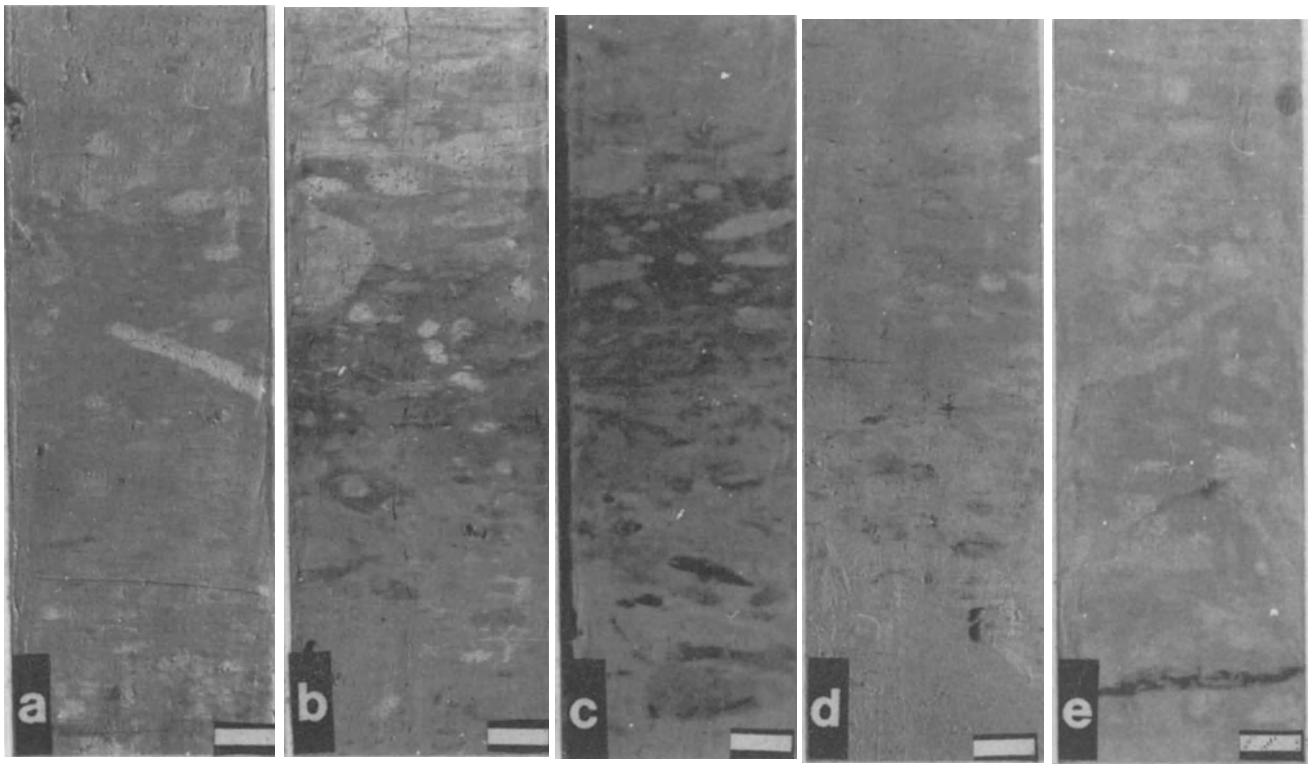

Figure 13. Typical trace fossils and bioturbation in split cores. Optimal preservation and visibility between lighter colored pelagic ooze (10YR 5/4) at ill-defined, possibly Fe/Mn-enriched darker horizons (10YR 3/2) (a,b, and c), and darker ashy intervals (10YR 3/2) (c and d) Chondrites, several Planolites variants, smeared-out forms as well as occasional rind and halo burrows are evident. Subtle color variations bring out a mottled ichnofabric with biodeformational wisps and streaks, together with (?) Teichichnus (e) (a from core PC-6, section 04; b from PC-7, section 04; c and d from PC-7, section 03; e from PC-5, section 08). Scale bars = 2 cm.

through a vertical extent of 10 cm or more (Figure 13). This would be consistent with the generally observed intense bioturbation and mixing of surficial seafloor sediments through depths of up to 20 cm below the sediment/water interface (e.g., Swinbanks and Shirayama, 1984) and which is evident in bottom photographs examined as described earlier (see Figures 8-11) as well as being noted in the tops of piston and trigger cores. Although many ashes have sharp basal contacts (Figure 14) there are several examples in intervals less than 4 cm thick of patchy reworking to 5 cm or more below these, while upper boundaries are diffuse over 5-8 cm or more.

Because the uppermost 5-20 cm of sediment is continually being churned over, lebensspuren identified in bottom photographs are unlikely to be preserved in the fossil record. Where preservation is good to optimal, intensity moderate and diversity generally greatest, the recognized ichnocoenosis is consistent with the tiering (or story) models involving habitat layering or stratification and the continual upwards migration of traces produced by later colonizing, deep burrowing organisms (e.g., Berger et al., 1979; Wetzel, 1983; Ekdale et al., 1984). It is only these later-formed traces which pass into the historical record.

The extent of bioturbation varies within cores, and horizons of optimal and/or moderate to intense bioturbation cannot be correlated between the cores. The temporal variation appears non-systematic and cannot be related to changes in carbonate and silt content, or textural and mineralogic character, other than becoming more conspicuous through ash-rich intervals. It is not possible to establish reasons for the selective diagenetic color enhancement (10YR 5/4 versus 10YR 4/3) of traces at some levels within the carbonate oozes of all cores. However these levels may define periods when sedimentation rates were reduced.

Nelson (1985), from a study of southwest Pacific DSDP Leg 90 sites, situated meridionally between the equator and 45°S, concluded that longer term variations in burrow intensity and progressive replacement at depth of a *Planolites*-like assemblage by a *Planolites-Chondrites-Zoophycos* one, could have been a response to changes in sedimentation rates and nutrient fluxes. These were taken to reflect paleoceanographic developments and in particular shifts in water mass boundaries. The North Fiji Basin cores are moderately bioturbated throughout most of their lengths and with only the *Planolites*-like assemblage evident, speculations of the kind made by Nelson (1985) are inappropriate.

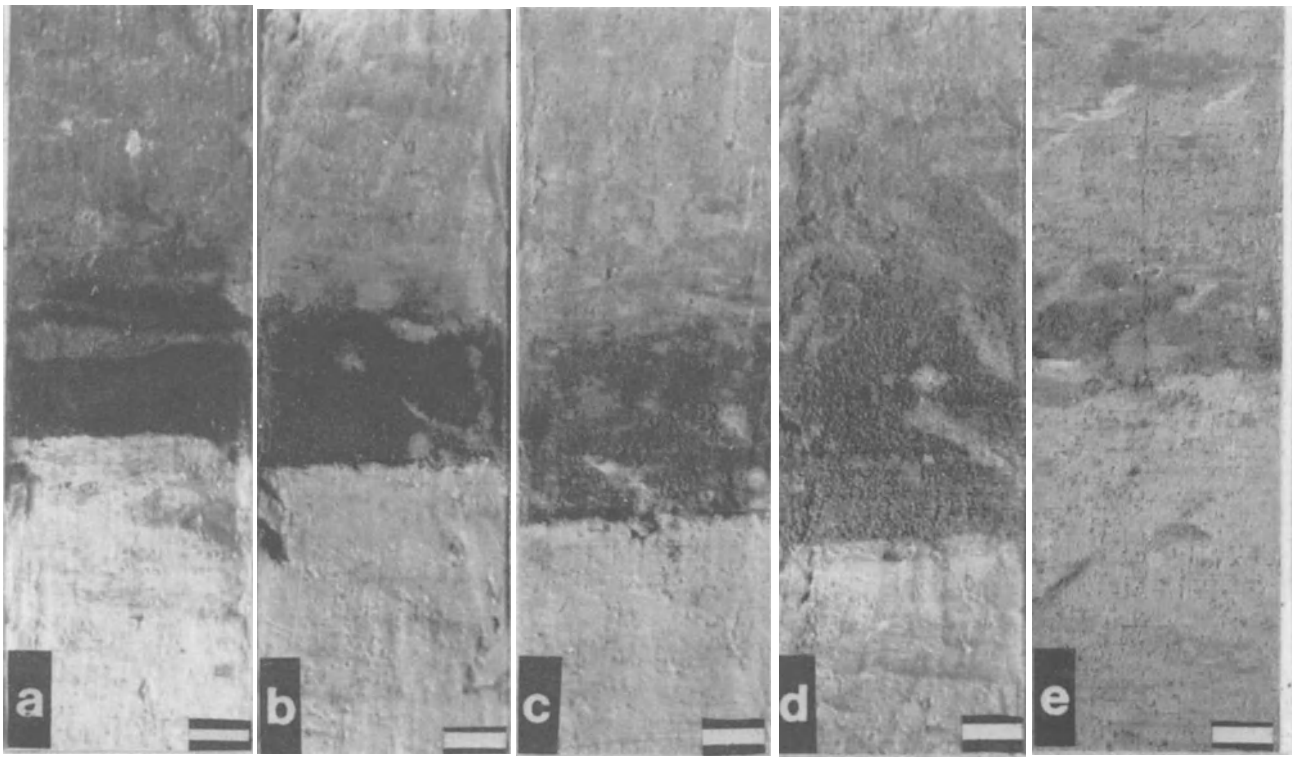

Figure 14. Graded ashes in split cores: (a) with sharp base and subtle burrow mottling above lowermost 5 cm; (b, c, and d) with little disturbance of basal contact but increasing biogenic reworking into and with overlying pale ooze; (e) non-graded ash with irregular basal contact, biogenic reworking throughout, and gradationally mottled into overlying ooze. Recognisable trace fossils include Planolites variants, smeared mottles and blobs, pyritised fillings, and (?)Teichichnus (e). (a from PC-6, section 04; b and c from PC-6, section 06; d from PC-8, section 05; e from PC-7, section 04). Scale bars = 2 cm.

CORE STRATIGRAPHY

Cores from the Abyssal Hills Terrain

Cores PC-5, PC-7, and PC-8 all have a similar stratigraphy consisting of ash-bearing, foram- and clay-rich nannofossil ooze with several ashy intervals. On the basis of the vertical distribution of ashy intervals three informal stratigraphic units are recognized and tentatively correlated (Figure 15). The upper and lower units (units 1 and 3) consist almost entirely of ash-bearing, foram- and clay-rich nannofossil ooze. A single ashy bed occurs in each of these two units. Apart from these, glass percentages are low (5%) and the sediments are uniform within each unit and similar between units. The middle unit in each core (unit 2) is characterized by having seven distinct ashy intervals inter-bedded with pelagic ooze. The pelagic ooze in unit 2 is indistinguishable from that in units 1 and 3.

The ashy intervals differ from the ooze in being darker, coarser, and having less carbonate and more volcanic glass. Glass percentages average 22%. The upper and lower boundaries of most ashy intervals are diffuse and gradational. Bioturbation is common throughout as already described. The ashy intervals may have been produced by mixing caused by bioturbation of glass in pure ash beds with underlying and overlying carbonate ooze. The ashy intervals range in thickness from 3 cm to 26 cm and are approximately twice as thick on average in PC-8 (14 cm) than in PC-7 (8 cm) and PC-5 (7 cm).

The lowest ashy interval in unit 2 in each core differs from the rest in being coarser, in having the greatest amount of ash of all intervals (average 76%) and in having a distinct, sharp base. It is referred to here as the "major ash". The lower boundary of unit 2 is placed at the base of the major ash. The upper boundary of unit 2 is less distinct but is placed at the top of the seven distinct ashy intervals above which pelagic ooze dominates.

Cores from the New Hebrides Apron

Cores PC-6 and PC-9 consist of ooze and ashy ooze interbedded with graded units (turbidites) made up mainly of volcanic grains. No stratigraphic subdivisions are recognized here but it is noted that turbidites are more common in the middle of PC-6 and the lower part of PC-9 and less common in the upper part of both cores. The differences between the two cores are a reflection

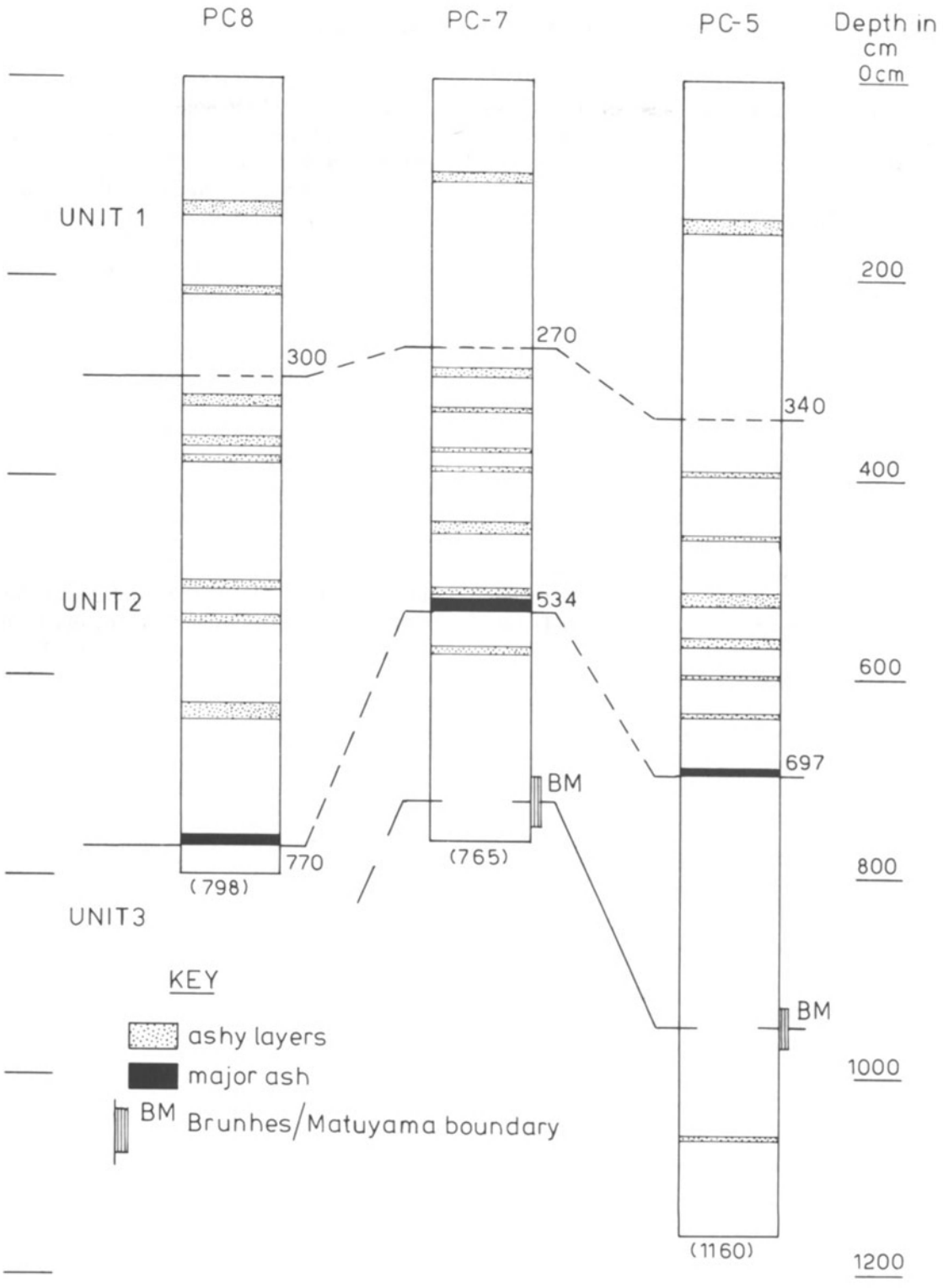

Figure 15. Stratigraphic correlation between cores PC-5, PC-7, and PC-8 from the central part of the North Fiji Basin. Unit 1/2 boundary is based on changes in volcanic glass content. Unit 2/3 boundary is placed at the base of the only major ash (containing more than 50% glass) in each core. Paleomagnetic dating by F. Theyer.

of the distance from the New Hebrides arc, the source of the turbidites. Volcanic glass is more common in PC-9, 150 km from the arc, than in PC-6; and pelagic ooze is more common in PC-6, 350 km from the arc, than in PC-9.

AGES OF CORES AND SEDIMENTATION RATES

Previous workers have found the cores they have studied from the North Fiji Basin to be no older than Quaternary (Chase, 1971; Luyendyk et al., 1974). Magnetostratigraphy (Table 6), foraminifera (A. Carter, personal communication), and nannofossils (D.A. Burns, personal communication) indicate that all five cores studied here are also no older than Quaternary. Two cores, PC-5 at 950 cm and PC-7 at 725 cm, contain the Brunhes-Matuyama magnetostratigraphic boundary which lies at 0.7 Ma (Table 6). As all other cores are magnetically positive it appears that none contain the Brunhes-Matuyama Boundary and it is assumed that all are less than 0.7 Ma.

Miocene and Pliocene foraminifera are present in core PC-5, where they occur in substantial numbers, and also in PC-8. As Quaternary species are also present and as both cores are from small basins at the foot of steep slopes down which sediment is likely to be moving, the pre-Quaternary fauna are considered reworked. Reworked foraminifera and nannofossils are also found in lithified sediments dredged at Station 21 (RD-16) (Gregory and Eade, this volume).

Using the known age and position of the Brunhes-Matuyama boundary in cores PC-5 and PC-7, average sediment accumulation rates for these two cores are calculated to be 13.6 m/m.y. and 10.3 m/m.y., respectively. These cores are almost entirely mixtures of sediments from two sources: biogenic carbonate from surface waters, and pumice and glass shards from volcanic sources.

Biogenic carbonate (pelagic ooze) accumulates at an approximate rate of 10 m/m.y. (Kennett, 1982). Brocher et al. (1985) found the average rate of sediment accumulation in the North Fiji Basin to be approximately 7 m/m.y. The pelagic sediments of PC-7 would probably have accumulated at a rate similar to these (i.e., 7-10 m/m.y.). As the pelagic oozes of PC-5 and PC-8 contain reworked carbonate, the rate of accumulation of pelagic sediments in these cores will be greater than PC-7.

The highest accumulation rate is most likely to be in PC-5 where reworking is greatest. Accepting a pelagic ooze accumulation of 7-10 m/m.y. and ignoring reworking, estimating the volume of ash present in each unit in each core from smear slide analyses and by a process of trial and error, the most likely accumulation rates are found to be 9 m/m.y. for pelagic carbonate ooze, up to 3 m/m.y. for reworked sediment, and up to 8 m/m.y. for volcanic sediment (Table 7). Using these figures, average accumulation rates are 9-12 m/m.y. for unit 1 and 14-20 m/m.y. for unit 2. The differences between the rates for unit 1 in different cores are due to differences in the amount of reworked sediment. The differences between rates for unit 2 are due to differences in both the amount of volcanic glass present and the amount of reworking (Table 7).

Using the rates derived above, ages for the unit boundaries can be calculated (Table 7). The ages for units 1/2 boundary and for units 2/3 boundary are in close agreement between cores averaging 0.28 Ma for units 1/2 and 0.49 Ma for units 2/3. These ages support the

Table 6. Paleomagnetic boundaries and average sedimentation rate.

	Paleomagnetics*			
	Brunhes/ Matuyama boundary (cm)	Base of core (cm)	Extrapolated age of base of core (Ma)	Average sedimentation rate for whole core (m/m.y.)
PC-5	930-970	1160	0.85	13.6
PC-6	normal throughout	-	<0.7	-
PC-7	700-750	765	0.74	10.3
PC-8	normal throughout	798	<0.7	-
PC-9	normal throughout	-	<0.7	-

*Data supplied by F. Theyer

Table 7. Summary of sedimentation rates (m/m.y.) and unit boundary ages (Ma)* for the central basin cores.

Stratigraphic units	Average boundary age	Cores PC-8	PC-7	PC-5
	(0)			
1		11.5	9	12
	(0.28)	(0.26)	(0.30)	(0.28)
2		20	14	17
	(0.49)	(0.49)	(0.49)	(0.49)
3		NA	9	12

*boundary ages shown in brackets

tentative correlations made between these three cores on the basis of core stratigraphy (Figure 15).

ORIGIN AND TRANSPORT OF VOLCANIC GLASS

The deepest parts of the North Fiji Basin are shallower than 4000 m. This is well above the CCD in this region which lies at approximately 4700 m. Consequently there is little dissolution of the carbonate material that accumulates readily on the seafloor to form the dominant sediment of the basin. The greatest variation in the sediment is in the amount of volcanic material present. Almost all the volcanic material is glass and variations in the amount and type of glass present represent different events, sources, and transport mechanisms.

Origin of Volcanic Glass

Few attempts have been made to establish the origin of glass in sediments of the North Fiji Basin. Jezek (1976) concluded that glasses in cores from the western part of the Basin were derived from the New Hebrides arc to the west. He considered all ash beds to be airfall ashes and did not identify the black graded beds as turbidites. He found a westerly source to be inconsistent with the fact that dominant winds are from the east and southeast.

Brocher et al. (1985) concluded that glasses in cores in the eastern North Fiji Basin were derived from degraded pumice transported from Tonga by surface wind-driven currents.

In the central North Fiji Basin glass may be derived either from back-arc spreading centers or from volcanoes in one of the volcanic arcs of the region. Despite the closeness of some core localities to active spreading centers, especially PC-8 to South Pandora Ridge, all glass grains studied are typical of volcanic arc magmas and bear no resemblance to glasses from back-arc spreading centers of the North Fiji Basin (Table 8).

The most characteristic feature of the North Fiji Basin glasses is the high K_2O content (Table 8, Appendix 2). Similar high K_2O values are found in some late Pliocene to Recent volcanics in the central chain of the New Hebrides arc, Vanuatu (Carney et al., 1985) and in Quaternary volcanics of Kandavu, Fiji (Colley and Hindle, 1984). From a K_2O-SiO_2 plot of high potash, late Pliocene to Recent volcanics from Efate, West Epi, and Tanna in the central chain, Carney et al. (1985)

Table 8. Chemical analyses of glass grains from North Fiji Basin and Quaternary volcanic rocks of Vanuatu.

Sample site	1	2	3	4	5	6	7
SiO_2	62.6	56.2	61.0	57.2	60.2	68.7	49.7
TiO_2	0.7	0.8	0.8	1.1	0.5	0.4	2.1
Al_2O_3	14.7	18.0	16.0	17.3	16.8	12.8	16.1
Fe_2O_3	-	4.4	1.2	2.2	1.7	1.3	-
FeO	7.1	3.7	5.9	5.5	3.6	4.1	9.4
MnO	0.3	0.2	0.2	-	0.1	0.1	0.1
MgO	1.6	1.5	2.2	2.4	3.2	3.2	6.4
CaO	4.0	3.9	5.2	6.6	6.0	5.6	10.8
Na_2O	4.1	5.5	3.5	4.8	4.2	2.5	3.0
K_2O	4.4	3.7	3.7	2.9	2.6	1.2	0.7
P_2O_5	0.8	0.7	0.5	0.2	0.3	-	0.3

1 North Fiji Basin (glass grains from cores PC-5, PC-7, and PC-8) average 65 samples, this study.
2 Vanuatu (Gaua) 1 sample, Mallick & Ash 1975
3 Vanuatu (West Epi) 1 sample, Gorton, 1977
4 Vanuatu (Tauna) average 5 samples, Colley & Warden, 1984
5 Fiji (Kandavu) average 2 samples, Colley & Hindle, 1984
6 Tonga (Metis Shoal) average 2 samples, Melson et al., 1970
7 North Fiji Basin (young seafloor basalts) average 14 samples, Sinton et al., this volume.

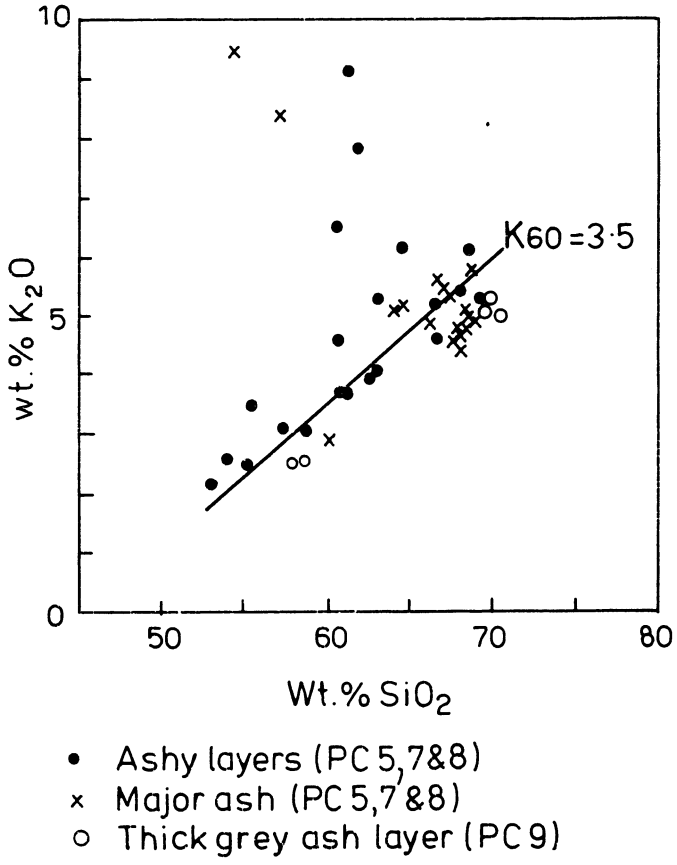

Figure 16. K_2O/SiO_2 plot for volcanic glass grains from ashes in cores from the central part of the North Fiji Basin.

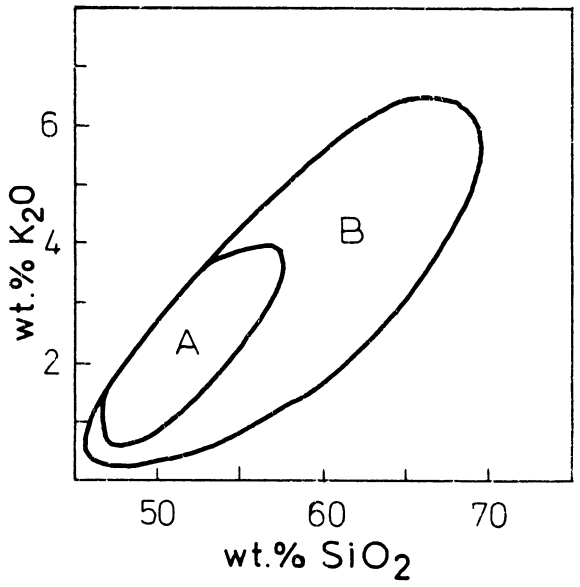

Figure 17. K_2O/SiO_2 plot for high potassic rocks from the central chain volcanoes of the New Hebrides arc (from Carney et al., 1985). A. Gaua Aoba Ambrym. B. Efate, W. Epi, Tanna.

derive a K_{60} value of 3.3. K_2O-SiO_2 plots for all glass grains analysed from the major ash and the ashy intervals in cores PC-5, PC-7, and PC-8 form a distinct trend with a K_{60} value of 3.5 (Figure 16). A few grains have much higher K_2O values and are clearly not associated with this trend. These may be from other central chain volcanoes such as Gaua, Aoba, or Ambrym (Figure 17) which have volcanics with the highest K_2O values relative to SiO_2 in the region, or they may be faulty analyses. On the basis of similarities between chemical analyses of North Fiji Basin glass grains with Quaternary volcanic rocks of Vanuatu (Table 8), especially K_2O content (Figure 18), the central chain volcanoes of Vanuatu are the most likely source of volcaniclastic sediment in the central part of the North Fiji Basin.

The same trend seen on K_2O-SiO_2 plots for grains from the major ash and ashy intervals is also seen for glass grains from pelagic ooze in the same three cores but the scatter is greater and the trend less obvious (Figure 19). This scatter in the pelagic ooze may have been produced by the vertical mixing caused by bioturbation. However there is bioturbation throughout the ashy intervals and grains from them do not show the same scatter on K_2O-SiO_2 plots. On the basis of chemical similarity, Jezek (1976) concluded that volcanic glass in sediments of the New Hebrides apron was probably derived from the New Hebrides arc. Results of chemical analyses of six glass grains from a graded bed in core PC-6 and four grains from a pure ash bed in core PC-9 support Jezek's conclusion.

Transport Mechanisms

The major ash which occurs in all three cores from the abyssal hill terrain (central basin area) forms a distinct bed with a sharp base. Glass grains make up most of the sediment. These are coarse silt- to very fine sand-sized shards and pumice grains with sharp edges showing no sign of mechanical weathering. Most grains belong chemically to the same suite. Glass grains in the

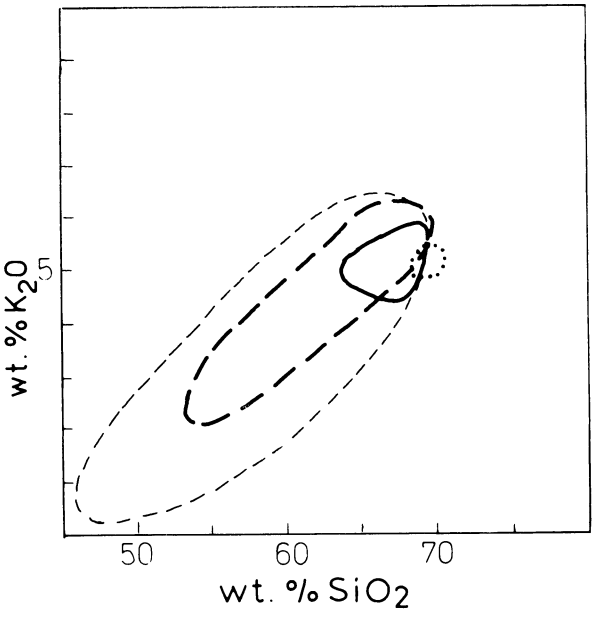

Figure 18. K_2O/SiO_2 showing the close relationship between the North Fiji Basin glasses (ashy layers of PC 5,7,8: light dashed line; major ash of PC 5,7,8: solid line; grey ash layer of PC 9: dotted line) and high potassic rocks of the central chain volcanoes, New Hebrides arc (light dashed line).

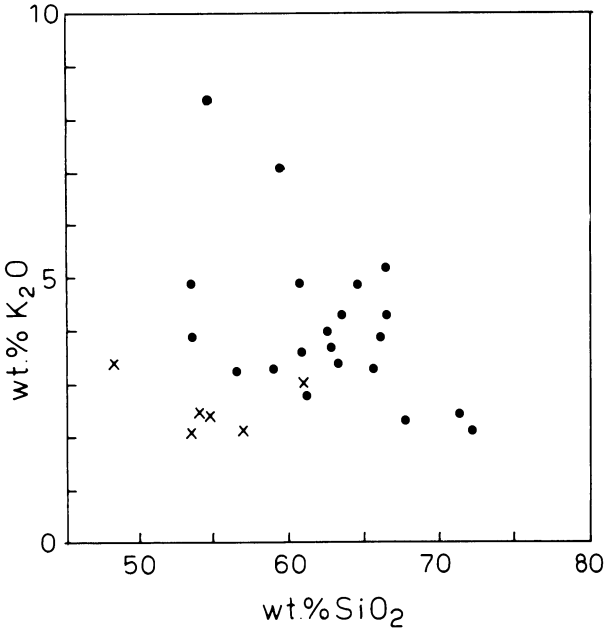

Figure 19. K_2O/SiO_2 plot for (a) glass grains from pelagic ooze from central basin cores PC 5, 7, and 8 (dots) and (b) glass grains from a turbidite PC 6 in the New Hebrides apron (crosses).

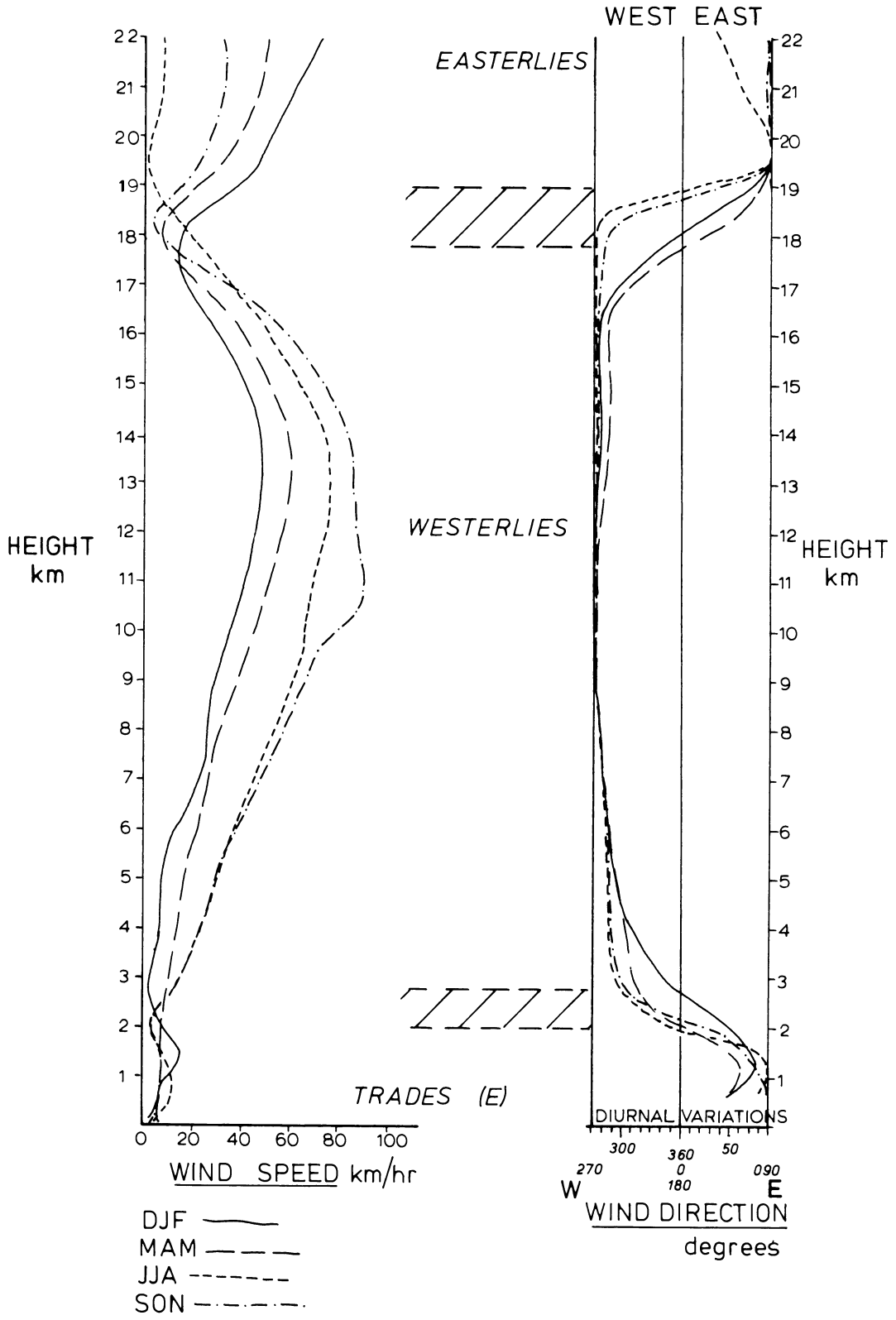

Figure 20. Wind speed and direction above Nadi, Fiji (latitude 17°45'S, longitude 177°27'W) (From de Lisle, 1969). (DJF = December, January, February; MAM = March, April, May; JJA = June, July, August; SON = September, October, November).

ashy intervals have the same physical and chemical characteristics, but differ from the major ash in being less common in the ashy intervals. These physical and chemical characteristics strongly point to these being airfall ashes.

The ashy intervals were probably derived from pure ashes by biological mixing of the ashes with overlying and underlying pelagic ooze. Glass in these intervals is therefore airfall material derived from a single eruptive event. Atmospheric dispersal of ash particles is primarily controlled by the wind velocity profile, variations in wind speed during an eruption, and the eruption column height (Wilson et al., 1978). An examination of weather records from Nadi, Fiji (deLisle, 1969; Reid and Penney, 1982) shows that at that locality the atmosphere is layered (Figure 20). At Nadi the east to southeasterly trade winds form a shallow layer 2-3 km thick. Three-monthly average wind speeds are in the order of 10-15 km/hr with maximum speeds rarely exceeding 60 km/hr. Above the trade winds there is a deep layer of tropospheric westerlies 15-17 km thick lying between 2-3 km and 18-19 km above sea level. Wind speeds are much higher than the trade winds reaching maximum speeds in excess of 200 km/hr at heights of 10-15 km above sea level. Three-monthly averages for the winds at 10-15 km are 50-90 km/hr. At more than 18-19 km above sea level easterlies predominate. The same structure occurs at similar latitudes (Gabites and Hutchings, 1961) and this would include the North Fiji Basin and its margins.

As the trade wind layer is very shallow and as most active volcanoes of the New Hebrides arc are higher than 0.5 km, almost all volcanic ash other than that from very small eruptions will be carried into the upper troposphere and transported to the east (Figure 21). Coarsest grains will fall first followed by progressively finer sediment further downwind. For explosive eruptions, the bigger the eruption, the more pyroclastic material produced, the higher the cloud, the farther the material will be carried. The very fine sand and coarse silt glass grains in the ashy intervals of the central North Fiji Basin cores were apparently derived from a source 500-750 km distant and transported by winds 50-90 km/hr. According to Shaw et al. (1974, see Figure 5) these ashes were probably derived from volcanic clouds 5-12 km high. The major ash which contains the coarsest volcanic grains was probably derived from a cloud higher than 12 km. Only the smallest eruptions along the New Hebrides arc, with cloud height less than about 5 km, will deposit pyroclastic material in the vicinity of the arc.

Ash occurs in all sediment in all central basin cores. Although only a minor component of pelagic ooze sediments, it is nevertheless persistently present, almost always at around 5%. Chemically the glass is different at any of the horizons sampled. This suggests a regular, non-episodic supply of grains from different sources.

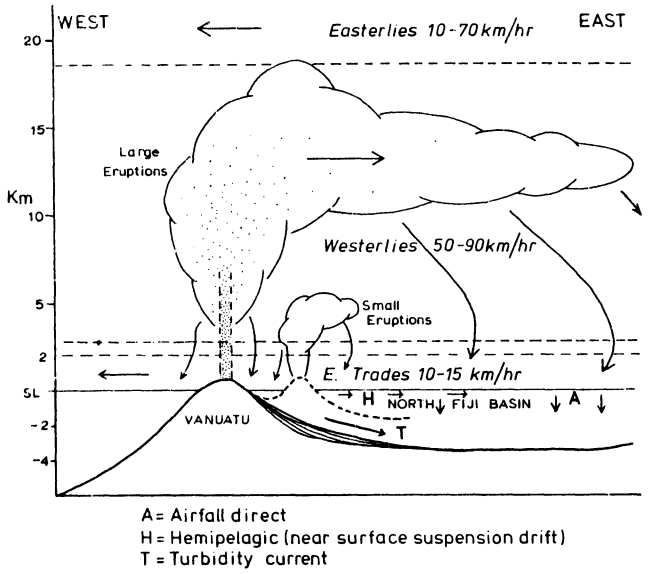

Figure 21. The effect of prevailing wind directions on the transport of airborne volcanic ash above Vanuatu and the North Fiji Basin. Also shown is the eastward transport of sediment from Vanuatu by turbidity current and formation of the New Hebrides apron on the western side of the North Fiji Basin.

Such glass may have been transported by air and after deposition been mixed biologically to such an extent that all bedding was destroyed and glass percentages reduced to a uniformly low level. Some ash may also have come from a persistent and constant supply, such as subaerial and shallow submarine deposits, and have been reworked and transported in suspension by oceanic currents. Existing currents in the region would carry fine sediment eastwards from central Vanuatu (Figure 22). The major westward-flowing currents, the trade wind drift south of Vanuatu, and the South Equatorial Current in northern Vanuatu are counterbalanced by a south tropical countercurrent (Donguy et al., 1975). The countercurrent with measured velocity of 15 cm/sec (Donguy et al., 1975) could well transport fine volcaniclastic sediment in suspension from the area around the Quaternary volcanoes of Ambryn, Epi, and Efate eastward to the central part of the North Fiji Basin. This sediment could have come from subaerially eroded ash, or reworking of coastal and shallow submarine sediments. Regular small eruptions and shallow submarine eruptions would also contribute the sediment which could remain in suspension long enough to be transported several hundreds of kilometers before being deposited. Plumes of fine sediment streaming downwind have been observed from shallow submarine eruptions (Davey, 1980). Coarse silt-sized particles would take between 15 and 50 days to settle 3000 meters in water. In this time they could travel up to 700 km from their source in currents of about 15 cm/sec, the speed of the south tropical countercurrent. Ash in the pelagic

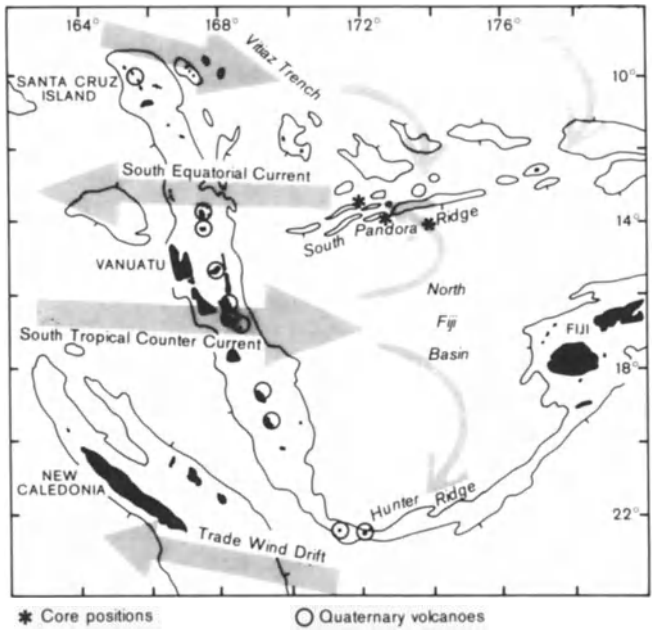

Figure 22. Surface currents in the vicinity of Vanuatu and the North Fiji Basin (from Donguy et al., 1975).

ooze is probably derived from a combination of all the above transport mechanisms. As two-thirds of the ash present in unit 2 in all three cores is present in the ooze and not in ashy intervals, combined transportation of airfall and oceanic suspension and subsequent biological mixing are important processes in the North Fiji Basin.

In the New Hebrides apron other transport mechanisms predominate. The apron consists of a wedge of sediment thickest at the foot of the New Hebrides arc, the source of sediment, and thinning eastward. Much of the sediment making up the apron has been transported across the floor of the North Fiji Basin by turbidity currents. If the source area of the turbidites is the arc, it is not surprising to find that almost all the sediment in these beds is volcaniclastic. Other processes have also contributed to the supply of volcaniclastic sediment to the apron. Much of the fine ash between the turbidites could have been transported by slow-moving bottom and surface suspension currents. Airfall ash is also present. Being close to the New Hebrides arc, major ash beds are thick. The thickest pure ash bed is 14 cm thick. Small subaerial eruptions will also have contributed significant amounts of ash to the non-turbidite sediment.

PRESERVATION OF ASHES

The effects of ash falls on bioturbation and the effects of mixing, predominantly bioturbation, on ash beds has been investigated by a number of authors (e.g., Ruddiman and Glover, 1982; Fisher and Schmincke, 1984). Ash falls, if large enough, will smother bioturbation and bioturbation will destroy ash beds if they are not too thick. If there is no bioturbation then ashes will be preserved in the sedimentary column as distinct beds with sharp bases and tops and containing only volcaniclastic grains. In the North Fiji Basin four pure undisturbed ashes were found in core PC-9 from the central part of the New Hebrides apron. There is very little evidence of bioturbation in this core and the ashes (2-14 cm thick) are the thickest seen in the cores studied. The locality of core PC-9 is closer to the New Hebrides arc than any other cores studied.

Bioturbation, if intense enough, will partially or completely mix volcaniclastic grains in an ash layer with underlying and overlying sediment. Ruddiman and Glover (1982) found that mixing in North Atlantic cores consisted of an intensely stirred near-surface layer averaging no more than 4 cm thick, and a mean depth of downward penetration of detectable mixing of 15 cm (range 5-25 cm). This is very similar to the 5-20 cm of mixing seen in the North Fiji Basin cores.

Ash falls will often muffle bioturbation and, if big enough, completely stop all biological mixing. Ruddiman and Glover (1982) found that ash thicknesses up to 1 cm do not measurably muffle the normal mixing process. Lewis and Kohn (1973) found that only ash beds thicker than about 2 cm were preserved, thinner ones being destroyed by bioturbation. In the central North Fiji Basin cores there is every gradation from fully preserved ash beds to completely mixed ash. Wherever conditions are favorable for burrowing organisms ashes will always be disturbed to some extent. Generally the lower contact is preserved as a sharp boundary, in contrast to a diffuse upper boundary formed by mixing. The major ash in cores PC-5, PC- 7, and PC-8 is typical of such a partially mixed layer. Glass grains are 60-80% of the sediment in the major ash and when restored to its original thickness as a pure ash it was 2.8-4.4 cm thick in the central North Fiji Basin. The youngest ash in PC-8 also has a sharp base and its original thickness was 2.5 cm.

The ashy intervals in these same cores represent ashes mixed to a greater extent than in the major ash. The whole ash has been partially mixed and both lower and upper sharp boundaries destroyed. Glass grains make up 10-46% of the sediment. The ashy intervals have restored ash thicknesses of 0.5-1.7 cm.

Other ash material occurs in low percentages (1-13%) throughout the pelagic ooze of all the central basin cores. At these levels ash layering was not detected. Hein et al. (1978) noted the important role of sediment mixing in interpreting explosive volcanic events along the Aleutian Ridge. They decided that if dispersed ash was more than 15% then that ash constituted a significant volcanic event. However, in the North Fiji Basin

cores, dispersed ash less than 13% of the sediment (averaging 5%) accounts for as much as twice the total volcanic sediment in unit 2 than that in the ashy intervals and the major ash combined. Clearly the input of this ash found in low concentrations is not insignificant in terms of total volcanic input.

Glass grains, apart from those in the ash and ashy intervals, are fairly evenly distributed throughout the pelagic ooze. As bioturbation is intense the even distribution of the glass may have been produced by biological mixing of ashes too thin to muffle bioturbation. As glass grains in the ooze from the same horizon have widely differing glass chemistry this material appears to have been derived from different sources and perhaps transported by different mechanisms. Small subaerial eruptions, submarine eruptions, and reworking of volcaniclastic sediment may all have contributed to the ash in the pelagic ooze. But regardless of the number of sources and transport mechanisms involved, bioturbation has been a major factor in producing low concentrations of evenly distributed ash material in the pelagic ooze of the North Fiji Basin.

Original ash thickness and level of bioturbation control whether or not an ash is preserved completely, partially, or is completely mixed with overlying and underlying sediment. In the central North Fiji Basin bioturbation levels during the last 0.5 million years have been such that ash beds thicker than about 2 cm have mostly retained their original form with only the upper part of the layer being mixed with the overlying ooze. Ash beds originally 0.5-2 cm thick have been mixed to such an extent that all sharp boundaries have been destroyed and glass grains make up less than half the sediment. However, in these ashy intervals glass percentages were high enough to be easily detected from the 'background' pelagic ooze.

Ash beds originally less than 0.5 cm thick appear to have been completely destroyed. While at least some and probably much of the dispersed ash in pelagic ooze was derived from small eruptions which produced ash beds less than 0.5 cm thick, the relative importance of small eruptions versus other transport mechanisms, notably oceanic-current suspension, cannot be measured. However in view of the relative proportions of dispersed ash versus ash in discrete layers the role of small eruptions and other mechanisms combined in transporting ash to the central North Fiji Basin is not insignificant and indeed is more important than major explosive volcanic events.

CONCLUSIONS

Our study of sediment cores from the North Fiji Basin has led to the following conclusions.

(1) There are two major sedimentary environments in the North Fiji Basin: (a) the abyssal hill area in the central part of the basin where the predominant sediment is pelagic ooze with variable amounts of volcaniclastic material (mostly glass); (b) the New Hebrides apron in the western part of the basin where sediments are graded, bedded, volcaniclastic turbidites alternating with ashy ooze.

(2) The cores represent a complete sedimentary sequence from 0.8 Ma to the present day.

(3) In the central basin area three stratigraphic units are recognised. The upper and lower units consist predominantly of pelagic ooze with only minor glass and containing one or two ashy intervals with more than about 15% but less than 50% volcanic glass. The middle unit also consists predominantly of pelagic ooze but differs from the other two units in containing a major ash bed ($<60\%$ volcanic glass) and several distinct ashy intervals. By extrapolation, the age of the boundary between the upper and middle unit is estimated to be 0.28 Ma and the middle and lower unit's boundary to be 0.5 Ma.

(4) Volcanic glass is present in all cores. One of the most distinctive features is the high K_2O content found in almost all grains analysed. The most likely source of the glass is the central volcanic chain of the New Hebrides arc. None of the volcanic sediment was apparently derived from volcanic activity associated with sea-floor spreading in the North Fiji Basin.

(5) Most of the volcanic sediment present was transported subaerially in volcanic clouds blown eastward over the basin from Vanuatu by strong tropospheric westerlies.

(6) Major eruptions which produced volcanic clouds higher than about 5 km produced enough ash to form beds thick enough to be preserved. The thickest of these was from an eruption which occurred at about 0.5 Ma, may have produced a cloud higher than 12 km, and formed an ash bed thicker than 2 cm in the central part of the North Fiji Basin. Bioturbation has mixed the upper part of this ash with the overlying ooze but the basal contact remains sharp. Other ashes, apparently from eruptive clouds 5-12 km high, were 0.5-2 cm thick when formed but have since been biologically mixed to the extent where both upper and lower sharp contacts have been destroyed and glass percentages in the ash reduced to 10-50%.

(7) Minor eruptions produced ashes which were less than 0.5 cm thick when formed and these are not preserved as recognisable layers. Ash from these beds has been completely dispersed thoughout the pelagic ooze by bioturbation and is found today as a minor component in all pelagic ooze. In addition to ash from minor eruptions transported subaerially into the North Fiji Basin, some fine volcanic grains in the ooze may have

been transported substantial distances in suspension by oceanic currents.

(8) Pumice grains, presumably transported floating on the sea surface and driven along by winds and surface currents, are not common but are scattered thoughout all cores.

(9) Glass grains are generally well preserved but the presence of montmorillonite clay in moderate amounts throughout all cores indicates ubiquitous alteration.

(10) During the period 0.5 Ma to 0.25 Ma explosive volcanic activity along the New Hebrides arc was significantly greater than during the periods 0.8 Ma to 0.5 Ma and 0.25 Ma to the present.

(11) Although three cores were collected from localities close to active spreading centers, no metallogenic enrichment was detected during this study.

ACKNOWLEDGMENTS

The authors gratefully acknowledge the assistance given in collecting the cores by their shipboard colleagues, especially the HIG technicians and University of Hawaii Marine Center technicians and crew onboard the R/V KANA KEOKI. Both authors are especially grateful to HIG and the Department of Oceanography, and in particular Chris Mato and her staff in the Core Laboratory at UH, for use of facilities and assistance in opening and describing the North Fiji Basin cores. Graeme Walker, Physics and Engineering Laboratory, DSIR Lower Hutt operated the SEM and photographed the glasses; John Mitchell and Ed Arron, both NZOI, did the grain size and carbonate determinations, respectively; Ann Kelly and Karl Majorhazi drafted some of the diagrams; and RoseMarie Thompson typed and edited the manuscript. All their contributions are gratefully acknowledged. Additional photography and drafting were undertaken by R. Harris, Geology Department, University of Auckland.

REFERENCES

Berger, W.H., A.A. Ekdale, and P.P. Bryant, 1979, Selective preservation of burrows in deep-sea carbonates: Marine Geology, v. 32, p. 205-230.

Brocher, T.M., S. Wirasantosa, F. Theyer, and C. Mato, 1985, Regional sedimentation patterns along the Northern Melanesian Borderland, in T.M. Brocher, ed., Investigations of the Northern Melanesian Borderland, Earth Science Series, v. 3: Houston, TX, Circum-Pacific Council for Energy and Mineral Resources, p. 75-101.

Carney, J.N., A. Macfarlane, and D.I.J. Mallick, 1985, The Vanuatu Island Arc: an outline of the stratigraphy, structure, and petrology, in Alan E.M. Nairn et al., eds., The Ocean Basins and Margins: vol. 7A: Plenum Publishing Corporation.

Chamberlain, C.K., 1975, Trace fossils in DSDP cores of the Pacific: Journal of Paleontology, v. 49, p. 1074-1096.

Chamberlain, C.K., 1978, Recognition of trace fossils in cores, in P. Basan, ed., Trace Fossil Concepts: Society of Economic Paleontologists and Mineralogists, Short Course No. 5, p. 133-184.

Chase, C.G., 1971, Tectonic history of the Fiji Plateau: GSA Bulletin, v. 82, p. 3087-3110.

Colley, H., and W.H. Hindle, 1984, Volcano-tectonic evolution of Fiji and adjoining marginal basins, in B.P. Kokelaar and M.F. Howells, eds., Marginal Basin Geology: Volcanic and associated sedimentary and tectonic processes in modern and ancient marginal basins: Special Publication of the Geological Society of London, no. 16, p. 151-162.

Colley, H., and A.J. Warden, 1974, Petrology of the New Hebrides: GSA Bulletin, v. 85, p. 1635-1646.

Davey, F.J., 1980, The Monowai seamount: an active submarine volcanic centre on the Tonga-Kermadec ridge (Note): New Zealand Journal of Geology and Geophysics: v. 23, p. 533-536.

De Lisle, J.F., 1969, Upper wind statistics for New Zealand stations: New Zealand Meteorological Service Miscellaneous Publication, no. 129, 62 p.

Donguy, J.R., C. Henin, and F. Rougerie, 1975, Surface water exchanges between the Coral Sea and the Pacific Ocean, in B.R. Stanton, ed., Proceedings of the Regional Workshop on Circulation Studies in the South West Pacific, Wellington, 11-15 November 1974: Miscellaneous Publication New Zealand Oceanographic Institute, no. 65, p. 8.

Ekdale, A.A., 1977, Abyssal trace fossils in worldwide Deep Sea Drilling Project cores, in T.P. Crimes and J.C. Harper, eds., Trace Fossils 2: Geological Journal Special Issue, no. 9, p. 163-182.

Ekdale, A.A., 1980, Trace fossils in Deep Sea Drilling Project Leg 58 cores: Initial Reports of the Deep Sea Drilling Project, v. 58, p. 601-605.

Ekdale, A.A., and W.H. Berger, 1978, Deep-sea ichnofacies: modern organism traces on and in pelagic carbonates of the western equatorial Pacific: Palaeogeography, Palaeoclimatology and Palaeoecology, v. 23, p. 263-278.

Ekdale, A.A., and R.G. Bromley, 1984, Comparative ichnology of shelf-sea and deep-sea chalk: Journal of Paleontology, v. 58, p. 322-332.

Ekdale, A.A., L.N. Muller, and M.T. Novak, 1984, Quantitative ichnology of modern pelagic deposits in the abyssal Atlantic: Palaeogeography, Palaeoclimatology and Palaeoecology, v. 45, p. 189-223.

Exon, N.F., and D.S. Cronan, 1983, Hydrothermal iron deposits and associated sediments from submarine volcanoes off Vanuatu, Southwest Pacific: Marine Geology, v. 52, p. M43-M52.

Fisher, R.V., and H.-U. Schmincke, 1984, Pyroclastic Rocks: Springer-Verlag, Berlin, 448 p.

Gabites, J.F., and J.W. Hutchings, 1961, Climatic features of the tropical Southwest Pacific Ocean: New Zealand Meteorological Service Technical Information Circular, no. 108, 10 p.

Gorton, M.P., 1977, The geochemistry and origin of Quaternary volcanism in the New Hebrides: Geochimica et Cosmochimica Acta, v. 41, p. 1257-1270.

Gregory, M.R., and J.V. Eade, 1990, Lithified sediments dredged from the North Fiji Basin: this volume.

Hein, J.R., D.W. Scholl, and J. Miller, 1978, Episodes of Aleutian Ridge explosive volcanism: Science, N.Y., v. 199, p. 137-141.

Jezek, P.A., 1976, Compositional variations within and among volcanic ash layers in the Fiji Plateau area: Journal of Geology, v. 84, p. 595-616.

Kennett, J.P., 1982, Marine Geology: Prentice-Hall, Englewood Cliffs, N.J., 813 p.

Kroenke, L.W., R. Smith, and K. Nemoto, Morphology and structure of the seafloor in the north central North Fiji Basin: this volume.

Kroenke, L.W., J.V. Eade, C.Y. Yan, and R. Smith, Sediment distribution in the north central North Fiji Basin: this volume.

Lewis, K.B., and B.P. Kohn, 1973, Ashes, turbidites, and rates of sedimentation on the continental slope off Hawkes Bay: New Zealand Journal of Geology and Geophysics, v. 16, 3, p. 439-454.

Luyendyk, B.P., W.B. Bryan, and P.A Jezek, 1974, Shallow structure of the New Hebrides Island Arc: GSA Bulletin, v. 85, p. 1287-1300.

McMurtry, G.M., E.H. de Carlo, and K.H. Kim, Geochemistry of north central North Fiji Basin sediments: this volume.

Mallick, D.I.J., and R.P. Ash, 1975, Geology of the Southern Banks Islands: New Hebrides Geological Survey Regional Report, 33 p.

Melson, W.G., E. Jarosewich, and C.A. Lundquist, 1970, Volcanic eruption at Metis Shoal, Tonga, 1967-1968: Description and Petrology: Smithsonian Contributions to the Earth Sciences, v. 4, p. 1-18.

Nelson, C.S., 1985, Bioturbation in middle bathyal, Cenozoic nannofossil oozes and chalks, Southwest Pacific: Initial Reports of the Deep Sea Drilling Project, v. 90, p. 1189-1200.

Neprochnov, Yu P., I.M. Belousov, V.P. Goncharov, A.A. Shreyder, V.N. Moskalenko, N.A. Marova, I.N. Yel'nikova, G.M. Valyashko, and N.A. Shishkina, 1974, Detailed geophysical investigations in the North-Central Fiji Basin: Doklady Akademii Nauk SSSR, v. 219, p. 688-691.

Reid, S.J., and A.C. Penney, 1982, Upper-level wind frequencies and mean speeds for New Zealand and Pacific island stations: New Zealand Meteorological Service Miscellaneous Publication no. 174.

Ruddiman, W.F., and L.K. Glover, 1982, Mixing of volcanic ash zones in subpolar North Atlantic sediments, in R.A. Scrutton and M. Talwani, eds., The Ocean Floor: John Wiley & Sons, p. 37-60.

Shaw, D.M., N.D. Watkins, and T.C. Huang, 1974, Atmospherically transported volcanic glass in deep-sea sediments: theoretical considerations: Journal of Geophysical Research, v. 79, 21, p. 3087-3094.

Sinton, J.M., R.C. Price, K.T.M. Johnson, H.J. Staudigel, and A. Zindler, Petrology and geochemistry of submarine lavas from the Lau and North Fiji back-arc basins: this volume.

Swinbanks, D.D., and Y. Shirayama, 1984, Burrow stratigraphy in relation to manganese diagenesis in modern deep-sea carbonates: Deep Sea Research, v. 31, p. 1197-1223.

Wetzel, A., 1983, Biogenic sedimentary structures in a modern upwelling area: the Northwest African continental margin, in J. Thiede and E. Suess, eds., Coastal Upwelling, its Sediment Record, Part B. Sedimentary Records of Ancient Coastal Upwelling: Plenum Press, New York, p. 123-144.

Wetzel, A., 1984, Bioturbation in deep-sea fine-grained sediments: Influence of sediment texture, turbidite frequency and rates of environmental change, in D.A.V. Stow and D.J.W. Piper, eds., Fine-grained sediments: Deep Water Processes and Facies: Geological Society of London, Special Publication, no. 14, p. 595-608.

Wilson, L., R.S.J. Sparks, T.C. Huang, and N.D. Watkins, 1978, The control of volcanic column heights by eruption energetics and dynamics: Journal of Geophysical Research, v. 83, B4, p. 1829-1836.

Young, D.K., W.H. Jahn, M.D. Richardson, and A.W. Lohanick, 1985, Photographs of deep-sea lebensspuren: a comparison of sedimentary provinces in the Venezuela Basin, Caribbean Sea: Marine Geology, v. 68, p. 269-301.

APPENDIX 1

Results of smear slide analyses.

Code to minerals and other sediment components identified:

Qu = quartz
Fs = feldspar
HM = heavy minerals
Cy = clay minerals
VG = volcanic glass
OM = opaque minerals and micronodules
Ze = zeolites
Ca = non-specific calcium carbonate
Fo = foraminifera
Nf = nannofossils
Si = siliceous microfossils

(Values in percent, tr = trace)

Core PC-5 Unit No.	Depth (cm)	Qu	Fs	HM	Cy	VG	OM	Ze	Ca	Fo	Nf	Si
	00	tr			13	4		1	10	5	65	1
	17	tr			18	5		1	12	12	50	1
	45	tr	tr		15	3	tr	1	10	8	60	2
	90	tr		tr	16	5	tr		12	9	55	2
1	150	tr			23	10	1		6	3	55	2
	200		tr		18	7	1		8	10	56	tr
	250		tr		23	5	1		5	21	45	tr
	297				20	5	tr		5	22	47	1
	300				20	5	1	tr	7	17	50	tr
------305----------												
	310				15	7	5	1	7	10	55	tr
	325	tr	tr	tr	18	13	tr	1	10	8	50	tr
	350	tr	tr		25	11	tr	1	5	6	50	1
	393	tr	tr		15	24	1	2	5	8	45	1
	394	tr	tr		10	46	tr	1	5	8	30	
	400		tr		17	9	1	2	5	22	45	
	440	tr	tr		23	11	tr	2	6	8	50	tr
	460	tr	tr		10	30	1	2	5	8	45	
	480		tr		15	6	1	1	5	27	45	
2	500		tr		25	12	1	2	6	3	50	1
	530	tr			20	22	1	2	7	3	45	
	550	tr			18	9	1	1		21	50	
	563	tr			23	21	1	2	3	15	35	
	585	tr	tr		19	18	1	2	2	15	40	
	610	tr			17	8		2	5	23	45	
	623			tr	18	15		2	5	15	45	tr
	638			tr	15	23	1	2	5	10	45	
	650				17	8		1	2	17	55	
	680	tr			20	8		2	2	23	45	
	694	tr	1	tr		85	1	2		1	9	1
------700----------												
	701	tr			20	8		2	2	23	45	
	742	tr	tr		11	5	tr	2	5	17	60	
	750				13	5				27	55	
	800				18	5				27	50	

Core PC-5 (continued)

Unit No.	Depth (cm)	Qu	Fs	HM	Cy	VG	OM	Ze	Ca	Fo	Nf	Si
	810				15	4	1			25	55	
	830		tr	tr	12	5			3	65	15	
	850				8	3			4	70	15	
	880		tr		17	5		1	2	15	60	
3	900		tr		17	5				17	55	
	950	tr			15	4		1	1	20	60	
	1000		tr	tr	25	5		2	5	13	50	
	1050	tr	tr		18	8	1	1	2	15	55	
	1062	tr		tr	25	14	tr	tr	5	40	16	tr
	1064				22	22		tr	2	40	14	tr
	1100	tr	tr		20	8		2	3	15	50	
	1150	tr	tr		18	5		2	2	18	55	

Core PC-6

Depth (cm)	Qu	Fs	HM	Cy	VG	OM	Ze	Ca	Fo	Nf	Si
00	3	1	5	18	40	3			20	10	tr
20	tr	tr		22	18				20	40	tr
65		tr	1	28	34				15	22	tr
100	tr	tr		28	20				15	37	tr
137	tr			16	8				5	65	1
190	1	tr		30	24	6			10	28	1
210	tr	1	1	18	42	7			8	22	1
244	5	4	tr	12	50	20			5	3	1
275	1	tr	1	24	40	5			9	20	tr
304				35	18	1			12	34	
343					85	15					
354	tr	1		21	40	8			2	18	
414	2	2		5	85	5				1	
420	1	1		30	23	5			12	28	
430	tr	1	4		84	11				tr	
475	1	1		30	24	3			20	20	1
500	tr	1	tr	26	15	3			20	30	2
520	1	1		1	97				tr	tr	
530	tr	1		30	7	1			8	50	3
564	1	2			95	2				tr	
570	tr	tr		40	8	1			8	42	1
606	1	2	2	15	65	5				10	
657	tr	tr			95	5					
673		tr		39	10	1			15	35	
694	tr		2	40	30	3			5	25	tr
700	1	2	1		85	11					
746	1	3	1	10	62	8				15	
816	1	1		27	5	1			15	50	tr
859	tr	3	1	20	50	1	tr			25	tr
877	tr	1	tr	27	35	1			5	30	1
896	1	5	6		85	3					
899			8		92						
960		1	2	40	20	1			5	30	1

Core Unit No.	Depth (cm)	Qu	Fs	HM	Cy	VG	OM	Ze	Ca	Fo	Nf	Si
	00		tr	tr	25	5	tr	2		25	40	tr
	25		tr	tr	19	3	tr	1	5	25	47	tr
	60		tr	tr	23	4	tr	1	2	25	45	tr
1	103	tr	2		17	35	3	tr	3	20	20	tr
	160	tr	tr		24	8			10	20	38	tr
	200		tr		20	3	tr	2	10	20	45	tr
	264	tr	tr		24	5		2	4	25	40	tr
------270----------												
	293	tr	tr	tr	25	15			5	20	35	tr
	312	tr	tr		25	3	tr	2	10	20	40	
	334		tr	tr	20	12	1	2	5	20	35	
	348			tr	22	3	tr	1	4	25	45	
	373		tr	tr	20	15	tr	2	8	15	40	
2	393	tr	tr		18	20		2	10	10	40	tr
	425		tr		22	4	tr	2	7	20	45	tr
	454		tr	tr	22	35	tr	tr	3	10	30	
	500	tr	tr		21	3	tr	tr	10	16	50	tr
	515		tr	tr	18	20		2	10	15	35	
	534	tr	1	tr	25	60	tr	1	3	5	5	
------534----------												
	572				15	20	3	2	10	25	25	
	576	tr	tr	tr	7	30	tr	1	5	42	15	
	610	tr			20	5	tr	tr	15	20	40	
3	637		tr		12	8	tr	tr	15	35	30	
	671				22	3	tr		10	20	45	
	685				17	3	tr	2	8	35	35	
	730		tr		22	3	2	tr	13	20	40	
	755		tr		22	3	2	tr	13	20	40	

Core Unit No.	Depth (cm)	Qu	Fs	HM	Cy	VG	OM	Ze	Ca	Fo	Nf	Si
	4	tr			22	2	1		3	25	45	2
	16			tr	5	25	5			60	5	
	30		1		15	1	3			15	65	tr
	68		tr		22	1	1	tr	5	25	45	1
	117		tr		27	1	tr		2	20	45	5
	130		1		22	12	3		5	20	35	2
1	138	1	3	3		40	35			6	11	1
	152		tr		25	8	5			10	50	2
	170		tr		20	2	1			15	60	2
	215		1	tr	8	22	16			22	30	1
	245		tr		16	5	1		5	25	45	3
	278				17	1	tr			50	30	2
-------300----------												
	329		tr	tr	22	15	tr			30	30	2
	368	tr	tr	1	15	20	2			15	45	2
	384		tr		22	12	2		3	20	40	1

Core PC-8 (continued) Unit No.	Depth (cm)	Qu	Fs	HM	Cy	VG	OM	Ze	Ca	Fo	Nf	Si
	404		tr		24	5	1		3	20	45	2
	420				20	2	tr			8	70	2
	490		1	1	17	2	1			8	70	tr
	511		1	3	22	12	1			10	50	1
2	546		1	1	15	30	1			10	41	1
	590		tr	tr	17	3	1		3	25	50	1
	635		tr	1	20	25	2			12	40	
	641		1		15	25	3			15	40	tr
	663			1	21	1				40	35	2
	710		tr	tr	17	1				20	60	2
	732		tr	tr	21	3				5	70	1
	769		1	1	5	82	5			6		
-------770----------												
	777		1		22	8	1			40	27	1
3	795		tr		17	8	tr			40	33	2

Core PC-9	Depth (cm)	Qu	Fs	HM	Cy	VG	OM	Ze	Ca	Fo	Nf	Si
	00	3	2	3	40	45	5	tr		2	tr	tr
	15	3	4	8	tr	60	15			3		
	28		tr	2	30	15	3		5	15	20	tr
	44	3	3	4	25	30	5	tr	1	4	15	
	74	tr	tr	tr	33		tr	2		25	30	tr
	100		3	tr	20	40			17	5	tr	15
	133	3	10	3	20	25	5	2		5	15	
	145		10	3	20	25	5	2		5	15	
	159		5	3	30	38	9			3	10	
	177		5	2	30	18	5	2		12	15	tr
	204	8		3	10	47	18					
	220	tr	tr	2	17	15		2	10	35	17	
	233	tr	tr	tr		95	3			2		
	243	tr	tr	tr		95	3			2		
	256		5	3	4	73	5					
	267					100						
	287			tr	25	22			5	27	tr	
	297					100	tr					
	304		7	2	33	35	3	2	3	4	5	
	317				15	78	2			3	2	
	332		6	2	22	20	3	tr	5	14	28	
	336		3	2	25	35	5		5	5	15	
	365		4	3		65	8			3		
	387	tr			35	45				5	tr	
	390		15	3	15	40	10			3		
	424		2	2	26	25	2	2		15	26	

APPENDIX 2

Glass analyses, North Fiji Basin piston cores.

Sample Total	Depth	SiO_2	TiO_2	Al_2O_3	FeO	MnO_2	MgO	CaO	Na_2O	K_2O	P_2O_5
PC-5	0000										
100.2		62.6	0.7	14.6	5.3	0.4	1.8	4.8	4.3	4.0	1.7
100.1		63.4	0.5	14.7	7.6	0.4	1.0	4.0	3.5	4.3	0.7
99.9		59.2	0.7	14.1	4.9	0.5	1.7	4.2	4.2	7.1	3.3
099.9		60.6	0.8	14.1	7.6	0.2	1.8	4.5	4.0	4.9	1.4
100.1		65.6	0.7	15.5	5.2	0.1	1.3	3.3	4.8	3.3	0.3
PC-5	0394										
100.1		63.0	1.6	15.0	7.7	0.2	1.1	3.7	2.9	5.3	0.1
100.2		58.5	0.9	15.9	8.9	0.1	3.7	5.6	3.7	2.6	0.3
100.6		66.6	0.6	14.6	5.3	0.2	1.0	2.6	4.3	4.6	0.8
100.1		64.3	0.6	14.6	6.3	0.2	1.0	3.6	3.4	5.2	0.9
99.9		57.3	0.8	15.6	9.3	0.3	3.4	5.7	3.5	3.1	0.9
PC-5	0468										
100.0		62.8	0.5	16.1	5.1	0.2	2.0	3.6	5.1	3.7	0.9
100.1		63.3	0.7	15.3	6.7	0.7	1.5	3.5	4.8	3.4	0.2
100.1		66.0	0.6	15.6	4.8	0.3	1.2	2.3	5.3	3.9	0.1
100.0		56.5	0.6	12.6	11.9	0.3	3.7	7.0	3.2	3.2	1.0
100.1		64.5	0.4	14.5	4.2	0.2	1.1	4.0	5.7	4.9	0.6
PC-5	0528										
100.0		61.8	0.8	14.1	7.3	0.6	0.4	2.3	4.1	7.8	0.8
100.2		58.6	1.1	15.1	8.7	0.6	2.7	5.1	4.4	3.1	0.8
100.1		61.2	0.8	13.3	6.1	0.5	0.4	3.5	2.9	9.1	2.3
99.9		64.6	0.6	14.6	5.7	0.4	1.1	2.4	4.1	6.1	0.3
100.1		53.9	0.9	15.3	12.5	0.3	3.1	7.2	3.7	2.6	0.6
PC-5	0694										
100.2		67.1	0.6	16.0	4.4	0.0	1.4	1.7	3.6	5.4	
100.0		68.7	0.3	15.2	3.6	0.3	0.8	1.7	3.6	5.8	
100.3		54.3	1.9	11.2	16.0	0.8	0.2	4.7	1.7	9.5	
99.9		68.5	0.6	15.6	2.8	0.2	0.7	1.7	4.7	5.1	
100.1		57.1	1.4	13.3	12.3	0.5	1.0	3.3	2.8	8.4	
100.1		66.7	0.6	15.4	4.4	0.2	0.9	2.0	4.3	5.6	
100.0		66.4	0.6	16.0	4.0	0.1	1.5	2.4	4.1	4.9	
100.0		67.5	0.6	15.7	3.3	0.3	1.2	1.7	4.4	5.3	
PC-5	1060										
100.1		66.8	0.8	15.8	4.0	0.2	0.9	2.1	4.4	5.1	
100.1		69.4	0.3	13.7	4.9	0.3	0.2	1.3	4.7	5.3	
100.1		68.0	0.4	14.1	5.1	0.4	0.4	1.8	4.5	5.4	
99.9		68.5	0.4	13.4	5.9	0.2	0.2	1.3	3.9	6.1	
100.2		66.6	0.8	15.5	4.3	0.2	0.8	2.8	4.1	5.1	
PC-6	0459										
100.0		48.4	1.0	13.6	15.7	0.3	3.2	8.3	2.4	3.4	1.0
100.0		57.0	0.9	15.5	10.5	0.4	3.5	5.7	4.0	2.1	0.4
100.2		54.2	1.2	13.3	15.6	0.1	2.8	7.2	2.9	2.5	0.3
100.0		61.0	0.8	14.3	8.7	0.2	2.9	3.8	4.4	3.0	0.9

Sample Total	Depth	SiO_2	TiO_2	Al_2O_3	FeO	MnO_2	MgO	CaO	Na_2O	K_2O	P_2O_5
100.0		53.6	1.1	14.1	14.3	0.4	4.1	7.0	2.7	2.1	0.6
100.1		54.7	1.1	15.8	11.6	0.2	3.7	7.1	3.2	2.4	0.3
PC-7	0297										
100.1		60.6	0.7	15.4	7.8	0.3	2.1	3.6	4.5	4.6	0.5
100.0		63.0	0.8	15.8	6.7	0.2	1.3	3.5	4.2	4.1	0.4
100.1		60.8	0.7	15.6	6.3	0.5	2.3	4.5	5.0	3.7	0.7
100.1		62.7	0.8	16.2	5.5	0.4	1.9	4.1	4.0	4.0	0.5
PC-7	0533										
100.1		67.6	0.7	15.3	4.0	0.2	1.0	2.3	4.3	4.7	
100.1		67.9	0.5	16.0	3.7	0.2	0.9	1.6	4.5	4.8	
99.9		68.0	0.7	15.9	3.7	0.3	1.0	1.7	4.2	4.7	
99.7		68.5	0.8	15.1	3.4	0.2	0.9	1.6	4.3	4.9	
99.9		68.0	0.8	15.6	3.8	0.0	1.0	1.8	4.5	4.4	
PC-8	0165										
100.2		72.1	0.4	11.6	6.0	0.3	0.7	3.7	2.8	2.1	0.5
100.0		67.7	0.5	11.6	5.9	0.1	1.5	5.1	3.3	2.3	2.0
100.1		53.3	1.1	14.7	10.7	0.7	3.2	5.8	4.3	4.9	1.4
99.9		53.5	1.0	16.7	9.7	0.5	3.5	6.0	4.5	3.9	0.6
99.9		71.2	0.3	11.8	4.5	0.3	0.9	3.6	3.5	2.4	1.4
PC-8	0213										
100.1		57.9	0.7	16.6	8.0	0.3	2.8	5.3	5.1	2.5	0.9
100.0		61.3	1.0	14.3	9.1	0.3	1.3	3.7	4.3	3.7	1.0
100.0		53.1	0.9	16.5	9.6	0.3	4.4	6.4	5.5	2.2	1.1
PC-8	0284										
100.1		66.4	0.4	15.9	4.2	0.1	0.8	2.0	5.6	4.3	0.4
100.0		54.5	1.0	11.6	16.9	0.7	0.8	2.8	2.5	8.4	0.8
100.2		66.3	0.8	14.6	4.9	0.2	0.6	2.2	4.7	5.2	0.7
100.1		58.9	0.9	15.6	8.5	0.2	2.2	5.3	4.6	3.3	0.6
99.7		60.7	1.0	15.2	8.7	0.4	1.3	4.8	4.0	3.6	
099.9		61.2	0.6	16.6	7.1	0.2	2.2	4.4	4.8	2.8	
PC-8	0383										
100.0		55.3	0.9	12.9	8.6	0.2	1.3	13.0	3.6	3.5	0.7
100.1		55.1	0.9	15.2	11.0	0.4	3.4	7.3	3.8	2.5	0.5
100.0		60.5	0.4	11.1	7.9	0.0	1.4	7.3	3.0	6.5	1.9
PC-8	0770										
99.8		67.7	0.6	15.5	3.9	0.2	0.8	2.9	3.6	4.6	
100.1		68.5	0.8	15.6	4.0	0.2	1.0	1.9	3.1	5.0	
99.7		60.1	0.7	16.0	8.1	0.1	2.3	5.1	4.4	2.9	
99.7		68.8	0.5	15.1	3.5	0.1	0.9	1.9	4.0	4.9	
99.7		64.1	1.0	14.6	6.4	0.0	1.1	3.7	3.7	5.1	
100.0		64.5	0.9	14.7	7.8	0.4	0.9	2.9	2.7	5.2	
PC-9	0315										
100.2		68.1	0.5	14.6	4.6	0.3	0.5	2.0	4.5	4.8	0.3
100.1		69.7	0.4	14.2	4.2	0.0	0.6	1.3	4.4	5.1	0.2
100.0		69.8	0.3	14.2	4.1	0.1	0.4	1.4	4.2	5.3	0.2
100.1		70.5	0.3	14.5	3.6	0.3	0.1	1.3	4.1	5.0	0.4

Kroenke, L.W., and J.V. Eade, editors, 1993, Basin Formation, Ridge Crest Processes, and Metallogenesis in the North Fiji Basin: Houston, TX, Circum-Pacific Council for Energy and Mineral Resources, Earth Science Series, Vol. 15, Springer-Verlag, New York.

LITHIFIED SEDIMENTS DREDGED FROM THE CENTRAL NORTH FIJI BASIN

MURRAY R. GREGORY
Geology Department, University of Auckland,
Auckland, New Zealand

JAMES V. EADE[1]
New Zealand Oceanographic Institute,
Wellington, New Zealand

ABSTRACT

Sedimentary rocks dredged from the seafloor in the north-central part of the North Fiji Basin at depths of 3000 m to 4500 m comprise a mixed volcanogenic and calcareous biogenic assemblage. Ages range from late Miocene to Pleistocene and are compatible with those established from magnetic data for the underlying oceanic crust which they veneer. There is no significant compaction of sediments, and lithification has occurred as a response to periodic stiff ground formation associated with depositional hiatuses or minor erosional episodes. Lithification has been diagenetically enhanced through alteration of glassy components to smectite and zeolite. The finer volcanogenic detritus of earliest sediments accumulating in this back-arc basin are mostly arc-derived, supplemented by slide- or slump-emplaced coarser epiclastic detritus with mid-ocean ridge basalt (MORB) affinities and of local origin. On the local scale sedimentation patterns and processes are complex. Although Mn encrustation of surfaces exposed on the seafloor is widespread, no shows of polymetallic sulfide deposits were encountered in the sedimentary rocks studied.

INTRODUCTION

There is general acceptance that the North Fiji Basin (Fiji Plateau of some authors) standing at 3000-3500 m, somewhat shallower than the adjacent Pacific Ocean basin at depths greater than 4500 m, is a young marginal basin (e.g., Chase, 1971; Falvey, 1975; Colley and Hindle, 1984). Seismotectonics (Eguchi, 1984; Hamburger and Isacks, this volume) and magnetic anomalies (Cherkis, 1980; Malahoff et al., 1982a,b, this volume) suggest active extensional back-arc spreading through at least the last 7.8 m.y. The broad geological and geophysical setting is reviewed elsewhere (Kroenke and Eade, this volume). Basaltic lavas which form acoustic basement in the North Fiji Basin are described by Sinton et al. (this volume).

Lying well above the calcium carbonate compensation depth (CCD), and bathymetrically isolated from any significant terrigenous input, the surficial sediments in the central part of the North Fiji Basin are dominantly calcareous pelagic ooze with 60-80% CaCO3 (Eade and Gregory, this volume) with varying and in some areas reasonably high amounts of volcanic ash (Chase, 1971; Jezek, 1976; Brocher et al., 1985; Eade and Gregory, this volume; McMurtry et al., this volume). In the central part of the basin the sediment cover is thin (Kroenke et al., this volume) and average sedimentation rates are about 10 m/m.y. at least for the last 700,000 years (Chase, 1971; Brocher et al., 1985; Eade and Gregory, this volume), a rate typical for calcareous pelagic ooze. The thin sediment veneer of the central part of the basin is locally concordant with acoustic basement, but westward it thickens and becomes increasingly discordant (Halunen, 1979; Eade and Gregory, this volume;

[1]Now with SOPAC Technical Secretariat, Suva, Fiji

Kroenke et al., this volume). In the western part of the basin, where the thicker sediments form the New Hebrides apron, arc-derived sediments predominate and sedimentation rates are considered to be much higher than in the central part of the basin (Chase, 1971; Luyendyk et al., 1974; Eade and Gregory, this volume).

The oldest sediments sampled in cores from the North Fiji Basin have suggested ages of 500,000 years (Chase, 1971) and 850,000 years (Eade and Gregory, this volume). Some cores contain reworked Pliocene foraminifera and coccoliths which indicate the existence of older sediments.

Dredgings were made on several escarpments in an attempt to recover older sediments that could assist in further elucidating basement ages already established on paleomagnetic evidence and also likely to afford information on early sedimentation processes and subsequent evolution of a back-arc basin.

DREDGE STATIONS

Successful dredgings were made at five stations in the North Fiji Basin from depths exceeding 4500 m to less than 3000 m (Figure 1; Table 1) during cruise KK820316 Leg 3 by the Hawaii Institute of Geophysics (HIG) vessel R/V KANA KEOKI.

Of the five dredge stations, two (RD-19 and RD-20) lay on or near the active rift axis of the South Pandora Ridge where sediment cover is virtually non-existent (Kroenke et al., this volume) and the samples recovered comprised entirely clean, fresh, fine-grained basalts, often with glassy selvedges and fragmented pillow-form shape. These samples are described elsewhere (Sinton et al., this volume). The other three stations (RD-16, RD-17, RD-21) were sited on escarpments at depths between 2690 m and 3500 m, which had minimal sediment cover as seen on continuous seismic reflection profiles and 3.5 kHz-records (Figure 2). These localities lie within the "smoothed abyssal hills" terrain of Kroenke et al. (this volume) where sediments distinctly drape acoustic basement, muting many topographic irregularities. Basement ages of 3-6 Ma are estimated for these areas. At these three stations several kinds and varying quantities of lithified sediment were recovered in addition to basaltic fragments, which were typically weathered with manganiferous encrustations up to 5 mm thick (RD-17) (Sinton et al., this volume).

A series of bottom photographs were taken in the vicinity of RD-17 (camera station BC-1) and RD-19 (BC-2). No lithified slab-shaped sedimentary crusts or ledges are evident in any of the photographs examined, although the shape of several recovered specimens suggests their presence. Pillow basalts of fresh appearance, and often lightly dusted with pelagic sediment which is also pocketed among them, are captured in several frames (see Eade and Gregory, this volume, Figure 12; McMurtry et al., this volume, Figure 8a).

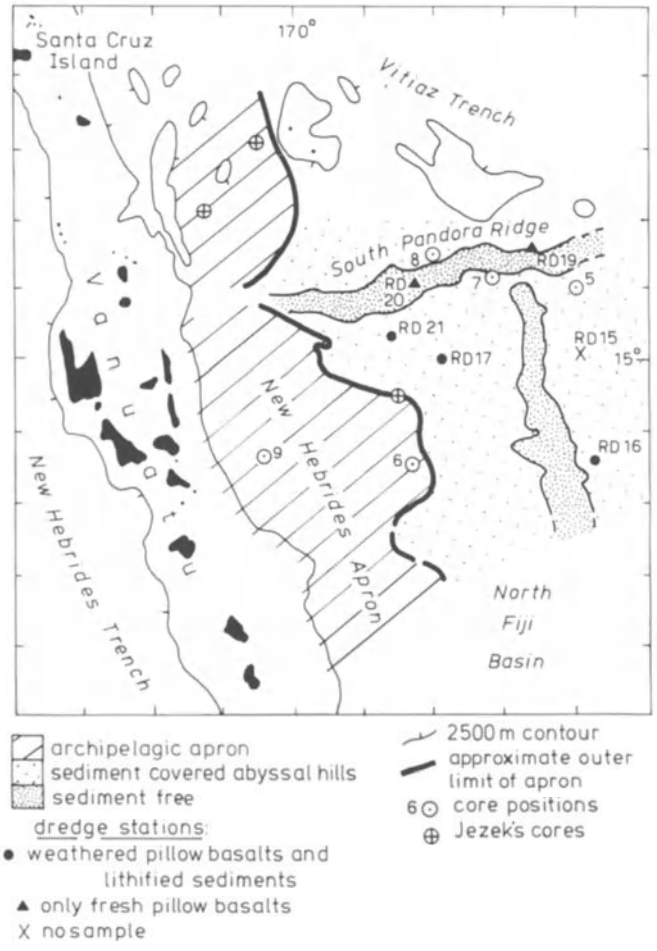

Figure 1. Locality map showing position of dredge stations in relation to the sediment terrains of the North Fiji Basin.

Dredge Site Descriptions (see Figure 2)

Station 21, RD-16

RD-16 comes from a prominent, steep, sediment-free, southeast-facing escarpment. In the area dredged the scarp is 1000-2000 m high with an average slope of about 35 degrees. Northwest and southeast of this escarpment the sediment covering basement is about 0.1 seconds thick (two-way time).

Station 23, RD-17 (also BC-1)

This locality is in an area of abyssal hills where sediment cover is continuous but thin (< 0.1 s thick, two-way time). The fabric of the seafloor trends WNW-ESE. RD-17 is located on the steep southwest-facing flank of an abyssal hill where the seafloor stands slightly elevated

Table 1. Summary of Dredging Station Data

Station No.	Dredge No.	Position Lat. S	Position Long. E	Depth (m)	Comments
20	15	14°53.3'	174°00.8'	3020	Dredge empty - no bites
21	16	16°29.7' to 16°30.4'	174°17.0' to 174°16.3'	?3445-2690	Moderately large haul: fragments of pillow basalt with glassy selvedges; up to >30 cm; across; weathered and Mn-encrusted. Several large slabby samples (>60 cm across) lithified volcanilutite; smaller rounded fragments stiff to weakly lithified chalky ooze. Rare pebble- to cobble-sized samples volcaniclastic breccia.
23	17	15°03.4' to 14°57.9'	171°57.5' to 171°57.4'	3160	Poor haul: solitary fragment weathered glassy (pillow) basalt. Single piece weakly lithified ashy chalky ooze light Mn coating, surface flutings and open borings.
25	18				Dredge lost.
	19	13°32.2'	173°20.2'	2350	Moderate haul: fresh pillow basalts. No lithified sediments.
27	20	13°46.0'	172°00.5'	4550	Moderate haul: very fresh pillow basalts. No lithified sediments.
28	21	14°31.5'	171°27.0'	3110	Small haul: solitary fragment (30 cm) weathered glassy pillow basalt. Few rounded samples consolidated/lithified (ashy) chalky ooze.

from that to the north and south. The thickness of the sediment cover tends to increase in both northerly and southerly directions.

Station 25, RD-19 (also BC-2)

RD-19 comes from the south side of a peak in a relatively shallow, high relief area lying within the axial rift of the WSW-ENE trending South Pandora Ridge. Within the rift there are numerous steep slopes, which on seismic reflection profiles are virtually devoid of any sediment cover.

Station 27, RD-20

RD-20 comes from much deeper water than RD-19 and on lower slopes of the South Pandora Ridge axial rift where it is at least 25 km wide and more than 1500 m deep. Locally the sides of the rift are very steep and from seismic reflection records appear to be sediment free.

Station 28, RD-21

RD-21 comes from within an area of abyssal hills where sediment cover appears continuous and about 0.1 s thick (two-way time) on seismic reflection records. RD-21 is from the steep side wall of the deepest part of a minor rift-like feature in a region where the seafloor has a prominent WNW-ESE trending fabric.

LITHOLOGIES

Three distinctive rock types were identified among the several lithified sediment samples recovered in the dredge hauls: volcaniclastic breccia, volcanilutite, and chalky, often ash-bearing calcilutites. These mixtures of volcaniclastic and pelagic carbonate lithologies are similar to those recovered from the southern Tonga platform by Exon et al. (1985), who found themselves presented with nomenclatural problems. Because the

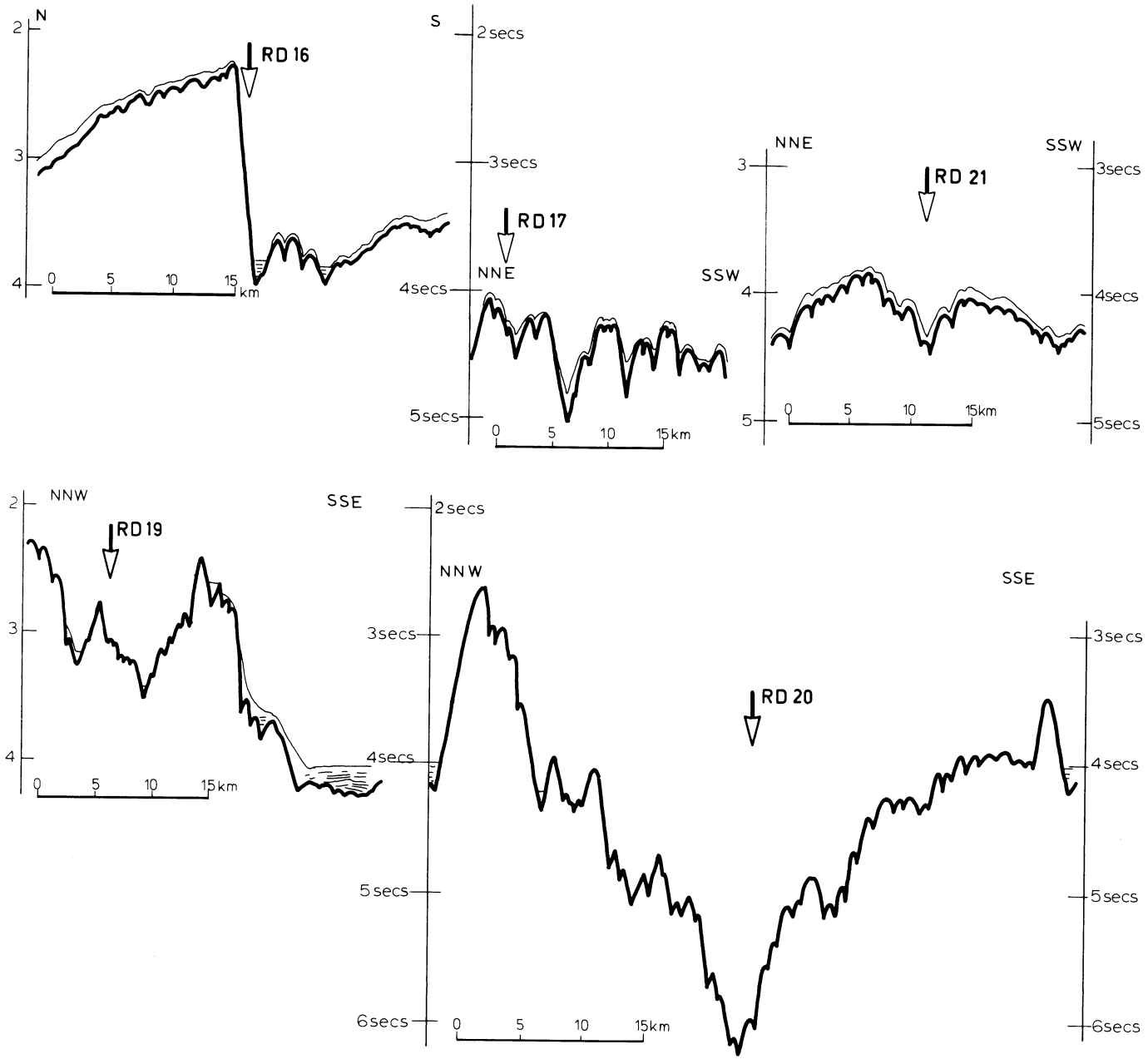

Figure 2. Simplified tracing of continuous seismic reflection profiles kaken on R/V KANA KEOKI across dredge station localities RD-16, RD-17, RD-19, RD-20, and RD-21. Successful bottom camera stations were at RD-17 (BC-1) and RD-19 (BC-2).

sand-sized components are typically either volcanic grains or foraminifera, some workers may consider variations around the terms "marly volcanic sandstone" or "sandy volcanic marl" more appropriate.

Most specimens had been extensively abraded and rounded during dredge operations, and many were coated with or heavily enrolled within modern pelagic carbonate ooze.

1. Volcaniclastic breccia (AU 39056)

Several irregularly shaped, sub-rounded cobbles of poorly sorted and loosely compacted, but weakly to moderately cemented volcaniclastic breccia were collected in RD-16 (Figure 3). The largest cobble exceeded 15 cm across but it broke into several smaller fragments during and after recovery. This breccia lithology comprises angular and subangular to sub-rounded, and rarely rounded clasts of weathered, fine grained, non-vesicular basalt with subordinate glass (Figure 3). These clasts commonly reach 1 cm in diameter and the

[1]Catalogue number of rock specimens and/or thin sections housed in collections of the Geology Department, University of Auckland.

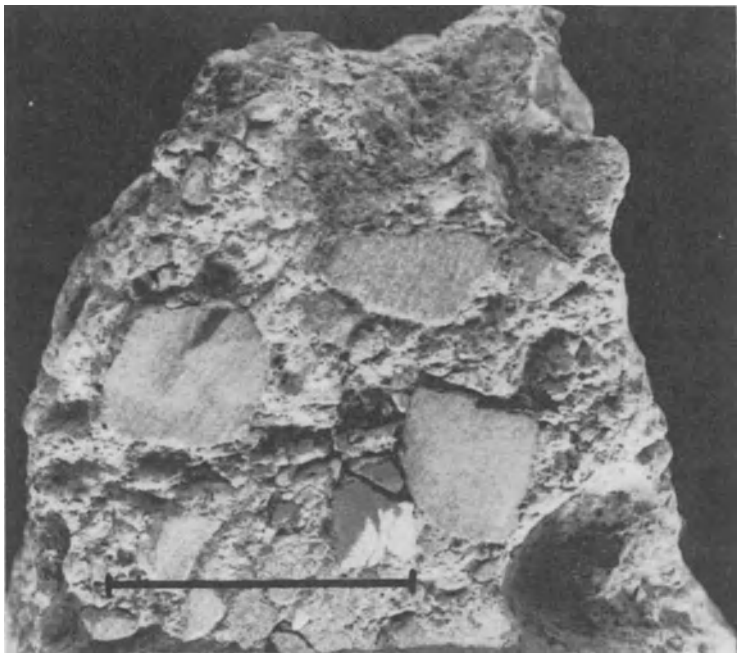

Figure 3. Volcaniclastic breccia from RD-16 (AU 39056). Bar scale 2 cm.

impression of one at least 4 cm across was evident on the broken surface of one of the cobbles. The clasts are set irregularly, and sometimes with grain-to-grain contact in a dull olive-green, volcanic-rich, non-calcareous muddy sand matrix. Pumice clasts were not recognised in any of the dredged breccia samples. Whilst a very poorly developed manganiferous coating is present on an irregularly planar surface of specimen AU 39056, it is not evident as veining along freshly broken surfaces more or less normal to this, suggesting breccia specimens were dredged from slabby exposures on the sea floor. There were no encrusting biota on this Mn-coated surface. Breccia samples are not graded and lack sedimentary structures other than a very crude planar fabric roughly paralleling the previously described Mn-coated surface. In none of the examined material is there any indication of a sedimentary contact with either of the other lithologies recovered as described below. Elsewhere in this volume (Sinton et al.) this volcaniclastic breccia lithology is termed a hyaloclastite. Whilst some of the characteristics of typical hyaloclastites are exhibited (cf. Schmincke et al., 1984; Moberly and Jenkyns, 1981; Batiza et al., 1984), for reasons outlined later we prefer an epiclastic origin for these deposits.

2. Volcanilutites (Tuffs) (AU 39057, AU 39058, AU 39059)

Two large slabs (60 cm x 30 cm x 10-20 cm), several smaller irregularly slabby pieces, and rounded pebble- to cobble-sized fragments of dark grey, sandy, volcanilutite (tuff) were also recovered in RD-16 (Figures 4, 5, 6, and 7). This lithology commonly exhibits a prominent, irregular, planar parting fabric, parallel to bedding. Parting develops along laminae made conspicuous by winnowed concentrations of larger, mostly unbroken foraminiferids (*Orbulina, Globigerinoides*) some of which are filled with an amorphous pale yellow-brown clay material. Occasional, small scale cross bedding (1-2 cm) is similarly emphasized by foraminiferal concentrations. Small scale scour and fill structures together with erosional truncation of planar and cross-bedded laminae are uncommon. Other than these phenomena, primary sedimentary features are lacking and there is no evidence of graded bedding in any of the tuff samples. Minor to moderate quantities of sand-sized, rounded, white pumice clasts degraded to clay were present in some foraminifera-rich laminae.

On surfaces cut normal to bedding, the tuff lithology is seen to be commonly overlain and rarely underlain by weakly to moderately lithified (stiff), pale cream calcilutite (below). Where present the basal contact is invariably sharp whilst the upper contact may be either sharp or diffuse with evidence of thorough biogenic reworking of both lithologies through a zone of 5-10 cm producing a characteristically mottled texture (Figures 4 and 5).

Where the upper contact is sharp, it is irregularly erosional and reminiscent of the bored stiff grounds described by Ekdale (1985). Here, vertical and oblique burrows, into and through the dark grey tuff, remained open for a time (Figure 7) before some were passively infilled from above by the pale creamy calcilutite (Figure 5). Occasionally the upper contact is defined by a crudely brecciated zone of irregularly angular to sub-rounded to rare wispy fragments of dark grey tuff, up to, but seldom more than, a centimeter across, set in the pale calcilutite. Sometimes this texture is clearly bioturbate. In other instances however, there is evidence for mechanical fragmentation of the kind that could originate through disruption of a firm ground. Collapse, with or without minor lateral displacement, is envisaged as some tuff fragments, whilst separated, maintain a fitted relationship.

There are also abundant indications that the tuff has been biogenically reworked in a patchy manner, with irregular and discontinuous disruption to foraminifera-rich planar laminae and small scale cross bedding by *Planolites*-like and other burrows (Figures 4 and 5). Several meniscate-filled burrows suggestive of

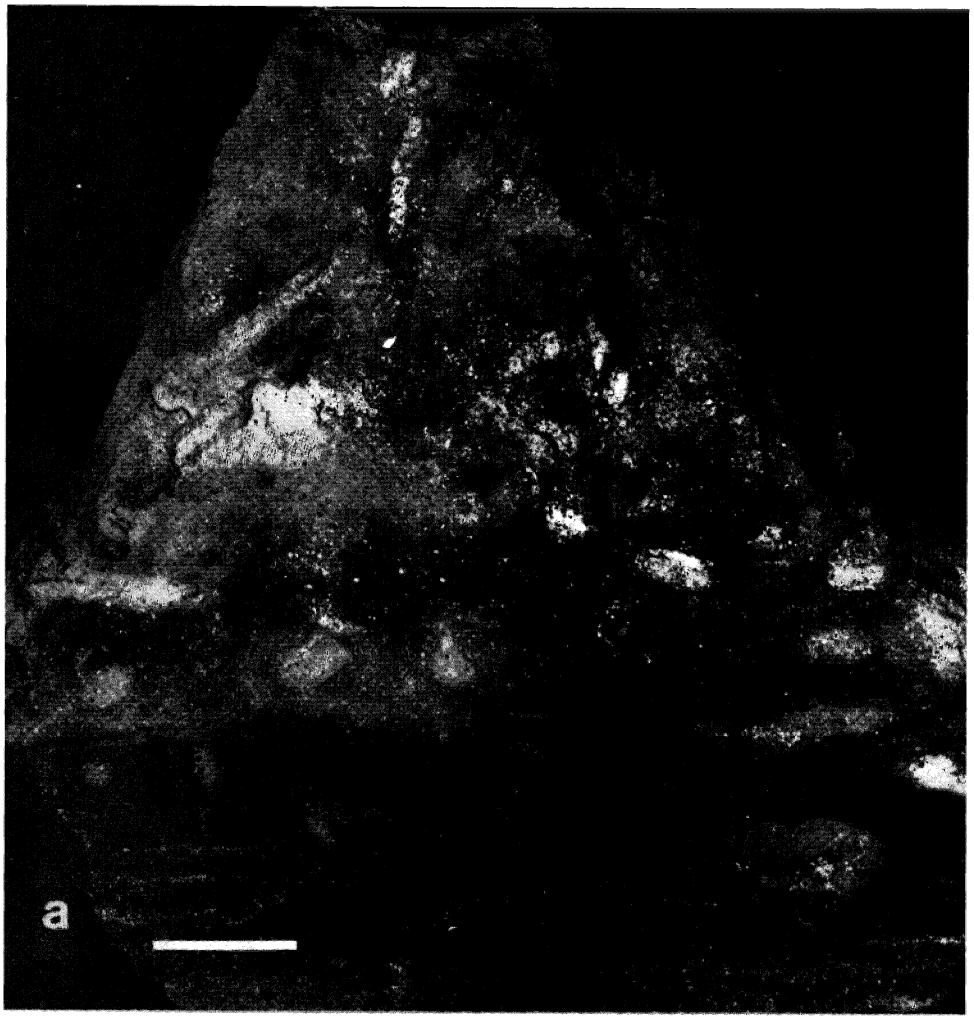

Figure 4. Semi-lithified fragment from RD-16 (AU 39057): (a) well cemented, dark grey, tuffaceous lithology with prominent foraminifera-rich laminae (lower), passing gradationally upward through a burrow mottled zone into overlying creamy pelagic carbonate ooze; (b) biogenic disturbance evident in foraminifera-rich laminae exposed on broken surfaces sub-parallel to bedding. Bar scale 2 cm.

Zoophycos were also present. Many trace fossils within the tuff lithology have infillings rich in larger planktonic foraminiferids and rounded sand-sized pumice clasts.

Sub-rounded to rounded, degraded and often quite rotten, creamy white pumice clasts (Figure 6), up to and rarely exceeding 3 cm across, are scattered irregularly through the diffuse bioturbated upper contact zone of the tuff lithology. Closer to the basal contact, pumice clasts are less common. Many of these pumice fragments have a conspicuous yellow-orange to pale brown weathering rind, and most also have a manganiferous coating.

3. Chalky calcilutite: (AU 39060, AU 39061, AU 39062)

Weakly to moderately lithified (stiff) pale creamy to creamy brown calcilutites were recovered at RD-16, RD-17, and RD-21 (Figures 8, 9, and 10). Most of the recovered samples had been rounded during dredging. However, some were not obviously rounded (AU 39060) but had irregular surfaces suggesting they were broken from protruding ledges, although no outcrops were seen in bottom photographs. Calcilutite also occurs in fragments in sedimentary contact with the previously described tuff lithology and these are commonly slab-shaped. These calcilutites are the weakly to moderately lithified (stiff) equivalents of ash-bearing, biogenic pelagic carbonate oozes that dominate modern sedimentation above the CCD around the present active plate boundary in the Southwest Pacific (e.g., Klein, 1985), including the North Fiji Basin (Jezek, 1976; Eade and Gregory, this volume). With the exception of a common faintly bioturbate (mottled) fabric and rare laminae of winnowed, larger planktonic foraminifera with subordinate pumice clasts, these samples are

Figure 5. Semi-lithified fragment from RD-16 (AU 39057): reasonably abrupt contact between tuff lithology and overlying ashy calcareous ooze. Note the manganiferous-lined, vertical tubular trace fossil, infilled from above and which passes through the contact. Bar scale 2 cm.

Figure 6. Semi-lithified fragment from RD-16 (AU 39058): rounded, clayey, degraded pumice clast with minor manganiferous coating, in sharp contrast to its enclosing host of a bioturbate mixture of foraminiferal pelagic ooze (calcilutite) and sandy volcanilutite (tuff) lithologies. Bar scale 2 cm.

devoid of sedimentary structures. Texturally, these calcareous lithologies range from lutites to foraminiferal sands, and many samples are speckled with manganiferous micro-nodules (Figure 9a).

Large open burrows were present in several calcilutite samples (Figure 8) as they were in tuffs (e.g., Figure 7). In all instances these burrows had a prominent manganiferous coating and there was no evidence for a passive contemporary ooze fill. It seems improbable any fill would have been washed out and lost during recovery as these samples were partially enrolled in sticky modern calcareous ooze. Prominent scratch marks on the walls of some of the burrows (Figure 8a) suggest a crustacean (? shrimp) progenitor.

Small simple non-diagnostic (and ?non-branching) tubular trace fossils, 2-3 mm across and sometimes exceeding 8 mm in length, are quite abundant in the calcilutites (Figure 9b and c). Most appear to be oriented normal to the apparent bedding. Their infilling is identical to the host sediment, but the manner of preservation hints at stable mucous-lined, and perhaps agglutinated walls. Very thin, poorly developed manganiferous linings (cf. Figure 5) suggest some burrow systems of this kind may have remained open at the sediment/water interface for some time, until they were passively infilled.

In one dredged calcilutite specimen (AU 39062; Figure 10) a probable depositional hiatus is emphasized by a thin, yet well developed manganiferous crust that also extends as apophyses irregularly into the sediment below. There are vague indications of simple tubular trace fossils in the lower unit being truncated at this level. Although the colour change at this boundary is subtle, and there is no apparent textural variation across it, the underlying calcilutite is stiffer than that which overlies it. There is no paleontologic (nannofossil) evidence for any age difference across this boundary.

Within the weakly lithified calcilutite, and also in the tuff lithologies, there is never any sign that trace fossils have been subjected to compactional deformation.

MINERALOGY AND PETROGRAPHY

Fresh, unbroken, and disaggregated samples of lithified sediments from RD-16, RD-17, and RD-21 were first examined microscopically under reflected light, and then under transmitted light in smear slides, thin sections and grain mounts. Identification of lithic and biogenic components was supplemented by SEM examination of selected samples. Conventional XRD techniques were used to clarify some mineral identifications and also to determine clay compositions.

The granule-sized and larger clasts of the breccias comprise in sub-equal quantities (i) plagioclase and clinopyroxene bearing, fresh basalts with ophitic texture and typically quench-ed character, (ii) glassy spherulitic basalts and tachylite, and (iii) pale yellow to brown glass (sideromelane), progressively

palagonitized and devitrified to varying extent. These clasts are typically non-vesicular and bound firmly in a poorly sorted, muddy sand matrix of granulated basaltic lithics, palagonite and glass, largely degraded to a finely felted mosaic of smectite and zeolite with rare grains of feldspar and augite. There is no carbonate cement, biogenic material is rare to absent, and in general manganiferous coatings and Mn micronodules are poorly developed. It can be noted that in the material examined by us there is no indication of the olivine reported by Sinton et al. (this volume) for similar breccia samples that they examined from RD-16.

The principal silt and fine sand size clasts of the tuff and ashy calcilutite lithologies, apart from biogenic detritus, are monotonously uniform, with plagioclase dominant, and lesser but varying quantities of augite and hypersthene (AU 39057) with minor biotite (AU 39059) and rare hornblende (AU 39061). Opaques are common. Olivine was never identified. There are pervasive zones of Mn encrustations or veining in many samples (AU 39062) and Mn micronodules are ubiquitous (Figure 9a). There is little and often no obvious glass shardy material in these lithologies, although palagonite grains are quite common. The glass has presumably been diagenetically altered to the smectite and zeolite identified by XRD. Rare, freshly broken, clear quartz grains are conspicuous in several samples (AU 39079). Quartz and illite are also prominent in several XRD records.

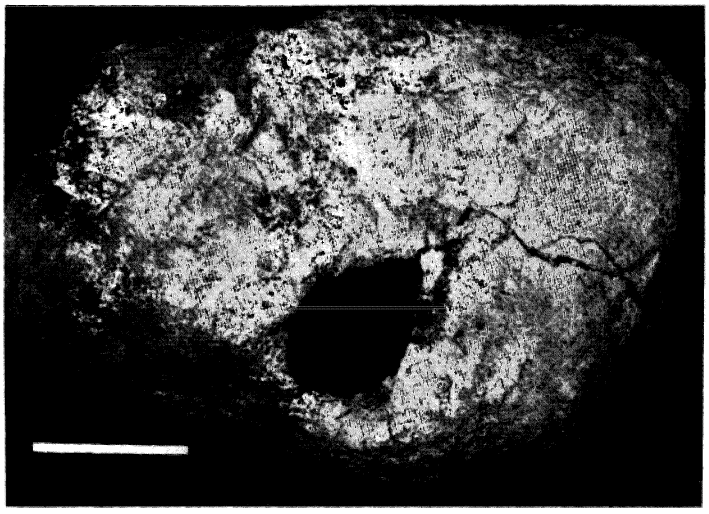

Figure 7. Tuff pebble from RD-16 (AU 39059): large open boring in tuff pebble, rounded during dredging and veneered with modern calcareous ooze. There is no evidence for any passive infilling of the boring, which is lined with a dark manganiferous coating. Bar scale 2 cm.

PROVENANCE

From the mineralogy and petrography of rock samples studied it is concluded that the origins of non-carbonate components are as follows:

(i) The volcaniclastic breccias have a mineralogy which Sinton et al. (this volume) indicate has typical MORB affinities;

(ii) The volcanic component of the tuffs and ashy calcilutites is typically calc-alkaline in character and probably arc-derived;

(iii) The pervasive Mn encrustations of these sedimentary rocks are considered indicative of hydrothermal activity across the North Fiji Basin (Cronan, 1983), however, polymetallic sulfides of the kind von Stackelberg et al. (1985) found impregnating basalts from the northeast part of the North Fiji Basin were never identified in the material examined here.

AGE

Nannofossil (A.D. Kadar, personal communication) and planktonic foraminiferal (A.N. Carter, personal communication) determinations indicate early to mid-Pliocene ages for lithified calcilutites from RD-17 and RD-21. Similar ages were also given for a tuff and several calcilutite samples from RD-16. A solitary, brownish cream, ashy calcilutite cobble from RD-16 (AU 39079) gave a foraminiferal age of uppermost mid-Miocene and a nannofossil age of early Pliocene with evidence for reworking of older taxa. These are to be compared with the no older than very late Pliocene age reported by Luyendyk et al. (1974) for a suite of sedimentary rocks dredged apparently from acoustic basement east of Maewo Island, Vanuatu, and some distance west of the present study area. The age determinations for this lithologically restricted suite of sedimentary rocks are compatible with those established from magnetic data for the oceanic crust on which they rest. Variations in lithology, and age from late Miocene to Pliocene and Pleistocene probably reflect a complex history of extensional back-arc spreading over the last 8 m.y. (Malahoff et al., 1982a,b, this volume).

In the samples examined there was never any indication of fossil age discrepancies or breaks across lithologic contacts, depositional hiatus boundaries, or at the "stiff ground" omission surfaces.

It was not possible to determine ages for the volcaniclastic breccia lithology.

SEDIMENTARY PROCESSES

Sinton et al. (this volume) described the volcaniclastic breccia lithology as hyaloclastite. However, rounding of larger basaltic clasts, lack of grading, and textural relationships, together with the indiscriminate mixtures of several volcanic rock types, suggest to us an epiclastic origin. Typical hyaloclastites have only rare lithic fragments and glass shards that are chemically homogeneous (Batiza et al., 1984). The breccias are probably mass emplaced, surficial slump or slide and fall deposits, accumulating as talus on or at the foot of steep escarpments. Some glass clasts perhaps represent spallation products of the pillow basalts with glassy selvedges which were also recovered in RD-16. Deposits of this kind with pebble- to cobble-sized lithic clasts scattered irregularly over and partially covered by fine grained seafloor sediments (ooze) are tentatively identified in several photographs from BC-2.

Although the evidence is not conclusive, the other volcanogenic sediments probably are mostly airfall deposits. Products of explosive eruptions settling directly through the water column or in part being derived from the erosion and disintegration of pyroclastic debris

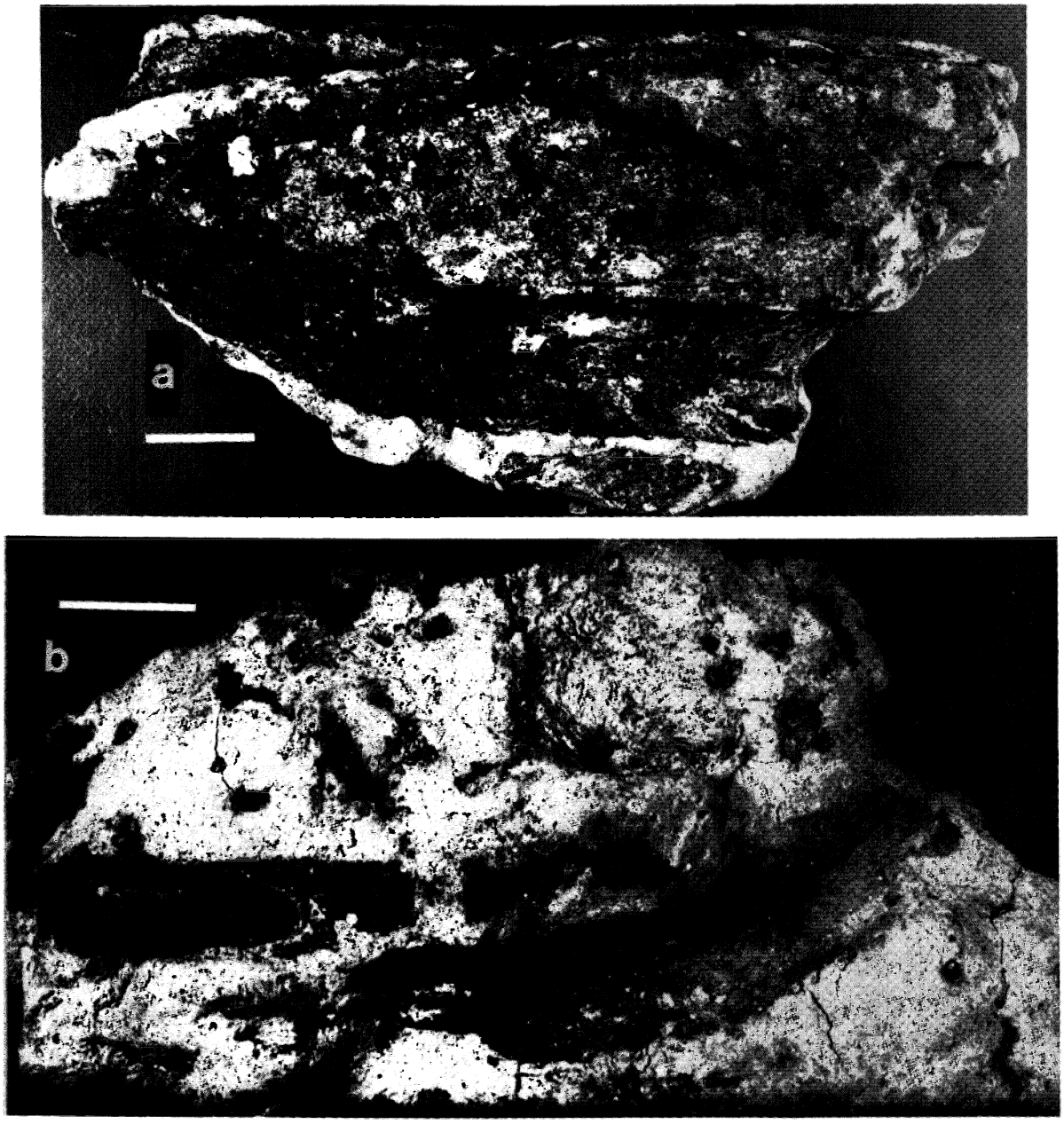

Figure 8. Weakly lithified and bored, chalky foraminiferal calcilutite from RD-17 (AU 39060), Pleistocene: (a) light manganiferous coating on its exposed (outer) surface; (b) broken surface (internal) with evidence of blotchy manganiferous development around and within biogenic structures, and open burrow systems with manganiferous linings. Note the pattern of chevron scratch marks in the open burrow in the exposed surface(s). Bar scales 2 cm.

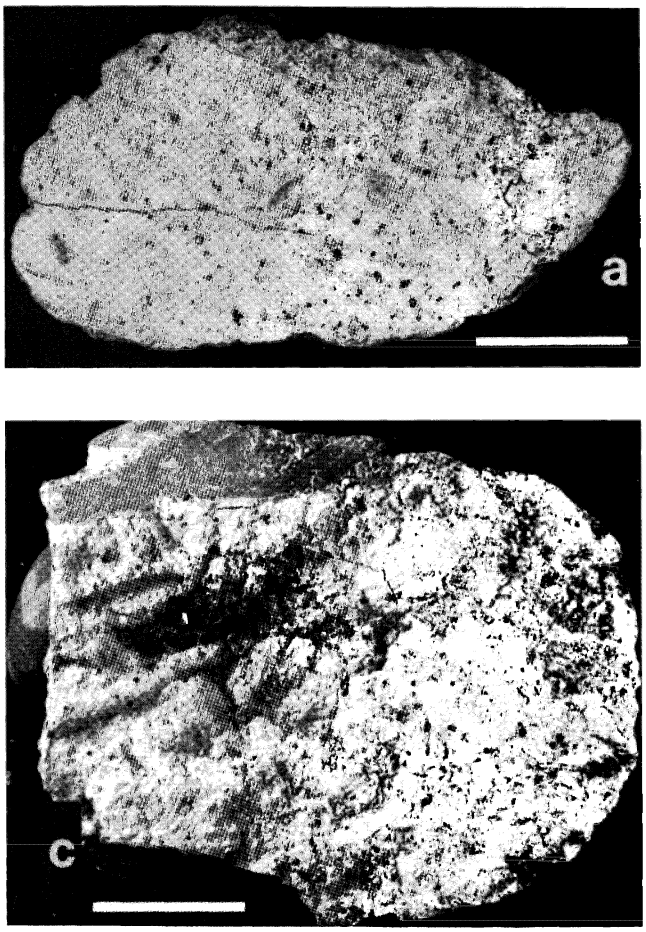

Figure 9. Chalky calilutite speckled with manganiferous micronodules from RD-21 (a, b, and c = AU 39061). ?Pliocene: (a) faintly bioturbate fabric; (b) and (c) molds and casts of simple tubular trace fossils on broken surfaces. The tube infillings are identical to the enclosing host sediment. Bar scales 2 cm.

of shallow marine phreatomagmatic eruptions (Carey and Sigurdsson, 1984). These tuffs and the ashy calcilutites are the lithified equivalents of sediments identified in cores from the region by Eade and Gregory (this volume). Winnowed, foraminifera-rich laminae, rare micro-crossbedding and small scour phenomena indicate intermittent current activity during the period these sediments were accumulating. The pure calcilutites are typical calcareous pelagic ooze deposits dominated by coccolith and foraminiferal detritus with minor contributions of siliceous sponge spicules and radiolaria and rare diatoms. Ash-bearing calcareous lithologies are testimony to a continual rain of small amounts of fine volcanic detritus onto the seafloor and thorough biogenic mixing(see Eade and Gregory, this volume). Some minor aeolian contribution from continental sources of fine quartz, illite, and kaolinite is probable (see Theide, 1979; McMurtry et al., this volume). Waterlogged pumice, transported by wind driven surface currents, sporadically settled onto the seafloor and was incorporated into these sediments (Eade and Gregory, this volume).

Intense bioturbation has mixed volcaniclastic (tuff) horizons with background pelagic carbonate ooze and in many instances sedimentary contacts are obliterated or gradational. Facing can often be determined through passive infilling by pale pelagic ooze of borings and burrows that remained open at the sediment/water interface for some time after formation. These bored surfaces, together with localized patchy intrastratal brecciation towards the top of tuff horizons are indicative of stiff ground formation during depositional hiatuses or minor erosional episodes.

Although there is no indication in any of the bottom photographs of ledges of sedimentary rock, the slabby character of the largest pieces recovered together with open Mn-encrusted burrows, suggests lithification takes place on the seafloor with stiff grounds periodically developed in the manner described by Pudsey et al. (1981). There is no evidence that any significant compaction is involved in this lithification process, although it is enhanced by degradation of volcanogenic detritus to smectite and zeolites. The envisaged general pattern of sediment accumulation, with transport from topographic highs to adjacent low areas, episodic (weak) bottom current activity, fluctuating volcanogenic input in a region otherwise dominated by biogenic pelagic carbonate oozes, some possible hydrothermal alteration, and continual churning of the seafloor through biological activity is not dissimilar to that described by Marks (1981) for sedimentation on new oceanic crust of a region of the Mid-Atlantic Ridge.

SYNTHESIS

Although the range of volcanogenic and biogenic rock types under investigation is somewhat limited and comes from only three dredge stations, the samples are representative of a broad variety of lithologies widely

reported from back-arc environments of the southwest Pacific (e.g., Leitch, 1984; Jenkins, 1985; Klein, 1985) and for which elegant and yet simplistic modelling of sedimentary environments and processes has been undertaken (e.g., Carey and Sigurdsson, 1984).

The North Fiji Basin is surrounded by largely submarine ridges and seamount chains, and stands proud of regional oceanic depths. The central part of the basin, from which these sedimentary rocks come, is isolated from any terrigenous input other than aoelian dust. It is not reached by distal turbidites of the New Hebrides apron (Eade and Gregory, this volume). However, throughout its development, calcareous pelagic ooze and varying amounts of volcaniclastics, both from local sources and from adjacent volcanic arcs, have accumulated in the North Fiji Basin.

Seafloor morphology at all dredge sites is locally complex with considerable relief, and depositional isolation is reflected in the varying lithofacies recovered. The dominance of arc-derived volcanogenic detritus in the earliest sediments accumulated on new oceanic crust in back-arc basins is a theme reported widely (Carey and Sigurdsson, 1984; Leitch, 1984). Intercalations of locally derived sediment, represented by the volcaniclastic breccias, are unlikely to spread far from source escarpments. It is evident from lithologies recorded in the cores (see Eade and Gregory, this volume) that arc volcanogenic input has decreased significantly in the central part of the North Fiji Basin since earliest sediment accumulation on the newly formed crust. This evolutionary pattern is similar to those recorded in other western Pacific back-arc basins described by Leitch (1984) and Carey and Sigurdsson (1984).

CONCLUSIONS

1. The semi-lithified epiclastic breccias, tuffs, and ash-bearing calcilutites are typical of volcaniclastic rocks found in back-arc basins immediately overlying basement.

2. The epiclastic breccias have a mineralogic and lithologic composition reflecting local slumps or slide derivation and mass emplaced talus accumulations at the foot of steep escarpments in a back-arc environment where rocks of MORB affinities outcrop.

3. The tuffs and ash-bearing calcilutites carry the mineralogic imprint of calc-alkaline rocks and are probably arc-derived.

4. It was not possible to establish any stratigraphic order or sequence for the various sedimentary lithologies identified amongst the dredged material.

5. The age ranges of the dredged sedimentary rocks are in accord with those established by magnetic data for the underlying oceanic crust, and reflect a complex history of back-arc spreading.

6. Sedimentation and lithification have been both episodic and irregular. Stiff grounds, with or without, open Mn-encrusted borings and burrows suggest lengthy periods of non-deposition, perhaps accompanied by erosion.

7. While lithification is primarily a response to stiff ground formation, it is enhanced by progressive degradation of volcanic glass with formation of smectite clays and zeolite.

8. Discontinuous weak current action is indicated during early sediment accumulation on new oceanic crust.

9. Partial to complete mixing of volcaniclastic and pelagic carbonate ooze lithologies is a response to extensive bioturbation.

10. While the presence of Mn-rich encrustations are possible evidence for hydrothermal activity and metallogenic enrichment of recent sediments across the North Fiji Basin as suggested by McMurtry et al. (this volume), there is no sign of polymetallic sulfide deposits in the dredged sedimentary rocks studied here.

Figure 10. Rounded calcilutite pebble from RD-21 (AU 39062), ?Pliocene: the Mn-enriched zone may represent a depositional hiatus although there is no nannofossil evidence for this (see text). Bar scale 2 cm.

ACKNOWLEDGMENTS

The assistance of shipboard colleagues, especially the HIG and University of Hawaii Marine Center technicians together with that of Captain Bob Hayes and the crew of R/V KANA KEOKI in collecting this dredged material is deeply appreciated. Both authors also express their gratitude to HIG and the Department of Oceanography, UH, and in particular Chris Mato and her core laboratory staff, for use of facilities and collaborative support. Further technical assistance came from N. Bovaird, S. Courtney, B. Curham, and K. Johnston, Geology Department, University of Auckland. The figures were prepared by R. Harris and early typescripts by R. Bunker.

REFERENCES

Batiza, R., D.J. Fornari, D.A. Vanko, P. Lonsdale, 1984, Craters, calderas and hyaloclastites on young Pacific seamounts: Journal of Geophysical Research, v. 89, p. 8371-8390.

Brocher, T.M., S. Wirasantosa, F. Theyer, and C. Mato, 1985, Regional sedimentation patterns along the Northern Melanesian Borderland, in T.M. Brocher, ed., Geological Investigations of the Northern Melanesian Borderland, Earth Science Series, Vol. 3: Houston, TX, Circum-Pacific Council for Energy and Mineral Resources, p. 75-101.

Carey, S., and H. Sigurdsson, 1984, A model of volcanogenic sedimentation in marginal basins, in B.P. Kokelaar and M.F. Howells, eds., Marginal Basin Geology: Volcanic and associated sedimentary and tectonic processes in modern and ancient marginal basins: Special Publication of the Geological Society of London, no. 16, p. 3758.

Chase, C.G., 1971, Tectonic history of the Fiji Plateau: GSA Bulletin, v. 82, p. 3087-3110.

Cherkis, N.Z., 1980, Aeromagnetic investigations and seafloor spreading history in the Lau Basin and Northern Fiji Plateau: U.N., ESCAP, CCOP/SOPAC Technical Bulletin, no. 3, p. 37-45.

Colley, H., and W.H. Hindle, 1984, Volcano-tectonic evolution of Fiji and adjoining marginal basins, in B.P. Kokelaar and M.F. Howells, eds., Marginal Basin Geology: Volcanic and associated sedimentary and tectonic processes in modern and ancient marginal basins: Special Publication of the Geological Society of London, no. 16, p. 151-162.

Cronan, D.S., 1983, Metalliferous sediments in the CCOP/SOPAC region of the Southwest Pacific, with particular reference to geochemical exploration for the deposits: U.N., ESCAP, CCOP/SOPAC Technical Bulletin, no. 4, 55 p.

Eade, J.V., and M.R. Gregory, Sediments of the North Fiji Basin: this volume.

Eguchi, T., 1984, Seismotectonics of the Fiji Plateau and Lau Basin: Tectonophysics, v. 102, p. 17-32.

Ekdale, A.A. 1985, Paleoecology of the marine endobenthos: Palaeogeography, Palaeoecology, Palaeoclimatology, v. 50, p. 63-81.

Exon, N.F., R.H. Herzer, and J.W. Cole, 1985, Mixed volcaniclastic and pelagic sedimentary rocks from the Cenozoic southern Tonga Platform and their implications for petroleum potential, in D.W. Scholl and T.L. Vallier, eds., Geology and offshore resources of Pacific island arcs - Tonga region, Earth Science Series, Vol. 2: Houston, TX, Circum-Pacific Council for Energy and Mineral Resources, p. 75-107.

Falvey, D., 1975, Arc reversals and a tectonic model for the North Fiji Basin: Australian Society of Exploration Geophysicists Bulletin, v. 9, p. 47-49.

Halunen, A.J., 1979, Tectonic history of the Fiji Plateau: unpublished PhD thesis, University of Hawaii, 127 p.

Hamburger, M.W., and B.L. Isacks, Shallow seismicity in the North Fiji Basin: this volume.

Jenkins, C.J., 1985, Late Cenozoic sedimentary rocks dredged from the North Tonga Ridge - preliminary analysis, in E. Honza, K.B. Lewis, and Shipboard Party, A marine geological and geophysical survey of the northern Tonga Ridge and adjacent Lau Basin: Mineral Resources of Tonga Field Report, no. 1, p. 73-83.

Jezek, P.A., 1976, Compositional variations within and among volcanic ash layers in the Fiji Plateau area: Journal of Geology, v. 84, p. 595-616.

Klein, G. deV., 1985, The control of depositional depth, tectonic uplift, and volcanism on sedimentation processes in back-arc basins of the western Pacific Ocean: Journal of Geology, v. 93, p. 1-25.

Kroenke, L.W., and J.V. Eade, Overview and principal results of the second leg of the first joint CCOP/SOPAC-Tripartite cruise of the R/V KANA KEOKI: North Fiji Basin survey (KK820316 Leg 03): this volume.

Kroenke, L.W., J.V. Eade, C.Y. Yan, and R. Smith, Sediment distribution in the north central North Fiji Basin: this volume.

Leitch, E.C., 1984, Marginal basins of the Southwest Pacific and the preservation and recognition of their ancient analogues: a review, in B.P. Kokelaar and M.F. Howells, eds., Marginal Basin Geology: Volcanic and associated sedimentary and tectonic processes in modern and ancient marginal basins: Special Publication of the Geological Society of London, no. 16, p. 97-108.

Luyendyk, B.P., W.B. Bryan, and P.A. Jezek, 1974, Shallow structure of the New Hebrides island arc: GSA Bulletin, v. 85, p. 1287-1300.

Malahoff, A., R.H. Feden, and H.S. Fleming, 1982a, Magnetic anomalies and tectonic fabric of marginal basins north of New Zealand: Journal of Geophysical Research, v. 87, p. 4109-4125.

Malahoff, A., S.R. Hammond, J.J. Naughton, D.L. Keeling, and R.N. Richmond, 1982b, Geophysical evidence for post-Miocene rotation of the island of Viti Levu, Fiji, and its relationship to the tectonic development of the North Fiji Basin: Earth and Planetary Science Letters, v. 57, p. 398-414.

Malahoff, A., L.W. Kroenke, N.Z. Cherkis, and J. Brozena, Magnetic and tectonic fabric of the North Fiji Basin and Lau Basin. this volume.

Marks, N.S., 1981, Sedimentation on new ocean crust: the Mid-Atlantic Ridge at 37'N: Marine Geology, v. 43, p. 65-82.

McMurtry, G.M., E.H. De Carlo, and K.H. Kim, Geochemistry of north central North Fiji Basin sediments: this volume.

Moberly, R., and H.C. Jenkyns, 1981, Cretaceous volcanogenic sediments of the Nauru Basin, Deep Sea Drilling Project Leg 61: Initial Reports of the Deep Sea Drilling Project, v. 61, p. 533-548.

Pudsey, C.J., D.G. Jenkins, and D. Curry, 1981, Sedimentology and palaeontology of samples from the Hellenic Trench: Marine Geology, v. 44, p. 273-288.

Schmincke, H-U., P.T. Robinson, W. Ohnmacht, and M.F.J. Flower, 1979, Basaltic hyaloclastites from hole 396B, DSDP Leg 46: Initial Reports of the Deep Sea Drilling Project, v. 46, p. 215-226.

Sinton. J.M., R.C. Price, K.M. Johnson, H. Staudigel, and A. Zindler, Petrology and geochemistry of submarine lavas from the Lau and North Fiji back-arc basins: this volume.

Thiede, J., 1979, Wind regimes over the late Quaternary Southwest Pacific Ocean: Geology, v. 7, p. 259-262.

von Stackelberg, U., and Shipboard Party, 1985, Hydrothermal sulfide deposits in back-arc spreading centers in the Southwest Pacific: Bundesanstalt fur Geowissenschaften und Rohstoffe Circular, no. 2, p. 3-14.

(one-column captions)

Kroenke, L.W., and J.V. Eade, editors, 1993, Basin Formation, Ridge Crest Processes, and Metallogenesis in the North Fiji Basin: Houston, TX, Circum-Pacific Council for Energy and Mineral Resources, Earth Science Series, Vol. 15, Springer-Verlag, New York.

FISSION TRACK DATES OF BASALTS FROM THE NORTH FIJI BASIN

DIANE SEWARD
Institute of Nuclear Sciences, DSIR, Lower Hutt, New Zealand

ABSTRACT

An attempt has been made to date three oceanic basalt samples from the North Fiji Basin, including South Pandora Ridge, by the fission track technique. All three samples are Quaternary in age. The South Pandora Ridge is a young feature, with associated basalts having been extruded in the last 100,000 years.

INTRODUCTION

Oceanic basalts contain few, if any, uranium-bearing mineral phases, and fission must therefore be confined to the glassy chilled margins. Absolute dates from such glasses have previously been reported by several workers, notably Storzer and Selo (1979), Selo and Storzer (1979, 1981), Mitchell and Aumento (1976, 1977), and McDougall (1976). Because of the very low uranium content of oceanic basaltic glasses (generally < 50 ppb), McDougall (1976) emphasized the difficulties of the fission track procedure associated with the very low spontaneous track density. Bearing this in mind, the basaltic material dredged from the North Fiji Basin (South Pandora Ridge) was subjected to the dating technique simply to test the hypothesis that the ridge is very young, confirming or denying the theories of Kroenke et al. (this volume).

SAMPLE COLLECTION AND DESCRIPTION

The basalts were dredged from the North Fiji Basin by the R/V KANA KEOKI, April-May 1982 (Kroenke and Eade, this volume). Basalt from RD-16 was dredged from the probable site of a major fracture zone which appeared as a steep escarpment. Sediments and basalts look "old"; they are heavily coated with a ferromanganese crust, and have a weathered appearance. As early to mid-Pliocene lithified sediments were also recovered from RD-16, it was thought that basement here was at least pre-Quaternary in age (Gregory and Eade, this volume). Basalts from RD-19 and RD-20 were dredged from the South Pandora Ridge. The basalts are fresh, and underwater photographs at the same site as RD-19 indicate fresh-looking pillows typical of those seen at mid-ocean ridges. As the South Pandora Ridge is suspected to be an active spreading ridge (Kroenke et al., this volume), rocks dredged from its central rift are thought to be very young.

EXPERIMENTAL PROCEDURE

Very little fresh looking glass was available, particularly for samples RD-16 and RD-20. One aliquot of glass from each sample was annealed at 400°C for four hours, and then irradiated together with the zircon standard Fish Canyon Tuff (age 27.9 + 0.7 Ma, IUGS constants, Steven et al., 1967) and two NBS (SRM 962) glass standards. Two aliquots (spontaneous and induced) were then mounted, polished, and etched for 1 min 45 s in the solution recommended by Storzer and Selo (1979). The tracks were counted at a magnification of 1000. Ages were calculated using the method of Hurford and Green (1982) with $\lambda_f = 6.85 \times 10^{-17}$/yr, and a nominal neutron dose determined from the "correct" age of the Fish Canyon Tuff zircons. The error is the "conventional error" of Green (1981).

RESULTS

As noted by McDougall (1976) fission track dating is essentially impractical at levels where the spontaneous

track density is less than 100/cm^2. Such is the result here (Table 1). In two samples, RD-16 and RD-20, no spontaneous tracks were present in 0.13 cm^2. One track per area counted was used to calculate a possible density per square centimeter such that some crude estimate of maximum ages could be made.

The RD-16 sample yields an early Quaternary age. This is younger than expected and may represent volcanism associated with the fracture zone, an event younger than the volcanism which formed basement in this part of the North Fiji Basin. It may also represent an annealed age if perhaps this basalt had come into close contact with heat from later basaltic eruptions.

As expected, the sample from RD-19 from the South Pandora Ridge is much younger than RD-16. Although the statistics are poor, the data confirm that sometime during the last few ten thousand years, basalt flows have been erupted onto the seafloor along the South Pandora Ridge, and that indeed the South Pandora Ridge is a young feature.

Table 1. Fission track ages of glasses from the North Fiji Basin.

Sample no.	RD-16	RD-19	RD-20
Latitude	16°30'S	13°31'S	13°46'S
Longitude	174°16'E	173°25.1'E	172°0.5'E
INS No.	R10446	R10447	R10448
N_s	0	4	0
area (cm^2)	(0.13)	(1.023)	(0.134)
ρ_s (cm^{-2})	< 7.5*	3.9	< 7.5*
N_i	182	249	141
area (cm^2)	(0.13)	(0.02)	(0.0004)
ρ_i (cm^{-2})	1400	12450	35250
Age ± 2σ (years)	< 1,166,000	68,000 ± 34,000	< 46,000

*Density based on a minimum of one track counted in the area covered.

Using the data from Fish Canyon Tuff zircons age standard a nominal dose of 35.5 x 10^{14} n •cm^{-2} is obtained with λ_f = 6.85 x 10^{-17}/yr. Other constants are λ_D = 1.551 × 10^{-10}/yr, $^{235}U/^{238}U$ = 7.2527 x 10^{-3}, σ^{235} = 580.2 x 10^{-24} cm^2.

s = spontaneous; i = induced

REFERENCES

Green, P.F., 1981, A new look at statistics in fission track dating: Nuclear Tracks, v. 5, p. 77-86.

Gregory, M.R., and J.V. Eade, Lithified sediments dredged from the North Fiji Basin: this volume.

Hurford, A.J., and P.F. Green, 1982, A users' guide to fission track dating calibration: Earth and Planetary Science Letters, v. 59, p. 343-354.

Kroenke, L.W., and J.V. Eade, Overview and principal results of the second leg of the first joint CCOP/SOPAC Tripartite Cruise of the R/V KANA KEOKI: North Fiji Basin Survey (KK820316 Leg 03): this volume.

Kroenke, L.W., R. Smith, K. Nemoto, Morphology and structure of the seafloor in the northern part of the North Fiji Basin: this volume.

McDougall, D., 1976, Fission track studies of basalt from Leg 34: Initial Reports of the Deep Sea Drilling Project: v. 34, p. 455-456.

Mitchell, W.S., and F. Aumento, 1976, Fission track chronology and uranium content of basalts from DSDP Leg 34: Initial Reports of the Deep Sea Drilling Project, v. 34, p. 451-453.

Mitchell, W.S., and F. Aumento, 1977, Fission track chronology of basaltic glasses from DSDP Leg 37: Initial Reports of the Deep Sea Drilling Project, v. 37, p. 625-628.

Selo, M., and D. Storzer, 1979, Chronologie des evenements volcaniques de la zone Famous: Compte rendu hebdomadaire des seances de l'Academie des sciences, Paris, v. 289, Serie D, p. 1125-1128.

Selo, M., and D. Storzer, 1981, Uranium distribution and age pattern of some deep-sea basalts from the Entrecasteaux area, southwestern Pacific: a fission track analysis: Nuclear Tracks, v. 5, p. 137-145

Steven, T.A., H.H. Mehnert, and J.D. Obradovich, 1967, Age of volcanic activity in the San Juan Mountains, Colorado: U.S. Geological Survey Professional Paper, 575-D, p. 47-55.

Storzer, D., and M. Selo, 1979, Fission track age of magnetic anomaly M-zero and some aspects of sea-water weathering: Initial Reports of the Deep Sea Drilling Project, v. 51, 52, 53, p. 1129-1133.

Kroenke, L.W., and J.V. Eade, editors, 1993, Basin Formation, Ridge Crest Processes, and Metallogenesis in the North Fiji Basin: Houston, TX, Circum-Pacific Council for Energy and Mineral Resources, Earth Science Series, Vol. 15, Springer-Verlag, New York.

PETROLOGY AND GEOCHEMISTRY OF SUBMARINE LAVAS FROM THE LAU AND NORTH FIJI BACK-ARC BASINS

JOHN M. SINTON
Hawaii Institute of Geophysics, School of Ocean and Earth Science and Technology
University of Hawaii, Honolulu, Hawaii 96822 USA

RICHARD C. PRICE
Department of Geology, LaTrobe University
Bundoora, Victoria 3083, Australia

KEVIN T.M. JOHNSON
Hawaii Institute of Geophysics, School of Ocean and Earth Science and Technology
University of Hawaii, Honolulu, Hawaii 96822 USA

HUBERT STAUDIGEL
Scripps Institution of Oceanography
La Jolla, CA 94093 USA

ALAN ZINDLER
Lamont-Doherty Geological Observatory of Columbia University
Palisades, NY 10964 USA

ABSTRACT

Basaltic lavas in seven new dredges from the Lau and North Fiji basins comprise eight distinct chemical groups, representing three magma types. Type I lavas from three sites including one dredge of abyssal ferrobasalt are low-K mid-ocean ridge basalt (MORB) similar to those of mid-ocean spreading centers, but with slightly higher $^{87}Sr/^{86}Sr$ = 0.7034. Lavas from two sites are slightly enriched in K, Rb, Zr, Ba, and possibly water, relative to normal MORB; these Type II lavas evolved from primary magmas formed by very high degrees of melting and have many similarities to lavas from the Mariana Trough back-arc basin. Type II lavas appear to be older than Type I, suggesting that the Lau and North Fiji basins evolved from initial eruption of a back-arc basin basalt (BABB) magma type, followed by later production of MORB magmas. Two sites on the South Pandora Ridge yielded alkali- and other incompatible-element enriched "transitional" basalts (Type III). The extremely fresh appearance of these lavas suggests that they are very young. We propose that the South Pandora Ridge represents a recently activated, pre-existing lineament that includes Rotuma Island. New isotope data from the North Fiji Basin suggest that a previously proposed southern-hemisphere, globe-encircling mantle anomaly may not be continuous west of the Samoa volcanic province.

INTRODUCTION

Karig (1971) proposed that many of the marginal basins of the western Pacific formed by extensional processes behind volcanic arc-trench systems. Subsequent work on extensional back-arc basins has resulted in controversy over the level of organization of back-arc spreading centers (see Taylor and Karner, 1983 for a review) and the extent to which lavas erupted at such centers differ from those at mid-ocean ridges. Hart et al. (1972), Ridley et al. (1974), Hawkins (1976, 1977), Tarney et al. (1977), Mattey et al. (1981) and Wood et

SOEST contribution no. 1756

al. (1981) analyzed whole rocks from back-arc basins and found little or no difference in major element compositions between those lavas and mid-ocean ridge basalts (MORB). However, Fryer et al. (1981) found that basaltic glasses from the Mariana Trough have lower total FeO and TiO_2 and higher Al_2O_3 and Na_2O than glasses from mid-ocean spreading centers. Wood et al. (1981) and Fryer et al. (1981) noted that the Mariana Trough lavas are enriched in K, Rb, Sr, Ba and light rare earth elements (LREE) relative to typical MORB. The most striking distinction is the enrichment in volatile components, particularly H_2O, in basaltic glasses from the Mariana Trough (Garcia et al., 1979) and East Scotia Sea (Muenow et al., 1980). High volatile contents are also indicated by the high vesicularity of some Shikoku Basin lavas (Dick, 1980). Fryer et al. (1981) found that the geochemical parameters that distinguish Mariana Trough basalts from typical N-MORB also pertain to basaltic glasses from the Lau, Parece Vela and East Scotia Sea back-arc basins. Thus back-arc basin basalts (BABB) may constitute a separate magma type reflecting petrogenetic processes unique to the back-arc environment. We propose an extension of the model proposed for BABB petrogenesis by Fryer et al. (1981): (1) The mantle source for BABB has been modified by addition of volatiles and other incompatible components derived from the nearby subducted slab; (2) the presence of significant water in the melting region promotes high rates of melting – this is manifested as low FeO in the BABB magmas; (3) the high Al_2O_3 and Na_2O contents result from the suppression of plagioclase crystallization to low MgO contents in the hydrous BABB magmas (e.g., Yoder and Tilley, 1962; Nicholls and Ringwood, 1973).

The world distribution of BABB lavas is as yet unknown although Fryer et al. (1981) cited evidence for their existence in the Mariana Trough, Parece Vela Basin, East Scotia Sea and at DSDP Site 503 in the Lau Basin. Hawkins and Melchior (1983) recognized an older population flanking the presently active axis of the Lau Basin, which they called "Mariana Trough Basalt", and an axial population of MORB. Since the principal distinctions between BABB and MORB concern volatile and alteration-sensitive elements that are best seen in glass analyses, the scant back-arc basin petrology literature, most of which contains only whole rock data, is of little use in further defining the distribution of BABB.

Previous petrological work on the Lau and North Fiji basins has mainly been by Hawkins and co-workers (Hawkins, 1974; 1976; 1977; Hawkins and Batiza, 1975; Hawkins and Melchior, 1983) and is dominated by Lau Basin studies. This paper reports the results of a petrological and geochemical study of samples from seven new dredges (Table l), six from the North Fiji Basin and one from the edge of the Lau Basin (Figure

Table 1. Basin dredges, KK820316, Legs 2 and 3.

Dredge #	Latitude	Longitude	Water depth (m)	Recovery
5	15°39.5'S	178°29.7'W	2200-1900	650 kg pillow basalt 20 kg pumice 90 kg mudstone
13	14°28.8'S	177°41.2'W	2600-2250	1400 kg pillow basalt 150 kg Mn crusts, consolidated ash
16	16°36.7'S	174°16.4'E	3475-2690	1200 kg pillow basalt 100 kg breccia 150 kg sediments
17	15°3.4'S	171°57.9'E	3160	15 kg pillow basalt 5 kg mudstone
19	13°32.6'S	173°28.6'E	2350	900 kg pillow basalt
20	13°31'S	171°58.4'E	4550	900 kg pillow basalt
21	14°33.1'S	171°28.2'E	3100	15 kg pillow basalt 5 kg mudstone

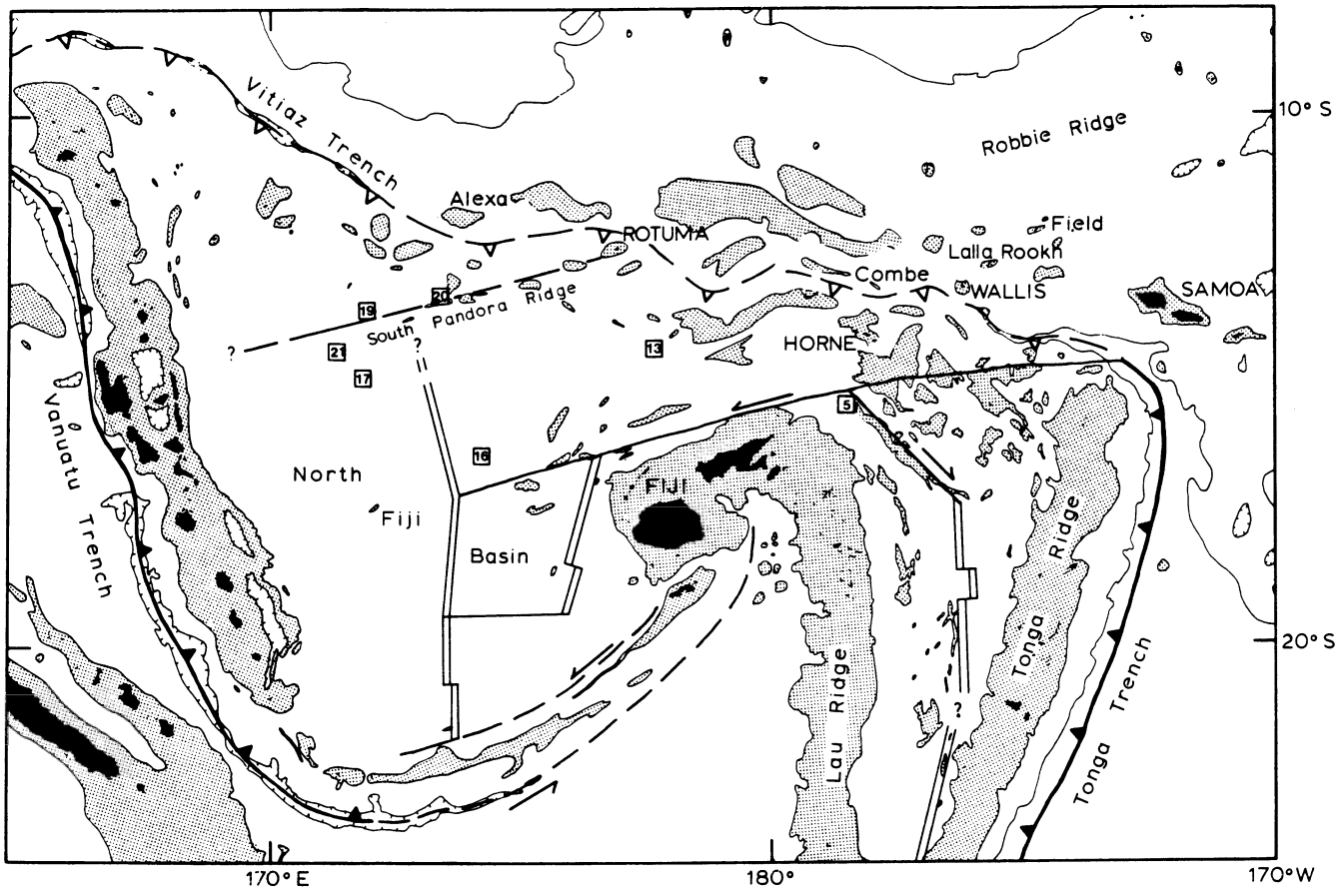

Figure 1. Map of the eastern Melanesian Borderland showing dredge locations (numbers in squares). The 2000- and 5000-m bathymetric contours are shown with features less than 2000 m stippled. Active spreading ridges are shown as double lines, transform faults and fracture zones as single heavy lines. The South Pandora Ridge may be an old fracture zone that is currently in extension (see text). The inactive Vitiaz Trench and its extension is a suture between Cretaceous Pacific lithosphere to the north and Cenozoic lithosphere to the south.

1). These dredges were recovered during R/V KANA KEOKI Cruise KK820316, Legs 2 and 3, the first two of three legs under the sponsorship of a tripartite consortium of government agencies from Australia, New Zealand, and the United States organized by the United Nations Committee for Coordination of Joint Prospecting for Mineral Resources in South Pacific Offshore Areas (CCOP/SOPAC).

ANALYTICAL PROCEDURES

The dredge collections were taken to Hawaii Institute of Geophysics where individual samples were selected for detailed study. These samples were thin-sectioned for petrographic analysis, and glassy fragments, where present, were picked for analysis. Glass major element analyses (Table 2) were done using a fully automated Cameca three-spectrometer microprobe following the procedure of Byerly et al. (1977). Selected glasses were hand picked to a volume of 5-7 grams, with all phenocrysts and altered pieces discarded after inspection with a binocular microscope. The glass separates were washed in an ultrasonic bath with distilled and deionized water prior to crushing.

Whole rocks and glass separates were crushed in a WC mill and analyzed by flame photometer (Na_2O), titration (FeO), gravimetric methods (H_2O, CO_2), and X-ray fluorescence (all other elements) at La-Trobe University. Major elements (Table 3) were analyzed on fused glass buttons using procedures similar to those of Norrish and Hutton (1969). Whole rocks and glass separates were analyzed for trace elements (Table 4) by X-ray fluorescence spectrometry on pressed powder pellets (Norrish and Chappell, 1977). All data were corrected for detector deadtime, matrix absorption and, where appropriate, inter-element interferences.

Glass separates were analyzed for Nd and Sr isotope ratios at Lamont-Doherty Geological Observatory using techniques described by Zindler et al. (1984). Isotope ratios are normalized to $^{86}Sr/^{88}Sr = 0.11940$, and $^{146}Nd/^{144}Nd = 0.72190$. Reported $^{87}Sr/^{86}Sr$ is relative

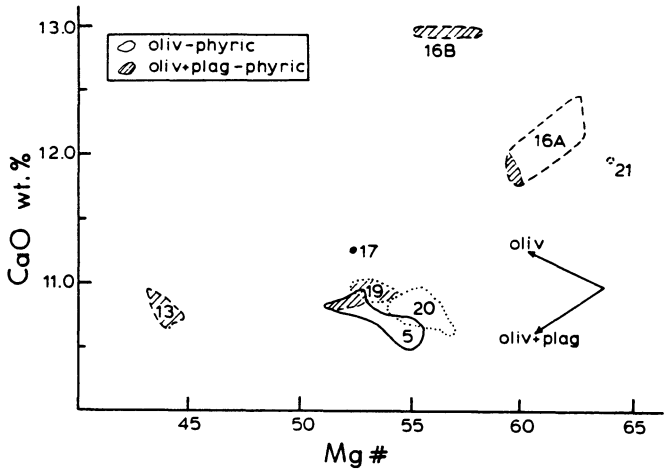

Figure 2. CaO (Wt %) versus Mg # (atomic 100 Mg/(Mg + Fe) where all Fe is FeO) for glass data of Table 2. Fields of plagioclase-saturated glasses are hachured. Other samples are saturated only with olivine. Arrows show trends produced by fractionation of olivine and of olivine + plagioclase. Note that group 16A follows an olivine + plagioclase trend even though only the lowest Mg # samples have modal plagioclase. See text for dicussion.

to 0.70800 for the Eimer and Amend Sr carbonate, and $^{143}Nd/^{144}Nd$ is relative to 0.512640 for BCR-1.

DREDGE DESCRIPTIONS

Rock Dredge 5

Dredge 5 recovered slightly Mn-encrusted pillow fragments from a small scarp just northeast of the northeast-trending Peggy Ridge (Figure 1). A sample from the dredge has been dated at 1.4 Ma by Duncan (1985). Five chemical subgroups (5A-1 through 5A-5, Table 2) have been recognized, which can be related by fractional crystallization involving the observed microphenocryst phases. Subgroups 5A-1 through 5A-4 are olivine microphyric with skeletal olivine microphenocrysts up to 2 mm long in a hyaline to hyalopilitic matrix. Subgroup 5A-5 has slender skeletal laths of plagioclase in addition to olivine microphenocrysts. These subgroups represent increasing degrees of differentiation with average Mg # (calculated as atomic 100 Mg/(Mg + Fe) with all Fe as FeO) decreasing from 55.2 (5A-1) through 54.7 (5A-2), 53.7 (5A-3), 53.1 (5A-4) to 52.2 (5A-5). The close textural similarity of all dredge 5 samples and the smooth inter-element variations on all plots, such as Figures 2 and 3, suggest that the five subgroups represent variation within a single eruptive event (i.e., single lava flow or series of closely related flows). A comparison of glass and whole rock data (Table 3) indicates that the dredge 5 rocks are enriched in total FeO and MgO and depleted in SiO_2, Al_2O_3 and CaO relative to the glasses. These differences are consistent with exclusion of the olivine microphenocrysts from the glass analyses. The slightly higher K_2O value of bulk rock sample 5-14 is almost certainly the result of enrichment during submarine alteration as the glass analysis displays much lower K_2O contents. All dredge 5 samples are low-K, olivine tholeiites, although they are slightly enriched in K_2O, Rb and Ba relative to N-MORB.

The $^{143}Nd/^{144}Nd$ of samples 5-14 and 5-15 (Table 5, Figure 4) is identical to that of N-MORBs from the East Pacific Rise, Mid-Atlantic Ridge, and Indian Ocean. The $^{87}Sr/^{86}Sr$, however, is more typical of that for enriched MORB. Similar isotopic characteristics have been found for BABB from the Lau Basin and Mariana Trough (Carlson et al., 1978; Stern, 1981) and for island arc tholeiites from Fiji (Gill, 1984). The slight enrichment in ^{87}Sr relative to most MORB possibly suggests that the Rb enrichment of the dredge 5 lavas may be a relatively long-term characteristic of their source.

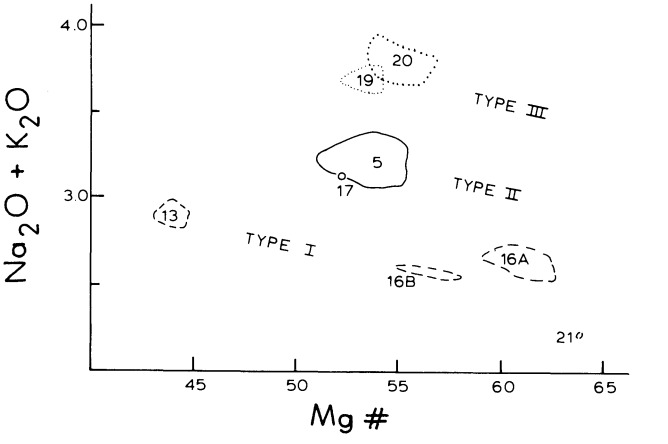

Figure 3. Type designations based on total alkalis versus Mg #. Only glass data from Table 2 are plotted.

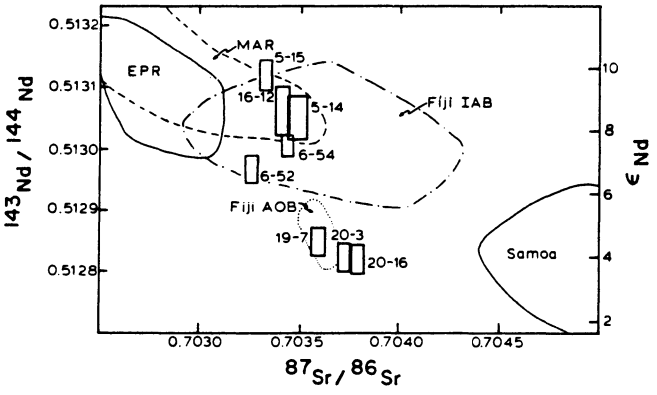

Figure 4. $^{143}Nd/^{144}Nd$ versus $^{87}Sr/^{86}Sr$ of glass separates listed in Table 5; samples 6-52 and 6-54 (Sinton et al., 1985) are arc tholeiites from the Horne Islands (Figure 1). Fields for the East Pacific Rise (EPR), Mid-Atlantic Ridge (MAR), and Samoa are those of Zindler et al. (1984); those for Fijian island arc basalts (IAB) and alkalic oliving basalts (AOB) are from Gill (1984).

Rock Dredge 6

Sinton et al. (1985) described the tectonic setting and detailed petrology and geochemistry of samples from dredge 6, taken on the southeastern flank of the Horne Islands (Figure 1). In this paper we report new Sr and Nd isotope data (Table 5) for two glass separate samples of group 6A which Sinton et al. (1985) interpreted as island arc tholeiitic in affinity. These samples have comparable $^{87}Sr/^{86}Sr$ but slightly lower $^{143}Nd/^{144}Nd$ than samples from dredge 5 ; they are similar with respect to these ratios to island arc basalts from Fiji (Figure 4).

Rock Dredge 13

Dredge 13 recovered a fairly uniform collection of pillow basalt fragments with 1- to 2-mm Mn crusts. Olivine, plagioclase, and rare clinopyroxene are microphenocryst phases. Whole rocks have average Mg # of 50.5 and have higher SiO_2, CaO, Na_2O and K_2O and lower FeO and MgO contents than do the glasses (Table 3). The glasses are strikingly enriched in FeO with up to 14 wt % (Table 2); average dredge 13 glass Mg # is 44.0. Thus, these samples are highly evolved, slightly quartz- to slightly olivine- normative abyssal tholeiites. Dredge 13 was taken in an area characterized by magnetic anomaly amplitudes of over 700 nT. The presence of ferrobasalts in an area of high magnetic anomaly amplitudes is consistent with the magnetic telechemistry hypothesis of Vogt and Johnson (1973). Brocher (1985) identified oblique bathymetric and magnetic fabric in the dredge 13 region that he tentatively ascribed to a now-defunct part of a propagating rift system. Rock dredge 13 was located about 15-20 km inside a proposed pseudofault (Brocher, 1985), a position predicted by Christie and Sinton (1981) and Sinton et al. (1983) to be most conducive to the eruption of highly differentiated lavas in association with propagating rifts.

Rock Dredge 16

Dredge 16 was taken from a southeast-facing escarpment at least 1000 m high. All dredge 16 samples have thin, 1-mm Mn crusts; this site is removed from an active spreading center. Two distinct chemical groups are present in the dredge. Group 16A, the dominant group, is olivine-phyric (16A-1,-2), plagioclase microphyric (16A-3) tholeiitic pillow basalt. Subgroups 16A-1 through 16A-3 (Table 2) represent progressively more differentiated populations that can be related either by fractionation of olivine + plagioclase or by magma mixing (see below). The analyzed 16A sample has Sr and Nd isotope characteristics similar to samples from dredge 5; the source for the basalts of the Lau and North Fiji basins appears to be isotopically similar to that for the Fiji island arc tholeiites (Figure 4). Group 16B samples are rare in the collection and mainly occur as cemented cobbles or hyaloclastic breccias. They are also olivine-phyric, but the high CaO and lower alkali contents of these samples (e.g., Figures 2 and 3) preclude their derivation from 16A parents by fractionation of the observed phenocryst phases.

Rock Dredge 17

Only one igneous rock was recovered in dredge 17. It is a pillow fragment of plagioclase + olivine-phyric tholeiitic basalt, with brown, weathered 2- to 5-mm Mn encrustation. This site is moderately sedimented and the weathered and Mn-encrusted nature of the sample indicates that this area is not an active spreading center. Glass from the dredge 17 pillow fragment has 0.24 wt % K_2O (Table 2) comparable to that of dredge 5. It is slightly olivine-normative (calculated with all Fe as FeO) and has a Mg # of about 52, indicating a moderate level of differentiation.

Rock Dredge 19

Dredge 19 was taken in a relatively shallow area of high relief and little or no sediment; this region has the characteristics of a spreading center. It is part of a generally east-west striking feature that has variably been called "Hazel Holme Fracture Zone" or "South Pandora Ridge." About 900 kg of fresh glassy pillow basalt fragments were recovered at this site. A thin brown film on fragment surfaces is the only evidence of weathering or alteration. The lava fragments are notably vesicular, with as many as 10% of vesicles up to 10 mm across, partially filled with black, glassy microvesicular segregations.

Dredge 19 lavas are olivine and plagioclase-phyric. Olivine phenocrysts range up to 3 mm, are typically slightly to moderately skeletal, and contain abundant inclusions of spinel. Some olivine phenocrysts are embayed and slightly rounded and may be partially resorbed; most are euhedral and the typical texture is one of rapid crystal growth. Plagioclase microphenocrysts are 1- to 3-mm skeletal laths. A crystallization sequence of spinel, spinel + olivine, olivine + plagioclase is indicated by the petrographic relations.

Only one chemical group is present in the dredge 19 collection. It is olivine- and hypersthene-normative and, relative to the other dredged rocks described so far, it has elevated K_2O and P_2O_5 values (Table 2). Only dredge 20 samples have higher values of these elements. Relative to the other basin samples (excluding dredge 20), dredge 19 is enriched in alkali and other incompatible elements with high Rb, Sr, Zr, Nb, Ba, La, and Ce contents (Table 4). The presence of hypersthene in the norm indicates that these lavas are not critically undersaturated; they are plotted just barely on the

Table 2. Glass analyses, Lau and North Fiji basins.

Sample	SiO_2	TiO_2	Al_2O_3	FeO*	MnO	MgO	CaO	Na_2O	K_2O	P2O5	Total
Dredge 5, Group 5A-1											
5-7	49.61	2.01	14.86	10.75	0.18	7.49	10.66	3.09	0.22	0.21	99.08
5-15	49.16	2.01	15.14	10.78	0.18	7.45	10.68	2.90	0.19	0.21	98.70
5-5	49.78	2.02	14.98	10.66	0.21	7.43	10.55	3.06	0.22	0.19	99.10
5-10	49.77	2.03	14.88	10.85	0.15	7.42	10.73	3.01	0.20	0.20	99.24
5-27	49.29	2.05	15.00	10.69	0.20	7.37	10.53	2.91	0.20	0.22	98.46
5-6	49.73	2.05	14.92	10.65	0.16	7.33	10.66	3.04	0.23	0.21	98.98
Dredge 5, Group 5A-2											
5-13	49.23	2.06	15.24	10.61	0.19	7.18	10.49	2.92	0.21	0.23	98.36
Dredge 5, Group 5A-3											
5-4	50.01	2.04	15.07	10.69	0.19	6.97	10.73	3.17	0.21	0.21	99.29
5-18	48.86	2.01	15.23	10.72	0.18	6.95	10.75	2.86	0.21	0.21	97.98
Dredge 5, Group 5A-4											
5-9	49.55	2.11	15.20	10.71	0.19	6.79	10.74	3.15	0.21	0.20	98.85
5-19	49.54	2.07	15.34	10.51	0.20	6.71	10.75	3.07	0.21	0.21	98.66
Dredge 5, Group 5A-5											
5-3	49.40	2.04	15.32	10.39	0.20	6.48	10.83	2.95	0.18	0.21	98.00
5-14	49.53	2.11	15.48	10.29	0.19	6.46	10.94	3.01	0.20	0.24	98.45
5-16	49.47	2.19	15.27	10.70	0.24	6.29	10.81	3.04	0.20	0.22	98.43
Dredge 13											
13-2	50.80	2.08	13.28	13.99	0.18	5.97	10.94	2.71	0.19	0.21	100.35
13-14	50.05	2.05	13.24	13.91	0.15	6.02	10.75	2.76	0.18	0.20	99.31
13-1	50.09	2.01	13.38	14.00	0.19	6.05	10.81	2.68	0.18	0.20	99.59
13-12	50.39	2.02	13.51	13.81	0.22	6.10	10.86	2.69	0.16	0.22	99.98
13-17	49.55	2.02	14.06	13.89	0.17	6.11	10.64	2.82	0.17	0.21	99.64
13-3	50.37	2.00	13.45	13.90	0.24	6.12	10.66	2.72	0.18	0.21	99.85
13-6	50.64	1.96	13.32	13.50	0.15	6.13	10.74	2.76	0.17	0.18	99.55
13-4	51.02	2.00	13.29	13.74	0.22	6.17	10.77	2.77	0.17	0.22	100.37
13-10	50.31	2.02	13.89	13.72	0.18	6.18	10.73	2.68	0.16	0.20	100.07
Dredge 16, Group 16A-1											
16-7	48.46	1.25	16.67	9.52	0.13	8.93	12.16	2.47	0.07	0.16	99.82
16-14	49.09	1.29	16.83	9.59	0.11	8.91	12.46	2.61	0.05	0.16	101.10
Dredge 16, Group 16A-2											
16-3	49.37	1.26	16.59	9.65	0.11	8.63	12.06	2.52	0.08	0.17	100.40
16-13	49.36	1.26	16.55	9.85	0.15	8.62	12.26	2.52	0.13	0.20	100.90
16-6	49.38	1.23	16.59	9.59	0.12	8.61	11.99	2.49	0.07	0.16	100.23
16-11	49.21	1.24	16.47	9.59	0.11	8.60	11.99	2.46	0.10	0.17	99.94
16-1	49.45	1.22	16.67	9.48	0.12	8.50	12.12	2.47	0.07	0.17	100.27
16-8	49.31	1.28	16.63	9.61	0.16	8.47	12.07	2.48	0.07	0.17	100.25
16-12	49.61	1.26	16.49	9.79	0.16	8.38	12.09	2.65	0.09	0.19	100.71
16-4	49.78	1.31	16.34	9.46	0.16	8.22	12.01	2.50	0.12	0.19	100.09
Dredge 16, Group 16A-3											
16-2	49.73	1.34	15.88	10.04	0.10	8.21	12.00	2.57	0.10	0.19	100.16
16-5	49.79	1.30	15.88	9.64	0.13	8.07	11.80	2.56	0.09	0.17	99.43
Dredge 16, Group 16B											
16-17	50.28	1.09	14.97	10.22	0.15	7.90	12.95	2.50	0.05	0.20	100.31
16-16	50.76	1.21	14.71	11.12	0.17	7.67	12.96	2.57	0.04	0.18	101.39

(table continued next page)

Sample	SiO_2	TiO_2	Al_2O_3	FeO*	MnO	MgO	CaO	Na_2O	K_2O	P2O5	Total
Dredge 17											
17-1	50.28	1.84	14.48	10.67	0.12	6.58	11.25	2.87	0.27	0.24	98.60
Dredge 19											
19-5	50.47	2.03	15.83	9.94	0.18	6.59	10.92	2.98	0.65	0.29	99.88
19-1	50.48	2.03	15.92	9.90	0.14	6.56	10.92	3.10	0.66	0.29	100.00
19-3	50.44	2.00	15.75	10.24	0.16	6.52	11.01	3.05	0.70	0.29	100.16
19-4	50.66	2.06	15.82	9.91	0.17	6.46	10.93	3.07	0.68	0.29	100.05
19-7	49.25	2.04	15.85	10.13	0.16	6.41	10.93	3.00	0.68	0.21	98.66
19-2	50.60	1.95	15.98	9.95	0.16	6.35	10.87	3.00	0.65	0.30	99.81
19-6	50.10	2.05	15.68	10.25	0.16	6.34	10.98	3.00	0.69	0.30	99.55
Dredge 20											
20-5	49.85	2.09	16.56	8.77	0.10	6.31	10.84	3.00	0.81	0.28	98.61
20-12	48.99	2.11	16.42	8.81	0.15	6.30	10.83	2.89	0.79	0.32	97.61
20-9	49.81	2.10	16.66	8.69	0.16	6.29	10.67	2.98	0.80	0.36	98.52
20-3	49.80	2.16	16.23	8.79	0.13	6.29	10.76	3.00	0.81	0.28	98.25
20-15	49.25	2.13	16.67	8.82	0.11	6.25	10.93	3.09	0.85	0.34	98.44
20-8	49.75	2.12	16.47	8.91	0.12	6.24	10.78	2.98	0.82	0.28	98.47
20-14	49.07	2.05	16.44	8.40	0.12	6.21	10.62	2.98	0.84	0.30	97.03
20-7	49.69	2.13	16.56	9.01	0.13	6.21	10.69	2.89	0.80	0.25	98.36
20-10	49.57	2.10	16.61	8.71	0.11	6.19	10.87	2.94	0.78	0.36	98.24
20-10	49.35	2.07	16.64	8.62	0.13	6.18	10.77	2.94	0.81	0.34	99.39
20-16	48.87	2.08	16.37	8.76	0.12	6.16	10.79	2.97	0.88	0.36	97.36
20-2	49.19	2.07	16.44	8.78	0.07	6.12	10.95	2.96	0.83	0.27	97.65
20-4	49.68	2.21	16.52	9.01	0.13	6.08	10.86	3.06	0.84	0.29	98.41
20-6	49.57	2.17	16.32	9.15	0.13	6.03	10.83	2.93	0.81	0.26	98.20
20-1	49.51	2.17	16.43	9.04	0.18	5.96	10.77	3.14	0.81	0.28	98.29
20-13	49.49	2.15	16.30	8.71	0.12	5.88	10.70	3.08	0.83	0.34	97.60
Dredge 21											
21-1	49.39	0.96	16.17	9.37	0.13	9.29	11.98	2.17	0.05	0.16	99.67

All analyses by HIG Cameca microprobe
*Total Fe as FeO

tholeiitic side of the Macdonald and Katsura (1964) line separating tholeiitic from alkalic lavas in Hawaii. These lavas are best described as alkali-enriched tholeiites or "transitional" basalts.

The Sr and Nd isotope ratios of sample 19-7 suggest a source that is significantly enriched relative to that for MORB. Though these ratios are displaced towards lower $^{87}Sr/^{86}Sr$ and $^{143}Nd/^{144}Nd$ when compared to most mantle-derived ocean island basalts, they are identical to those of other oceanic islands in the southern hemisphere and the alkalic olivine basalts of Fiji (Gill, 1984) (Figure 4).

Rock Dredge 20

Dredge 20 was also taken along the South Pandora Ridge, but in much deeper water than dredge 19. Recovered lavas are virtually without signs of alteration or weathering and must be extremely young. Glassy pillow fragments and thin (5-cm), flat lava fragments with two subparallel glassy chilled margins are identical in composition and must represent different parts of the same lava flow; the thin fragments are probably fragments of collapsed pillows. Dredge 20 lavas are vesicular, olivine-phyric basalts with 1-mm skeletal plagioclase microphenocrysts in a glassy to incipiently crystallized matrix. Olivine phenocrysts typically have spinel inclusions. These lavas are petrographically similar to those from dredge 19, although they are generally even fresher in appearance and have less plagioclase. They are also chemically similar (Tables 2,4) although they are somewhat less evolved (average Mg # = 55.5, compared to 53.4 for average dredge 19; less plagioclase, higher Ni) and more enriched in alkali and other incompatible elements. Dredge 20 lavas have up to 4 wt % hypersthene in the norm and can also be

Table 3. Whole rock and selected glass major element analyses.

Sample No.	5-5		5-11	5-14		5-15		13-1		13-16	13-17	
	GL	WR	WR	GL	WR	GL	WR	GL	WR	WR	GL	WR
SiO_2	49.78	48.89	48.00	49.53	48.38	49.16	49.00	50.09	50.75	51.37	49.55	51.11
TiO_2	2.02	2.01	2.03	2.11	2.05	2.01	2.01	2.01	2.02	2.03	2.02	2.05
Al_2O_3	14.98	14.73	14.90	15.48	14.95	15.14	14.72	13.38	13.86	13.84	14.06	14.07
FeO*	10.66	11.02	10.84	10.29	10.79	10.78	11.01	14.00	10.99	10.31	13.89	10.07
MnO	0.21	0.20	0.19	0.19	0.19	0.18	0.21	0.19	0.22	0.24	0.17	0.22
MgO	7.43	8.44	7.77	6.46	7.87	7.45	8.39	6.05	5.95	6.36	6.11	5.68
CaO	10.55	10.40	10.47	10.94	10.43	10.68	10.38	10.81	11.05	10.98	10.64	11.29
Na_2O	3.06	2.97	2.98	3.01	2.93	2.90	2.94	2.68	2.87	2.91	2.82	2.97
K_2O	0.22	0.21	0.32	0.20	0.43	0.19	0.21	0.18	0.29	0.26	0.17	0.30
P_2O_5	0.19	0.23	0.23	0.24	0.24	0.21	0.23	0.20	0.22	0.22	0.21	0.22
H_2O+	n.a.	0.77	1.31	n.a.	0.96	n.a.	0.69	n.a.	0.64	0.62	n.a.	0.71
H_2O-	n.a.	0.00	0.79	n.a.	0.48	n.a.	0.02	n.a.	0.47	0.38	n.a.	0.40
CO_2	n.a.	0.08	0.13	n.a.	0.00	n.a.	0.05	n.a.	0.14	0.00	n.a.	0.14
S	n.a.	0.15	0.08	n.a.	0.07	n.a.	0.14	n.a.	0.23	0.02	n.a.	0.21
Less S = O		0.08	0.04		0.04		0.07		0.12	0.01		0.11
Total	99.10	100.02	100.00	98.34	99.73	98.70	99.93	99.59	99.58	99.53	99.64	99.33

Glass (GL) analyses by HIG Cameca microprobe.
Whole rocks (WR) analyzed at LaTrobe University, mainly by XRF.
* Total Fe as FeO.
n.a. - element not analyzed.

described as transitional between tholeiitic and alkalic basalts. Analyzed dredge 20 basalts have similar $^{87}Sr/^{86}Sr$ and $^{143}Nd/^{144}Nd$ to dredge 19, suggesting that these characteristics may be common for the South Pandora Ridge.

Rock Dredge 21

Only one igneous rock was recovered from this site on the edge of a steep-walled, west-northwest striking ridge, slightly veneered with sediment. The recovered sample has a brown weathered surface, and a thin -mm Mn crust. It is a nearly aphyric pillow fragment with a partially devitrified glassy selvedge containing scattered, generally < 1-mm olivine microphenocrysts making up less than 2% of the rock. This sample is the least evolved basin sample recovered with Mg # = 63.9. It is a strongly depleted, low-K, -Na, -P, -Ti olivine tholeiite (Table 2).

DISCUSSION

We recognize eight chemical groups in the seven dredges described above – two groups in dredge 16 and one in each of the other seven. All eight groups are hypersthene-normative, and hence silica-saturated, but there are variations in alkalicity among them. Chemical groups 13, 16A, 16B and 21 are the most depleted in alkalis (Figure 3) and have the highest K/P ratios (Table 6), and for those samples for which trace element and isotope data are available, have the lowest Zr contents, Zr/Y and $^{87}Sr/^{86}Sr$ ratios, and the highest Zr/Nb, K/Rb and $^{143}Nd/^{144}Nd$ ratios. There is correlation between $^{87}Sr/^{86}Sr$ and Zr/Y (Figure 5), but in terms of $^{143}Nd/^{144}Nd$ versus Zr/Y (not shown) dredges 19 and 20 define a group distinct from the other basin samples. Lavas in dredges 5 and 17 are intermediate in most of the above parameters and those from dredges 19 and 20 are the most enriched in the more incompatible ele-

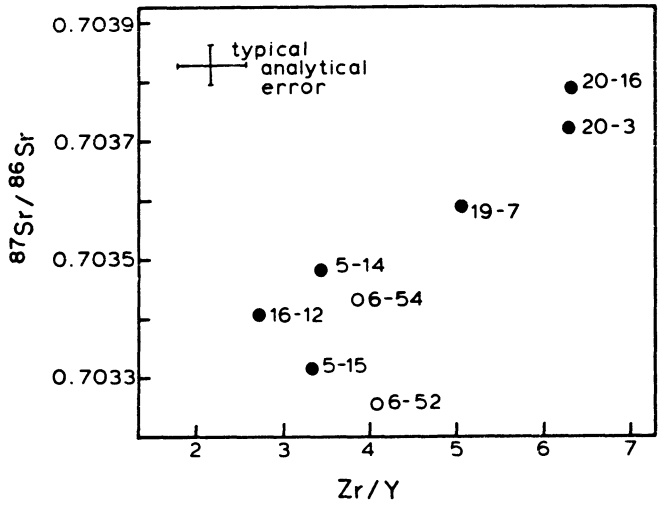

Figure 5. $^{87}Sr/^{86}Sr$ versus Zr/Y for glass separates of Table 5. Arc tholeiites from the flanks of the Horne Islands are shown as open circles; basin samples are closed circles.

ments. Thus, three distinct magma types are present in the collection. Type I (groups 13, 16A, 16B, and 21) lavas are indistinguishable from N-MORB in being strongly depleted in the more incompatible elements (Figure 6, top) and in high $^{143}Nd/^{144}Nd$ ratios. Their $^{87}Sr/^{86}Sr$, however, indicate that, relative to MORB, their source regions were slightly enriched in Rb. Relative to the other Type I chemical groups, group 13 is significantly more differentiated as reflected in its lower Mg # and higher contents of K_2O, FeO, V, Y, Zr, and Ba. Type II (groups 5 and 17) are slightly enriched in K, Rb, Zr, and Nb relative to Type I, but also have light rare earth element-depleted patterns (Figure 6, center). Type III (groups 19 and 20) are enriched in incompatible elements (Figure 6, bottom) and in $^{87}Sr/^{86}Sr$. They have Nd isotope characteristics that are typical of most light rare earth element-enriched magmas, including alkalic basalts of Fiji (Gill, 1984). The differences among the three types in the parameters listed in Table 6 cannot be accounted for by fractional crystallization and must reflect differences in the parental magmas of each group. Variations in the degree of melting and/or composition of the source material can contribute to the variation in parental magmas. Before assessing these

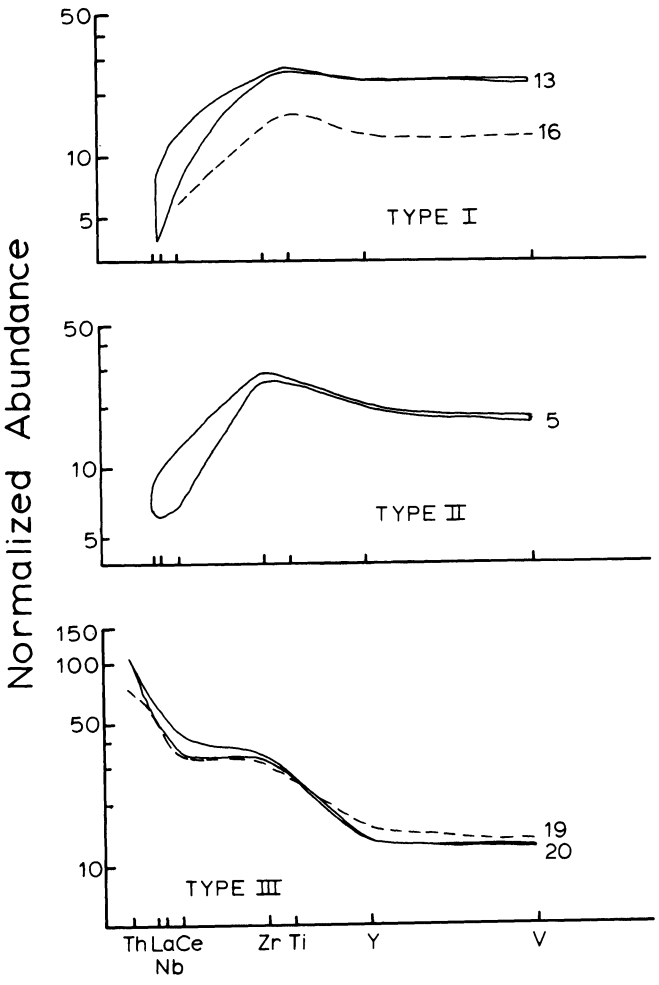

Figure 6. Normalized abundance patterns for samples listed in Table 4. Element concentrations have been normalized by division by factors of 0.028 (Th), 0.32 (La), 0.58 (Nb), 0.85 (Ce), 5.13 (Zr), 460 (Ti), 2.16 (Y), and 22 (V). These empirically derived factors and the relative positions of the elements are from Bougault (1980); the patterns approximate rare earth patterns.

Table 4. Whole rock (WR) and selected glass (GL) XRF trace element analyses (ppm)

Sample	5-5	5-11	5-14		5-15		13-1	13-16	13-17	16-12	19-7	20-3	20-16
No.	WR	WR	WR	GL	WR	GL	WR	WR	WR	GL	GL	GL	GL
CR	291	294	285	278	291	278	143	134	144	383	430	372	343
V	365	365	365	356	363	358	512	510	499	289	286	280	270
Ni	149	152	146	144	148	153	83	89	67	220	159	188	176
Cu	76	77	76	75	78	74	250	178	183	172	100	72	67
Zn	100	102	100	97	100	97	143	131	157	74	96	85	83
Ga	21	22	20	20	22	22	21	21	22	17	19	19	19
Rb	4	6	7	4	4	3	3	4	4	1	18	20	20
Sr	159	165	165	157	159	158	161	167	185	128	249	245	242
Y	42	42	43	41	42	41	52	51	51	27	32	28	28
Zr	143	142	146	140	142	139	124	124	126	73	162	176	177
Nb	3	3	5	4	3	4	2	1	4	1	24	27	30
Ba	30	24	30	30	288	31	55	69	62	3	199	234	224
La	-	-	-	2	-	-	-	-	-	-	19	19	18
Ce	8	7	7	7	9	5	8	9	11	5	28	36	30
Pb	1.5	2.4	1.8	-	-	-	1.4	2.3	-	-	2	2	2
Th	-	-	-	-	-	-	-	-	-	-	2	3	3

All analyses by XRF at LaTrobe University.
- below detection limits: Pb(1.2), Th(1.2), La(1.3), Ce(4)
All samples have less than 1.4 ppm U.

Table 5. K, Rb, Sr, Nd, and Sm concentrations determined by isotope dilution and $^{87}Sr/^{86}Sr$, and $^{143}Nd/^{144}Nd$ isotope ratios of glasses from KK820316, Legs 2 and 3.

Sample No.	K (ppm)	Rb (ppm)	Sr (ppm)	$^{87}Sr/^{86}Sr$	2σ x 10^6	Nd (ppm)	Sm (ppm)	$^{143}Nd/^{144}Nd$	2σ x 10^6
5-14	1370	3.53	140	.703482	49	11.21	4.76	.513051	35
5-15	1440	3.21	152	.703317	29	14.09	4.68	.513118	23
6-52	950	1.28	155	.703257	25	5.79	1.99	.512968	24
6-54	755	1.37	174	.703434	26	6.08	2.10	.513017	16
16-12	557	.58	109	.703407	34	7.03	2.54	.513061	39
19-7	3600	15.4	216	.703589	34	18.65	4.76	.512849	23
20-3	3400	11.3	270	.703720	28	n.e.	5.11	.512823	23
20-16	1960	9.8	256	.703791	35	21.9	4.93	.512821	24

Isotope dilution and mass spectrometric techniques are described in Zindler et al. (1984). $^{86}Sr/^{88}Sr$ normalized to 0.1194; $^{87}Sr/^{86}Sr$ relative to E&A = 0.7080; $^{146}Nd/^{144}Nd$ = 0.72190. Only significant figures given for concentration data.

variations, however, several important points concerning the low-pressure, pre-eruptive history of these magmas can be made.

Shallow Magmatic History of the Lavas

Low-pressure magmatic processes affecting magma composition are generally assumed to be dominated by crystal fractionation, although a variety of other processes including magma mixing and assimilation (e.g. Bowen, 1928; O'Hara, 1980), liquid immiscibility (e.g. Bowen, 1928; Philpotts, 1979) and thermally driven diffusion (e.g. Hildreth, 1981; Walker and DeLong, 1982) also can be locally important. As noted above, the variations in whole rock and glass compositions for samples from dredges 5 and 13 can, at least qualitatively, be attributed to the effects of the observed phenocryst phases on the whole rock compositions.

Projection of the glass data of Table 2 from plagioclase onto the cpx-olivine-quartz plane of the cpx-olivine-plagioclase-quartz tetrahedron (Figure 7) indicates that most of the chemical groups are very near to three-phase saturation with olivine, plagioclase, and clinopyroxene, even though only dredge 13 lavas actually have clinopyroxene as a (micro)phenocryst phase. With the exception of group 16A the variation within each chemical group on this projection can be explained either by crystal fractionation effects or by analytical error (Figure 8). Group 16A lava compositions project in an array that trends subparallel to the base of the projection, a trend that is transverse to olivine fractionation control lines. Although this array could be produced by a spectrum of parental magmas derived from a range of depths, Mg # progressively decreases across the array (Figure 8), and it seems unlikely that derivatives of a range of parental magmas could be represented in what is probably a single lava flow. More plausibly, the 16A trend is a magma mixing trend, whereby the spectrum of compositions represents mixing between relatively primitive (high Mg #, olivine saturated) and more evolved (low Mg #, olivine + plagioclase + clinopyroxene saturated) magmas. This mixing trend is also apparent in Figure 2, where a decrease in CaO with decreasing Mg # occurs in 16A-1 and 16A-2 subgroups even though olivine is the only phenocryst phase. Although chemical groups 16A and

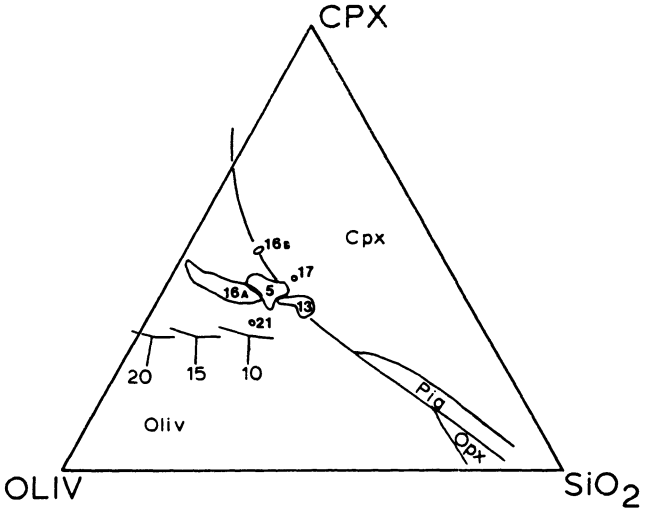

Figure 7. Types I and II glass data (Table 2) projected from plagioclase onto the cpx-oliv SiO_2 plane, after Walker et al. (1979). Projection equations, 1-atmosphere multiple saturation surfaces, and phase fields for olivine (oliv), clinopyroxene (cpx), pigeonite (pig), and orthopyroxene (opx) are from Grove et al. (1982). High-pressure phase boundaries at 10, 15, and 20 kb are those of Stolper (1980).

16B cannot be related by low-pressure crystal fractionation, both could be related to a parental magma with Mg # of 66 and 13 wt % CaO. In this case, 16B magmas have evolved by fractionation of olivine and 16A magmas by mixing with a low-Mg #, low-CaO, olivine + plagioclase ± clinopyroxene-saturated liquid.

An interesting distinction among the three magma types defined above can be made on the basis of the position of the olivine + plagioclase (+ liquid) multiple saturation surface. Type I magmas are saturated with plagioclase at about 8 wt % MgO, and plagioclase-saturated liquids conform to a MORB cotectic (Figure 9). However, dredge 5 magmas are saturated with only olivine (subgroups 5A-1,-2,-3 and -4) until about 6.5 wt % MgO (subgroup 5A-5), where plagioclase joins olivine as a crystallizing phase. The position of the olivine + plagioclase + liquid cotectic is sensitive to total alkali content (e.g. Bryan and Dick, 1982; Dick et al., 1984) and to water content (e.g. Yoder and Tilley, 1962; Nicholls and Ringwood, 1973; Bender et al., 1978). Types II and III lavas appear to define a plagioclase + olivine cotectic that is distinctly displaced toward plagioclase from that for Type I magmas, and that is essentially coincident with that for BABB lavas from the Mariana Trough and East Scotia Sea (Figure 9). The position of the Mariana and Scotia cotectic probably reflects the high water content of those magmas. Analytical totals for dredge 5 and 17 glass analyses (Table 2) average 98.7 and 98.6 wt % respectively, suggesting that these glasses could contain an excess of 1.0 wt % volatiles; alternatively, the low totals could reflect analytical errors. Although the evidence for high volatile abundances of these lavas is indirect, it is clear that Type II lavas share many characteristics with BABB lavas from the Mariana Trough and elsewhere. However, North Fiji Basin Type II lavas differ from Mariana Trough basalts in being more like MORB with respect to their Al_2O_3 and FeO abundances relative to MgO, and in their light rare earth element-depleted patterns (cf. Fryer et al., 1981).

Petrogenesis of Lau and North Fiji Basin Lavas

The positions of the individual lava groups on the cpx-oliv-SiO_2 projection (Figure 7) allows the relative depths of segregation of their parental liquids from residual mantle to be inferred. At low pressure, liquids in the olivine volume evolve by olivine + plagioclase fractionation until they become saturated with clinopyroxene, at which time they move down the cotectic toward SiO_2. Thus liquids that have not yet become saturated with clinopyroxene can be projected back toward olivine to derive an inferred depth of melt segregation. Although the high pressure pseudoinvariant points shown in Figure 7 are not truly invariant (e.g. Stolper, 1980; Takahashi and Kushiro, 1983) and their positions are composition-sensitive (e.g. Jaques and Green, 1979), results of all experiments to date agree that increasing depth of melt segregation coincides with

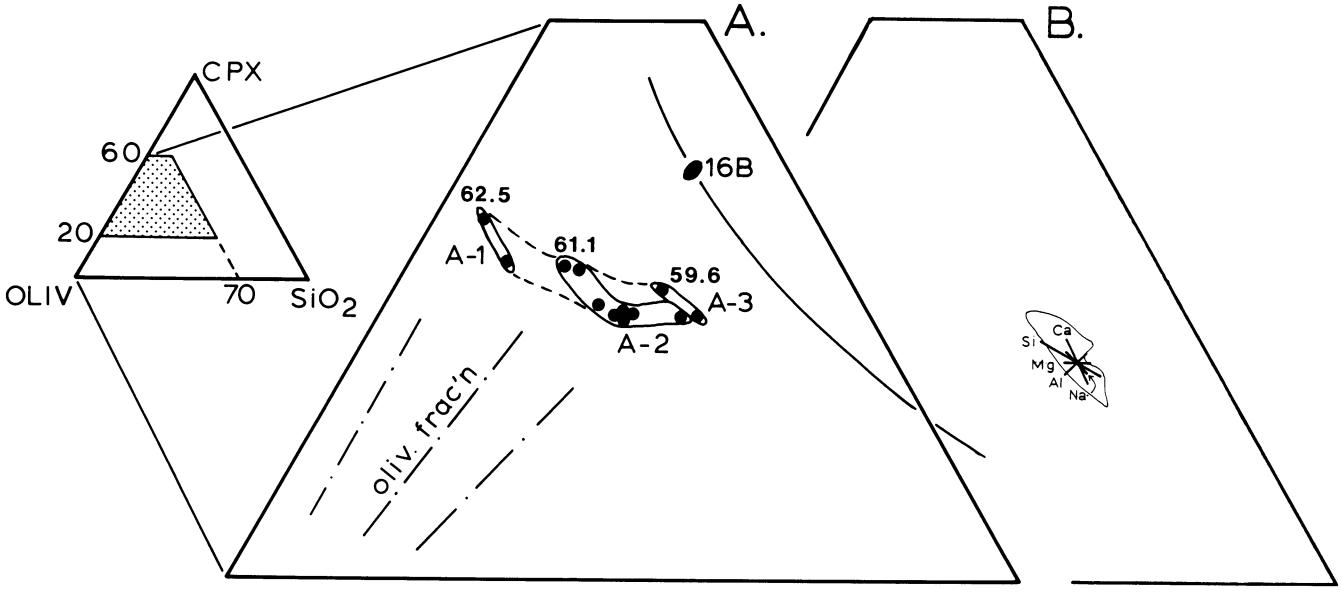

Figure 8. A. Enlarged portion of the cpx-oliv-SiO_2 projection (Figure 5) showing glasses from dredge 16. The decrease in Mg # of the 16A glasses along a trend transverse to olivine control lines cannot be accounted for by fractionation, but may be explained by mixing between a high Mg #, olivine-saturated liquid, and a low Mg #, olivine + plagioclase ± clinopyroxene-saturated liquid. B. Effects of analytical uncertainty on projection position. Enclosed field is for 50 of the 76 Galapagos group D5 glasses of Byerly et al. (1976); data from Melson et al. (1977). Heavy lines show the effect on the projection position of plus and minus one standard deviation from the group mean for each element shown (after Christie, 1984).

Table 6. Sample characteristics and type designations.

Lava Type #	I	II	III
Chemical group	13, 16A, 16B, 21	5, 17	19, 20
Chemical characteristics*			
Glass K_2O	0.11 ± 0.05	0.21 ± 0.02	0.77 ± 0.07
Glass P_2O_5	0.19 ± 0.02	0.21 ± 0.001	0.30 ± 0.04
Glass K/P	1.1 ± 0.4	1.9 ± 0.2	5.0 ± 0.7
K/Rb	678 ± 119	461 ± 45	338 ± 26
Zr/Nb	92.8 ± 38.3	40.2 ± 8.2	6.7 ± 0.6
Zr/Y	2.5 ± 0.14	3.4 ± 0.01	5.9 ± 0.72
$^{87}Sr/^{86}Sr$	0.70341	0.70340 ± 0 .00012	0.70370 ± 0.00010
$^{143}Nd/^{144}Nd$	0.51306	0.51308 ±0.00005	0.51283 ± 0.00001
Magma type	MORB	BABB	Transitional

*Reported values are mean ± 1σ, K_2O, P_2O_5 and K/P all increase with differentiation.

a shift of primary liquid composition to the left on the projection.

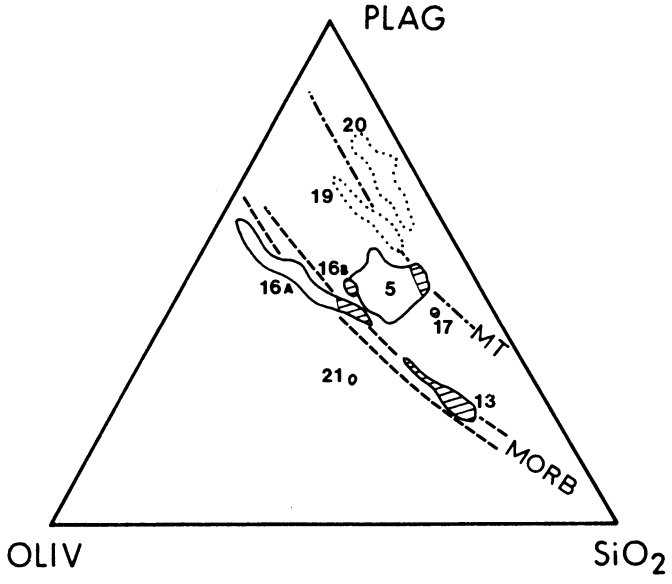

Figure 9. Projection of glass data (Table 2) from cpx onto the plag-oliv-SiO_2 plane, after Walker et al. (1979), using equations of Grove et al. (1982). Pagioclase-saturated glasses are hachured, except for dredges 19 and 20, which are unpatterned for clarity. Type I glasses conform to (dashed) olivine + plagioclase (+ liquid) cotectic approximately like that for MORB glasses from the Galapagos spreading center (Christie and Sinton, 1981, and unpublished data) and the East Pacific Rise near the Tamayo Fracture Zone (Bender et al., 1984). Types II and III plagioclase-saturated glasses are nearly coincident with a BABB cotectic defined by data from the Mariana Trough and East Scotia Sea (data of Fryer et al., 1981).

Of the samples in this study, those from dredge 5 are most conducive to this approach because the range of compositions represented in that dredge is primarily controlled by olivine fractionation. Chemical subgroup 5A-1 is the most primitive representative in that dredge. Primary magmas that could be parental to 5A-1 must lie on an olivine addition path, calculated by successive addition of fractions of equilibrium olivine composition. We have calculated olivine addition paths using a method developed by Diller (1982) and Christie (1984). Equilibrium olivine compositions are calculated from input two-component distribution coefficients (e.g., $(Fe/Mg)_{oliv\text{-}liq} = 0.30$) using the equations of Takahashi and Irvine (1981), which assume stoichiometric control of mineral/liquid partitioning. Relative to the single-element partition coefficients calculated by the program, the input two-component distribution coefficients are relatively insensitive to variations in temperature and composition (Takahashi and Irvine, 1981). This procedure can be repeated using small, in this case 0.5 mol %, steps with a new equilibrium olivine composition calculated for each new derived liquid composition. Thus, a spectrum of liquid and coexisting olivine compositions can be calculated for olivine control lines for any given starting composition.

The results of the olivine addition models for dredge 5 are shown in Figure 10. By inspection of the results in both projections, it is possible to determine a composition that has a consistent relation to the high pressure phase boundaries in both projections. For the dredge 5 models, that composition is where liquid Mg # is about 69-70. Such a composition would lie on the olivine +

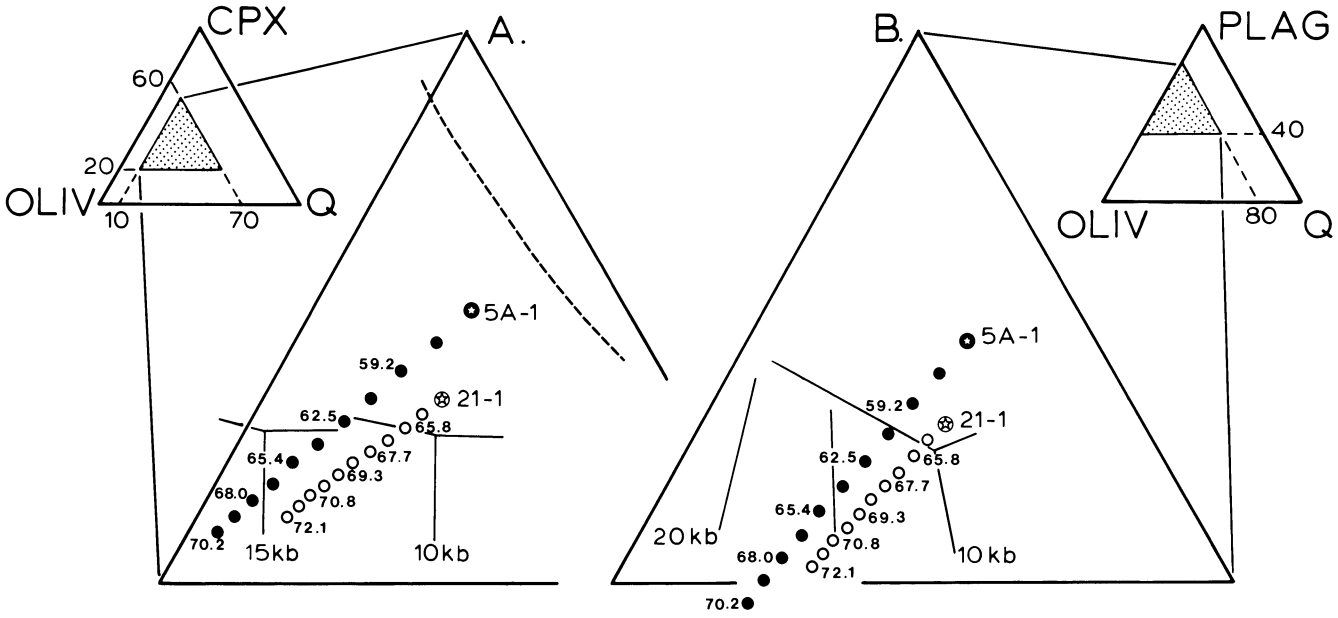

Figure 10. Liquid compositions derived by addition of incremental 0.5 mol % steps of equilibrium olivine to compositions 5A-1 (solid symbols) and 21-1 (open symbols), plotted in the projections of Walker et al. (1979) and Grove et al. (1982). Starting compositions (Table 6) are shown as circled stars. For clarity, only points for every five (5A-1) and three (21-1) steps, and the Mg # of every other plotted point, are shown. High-pressure phase boundaries are those of Stolper (1980). See text for discussion.

orthopyroxene cotectic at 16-17 kbar, suggesting that, at this pressure, primary liquids parental to dredge 5 lavas separated from a harzburgitic residue after very high rates of melting. Obviously there are considerable uncertainties, particularly with respect to the position of the high pressure phase boundaries and actual pressures of segregation. Nonetheless, the result that derived liquids do not reach Mg # close to 70 except at low normative cpx (close to the olivine-SiO join on Figure 10A) is compelling evidence that dredge 5 lavas are derived from melts generated by very high rates of fusion.

The calculated "parental" liquid inferred from this model is given in Table 7. It is unusually high in Ni, but this result is in accord with the very high percent of melting. Compared to "parental" liquids generally assumed for most abyssal lavas, it is also rather high in FeO, TiO_2, K_2O, P_2O_5, Rb and Zr. This result for the more incompatible elements is consistent with derivation from a metasomatized mantle, as previously suggested for BABB lavas from the Mariana Trough (Fryer et al., 1981).

A similar approach has been taken for sample 21-1, a Type I lava. The result is shown in Figure 10 and Table 7. A "best fit" result suggests segregation from a harzburgitic residue at about 12-13 kbar after somewhat lower rates of melting than for the dredge 5 "parental" composition. It is clear from Figure 7 that parental lavas for other Type I lavas (e.g. 16A, 16B) must have segregated at pressures at least as high as 15-20 kbar, so the shallow segregation pressure inferred for dredge 21 should not be taken as indicative of all Type I lavas. The calculated parental liquid for dredge 21 (Table 7) is somewhat low in magnesium but otherwise it reflects the strongly depleted nature of Type I lavas. Sample 21-1 has not been analyzed for trace elements.

With respect to lavas in Types I and II, a number of important conclusions can be made:

1. Type I lavas are very similar to highly depleted N-MORB. They are derived from parental liquids segregated from residual mantle over a range of pressures from 13-20 kbar.

2. Relative to Type I, Type II lavas are enriched in incompatible elements, but only slightly in Sr isotope composition. The incompatible-element enrichment probably reflects a recent enrichment of the mantle source for Type II magmas.

3. Type II magmas are saturated with plagioclase at significantly lower MgO contents than are Type I lavas. The Type II olivine + plagioclase cotectic projects to a position essentially coincident with that for hydrous magmas from the Mariana Trough.

4. Type II lavas may be hydrous and this, together with their slight incompatible element enrichments and the position of their olivine + plagioclase cotectic, suggests that these magmas are representatives of BABB magma type.

5. Type II parental magmas formed by very high degrees of melting, consistent with the interpretation that the melting may have occurred under hydrous conditions.

Table 7. Olivine addition models.

Dredge #	5		21	
	Ave. 5A-1	Calc. "parent"	Ave. 21-1	Calc. "parent"
SiO_2	49.56	48.60	49.39	49.17
TiO_2	2.03	1.76	0.96	0.93
Al_2O_3	14.96	12.93	16.17	15.59
FeO	10.73	11.45	9.37	9.55
MgO	7.41	12.90	9.29	10.78
CaO	10.63	9.23	11.98	11.56
Na_2O	3.00	2.59	2.17	2.09
K_2O	0.21	0.18	0.05	0.05
P_2O_5	0.21	0.18	0.16	0.15
Mg #	57.8	69.1	66.3	69.1
Ni	153	691	--	--
Rb	3	2.4	--	--
Zr	139	112	--	--
Eq. Oliv	Fo 80.4	Fo 87.0	Fo 85.5	Fo 87.0
wt % oliv added	0	24	0	4

Type III lavas are unusual, particularly with respect to their alkali and other incompatible element abundances. Such lavas are rare from normal spreading centers (but see Groups 2 and 27 of Christie and Sinton, 1981); they are more similar to lavas from seamounts. Their relatively low TiO_2 contents distinguish them from mid-plate hotspot basalts like those from Hawaii (e.g. Macdonald and Katsura, 1964). Compared to lavas in Types I and II, Type III lavas have lower Zr/Nb, K/Rb, K/Ba, $^{143}Nd/^{144}Nd$ and higher K/P, Zr/Y and $^{87}Sr/^{86}Sr$. These characteristics indicate that the mantle source for each of the Types I-III is distinct. Although Type III magmas are strongly enriched in light rare earth elements, they are not particularly depleted in yttrium (e.g. Figure 6), and garnet need not have been a residual phase from the melting events that produced those magmas.

The $^{87}Sr/^{86}Sr$ of all the analyzed samples are too low when compared to expectations based on Hart's (1984) globe-encircling high $^{87}Sr/^{86}Sr$ mantle anomaly. According to our new data, the <0.704-contour must be considerably farther to the north than suggested by Hart (1984), thus nearly isolating the source region for the

Table 8. Weathering, Mn crusts and lava ages.

Dredge #	Type	Weathering Characteristics	Estimated Age
20	III	None	< 50,000 yrs.
19	III	Slight discoloration	< 50,000 yrs.
21	I	1 mm Mn crusts	0.1-1.0 Ma
16	I	1 mm Mn crusts	0.1-1.0 Ma
13	I	1-2 mm Mn crusts	1-2 Ma
5	II	1-2 mm Mn crusts	1.4 Ma (Duncan, 1985)
17	II	2-5 mm Mn crusts	> 2 Ma

Samoan volcanic province. Our data further suggest that either the large scale southern hemisphere anomaly is not "globe-encircling," or that the sources of our analyzed basalts do not represent "normal" ocean island or MORB sources. As we can preclude a typical island arc origin for the analyzed lavas, we prefer the former interpretation.

LAVA AGES AND VOLCANO-TECTONIC IMPLICATIONS

Of the recovered lavas in this study, only one sample from dredge 5 has been radiometrically dated, yielding a K/Ar age of 1.4 Ma (Duncan, 1985). Relative ages of the other samples can be inferred based on the degree of weathering and development of Mn encrustations. Relative and estimated absolute age ranges of the recovered lavas are given in Table 8. In many respects these ages are in marked conflict with magnetic anomaly assignations of Cherkis (1980) and Malahoff et al. (1982) for the dredge sites and indicate that realistic tectonic reconstructions of the North Fiji Basin are yet to be made. Nonetheless, several important conclusions can be drawn from the results in Table 8.

The Type II lavas are among the oldest recovered. The data suggest that early opening of the Lau and North Fiji basins may have involved the production of BABB magmas, followed by evolution to production of MORB magmas. Thus, the influence of a slab-derived component may be restricted to early back-arc basin magma genesis. This conclusion is identical to, and strongly supports, that of Hawkins and Melchior (1983) with respect to the Lau Basin.

The youngest recovered lavas are from the South Pandora Ridge and those in dredge 20 are exceedingly young; this feature must be considered to be volcanically active. The recovery of very young dredge 20 lavas from a deep graben-like structure suggests that the area is in active extension. The South Pandora Ridge strikes east-northeast until it intersects the Northern Melanesian Borderland paleo-Vitiaz suture at Rotuma Island (Figure 1). Rotuma, like Wallis Island to the west (Figure 1), appears to be a rejuvenated edifice (e.g. Sinton et al., 1985). There is a well-developed barrier reef, yet the island contains probable Holocene alkali basaltic lavas (Hindle, 1970; Price and Woodhall, unpublished data). Thus the rejuvenated activity on Rotuma and the recent activity on the South Pandora Ridge may be related. This conclusion is not necessarily in conflict with interpretation of the South Pandora Ridge as a fracture zone (Chase, 1971). There is evidence for continual and recent plate reorganization in this region; we propose that the young activity along the lineament including dredges 19 and 20 and Rotuma Island reflects extension during the last one million years along a pre-existing zone of weakness. The alkali-enriched lavas from along this lineament could reflect low degrees of melting from a poorly developed asthenospheric upwelling zone beneath the, now extensional, South Pandora Ridge.

SUMMARY AND CONCLUSIONS

1. Seven new dredges from the Lau and North Fiji basins contain eight chemical groups. These eight groups can be described in terms of three distinct types that primarily reflect distinct mantle sources and degree of melting. Type I mantle sources most closely resemble those of MORB; Type III display isotope characteristics that are enriched in terms of their long-term Rb/Sr and Nd/Sm ratios.

2. The oldest recovered lavas (Type II) are enriched in incompatible elements, and possibly water, relative to normal MORB. They evolved from parental magmas formed by very high rates of melting and share many characteristics with BABB lavas from the Mariana Trough and some other back-arc basins.

3. Type I lavas, of intermediate age, are low-K MORB like those of mid-ocean spreading centers but with slightly higher $^{87}Sr/^{86}Sr$. Although our sample coverage is limited, the conclusion that early production of BABB was followed by MORB-dominated spreading is in accord with a similar conclusion of Hawkins and Melchior (1983) for the Lau Basin.

4. Ferrobasalts with MORB affinity were recovered from a region of high-amplitude magnetic anomalies and oblique seafloor structure. This result suggests that the magnetic telechemistry hypothesis (Vogt and Johnson, 1973) may, at least locally, be valid in back-arc spreading environments and that some back-arc spreading centers may be characterized by rift propagation.

5. We did not sample active spreading centers west of Viti Levu (Figure 1), but, based on conclusion 3 above, MORB lavas can be expected in the active zones of those centers (see also Hawkins and Batiza, 1975).

6. The youngest recovered lavas are alkali and other incompatible-element enriched basalts from the South Pandora Ridge. These lavas may have been erupted from a recently activated pre-existing lineament that includes Rotuma Island. The enriched nature of the lavas is consistent with low degrees of melting from a poorly developed mantle upwelling zone, but the source for these lavas was also enriched relative to that for the other lavas on the North Fiji Basin.

7. The $^{87}Sr/^{86}Sr$ of all samples are too low when compared to predictions based on a hypothetical globe-encircling mantle anomaly (Hart, 1984), suggesting that this anomaly may not be continuous to the west of the Samoa volcanic province.

REFERENCES

Bender, J.F., F.N. Hodges, and A.E. Bence, 1978, Petrogenesis of basalts from the project FAMOUS area experimental study from 0 to 15 kbars: Earth and Planetary Science Letters, v. 41, p. 277-302.

Bender, J.F., C.H. Langmuir, and G.N. Hanson, 1984, Petrogenesis of basalt glasses from the Tamayo Region, East Pacific Rise: Journal of Petrology, v. 25, p. 213-254.

Bougault, H., 1980, Contribution des elements de transition a la comprehension de la genese des basalts oceaniques: Thesis, University of Paris VII.

Bowen, N.L., 1928, The Evolution of the Igneous Rocks: New York, Dover Publications, Inc., 332 pp.

Brocher, T.M., 1985, On the formation of the Vitiaz Trench lineament and North Fiji Basin, in T.M. Brocher, ed., Geological Investigations of the Northern Melanesian Borderland, Earth Science Series, v. 3: Houston, TX, Circum-Pacific Council for Energy and Mineral Resources, p. 13-34.

Bryan, W.B., and H.J.B. Dick, 1982, Contrasted abyssal basalt liquidus trends: evidence for mantle major element heterogeneity: Earth and Planetary Science Letters, v. 58, p. 15-26.

Byerly, G.R., W.G. Melson, J.A. Nelen, and E. Jarosewich, 1977, Abyssal basaltic glasses as indicators of magma compositions: Smithsonian Contributions to the Earth Sciences, v. 19, p. 22-30.

Byerly, G.R., W.G. Melson, and P.R. Vogt, 1976, Rhyodacites, andesites, ferrobasalts and ocean tholeiites from the Galapagos spreading center: Earth and Planetary Science Letters, v. 30, p. 215-221.

Carlson, R.W., J.D. Macdougall and G.W. Lugmair, 1978, Differential Sm/Nd evolution in oceanic basalts: Geophysical Research Letters, v. 5, p. 229-232.

Chase, C.G., 1971, Tectonic history of the Fiji Plateau: GSA Bulletin, v. 82, p. 3087-3110.

Cherkis, N.Z., 1980, Aeromagnetic investigations and sea floor spreading history in the Lau Basin and northern Fiji Plateau: U.N. ESCAP, CCOP/SOPAC Technical Bulletin, v. 3, p. 37-45.

Christie, D.M., 1984, Petrological effects of mid-oceanic rift propagation: the Galapagos spreading center at 95.5°W: Ph.D. Dissertation, University of Hawaii, Honolulu, Hawaii..

Christie, D.M., and J.M. Sinton, 1981, Evolution of abyssal lavas along propagating segments of the Galapagos spreading center: Earth and Planetary Science Letters, v. 56, p. 321-335.

Dick, H.J.B., 1980, Vesicularity of Shikoku Basin basalt: a possible correlation with the anomalous depths of back-arc basins: Initial Reports of the Deep Sea Drilling Project, v. 58, p. 895-904.

Dick, H.J.B., R.L. Fisher, and W.B. Bryan, 1984, Mineralogic variability of the uppermost mantle along mid-ocean ridges: Earth and Planetary Science Letters, v. 69, p. 88-106.

Diller, D.E., 1982, Contributions to the geology of West Maui Volcano, Hawaii: M.S. Thesis, Univ. of Hawaii, Honolulu, 237 pp.

Duncan, R., 1985, Radiometric ages from volcanic rocks along the New Hebrides-Samoa Lineament, in T.M. Brocher, ed., Geological Investigations of the Northern Melanesian Borderland, Earth Science Series, v. 3: Houston, TX, Circum-Pacific Council for Energy and Mineral Resources, p. 67-76.

Fryer, P., J.M. Sinton, and J.A. Philpotts, 1981, Basaltic glasses from the Mariana Trough: Initial Reports of the Deep Sea Drilling Project, v. 60, p. 601-609.

Garcia, M.O., N.W.K. Liu, and D.W. Muenow, 1979, Volatiles in submarine volcanic rocks from the Mariana island arc and trough: Geochimica et Cosmochimica Acta, v. 43, p. 305-312.

Gill, J.B., 1984, Sr-Pb-Nd isotopic evidence that both MORB and OIB sources contribute to oceanic island arc magmas in Fiji: Earth and Planetary Science Letters, v. 68, p. 443-458.

Grove, T.L., D.C. Gerlach, and T.W. Sando, 1982, Origin of calc-alkaline series lavas at Medicine Lake Volcano by fractionation, assimilation and mixing: Contributions to Mineralogy and Petrology, v. 80, p. 160-182.

Hart, S.R., 1984, A large scale isotope anomaly in the southern hemisphere mantle: Nature, v. 309, p. 753-757.

Hart, S.R., W.E. Glassley, and D.E. Karig, 1972, Basalts and seafloor spreading behind the Mariana Island arc: Earth and Planetary Science Letters, v. 15, p. 12-18.

Hawkins, J.W., 1974, Geology of the Lau Basin, a marginal sea behind the Tonga Arc, in C. Burke and C. Drake, eds., Geology of Continental Margins: New York, Springer-Verlag, p. 505-520.

Hawkins, J.W., 1976, Petrology and geochemistry of basaltic rocks of the Lau Basin: Earth and Planetary Science Letters, v. 21, p. 283-297.

Hawkins, J.W., 1977, Petrology and geochemical characteristics of marginal basin basalt, in M. Talwani and W.C. Pitman, eds., Island Arcs, Deep Sea Trenches and Back-arc Basins: Washington, D.C., American Geophysical Union, p. 355-365.

Hawkins, J.W., and R. Batiza, 1975, Tholeiitic basalt from an active spreading center on the North Fiji Plateau 15°30'S, 173°30'E: Eos, Transactions of the American Geophysical Union, v. 56, p. 1078.

Hawkins, J.W., and J.T. Melchior, 1983, Petrology of back-arc basin basalts: implications for mantle heterogeneity: Eos, Transactions of the American Geophysical Union, v. 64, p. 332.

Hildreth, W., 1981, Gradients in silicic magma chambers: implications for lithospheric magmatism: Journal of Geophysical Research, v. 86, p. 10153-10192.

Hindle, W.H., 1970, The geochemistry of volcanism from Vanua Levu and other islands of the Fiji group and their petrogenetic significance: M.Sc. Thesis, University of Leeds, 1970.

Jaques, A.L., and D.H. Green, 1979, Anhydrous melting of peridotite at 0-15 kb pressure and the genesis of tholeiitic basalts: Contributions to Mineralogy and Petrology, v. 73, p. 287-310.

Johnson, K.T.M., J.M. Sinton, and R.C. Price, 1983, Submarine arc and back-arc lavas of the N. Melanesian Borderland, Lau and N. Fiji basins: Eos, Transactions of the American Geophysical Union, v. 64, p. 335.

Karig, D.E., 1971, Structural history of the Mariana Island arc system: GSA Bulletin, v. 83, p. 323-344.

Macdonald, G.A., and T. Katsura, 1964, Chemical composition of Hawaiian lavas: Journal of Petrology, v. 5, p. 82-133.

Malahoff, A., R.H. Feden, and H.S. Fleming, 1982, Magnetic anomalies and tectonic fabric of marginal basins north of New Zealand: Journal of Geophysical Research, v. 87, p. 4109-4125.

Mattey, D., B. Marsh, and J. Tarney, 1981, The geochemistry, mineralogy and petrology of basalts from the West Philippine and Parece Vela basins and from the Palau-Kyushu and West Mariana ridges, Deep Sea Drilling Project Leg 59: Initial Reports of the Deep Sea Drilling Project, v. 59, p. 753-800.

Melson, W.G., G.R. Byerly, J.A. Nelen, T. O'Hearn, T.L. Wright, and T.L. Vallier, 1977, A catalog of the major element chemistry of abyssal volcanic glasses: Smithsonian Contributions to Earth Sciences, v. 19, p. 31-60.

Muenow, D.W., N.W.K. Liu, M.O. Garcia, and A.D. Saunders, 1980, Volatiles in submarine volcanic rocks from the East Scotia Sea back-arc basin: Earth and Planetary Science Letters, v. 47, p. 272-278.

Nicholls, I.A., and A.E. Ringwood, 1973, Effect of water on olivine stability in tholeiites and the production of silica-saturated magmas in the island arc environment: Journal of Geology, v. 81, p. 285-300.

Norrish, K., and J.T. Hutton, 1969, An accurate X-ray spectrographic method for the analysis of a wide range of geologic samples: Geochimica et Cosmochimica Acta, v. 33, p. 431-451.

Norrish, K., and B.W. Chappell, 1977, X-ray fluorescence spectrometry, in J. Zussman, ed., Physical Methods in Determinative Mineralogy, 2nd edition: New York, Academic Press, p. 201-272.

O'Hara, M.J., 1980, Nonlinear nature of the unavoidable long-lived isotopic, trace and major element contamination of a developing magma chamber: Philosophical Transactions of the Royal Society of London, v. 297A, p. 215-227.

Philpotts, A.R., 1979, Silicate liquid immiscibility in tholeiitic basalts: Journal of Petrology, v. 20, p. 99-118.

Ridley, W.I., J.M. Rhodes, A.M. Reid, P. Jakes, C. Shih, and M.N. Bass, 1974, Basalts from Leg 6 of the Deep Sea Drilling Project: Journal of Petrology, v. 15, p. 140-159.

Sinton, J.M., D.S. Wilson, D.M. Christie, R.N. Hey, and J.R. Delaney, 1983, Petrologic consequences of rift propagation on oceanic spreading ridges: Earth and Planetary Science Letters, v. 62, p. 193-207.

Sinton, J.M., K.T.M. Johnson, and R.C. Price, 1985, Petrology and geochemistry of volcanic rocks from the Northern Melanesian Borderland, in T.M. Brocher, ed., Geological Investigations of the Northern Melanesian Borderland, Earth Science Series, v. 3: Houston, TX, Circum-Pacific Council for Energy and Mineral resources, p. 35-66.

Stern, R.J., 1981, A common mantle source for western Pacific island arc and "hot-spot" magmas-implications for layering in the upper mantle: Carnegie Institution of Washington Yearbook, v. 80, p. 455-462.

Stolper, E., 1980, A phase diagram for mid-ocean ridge basalts: preliminary results and implications: Contributions to Mineralogy and Petrology, v. 74, p. 13-27.

Takahashi, E., and T.N. Irvine, 1981, Stoichiometric control of crystal/ liquid single-component partition coefficients: Geochimica et Cosmochimica Acta, v. 45, p. 1181-1186.

Takahashi, E., and I. Kushiro, 1983, Melting of a dry peridotite at high pressures and basalt magma genesis: American Mineralogist, v. 68, p. 859-879.

Tarney, J., A.D. Saunders, and S.D. Weaver, 1977, Geochemistry of volcanic rocks from the island arcs and marginal basins of the Scotia Sea region, in M. Talwani and W.C. Pitman, eds., Island arcs, deep sea trenches and back-arc basins: Washington, DC, American Geophysical Union, p. 367- 377.

Taylor, B., and G.D. Karner, 1983, On the evolution of marginal basins: Reviews of Geophysics and Space Physics, v. 21, p. 1727-1741.

Vogt, P.R., and G.L. Johnson, 1973, Magnetic telechemistry of oceanic crust? Nature, v. 245, p. 373-375.

Walker, D., and S.E. DeLong, 1982, Soret separation of mid-ocean ridge basalt magma: Contributions to Mineralogy and Petrology, v. 79, p. 231-240.

Walker, D., T. Shibata, and S.E. DeLong, 1979, Abyssal tholeiites from the Oceanographer Fracture Zone, II. Phase equilibria and mixing: Contributions to Mineralogy and Petrology, v. 70, p. 111-125.

Wood, D.A., N.G. Marsh, J. Tarney, J.-L. Joron, P. Fryer, and M. Treuil, 1981, Geochemistry of igneous rocks from a transect across the Mariana Trough, arc, fore-arc and trench, Sites 453 through 461, Deep Sea Drilling Project Leg 60: Initial Reports of the Deep Sea Drilling Project, v. 60, p. 611-645.

Yoder, H.S., Jr., and C.E. Tilley, 1962, Origin of basalt magmas: an experimental study of natural and synthetic rock systems: Journal of Petrology, v. 3, p. 342-532.

Zindler, A., H. Staudigel and R. Batiza, 1984, Isotope and trace element geochemistry of young Pacific seamounts: implications for the scale of upper mantle heterogeneity: Earth and Planetary Science Letters, v. 70, p. 175-195.

Kroenke, L.W., and J.V. Eade, editors, 1993, Basin Formation, Ridge Crest Processes, and Metallogenesis in the North Fiji Basin: Houston, TX, Circum-Pacific Council for Energy and Mineral Resources, Earth Science Series, Vol. 15, Springer-Verlag, New York.

GEOCHEMISTRY OF NORTH CENTRAL NORTH FIJI BASIN SEDIMENTS

GARY M. McMURTRY, ERIC H. DeCARLO, and KEE HYUN KIM[1]
Hawaii Institute of Geophysics, School of Ocean and Earth Science and Technology
University of Hawaii, Honolulu, Hawaii 96822

ABSTRACT

Pelagic sediment cores from eleven stations in the north central North Fiji Basin plus a coring station on the Vanuatu archipelagic apron were geochemically characterized as part of an intensive geological survey of backarc spreading centers in the region. In order to assess recent hydrothermal contributions to these sediments from active backarc spreading, surface samples were chemically and mineralogically analyzed. Analyses included phase and size partitioning and Q-mode factor analysis of the chemical data. The cores were analyzed for sedimentation and element accumulation rates by the excess ^{230}Th method, using alpha-track autoradiography.

The sampled sediments are largely carbonate oozes whose noncarbonate material is dominated by volcanic detritus in the >2-μm fraction and by Fe-montmorillonite, amorphous ferromanganese oxides and fine-grained volcanic ash in the <2-μm fraction. The sediments are slightly enriched in Fe, Mn, Cu, Zn, Ni and Pb relative to other North Fiji Basin and southwest Pacific sediments. Iron accumulation rates are similar to those of metalliferous sediments from the East Pacific Rise. The mean Mn accumulation rate is only about twice the global authigenic rate, whereas Al, because of volcanic ash contributions from the Vanuatu island arc and intra-basin volcanism, is accumulating at rates that are about ten times those of eastern and equatorial Pacific pelagic sediments.

Q-mode factor analysis produced three major factors—hydrothermal, authigenic and detrital—which together account for more than 90% of the sample variance in both size fractions of the noncarbonate material. The aerial distribution of the <2-μm fraction factor components reveals a major hydrothermal source associated with the South Pandora Ridge spreading center, in general agreement with the Mn and As accumulation rate patterns. Two smaller hydrothermal sources were revealed by the factor analysis which are not associated with any known active tectonic features, suggesting that back-arc rifting and associated hydrothermal activity in this portion of the North Fiji Basin may follow both ordered and complex regional modes.

INTRODUCTION

Back-arc spreading centers are a principal component in the tectonic evolution of marginal basins and seas (Chase, 1971; Karig, 1971; Moberly, 1972; Watts et al., 1977; Taylor, 1979; Weissel, 1981; Taylor and Karner, 1983; Kroenke and Rodda, 1984). These spreading centers have recently been added to a growing number of tectonic regimes that are known to possess active hydrothermal systems. The systems result from convective cooling of rising magma bodies by seawater near the axis of spreading. They are often associated with intense mineralization of the seafloor, vent plumes and unique ecosystems (Corliss et al., 1979; Francheteau et al., 1979; Karl et al., 1980; Spiess et al., 1980; Grassle, 1982;

[1]Now at Department of Oceanography, Chungnam National University, Taejong, Korea

Malahoff, 1982; Rona et al., 1983). The first indications that such systems were associated with spreading centers were anomalous heat flow and metal enrichment in the pelagic sediments and encrustations on the midocean ridges (Bonatti and Joennsu, 1966; Bostrom and Peterson, 1966, 1969; Degens and Ross, 1969; Scott et al., 1974). More recently, water column tracers such as ^3He, CH_4, dissolved and particulate Mn and Fe, anhydrite particles, microorganisms and dissolved microbiological metabolites (Klinkhammer et al., 1977; Weiss et al., 1977; Lupton and Craig, 1981; Kim and Craig, 1983; Feely et al., 1984; Winn et al., 1986) as well as direct observations by bottom camera/temperature systems and manned submersibles (Crane and Normark, 1977; Lonsdale, 1977a,b; Ballard et al., 1979, 1982; Ballard and Francheteau, 1983) have been used to locate active hydrothermal fields. The tectonic regimes known or suspected to contain active hydrothermal systems now include on-axis volcanoes (Lonsdale et al., 1982; Chase et al., 1985), hotspot volcanoes (Malahoff et al., 1982a; De Carlo et al., 1983; Horibe et al., 1983), fault zones (Vidal et al., 1978; Lonsdale, 1979), island-arc ridges (Cronan et al., 1982), and spreading centers in the Lau (Bertine and Keene, 1975; von Stackelberg et al., 1985) and Mariana back-arc basins (Leinen and Anderson, 1981; Horibe et al., 1983).

The present study describes the geochemistry of sediments recovered from the north central North Fiji Basin during cruise KK820316 Leg 3 of the R/V KANA KEOKI. The primary objective of the survey was to locate and define the structure of the North Fiji Basin triple junction (a locus of three back-arc spreading centers) suggested by previous airborne magnetic surveys (Malahoff et al., 1982b; Cherkis and Malahoff, unpublished data, 1982) (Figure 1). Rationale for this objective was the premise that such backarc spreading centers may contain presently or recently active hydrothermal systems and their associated deposits, particularly metalliferous sediments and massive polymetallic sulfides.

Previous geophysical and geochemical surveys in the southwestern Pacific have indicated the presence of active hydrothermal circulation systems on the Fiji Plateau (North Fiji Basin). Conductive heat flow is four times the oceanic crustal average there and is bimodally distributed with anomalously high values that range to greater than 30 HFU (Sclater and Menard, 1967; Halunen, 1979). The region is also seismically active with epicenters generally coincident with the magnetically and bathymetrically defined ridges and transform faults (Haxby et al., 1983; Hamburger and Isacks, this volume). Cox (1980) studied marine sediment Hg in the region around Fiji and found concentrations to increase from background values of less than 20 ppb associated with shallow basins to 70 ppb in areas of high heat flow west of Fiji. On the basis of Fe and Mn enrichment over southwestern Pacific regional averages, Cronan and Thompson (1978) and Cronan (1983) suggested the area northwest of Fiji be targeted for more detailed sampling.

We present in this study detailed geochemical analyses of oriented piston cores, companion trigger cores, and free-fall cores from eleven stations in the north central North Fiji Basin, plus a coring station on the Vanuatu archipelagic apron (Figures 1 and 2). In order to determine the presence of hydrothermal contributions to the sediments, chemical, mineralogical and radiochemical analyses, including elemental phase and size partitioning, element accumulation rate determinations, and multivariate factor analysis of the geochemical data were performed.

METHODS

The topmost 5-cm sections of the free-fall cores (FFC) and trigger cores (TC) were selected for the following detailed chemical treatments and analyses because these samples were more likely to represent the most recently deposited material. Piston cores (PC) were not sampled for this work because the topmost portion is often disturbed by the coring process, as discussed in the results section below.

Chemical Treatments

All sediment samples were rinsed several times with distilled-deionized water followed by centrifugation to remove sea salts. After drying for a minimum period of 24 hours at 110°C, samples were cooled in a desiccator and weighed.

Weighed subsamples were treated with a sodium acetate-acetic acid buffer solution (SAAB) (pH 5.0) to remove carbonates and exchangeable divalent cations (Jackson, 1974). After apparent reaction completion (as evidenced by no further evolution of CO_2), the solid residue was separated from the supernate by centrifugation followed by repeated rinses with distilled-deionized water. The supernate and rinse water were collected for subsequent analysis. The solid residue was dried for a minimum period of 24 hours at 110°C prior to weighing.

Following SAAB treatment, the carbonate-free samples were separated into <2-μm and >2-μm

fractions by centrifugation. Both size fractions were redried at 110°C and weighed, yielding the relative percentages of these fractions reported in Table 1. The weight percentage of the carbonate fraction was determined by weight difference and by analysis of the supernate for Ca and Mg. Comparison of the two methods reveals no difference beyond the analytical error.

Additional subsamples of the carbonate-free sediment, <2-μm fraction, were treated with a sodium citrate-bicarbonate-dithionite buffer solution (CBD) to remove amorphous iron oxides and associated elements and compounds (Mehra and Jackson, 1960; McMurtry and Yeh, 1981; McMurtry et al., 1983; De Carlo et al., 1983). After extraction, the solid residue and supernate were separated by centrifugation followed by several rinses of the residue with distilled-deionized water. The supernate and rinse water were collected for subsequent analysis. The solid residue was dried at 110°C for a minimum of 24 hours before weighing.

Chemical Analysis

Appropriately weighed duplicate splits of all solid residues from the above chemical treatments were dissolved by heated, pressurized acid digestion using ultrapure HF-HCl-HNO_3. Sample solutions were diluted with a H_3BO_3 solution to complex insoluble fluorosilicates in a method modified after Bernas (1968) and De Carlo et al. (1983).

In certain cases the <2-μm fraction of the carbonate-free sediment was found to contain significant amounts of organic material which would not dissolve with the acid digestion procedures. In such instances, the organic matter was decomposed directly in the Teflon crucibles by treatment with 30% H_2O prior to acid digestion. This procedure avoided loss of manganese oxides that are dissolved by H_2O.

Major and minor elemental analyses of the digested solid residues and supernate solutions were performed by atomic absorption spectrophotometry

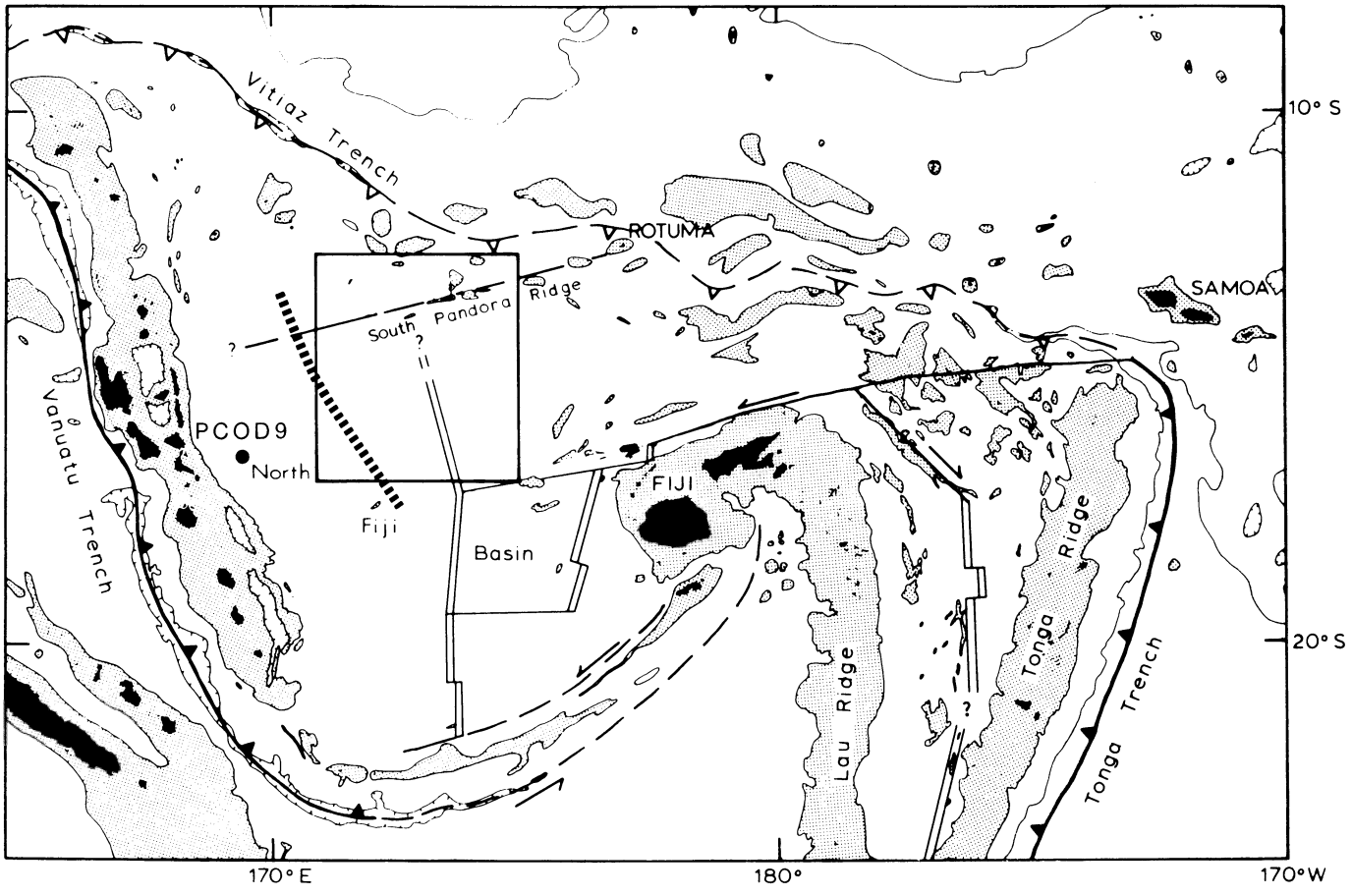

Figure 1. Bathymetric and tectonic map of the North Fiji Basin showing major physiographic features and locations of detailed survey area (Figure 2) and core KK82-PCOD-9. Dotted line indicates boundary between Vanuatu archipelagic apron sediments and pelagic sediments of the North Fiji Basin (Eade and Gregory, this volume). Bathymetry and tectonic interpretations modified after Kroenke et al. (1983) and Taylor and Karner (1983).

using a Perkin-Elmer Model 603 double-beam spectrophotometer equipped with deuterium background correction. Standard flame methods were employed for all elements except arsenic, which was determined by the method of hydride generation. Emission mode was utilized for the determination of Li, Na and K. The method of standard additions was employed in cases where significant matrix interferences were expected. The accuracy of the analyses was checked by simultaneous analysis of USGS standard rock AGV-1 (andesite) and HIG standard rocks HIGS-1 and HIGS-2 (tholeiitic basalts) (Macdonald et al., 1972; Flanagan, 1973). All analyses were found to agree with the reported or recommended values for the standards.

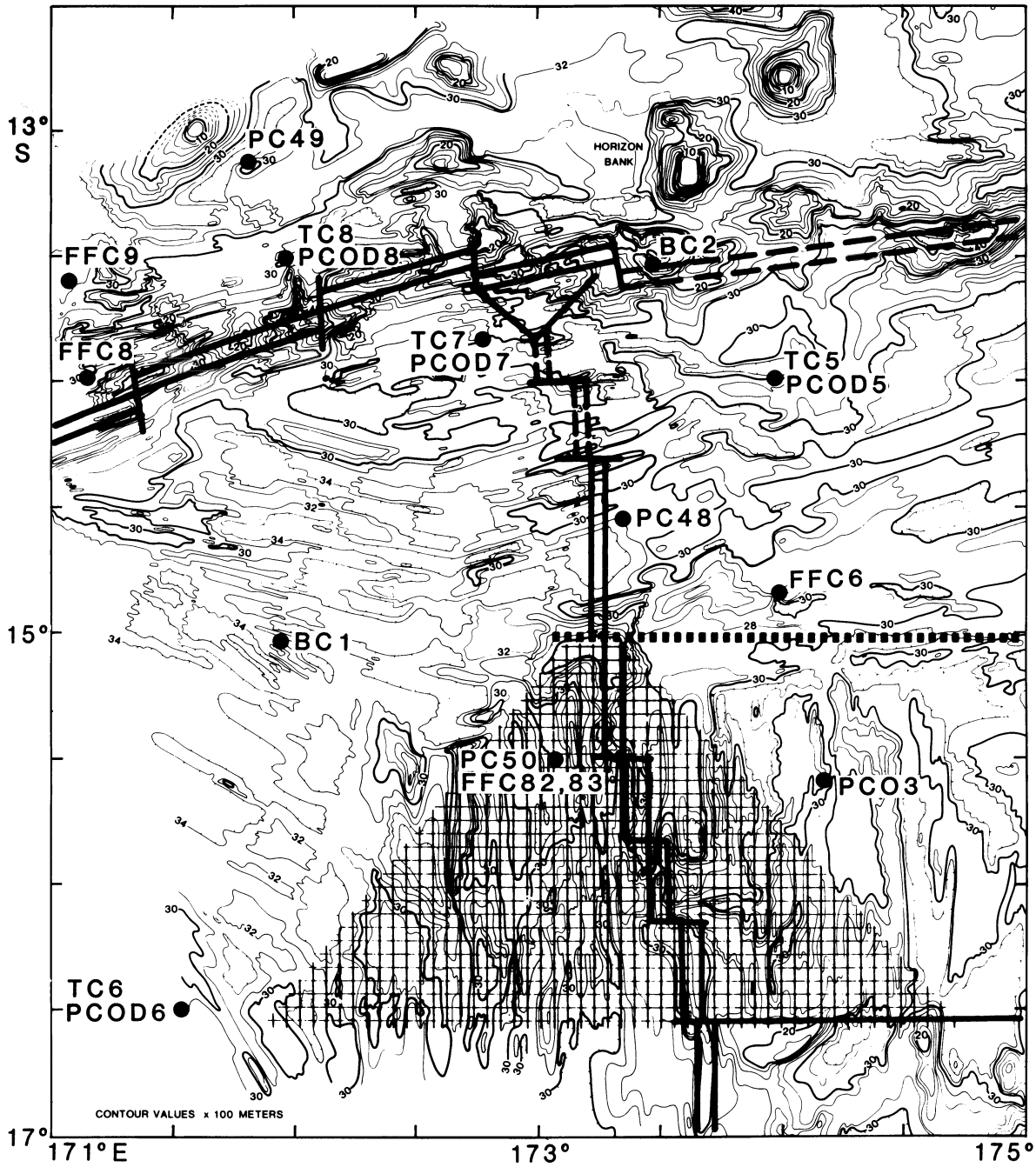

Figure 2. Detailed study area of north central North Fiji Basin, showing core and bottom camera (BC) locations. Bathymetric contours in 100-m intervals. Tectonic interpretations are: single line – transform fault; double line – spreading center; hatchured – propagating rift fabric. All symbols dashed where inferred (after Kroenke et al., this volume).

Table 1. North central North Fiji Basin sediment core locations and description.

Core Identification	Latitude (S)	Longitude (E)	Water depth (m)	$CaCO_3$[1] (wt%)	Noncarbonate[2]	
					>2 μm (wt%)	<2 μm(wt%)
KK82-FFC- 6	14°50.3′	174°00.0′	2580	81.7	45.8	54.2
KK82-FFC-8	13°58.5′	171°09.3′	2680	81.1	75.4	24.6
KK82-FFC-9	13°35.8′	171°03.9′	3350	78.6	72.1	21.9
KK82-TC-5 KK82-PCOD-5	13°58.4′	173°57.5′	3400	77.6	77.3	22.7
KK82-TC-6 KK82-PCOD-6	16°30.4′	171°32.3′	3165	41.2	89.0	11.0
KK82-TC-7 KK82-PCOD-7	13°49.7′	172°46.1′	3150	79.7	70.5	29.5
KK82-TC-8 KK82-PCOD-8	13°31.3′	171°58.2′	3020	85.0	70.3	29.7
KK82-TC-9 KK82-PCOD-9	16°28.8′	169°30.6′	3040	3.4	91.2	8.8
KK71-FFC-82	15°30.2′	173°04.2′	2945	74.4	79.7	20.3
KK71-FFC-83	15°30.3′	173°04.2′	2945	25.6	95.6	4.4
KK72-PC-03	15°34.7′	174°10.2′	2655	37.0	96.8	3.2
KK71-PC-48	14°33.2′	173°21.4′	3140	76.7	78.8	21.2
KK71-PC-49	13°06.71′	171°48.5′	3290	83.6	70.5	29.5
KK71-PC-50	15°30.0′	173°03.6′	2900	45.9	91.3	8.7

[1] Samples from topmost 0-5 cm, oven-dried at 110°C. $CaCO_3$ calculated by weight difference (Table 3).
[2] Loss-corrected relative weight percentage.

Mineralogy

Mineralogy was determined by X-ray diffraction analysis using a Philips XRG 3100 automatic diffractometer system equipped with long-fine-focus CuKα radiation, graphite curved-crystal monochromator and scintillation detector. Carbonate-free, >2-μm and <2-μm samples were analyzed as bulk powders and as oriented mounts on glass and molybdenum slides.

Radiochemical Analysis

Recovered free-fall cores (FFC), trigger cores (TC) and piston cores (PC) were surveyed for accumulation rates by the excess ^{230}Th method using alpha track autoradiography (Andersen and Macdougall, 1977; Fisher, 1977a,b). Alpha-sensitive, Kodak CN-85 cellulose nitrate film was placed directly on the cores and exposed for 6 months. Films were etched in a 10% NaOH solution at a constant temperature of 60°C. Etching efficiencies were monitored with a ^{241}Am source. Alpha tracks were counted by a random field-of-view method using a light microscope. Errors reported are based on counting statistics ($\pm 1\sigma$).

Accumulation Rates

Sedimentation rates for the cores were calculated by a least-squares fit of the logarithm of the excess ^{230}Th activity (expressed as the alpha track production density in tracks/cm^2 day) versus the core depth in cm. Three major assumptions of this method are (1) the total alpha track production reflects the total alpha activity of ^{230}Th, ^{238}U and their daughters, i.e. secular equilibrium is established; (2) the total alpha activity in the deepest sections of the cores solely reflects the level of ^{238}U

support; and (3) no significant post-depositional migration of ^{226}Ra and its daughters has occurred (closed system assumption). Excess ^{230}Th was calculated by subtracting the mean value of ^{238}U support from the total alpha activity at each sample interval.

Element accumulation rates were calculated using the relation:

$$A_e = C_e \rho S \quad (1)$$

where A_e = the accumulation rate of element e in either mg or $\mu g/cm^2\ 10^3$ yrs, C_e = the bulk concentration of element e in either mg or $\mu g/g$, ρ = the average dry bulk density in g/cm^3, and S = the average sedimentation rate in $cm/10^3$ yrs (McMurtry et al., 1981).

Bulk concentrations of elements were calculated from the data in Tables 1, 2 and 3 using the relation

$$C_e = (X_c/100)(C_c) + [1 - (X_c/100)] \cdot [(X_G/100)C_G + (X_L/100)C_L] \quad (2)$$

where X_c = the weight percentage of $CaCO_3$, C_c = the concentration of element e in the carbonate (SAAB extractable) fraction, X_G = the weight percentage of the carbonate-free, >2-μm fraction, C_G = the concentration of element e in the carbonate-free, >2-μm fraction, X_L = the weight percentage of the carbonate-free, <2-μm fraction, and C_L = the concentration of element e in the carbonate-free, <2-μm fraction.

RESULTS

Chemical Partitioning

The sediment samples were quantitatively partitioned into carbonate and noncarbonate fractions, and the noncarbonate sediment sized into >2-μm and <2-μm fractions to study the distribution of elements. The results of this study for 18 elements are presented in Tables 1, 2 and 3. The <2-μm fraction was further partitioned into amorphous iron oxide (CBD extractable) and silicate (CBD nonextractable) fractions (Table 4). From visual inspection of the cores after splitting and from results of previous work on metalliferous sediments in the eastern Pacific (Heath and Dymond, 1977; Dymond, 1981; McMurtry and Yeh; 1981; McMurtry et al., 1981), it was anticipated that some element partitioning into the various fractions would be found and that the noncarbonate >2-μm fraction would largely be composed of volcanic ash and/or hyaloclastite, whereas the noncarbonate <2-μm fraction would largely be composed of authigenic clay minerals, amorphous ferromanganese oxides and some clay-sized aeolian component.

Partitioning results for 15 of the 18 elements analyzed are presented for the carbonate and noncarbonate fractions of the sediment in Figure 3. The relative weight distributions of elements in the >2-μm and <2-μm fractions of the noncarbonate sediment are also shown. The 'carbonate fraction' is more accurately termed the 'SAAB extractable fraction' because it may also include weakly bound or exchangeable divalent cations from other sediment components such as organics or the inorganic noncarbonate material. With this ambiguity in mind, it is nevertheless remarkable that on average greater than 90% of the Cd, 60% of the Pb, 40% of the Li, 30% of the Co, and 20% of the K, Cu, Ni and Zn are associated with the SAAB extractable (carbonate) fraction. Only an average of 8 and 3% of the Mn and Si, respectively, associate with this fraction, whereas little if any Al, Fe or Cr are detected in this material (Figure 3). An average of 96% of the Ca and 19% of the Mg associate with the SAAB extractable fraction, presumably as Ca-Mg carbonates. The large amounts of Cd and Pb found in this fraction may also be bound as carbonates as their ionic radii (Cd^{2+}: 0.97 Å; Pb^{2+}: 1.20 Å) are similar to that of Ca (Ca^{2+} : 0.99 Å). Organic associations are known for these metals as well as for the others found in this fraction, however, (Patterson et al., 1976; Gong et al., 1977; Moore and Bostrom, 1978; Boylan et al. 1980) and it is uncertain what portion may also occupy weakly bound or exchangeable sites in the inorganic noncarbonate material.

Partitioning between the >2-μm and <2-μm fractions of the noncarbonate material is presented for all 18 elements in Figure 4. Figure 4a presents the mean and range of relative weight percentages for all samples except KK82-TC9 and KK72-PC03. Partitioning of these two samples are shown separately as Figures 4b

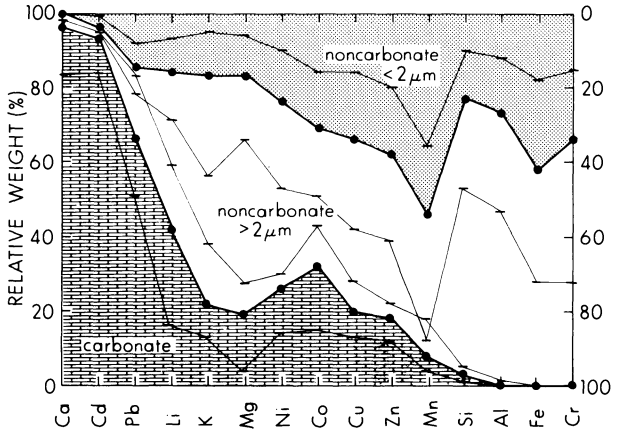

Figure 3. Chemical partitioning into SAAB extractable (carbonate) and SAAB nonextractable (noncarbonate) fractions. The size partitioning of the noncarbonate material into $>2-\mu$m and $<2-\mu$m fractions is also shown. Mean and range of values in relative weight percentage.

Table 2A. Major and minor element chemistry of North Fiji Basin sediments, $<2\mu m$[1]

Wt.%	FFC-6	FFC-8	FFC-9	TC-5	TC-6	TC-7	TC-8	TC-9	FFC-82	FFC-83	PC-03	PC-48	PC-49	PC-49[2]	PC-50
Na_2O	1.63[3]	0.93	0.93	1.75	3.37	1.38	1.83	3.36	1.32	1.26	1.28	1.04	0.95	1.31	1.00
K_2O	1.12	0.63	0.68	0.69	0.86	0.66	0.64	1.77	0.57	1.04	0.77	0.57	0.51	0.53	0.78
CaO	4.11	3.50	2.87	3.08	2.53	2.76	4.08	3.24	3.25	2.41	2.70	3.40	3.42	3.18	3.54
MgO	2.45	2.61	2.85	2.34	2.59	2.27	2.52	3.05	2.00	2.42	1.93	2.28	2.48	2.51	2.30
Al_2O_3	14.9	14.7	16.1	13.6	12.8	13.3	13.3	15.8	13.1	15.0	10.6	13.4	13.7	13.8	14.4
SiO_2	45.3	42.2	41.2	41.9	44.5	41.8	40.8	49.3	45.2	47.9	34.0	46.3	42.4	41.9	48.1
Fe_2O_3	17.4	20.1	18.6	21.5	19.0	21.4	18.8	11.1	20.3	17.0	28.6	20.7	19.1	20.3	19.1
MnO_2	2.97	3.37	3.39	4.16	2.55	4.22	3.73	0.32	2.48	1.33	6.39	2.22	3.07	3.05	2.17
TiO_2	1.03	1.21	1.21	1.05	1.11	1.05	1.24	0.84	0.90	0.76	1.20	0.93	1.00	0.88	0.77
Sub-total	90.9	89.3	87.8	90.1	89.3	88.8	86.9	88.8	89.1	89.1	87.5	90.8	86.6	87.5	92.2
LOI	9.0	11.7	12.6	10.7	9.2	11.5	13.5	9.6	--	--	--	--	--	--	--
Total	99.9	101.0	100.4	100.8	98.5	100.3	100.4	98.4	--	--	--	--	--	--	--
ppm															
Cu	369	544	452	649	402	590	704	206	400	330	780	510	520	570	400
Ni	133	167	180	162	92	154	190	55	200	180	1190	290	360	360	200
Zn	246	297	256	525	257	307	306	116	650	290	860	487	360	380	286
Pb	90	140	120	154	86	150	150	30	140	104	180	150	140	163	80
Co	119	173	188	137	115	131	135	92	120	104	490	140	160	160	110
Cr	80	90	110	100	80	100	100	36	96	100	99	120	150	190	125
Cd	1.3	1.9	1.2	2.9	1.8	1.8	1.2	1.1	0.5	1.7	1.8	1.9	0.4	0.7	0.6
As	40	55	38	56	44	58	44	10	57	65	110	53	75	56	88
Li	18	19	23	23	13	23	25	12	27	25	31	32	37	37	27

[1] All samples from topmost 0-5 cm, oven-dried at 110°C. Carbonate phases were removed prior to analysis by SAAB treatment (Table 3).
[2] Replicate determination.
[3] Coefficients of variation based on replicate analyses are within 5% for all elements except Ti (%), Mn, As, Li (%) and Cd (%).

Table 2B. Major and minor element chemistry of North Fiji Basin sediments, $>2\mu m$[1].

Wt.%	FFC-6	FFC-8	FFC-8[2]	FFC-9	FFC-9[2]	TC-5	TC-6	TC-7	TC-8	TC-9	FFC-82	FFC-83	PC-03	PC-48	PC-49	PC-50
Na_2O	3.17	2.36	2.23	2.34	2.14	2.27	2.78	1.95	2.14	3.55	2.09	3.56	0.73	2.03	1.82	2.99
K_2O	1.16	0.98	0.90	0.94	0.91	1.02	1.56	0.83	0.82	2.03	0.91	2.04	0.44	0.94	0.76	1.59
CaO	6.92	7.63	7.79	7.04	7.22	5.42	8.23	5.73	6.47	5.56	6.51	4.75	3.21	6.26	5.70	6.27
MgO	3.25	4.46	4.68	4.24	4.45	3.15	4.60	3.54	3.70	2.55	3.47	2.11	1.14	3.14	3.53	3.03
$A1_2O_3$	15.4	15.5	15.1	15.8	15.5	14.5	15.6	14.2	15.4	15.3	14.8	15.6	8.33	13.8	14.7	15.3
SiO_2	58.0	52.1	52.7	53.5	54.8	53.7	51.8	50.5	52.0	59.3	53.0	62.8	24.9	48.8	53.6	57.5
Fe_2O_3	8.17	9.72	10.2	9.28	9.52	11.1	10.5	11.7	10.4	8.02	11.0	7.27	25.4	17.9	10.7	8.85
MnO_2	0.27	0.68	0.68	0.61	0.59	1.61	0.45	1.69	1.03	0.20	0.71	0.25	18.6	0.67	1.06	0.39
TiO2	0.72	0.74	0.81	0.12	0.81	0.82	0.89	0.86	0.90	0.76	0.81	0.65	1.41	0.78	0.86	0.71
Sub total	97.1	94.2	95.1	94.5	95.9	93.6	96.4	91.0	92.9	97.3	93.3	99.0	84.2	94.3	92.7	96.6
LOI	1.6	3.7	4.4	4.2	4.6	5.9	2.1	7.5	6.8	1.1	5.8	1.4	14.4	4.0	6.3	1.7
Total	98.7	97.9	99.5	98.7	100.5	99.5	98.5	98.5	99.7	98.4	99.1	100.4	98.6	98.3	99.0	98.3
ppm																
Cu	153	209	253	221	262	284	226	366	306	143	242	84	992	265	340	143
Ni	81	108	123	109	110	138	93	141	154	77	105	53	1350	125	141	73
Zn	108	107	115	106	112	140	109	158	157	94	119	103	498	174	133	109
Pb	19	50	44	52	43	83	22	82	74	18	48	23	333	61	81	24
Co	39	54	61	56	53	60	59	69	64	30	54	27	1600	57	82	38
Cr	37	95	84	77	87	66	55	83	86	21	46	18	24	113	72	31
Cd	0.4	0.3	0.3	0.3	0.4	0.4	0.3	0.4	0.4	0.4	0.3	0.2	4.4	0.2	0.3	0.3
As	6	7	15	10	6	19	4	14	9	3	13	5	142	4	13	5
Li	16	18	18	20	19	22	18	20	21	16	17	17	9	18	20	17

[1] All samples from topmost 0.5 cm, oven-dried at 110°C. Carbonate phases were removed prior to analysis by SAAB Treatment (Table 3).
[2] Replicate determination.

and 4c. Sample KK82-TC9 represents sediment from the Vanuatu archipelagic apron (largely andesitic ash). Sample KK72-PC03 is from an unusually ferromanganese-rich layer in the topmost 38 cm of this core.

For all samples except KK82-TC9 and KK72-PC03, the average abundances in the >2-μm fraction are, in decreasing order, Ca, Na, K, Mg, Si and Al. This grouping suggests detrital material which is consistent with the visual and microscopic observations of ash/hyaloclastite. The average abundances in the <2-μm fraction are, in decreasing order, As, Mn, Cd, Zn, Pb, Co, Cu, Fe, Cr, Ni, Li and Ti. This grouping suggests trace metal adsorption onto ferromanganese oxides and smectite, which is consistent with the mineralogy and CBD extraction results (see below) and with previous work (Heath and Dymond, 1977; Dymond, 1981; McMurtry and Yeh, 1981; McMurtry et al., 1981; De Carlo et al., 1983).

For sample KK82-TC9, the abundances in the >2-μm fraction are, in decreasing order, Ca, Ni, Li, Si, K and Na. With the exception of Ni, Li, Mg and Al, this grouping is the same as for all samples except KK72-PC03. The presence of Ni may reflect a mafic component in the detrital material; Al, Ti, Mg and Zn, Fe, Cu show no significant size partitioning (Figure 4b). The partitioning of Li into this fraction is surprising, since Li is suggested to incorporate into authigenic marine smectites (Stoffyn-Egli and Mackenzie, 1984), which are not concentrated in the >2-μm fraction of this sample. The abundances in the <2-μm fraction are, in decreasing order, As, Co, Cd, Pb, Cr, Mn, Cu, Fe, Zn, Mg, Ti and Al. This grouping is similar to that of all samples except KK72-PC03. Trace metal adsorption onto ferromanganese oxides and smectite is also consistent with the mineralogy and CBD extraction results (see below).

For sample KK72-PC03, the abundances in the >2-μm fraction are, in decreasing order, Co, Mn, Cd, Pb, As, Cu, Ti, Ca and Ni. With the exception of the Ca presence and Fe absence (no significant partitioning), this grouping suggests ferromanganese oxides, which is consistent with the mineralogy (abundant δ-MnO_2, see below). The abundances in the <2-μm fraction are, in decreasing order, Cr, Li, Na, K, Mg, Zn, Si, Al and Fe. This grouping is suggestive of a smectite, which is again consistent with the mineralogy (see below). Note that in this particular case, the groupings are apparently size reversed, and that little if any detrital associations exist.

In order to better delineate the size partitioning results and characterize the mineralogy and chemical composition of the <2-μm fraction, CBD extracts of selected samples were analyzed and compared with the chemical composition of the <2-μm fraction (Table 4 and Figure 5). The CBD treatments extracted between 37% and 73% of the Fe_2O_3 in the samples. On the basis of whether more or less than 50±10% of the element was

Table 3. Chemical composition of carbonate fraction of North Fiji Basin sediments[1].

Wt. %	FFC-6	FFC-8	FFC-9	TC-5	TC-6	TC-7	TC-8	TC-9
$CaCO_3$[2]	81.7	81.1	78.6	77.6	41.2	79.7	85.0	3.4
$CaCO_3$[3]	78.3	81.7	73.8	72.4	39.7	80.0	81.8	3.5
$MgCO_3$[3]	0.40	0.38	0.39	0.48	0.44	0.48	0.40	0.19
ppm								
K	400	540	630	700	2560	660	670	--
Al	110	85	194	100	390	160	33	--
Si	1400	1200	1900	2200	4400	1700	2200	--
Fe	31	28	34	28	86	38	36	--
Mn	155	95	134	444	602	306	424	
Cu	16	16	29	33	52	26	17	--
Ni	10	9	15	15	22	16	12	--
Zn	8	8	11	16	24	12	8	--
Pb	34	38	42	34	44	40	87	--
Co	11	10	10	9	16	13	11	--
Cd	2.9	3.0	3.0	3.3	3.5	3.0	4.5	--
Li	3.8	3.7	3.8	4.3	4.7	4.0	5.5	--

[1] Samples treated with a sodium acetate-acetic acid buffer solution (SAAB) after Jackson (1974). Analyses based on SAAB solution extracts and reported on a bulk sample basis.
[2] Calculated from weight difference assuming all losses are due to $CaCO_3$.
[3] Calculated from Ca, Mg analyses.

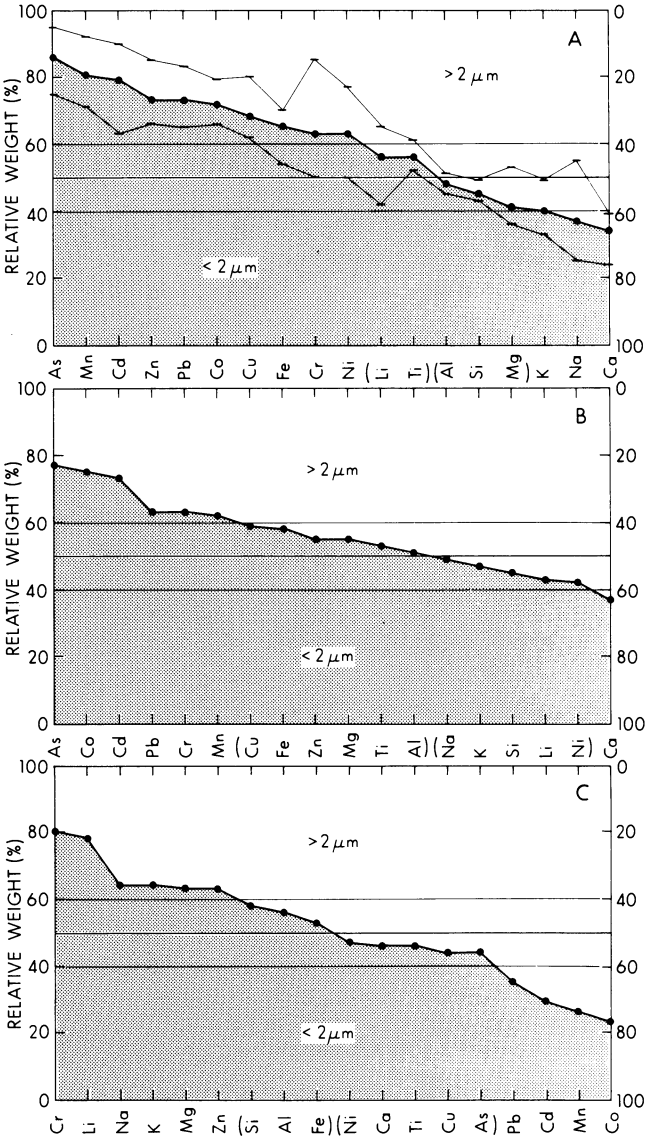

Figure 4. Chemical partitioning of noncarbonate material into >2-μm and <2-μm size fractions for all elements analyzed. Bracketed elements show no significant partitioning (50±10%). (a) All samples except KK82-TC9 and KK72-PC03. Mean and range of values in relative weight percentage. (b) Sample KK82-TC9. Vanuatu archipelagic apron (Figure 1). (c) Sample KK72-PC03. Ferromanganese-rich layer.

extracted with the iron oxide, three groups of element associations can be distinguished: (1) iron oxide; (2) intermediate; and (3) silicate. Arsenic, Mn and Cd are primarily associated with the extractable iron, whereas Fe, Cr, Co, Ni and Ca show both oxide and silicate associations. Lead, Cu, Zn, Ti, Li, Mg, Al, Si and K display increasing silicate associations that probably represent smectite scavenging (Pb, Cu, Zn) and structural assignments (Si, Al, Fe, Mg, Ti, K, Li) (Figure 5). In general, these results agree with similar CBD extraction of iron oxide-Fe-montmorillonite-nontronite deposits from Loihi submarine volcano (De Carlo et al., 1983). Elements extracted by this treatment may also include weakly bound cations on the silicate. The absolute concentrations of elements reported for the CBD extracts in Table 4 may therefore represent maximum values, and the relative concentrations of some elements may be affected because of their selective removal.

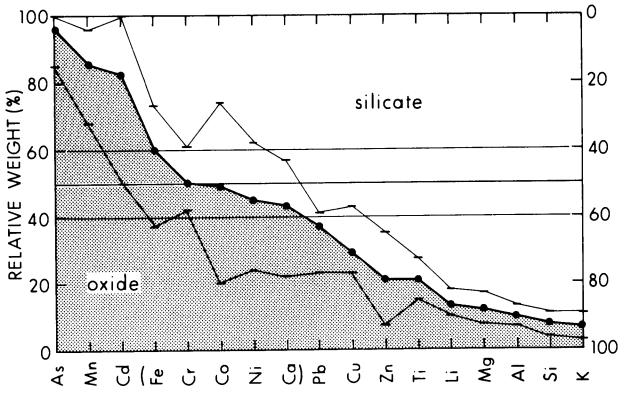

Figure 5. Chemical partitioning of noncarbonate, <2-μm fraction into CBD extractable (oxide) and CBD nonextractable (silicate) fractions. Mean and range of values in relative weight percentage. Bracketed elements show no significant partitioning (50±10%).

Mineralogy

The noncarbonate mineralogy of the <2-μm fraction of the sediment cores is summarized in Table 5. The relative abundances of the minerals are estimated semi-quantitatively based on characteristic X-ray peak areas generated from bulk-powder mounts. The semi-quantitative mineralogy of the >2-μm fraction is not presented because of the relatively constant composition of this material. X-ray diffraction revealed abundant and ubiquitous plagioclase feldspar, a broad hump centered at approximately 25° 2θ (3.56 Å) that is characteristic of amorphous volcanic glass, and minor amounts of smectite, quartz and kaolinite in some of the samples (Figure 6a). Light microscopy confirms the dominance of these volcanic detrital phases in the >2-μm fraction. One exception to the predominantly detrital composition of the >2-μm fraction is the presence of abundant δ-MnO_2 in sample KK72-PC03 (Figure 6b).

Smectite predominates in the <2-μm fraction. Some clay-sized plagioclase (and by association, clay-sized volcanic glass) is always present and sometimes abundant in this fraction. Kaolinite and quartz of probable aeolian origin are present in lesser and varying amounts (Table 5).

Amorphous iron and manganese oxides are also present in the <2-μm fraction of all samples, as discussed above (see chemical partitioning section). For selected samples, these phases were removed by CBD extraction prior to further characterization of the clay

Table 4. Chemical composition of armorphous iron oxide fraction of North Fiji Basin sediments[1].

Wt.%	FFC-6	%Ext.[2]	FFC-8	%Ext.	FFC-9	%Ext.	TC-7	%Ext.	TC-9	%Ext.	TC-9[3]	%Ext.
Na_2O	--	--	--	--	--	--	--	--	--	--	--	--
K_2O	0.03	3.0	0.07	11	0.06	8.5	0.04	6.1	0.14	7.9	0.12	6.8
CaO	1.57	38	1.48	42	1.58	55	1.57	57	0.75	23	0.68	21
MgO	0.22	9.0	0.44	17	0.33	12	0.25	11	0.29	9.4	0.23	1.6
Al_2O_3	1.36	9.1	1.96	13	1.66	10	1.59	12	1.16	7.3	0.94	5.9
SiO_2	2.8	6.1	4.0	9.4	3.1	7.5	4.7	11	2.5	5.1	2.0	4.1
Fe_2O_3	9.90	51	14.6	73	12.1	65	14.7	69	4.27	39	3.84	35
MnO_2	2.64	90	3.05	90	2.83	84	4.05	96	0.22	70	0.21	65
TiO_2	0.16	16	0.33	27	0.27	23	0.22	21	0.14	17	0.12	14
ppm												
Cu	100	27	161	30	198	43	143	24	58	28	36	18
Ni	75	42	80	48	87	48	95	62	14	26	12	22
Zn	90	35	30	10	18	6.8	94	31				
Pb	37	41	57	41	47	39	59	40	10	33	4	13
Co	68	57	84	49	87	46	97	74	21	23	15	16
Cr	39	49	53	61	46	43	45	45	--	--	--	--
Cd	1.4	100	1.5	80	1.2	100	0.9	50	--	--	--	--
As	37	97	47	85	42	100	66	100	15	100	14	100
Li	2.3	13	3.5	18	2.6	11	2.8	12	1.8	15	1.4	11

[1] Samples treated with a sodium citrate-bicarbonate-dithionate buffer solution (CBD) after Mehra and Jackson (1960). Analyses based on CBD extracts and reported on a $<2\mu m$, carbonate-free basis (Table 2).
[2] Extraction percentage relative to concentrations reported in Table 2.
[3] Replicate extraction.

mineralogy and chemistry. Typical X-ray diffraction patterns for the CBD-treated samples are presented in Figures 6c and 6d. The predominant 15 Å smectite is dioctahedral and expandable to 18 Å upon glycolation. Structural formulas calculated for the smectite suggest that it is an Fe-rich montmorillonite which is similar to those found in pelagic sediments of the Eastern Pacific (Table 6). Further, the Fe-montmorillonite in the North Fiji Basin cores (FFC-8, TC-7) appears to be identical to that found in the Vanuatu archipelagic apron (TC-9, Table 6). These structural formulas must be viewed with some caution, however, because of the residual contamination of minor amounts of clay-sized quartz, kaolinite, plagioclase and associated volcanic glass (Table 5 and Figure 6c). These additional phases would tend to enrich the Al and Si proportions of the smectite, suggesting that it could be more Fe-rich than indicated in Table 6.

Sediment Accumulation Rates

The results of the alpha track autoradiography surveys are presented in Table 7 and Figures 7a and 7b. Figure 7a presents total alpha activity profiles for those cores which, because they were either too short or disturbed, did not display a sufficiently coherent pattern of ^{230}Th decay to attempt a sedimentation rate determination. Surprisingly, these cores include the trigger cores, which were employed on the premise that they would recover the topmost materials relatively undisturbed. Instead, most appear to suffer from the same disturbance problem as the piston cores (see below). Although relatively long, PCOD-9 did not display a coherent ^{230}Th decay pattern. This core (from the Vanuatu archipelagic apron) contains numerous ash layers which violate the primary dating assumption of uniform deposition (McMurtry et al., 1981).

Figure 7b presents the total and excess alpha activity (^{230}Th) profiles for those cores with coherent patterns. Even with these cores, there are some (PCOD-5, PCOD-8, PC-49, PC-50) that display regions of relatively flat or counter (PC-50) activity gradients. For cores PCOD-5, PCOD-8 and PC-49, these regions (down to 150 cm) as well as those for the trigger and free-fall cores (Figure 7a) could be the result of (1) coring disturbance; (2) slumping; (3) deep bioturbation; or (4) ^{226}Ra dif-

Table 5. Semi-quantitative mineralogy of North Fiji Basin sediments, $<2\mu m$[1].

Core no.	Smectite	Plagioclase	Kaolinite	Quartz
FFC-6	43.8	48.2	5.1	2.9
FFC-8	56.1	38.2	4.1	1.6
FFC-9	49.0	43.1	4.1	3.2
TC-5	60.2	27.3	9.4	3.0
TC-6	63.9	30.5	4.9	0.8
TC-7	59.7	29.4	9.5	1.4
TC-8	69.3	24.3	5.0	1.4
TC-9	54.2	39.4	4.7	1.6
FFC-82	67.3	22.0	10.0	0.6
FFC-83	58.5	30.8	9.2	1.5
PC-03[2]	27.3	63.6	5.8	3.3
PC-48	61.9	29.7	7.2	1.2
PC-49	54.6	33.8	9.1	2.6
PC-50	54.2	32.4	12.0	1.3

[1] Relative weight percentage (normalized to the crystalline fraction) based on X-ray diffraction analyses of the carbonate-free (SAAB treated) samples, bulk-powder mounts, and using intensity factors for diagnostic peaks determined from 1:1 mixtures with quartz (Cook et al., 1975).

[2] This sample also contains δ-MnO_2, which does not have an intensity factor. The relative proportions of the minerals determined for this sample are suspected to be diferent from those of one from the same depth interval reported in Tables 1 and 2, which was consumed during chemical analysis.

fusion. For core PC-50, the most reasonable explanation for its counter profile is an inadequate correction for ^{238}U support due to the nature of the excess activity calculation used. For cores PCOD-5, PCOD-8, PC-49 and PC-50, the data from these anomalous regions were excluded from the sedimentation rate determinations (Figure 7b).

As pointed out in a companion paleomagnetism study of the piston cores, paleomagnetic directions are often generally distorted in the topmost 1-3 m (Brocher et al., 1985). These authors suggest that this disturbance is caused by the vacuum of the piston-coring process acting on the watery surficial sediments. This explanation, modified somewhat to include the trigger and free-fall cores studied here, seems more reasonable than widespread recent slumping, deep bioturbation or ^{226}Ra diffusion acting on only a few of the cores. In any case, ^{226}Ra diffusion would be limited in sediments accumulating at rates of 1.0 cm/10^3 years or more (McMurtry et al., 1981). Deep bioturbation, although not totally unreasonable considering the bottom camera evidence (Figure 8) and results of studies elsewhere (McMurtry et al., 1985 and references therein), could not have occurred in the region until recently or there would be no recognizable activity profiles in these sediments over the entire depth interval studied.

Derived sedimentation and sediment accumulation rates are presented in Table 8. Also shown are rates determined from paleomagnetic stratigraphy. Comparison of the sedimentation rates determined from these two completely independent methods indicates that they agree to within 10%, considering their respective errors (Table 8). Note that where paleomagnetism could only provide minimum rate values for cores PCOD-6 and PCOD-8 because the Brunhes-Matuyama boundary was not encountered, the excess ^{230}Th method is able to determine an absolute value; this is one of the advantages of the radiometric technique. Comparison of the respective accumulation rates is even closer because of the added error from the average dry bulk density. Accumulation rate errors range from 8% to 48%, primarily because of the error introduced from the heterogenous lithology of the cores that is in turn reflected in the dry bulk density measurements (Table 8).

Element accumulation rates determined from the average accumulation rates in Table 8 and the chemical composition data in Table 2 are presented in Table 9. Besides the errors extrapolated from the accumulation rates (Table 8) and chemical determinations (Table 2), the element accumulation rates reflect in addition the value from the topmost 0-5 cm of the cores and should therefore only represent the most recent few thousand years of accumulation. If the trigger cores and free-fall cores sampled for chemical determinations are indeed homogenized by coring disturbance, as indicated by their alpha activity profiles, these data may, however, reflect element accumulations over even longer periods (about 30 to 150 thousand years, Figures 7a and 7b).

Selected accumulation rate patterns are superimposed upon the recent tectonic configuration of the detailed survey area (Kroenke et al., this volume) in Figure 9. The noncarbonate, carbonate, Fe and Mn patterns all display high rates of accumulation in the southwest corner of the survey area (TC-6 and PCOD-6), which is interpreted by Eade and Gregory (this volume) and Kroenke et al. (this volume) to represent the eastern border of the Vanuatu archipelagic apron. A second area of high accumulation rates is located in the north central survey area (Figure 9). This area, which contains the highest carbonate accumulation rates, coincides with the South Pandora Ridge and the northern extension of the central North Fiji Basin spreading center. Like Fe, the Cu, Cr, Co, Ni, Ti, Zn, Mg, Al, Si, K and Ca accumulation rate patterns (not shown) resemble that of noncarbonate material (Figure 9a and 9b), indicating similar patterns of iron oxide, smectite and detrital (ash) accumulation for this region. Cadmium and lead accumulation patterns are similar to the car-

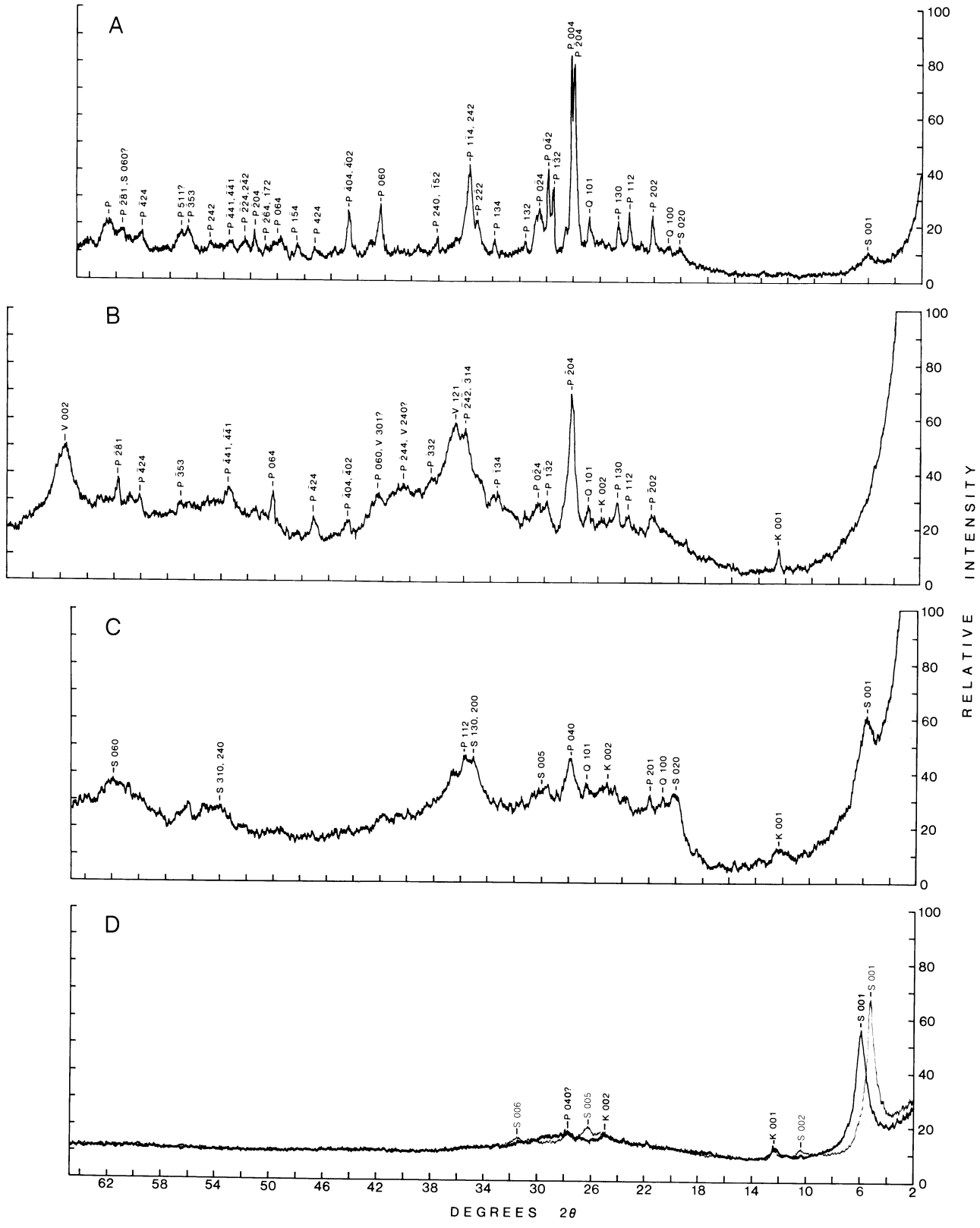

Figure 6. X-ray diffraction patterns of selected samples as bulk powder and oriented mounts. CuKα radiation, scan speed of 2° 2θ /min. (a) KK71-PC48, >2-μm, bulk; (b) KK72-PC3, >2-μm, bulk; (c) KK82-TC7, <2-μm, CBD-treated, bulk; (d) KK82-TC9, <2-μm, CBD-treated, oriented. Light trace after 48-hour exposure to ethylene glycol. S = smectite; K = kaolinite; P = plagioclase; Q = quartz; V = vernadite (δ-MnO_2).

Table 6. Atomic proportions and site occupancy of North Fiji Basin smectites[1].

		FFC-8 CBD[3]	TC-7 CBD	TC-9 CBD	Galapagos Mounds[2] Fe-Mont.	Galapagos Mounds[2] Nontronite	Loihi 20-2G CBD
Oxides Wt.%	Na_2O	1.31	1.99	3.73	0.41	0.16	2.00
	K_2O	0.79	0.89	1.82	0.93	2.43	0.61
	CaO	2.85	1.11	2.81	2.55	0.78	1.04
	MgO	3.06	2.91	3.09	2.73	3.13	2.94
	Al_2O_3	17.9	16.8	16.4	11.4	1.06	2.71
	SiO_2	53.9	53.4	52.2	60.0	52.8	56.6
	Fe_2O_3	7.76	9.64	7.82	7.39	27.4	25.5
	MnO	0.45	0.24	0.11	0.26	0.32	0.04
	TiO_2	1.24	1.19	0.79	0.39	0.10	0.76
	Subtotal	89.3	88.8	88.8	86.1	88.2	92.2
Tetrahedral	Si^{4+}	7.41	7.44	7.37	7.99	7.96	7.99
	Al^{3+}	0.59	0.56	0.63	0.01	0.04	0.01
	Fe^{3+}						
		8.00	8.00	8.00	8.00	8.00	8.00
Octahedral	Al^{3+}	2.33	2.20	2.10	2.17	0.15	0.44
	Fe^{3+}	0.79	1.00	0.83	0.90	3.10	2.71
	Ti^{4+}	0.13	0.13	0.08	0.05	0.01	0.08
	Mg^{2+}	0.63	0.60	0.65	0.66	0.70	0.62
		3.88	3.93	3.66	3.78	3.96	3.85
Interlayer	Ca^{2+}	0.42	0.25	0.43	0.44	0.13	0.16
	Mg^{2+}						
	Mn^{2+}	0.04	0.02	0.01	0.04	0.04	0.01
	Na^{+}	0.35	0.53	1.02	0.13	0.05	0.55
	K^{+}	0.17	0.16	0.33	0.19	0.47	0.11
		0.98	0.90	1.79	0.80	0.69	0.83
Layer Charge		1.45	1.23	2.22	1.28	0.85	1.00
Interlayer		1.44	1.24	2.23	1.28	0.86	1.00

[1] Calculated on the basis of 20 oxygens and 4 hydroxyls per formula unit and assuming all Fe as Fe^{3+}.

[2] Galapagos Mounds average nontronite and Fe-montmorillonite, SAAB and CBD treated, $< 0.2\,\mu m$. The Fe-montmorillonite has been corrected for an average of 11% amorphous silica as a contaminant (McMurtry et al., 1983). Loihi Seamount Al-nontronite, CBD treated, $< 75\,\mu m$ from DeCarlo et al. (1983).

[3] Data calculated by difference from $< 2\,\mu m$, carbonate-free and CBD extracted values (Tables 2 and 4). Na values calculated from $2\,\mu m$, carbonate-free analyses, assuming no CBD extraction.

bonate accumulation rate pattern (Figure 9c), which is consistent with the phase partitioning results (Figure 3). Arsenic shows a similar accumulation rate pattern to that of manganese (Figure 9d), which displays a northern shift of the second high accumulation area toward the South Pandora Ridge. Rapid manganese and arsenic accumulation rates are indicators of recent metalliferous sediments and active hydrothermal systems (McMurtry et al., 1981; Marchig et al., 1982).

The highest metal accumulation rates for the North Fiji Basin sediments listed in Table 9 represent an area that is probably receiving a large contribution of detrital material from the Vanuatu island arc (Figure 1). In order to estimate the various contributions of detrital, authigenic and hydrothermal material to this area, the following Mn flux calculation is made:

$$[\text{Mn flux}]_{\text{total}} = [\text{Mn flux}]_{\text{detrital}} + [\text{Mn flux}]_{\text{authigenic}} + [\text{Mn flux}]_{\text{hydrothermal}} \quad (3)$$

where

$$[\text{Mn flux}]_{\text{detrital}} = [\text{Mn/Al}]_{\text{ash}} \cdot [\text{Al flux}],$$

$$[\text{Mn/Al}]_{\text{ash}} = 0.016 \text{ (from TC9 } > 2\text{-}\mu\text{m, Table 2)},$$

and

$$[\text{Mn flux}]_{\text{authigenic}} = 1.0 \text{ (from values listed in Table 10)}.$$

Table 7. Alpha track autoradiography results for North Fiji Basin sediments.

Depth (cm)	Total[1] activity (tracks/ cm^2 day)	Excess[2] activity (tracks/ cm^2 day)	Depth (cm)	Total activity (tracks/ cm^2 day)	Excess activity (tracks/ cm^2 day)	Depth (cm)	Total activity (tracks/ cm^2 day)	Excess activity (tracks/ cm^2 day)
	KK82-FFC-6			KK82-TC-5			KK82-TC-8	
0-3	12±1		0-3	113±3		0-3	31±2	
3-6	10±1		3-6	106±3		3-6	40±2	
10-13	9±1		10-13	95±3		10-13	42±2	
17-20	8±1		17-20	52±2		17-20	60±2	
23-26	8±1		23-26	55±2		23-26	67±2	
30-33	5.8±0.8		30-33	60±2		29-32	43±2	
40-43	6.7±0.8		40-43	62±3		35-38	42±2	
50-53	21±1		50-53	39±2		41-44	38±2	
70-73	16±1		60-63	33±2		47-50	39±2	
90-93	8±1		66-69	48±2		53-56	45±2	
	KK82-FFC-8			KK82-TC-6			KK82-PCOD-5	
0-3	51±2		0-3	14±1		0-3	59±2	58±2
3-6	56±2		3-6	43±2		10-13	88±3	87±3
10-13	49±2		6-9	31±2		20-23	55±2	54±2
17-20	41±2		10-13	39±2		30-33	48±2	47±2
23-26	40±2		17-20	45±2		40-43	89±3	88±3
30-33	26±2		23-26	37±2		60-63	32±2	31±2
40-43	31±2		30-33	31±2		80-83	49±2	48±2
50-53	28±2		35-38	18±1		100-103	32±2	32±2
70-73	33±2		40-43	37±2		120-123	47±2	46±2
90-93	28±2		45-48	26±2		140-143	9±1	8±1
						180-183	48±2	48±2
						220-223	55±2	54±2
	KK82-FFC-9			KK82-TC-7		260-263	28±2	27±2
						360-363	15±1	14±1
0-3	18±1		0-3	99±3		460-463	7±1	6±1
3-6	17±1		3-6	63±3		560-563	2.9±0.5	1.9±0.7
10-13	17±1		6-9	56±2		660-663	2.5±0.5	1.5±0.7
17-20	17±1		9-12	66±3		760-763	0.8±0.3	
23-26	27±2		12-15	60±2		860-863	1.1±0.3	
30-33	24±2		15-18	57±2		963-966	1.1±0.3	
40-43	15±1		18-21	48±2				
50-53	33±2		25-27	33±2				
70-73	26±2		27-30	23±2				
90-93	17±1		30-33	36±2				

(Table continues)

[1]Reflects total alpha activity of ^{230}Th, ^{238}U, and their daughters, assuming secular equilibrium.
[2]Excess alpha activity of ^{230}Th and its daughters after correction for ^{238}U support.

Depth (cm)	Total[1] activity (tracks/ cm^2 day)	Excess[2] activity (tracks/ cm^2 day)	Depth (cm)	Total activity (tracks/ cm^2 day)	Excess activity (tracks/ cm^2 day)	Depth (cm)	Total activity (tracks/ cm^2 day)	Excess activity (tracks/ cm^2 day)

(Table continues)

KK82-PCOD-6			KK2-PCOD-8			KK82-PCOD-9		
0-3	27±2	25±2	0-3	66±3	64±3	0-3	9±1	
10-13	33±2	31±2	10-13	45±2	43±2	10-13	4.6±0.7	
20-23	34±2	32±2	20-23	43±2	41±2	20-23	10±1	
30-33	32±2	30±2	30-33	59±2	58±2	30-33	6.8±0.8	
40-43	31±2	28±2	40-43	77±3	75±3	40-43	7.6±0.8	
60-63	30±2	28±2	60-63	16±1	14±1	60-63	17±1	
80-83	46±2	44±2	80-83	61±2	60±2	80-83	7.3±0.8	
100-103	50±2	47±2	100-103	40±2	38±2	100-103	12±1	
120-123	32±2	29±2	120-123	34±2	32±2	120-123	6.4±0.8	
140-143	20±1	18±1	180-183	58±2	56±2	140-143	7.0±0.8	
220-223	27±2	25±2	220-223	38±2	36±2	160-163	4.3±0.6	
260-263	16±1	14±1	260-263	50±2	48±2	180-183	7.6±0.8	
363-366	4.8±0.7	2.6±0.8	300-303	23±2	21±2	200-203	12±1	
461-464	10±1	7±1	340-343	22±1	20±2	220-223	10±1	
560-563	5.2±0.7	3.0±0.8	380-383	18±1	16±1	240-243	4.2±0.6	
660-663	4.1±0.6	2.0±0.8	420-423	18±1	16±1	260-263	4.4±0.6	
760-763	4.6±0.6	2.4±0.8	520-523	6.6±0.8	5±1	300-303	5.1±0.7	
860-863	2.2±0.4		620-623	4.0±0.6	2.1±0.8	340-343	8.7±0.9	
957-960	5.0±0.7	2.8±0.8	720-723	1.9±0.4		380-383	2.2±0.5	
						419-422	2.9±0.5	

KK82-PCOD-7			KK71-FFC-82		KK71-FFC-83	
3-6	57±2	55±2	0-3	27±2	8-11	19±2
6-9	67±2	65±2	3-6	20±2	12-15	13±1
10-13	69±2	66±2	6-9	19±2	16-19	18±2
20-23	53±2	51±2	13-15	22±2	19-22	16±1
30-33	56±2	54±2	16-19	17±1	22-24.5	20±2
40-43	48±2	46±2	20-22	17±1	29-32	23±2
60-63	43±2	41±2	24-26.5	19±2	36.5-40	19±2
80-83	36±2	34±2	28-30	16±1	50-53	17±2
100-103	28±2	26±2	32-35	22±2	62-65	15±1
120-123	31±2	28±2	39-41.5	16±1	76–79	21±2
140-143	44±2	42±2				
180-183	41±2	38±2				
220-223	7.5±0.8	5±1				
260-263	19±1	17±1				
300-303	12±1	10±1				
340-343	7.8±0.8	6±1				
380-383	8.3±0.8	6±1				
420-423	4.6±0.6	2.3±0.9				
520-523	3.3±0.5	1.0±0.8				
620-623	2.1±0.4					
720-723	2.4±0.4					

(Table continues)

Depth (cm)	Total[1] activity (tracks/ cm^2 day)	Excess[2] activity (tracks/ cm^2 day)	Depth (cm)	Total activity (tracks/ cm^2 day)	Excess activity (tracks/ cm^2 day)	Depth (cm)	Total activity (tracks/ cm^2 day)	Excess activity (tracks/ cm^2 day)
			(Table continues)					
	KK71-PC-48			KK71-PC-49			KK71-PC-50	
3-6	25±2	22±2	0-3	39±2	35±2	11-13	29±2	26±2
6-9	27±2	25±2	3-6	34±2	30±2	15-17	24±2	20±2
9-12	23±2	21±2	11-14	22±2	19±2	20-23	17±1	14±2
19-21	11±1	9±1	14-17	33±2	30±2	25-28	16±1	12±2
29-32	26±2	24±2	23-25	28±2	24±2	30-33	11±1	8±2
39-42	26±2	24±2	37-40	29±2	25±2	35-38	7±1	4±2
59-62	23±2	21±2	65-68	31±2	27±2	40-43	8±1	5±2
81-83	8±1	6±1	75-78	45±2	41±2	45-48	7±1	4±2
97-100	7±1	4±1	85-88	26±2	22±2	50-53	4.7±0.8	1±1
120-123	6±1	4±1	95-98	28±2	24±2	60-63	5.0±0.8	2±1
140-143	6±1	3±1	115-118	40±2	37±2	70-73	6±1	2±1
180-183	3.7±0.7	1±1	135-138	39±2	35±2	80-83	7±1	3±1
220-223	6±1	4±1	155-158	32±2	28±2	90-93	7±1	4±2
258-261	4.7±0.8	2±1	175-178	34±2	30±2	100-103	16±1	12±2
310-313	4.2±0.7	2±1	195-198	26±2	23±2	110-113	3.5±0.6	0.2±1.3
360-363	4.4±0.7	2±1	230-233	17±1	13±2	120-123	4.2±0.7	0.9±1.4
460-463	5±1	2±1	260-263	13±1	9±1	130-133	4.0±0.7	0.7±1.3
560-563	2.4±0.6		290-293	8±1	5±1	140-143	3.1±0.6	
648-651	2.9±0.6		320-323	5.4±0.8	2±1	152-155	3.2±0.6	
			347-350	3.8±0.7		160-163	3.7±0.7	

Therefore, for TC-6,

$$4.1 = (0.016)(79) + 1.0 + [\text{Mn flux}]_{\text{hydrothermal}}$$

$$[\text{Mn flux}]_{\text{hydrothermal}} = 4.1 - (1.3 + 1.0) = 1.8.$$

The relative contributions of detrital, authigenic and hydrothermal material to TC-6 are 32, 24 and 44%, respectively.

For the second highest Mn accumulation site, TC-7, the Mn flux calculations yield the following:

$$2.6 = (0.016)(12) + 1.0 + [\text{Mn flux}]_{\text{hydrothermal}}$$

$$[\text{Mn flux}]\text{hydrothermal} = 2.6 - (0.2 + 1.0) = 1.4.$$

The relative contributions of detrital, authigenic and hydrothermal material to TC-7 are 8, 38 and 54%, respectively. The above calculations, which are based solely on the Mn flux, are in generally good agreement with the relative contributions of these sources to TC-6 and TC-7 estimated from the multivariate factor analysis presented next.

Multivariate Factor Analysis

Multivariate factor analysis has been very successful in deconvoluting major sources or endmembers from large elemental/sample data sets in geochemical studies of Pacific pelagic sediments (Heath and Dymond, 1977; Leinen and Stakes, 1979; Dymond, 1981; McMurtry et al., 1981). In order to extract information on major sources underlying the variability in the North Fiji Basin major and minor elemental data, Q-mode factor analysis was performed on two separate data matrices representing samples from the >2-μm and <2-μm fractions. We employed a program developed by Klovan and Imbrie (1971) for this analysis utilizing a cosine theta coefficient (Imbrie and Purdy, 1962) as a measure of proportional similarity between sample vectors.

>2-μm Fraction

Three varimax factors extracted and rotated from the data matrix of the >2-μm fraction (14 samples by 18

Figure 7a

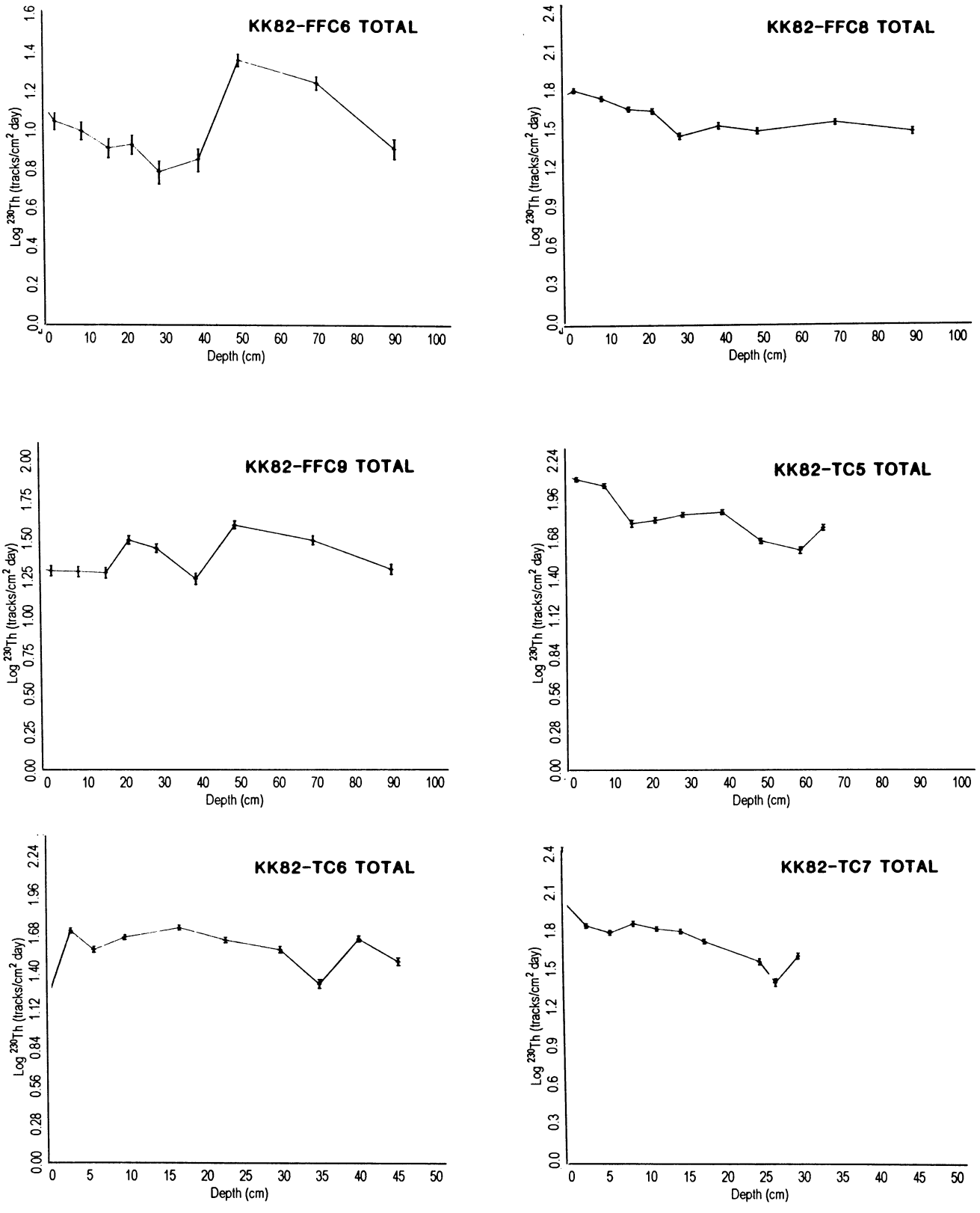

Figure 7. (a) Plots of log[total ^{230}Th activity] versus core depth for those cores that do not display coherent decay profiles. (b) Plots of log[total ^{230}Th activity] versus core depth (left) and log[excess ^{230}Th activity] versus core depth (right) for those cores that display coherent decay profiles. Errors are based on counting statistics ($\pm 1\sigma$). Sedimentation rates determined from slope of least-squares linear fit. All connected data rejected (see text).

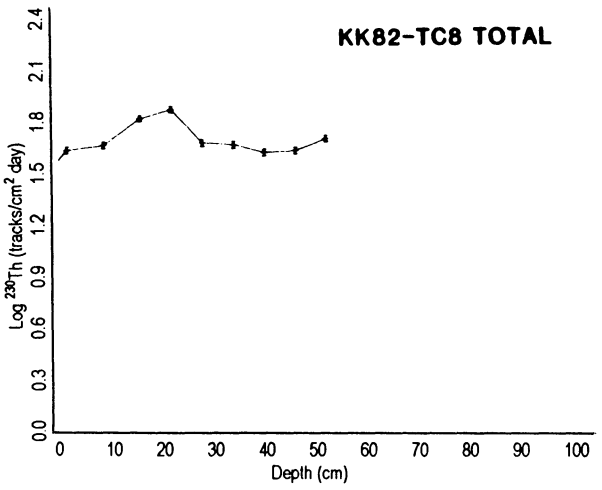
KK82-TC8 TOTAL
Log 230Th (tracks/cm2 day)
Depth (cm)

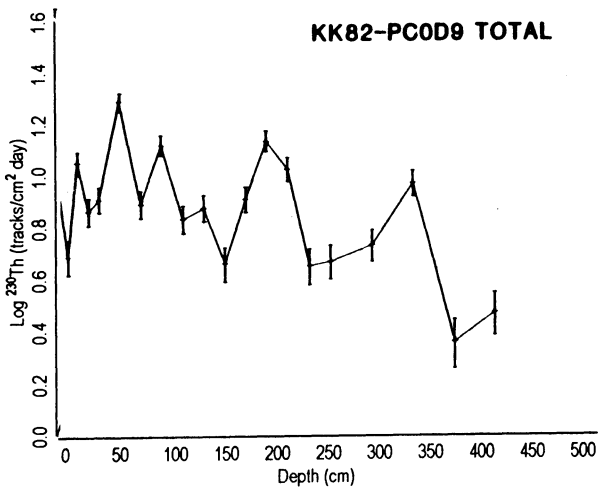
KK82-PC0D9 TOTAL
Log 230Th (tracks/cm2 day)
Depth (cm)

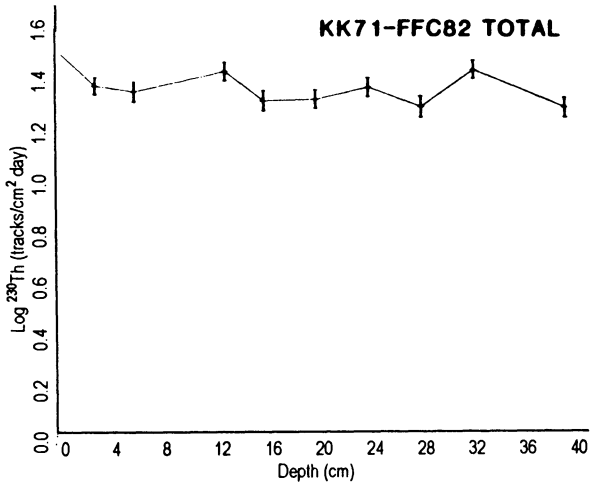
KK71-FFC82 TOTAL
Log 230Th (tracks/cm2 day)
Depth (cm)

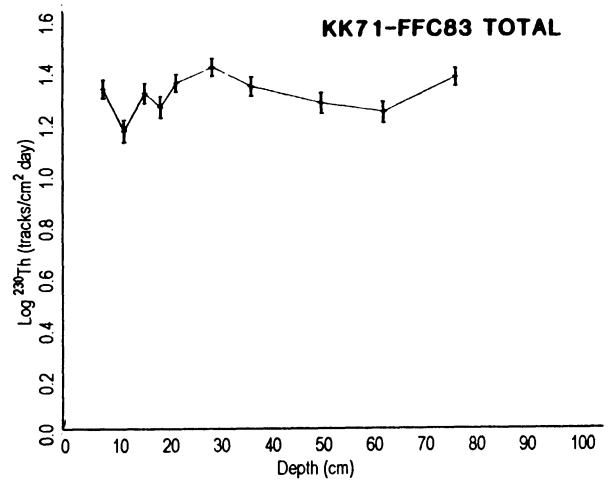
KK71-FFC83 TOTAL
Log 230Th (tracks/cm2 day)
Depth (cm)

Figure 7b

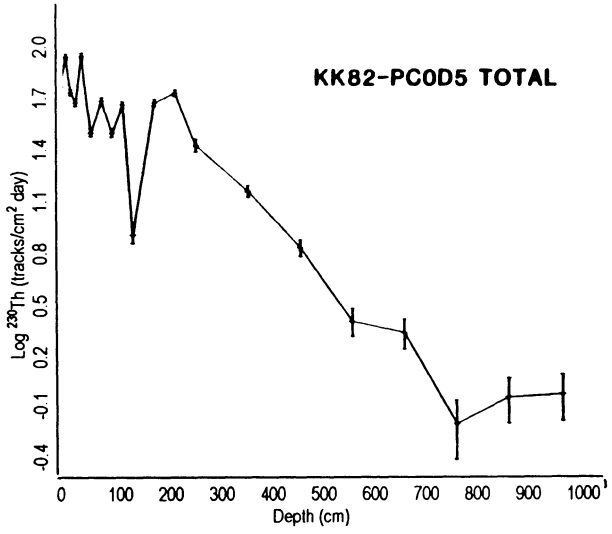
KK82-PC0D5 TOTAL
Log 230Th (tracks/cm2 day)
Depth (cm)

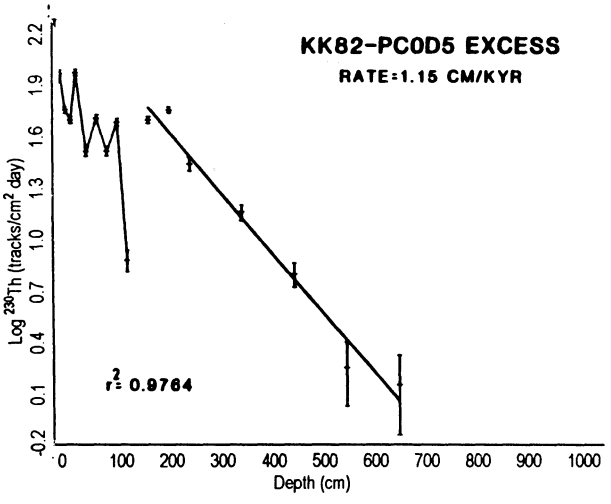
KK82-PC0D5 EXCESS
RATE=1.15 CM/KYR
r2= 0.9764
Log 230Th (tracks/cm2 day)
Depth (cm)

Figure 7b. (continued)

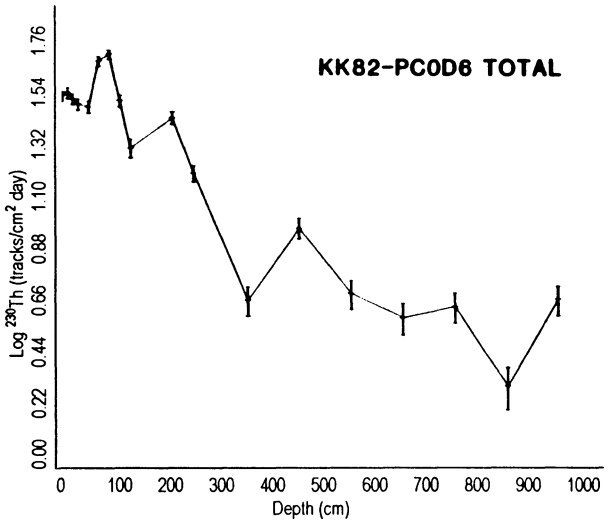

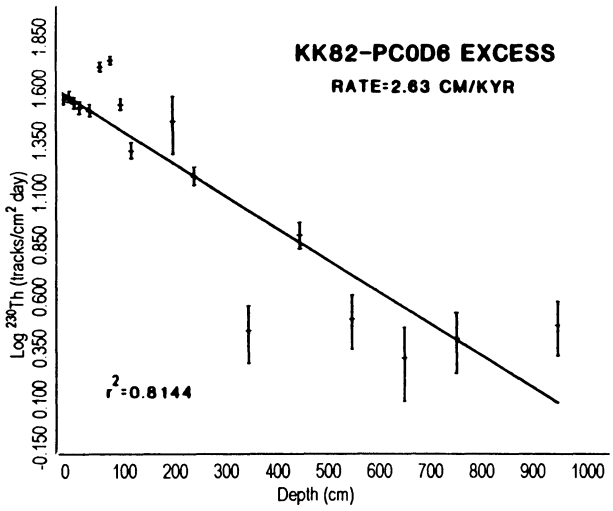

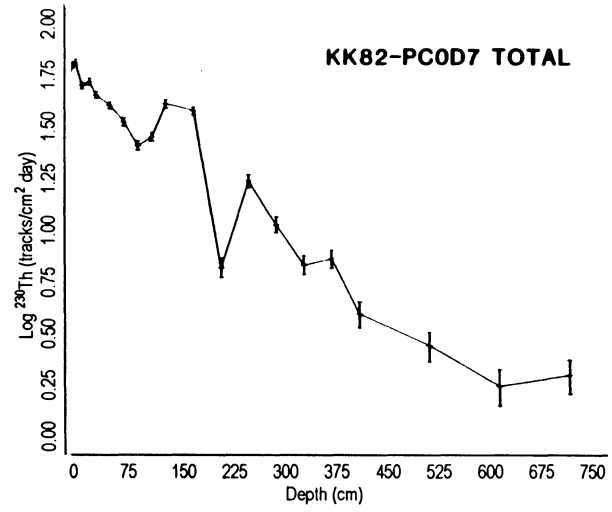

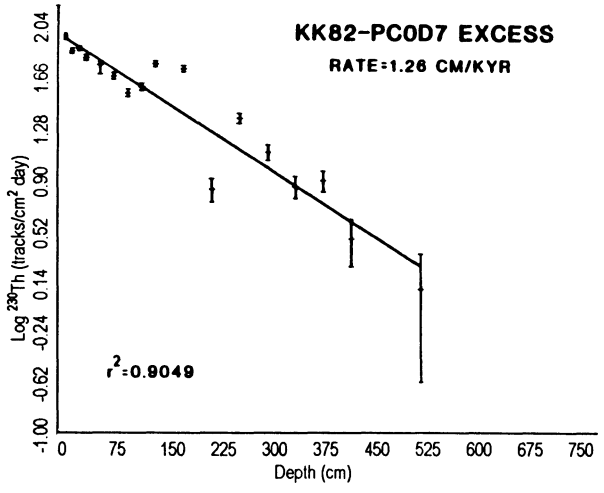

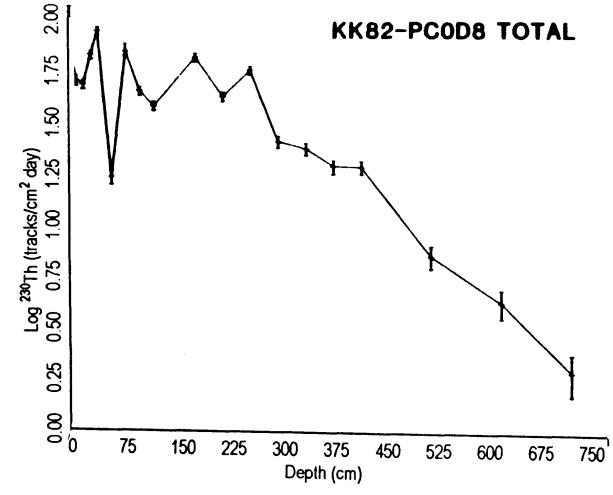

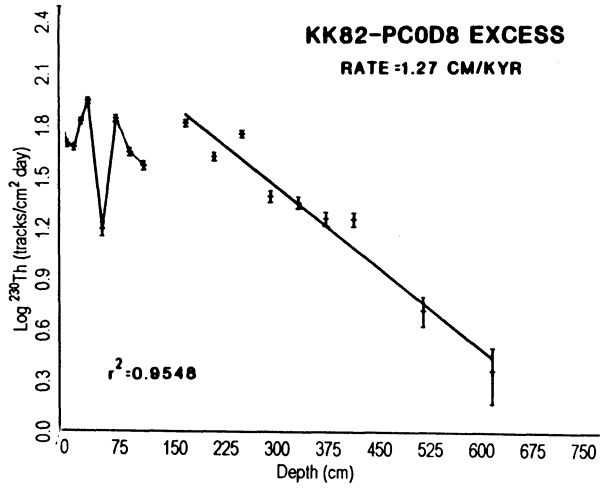

Figure 7b. (continued)

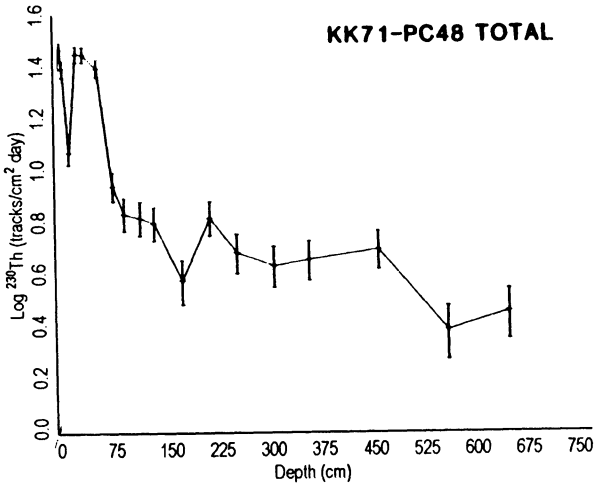

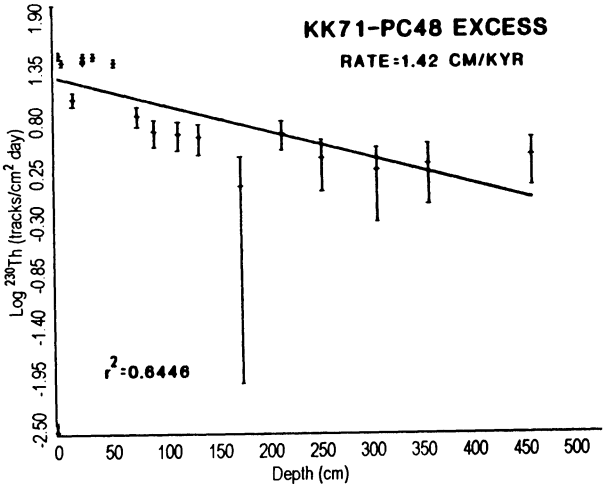

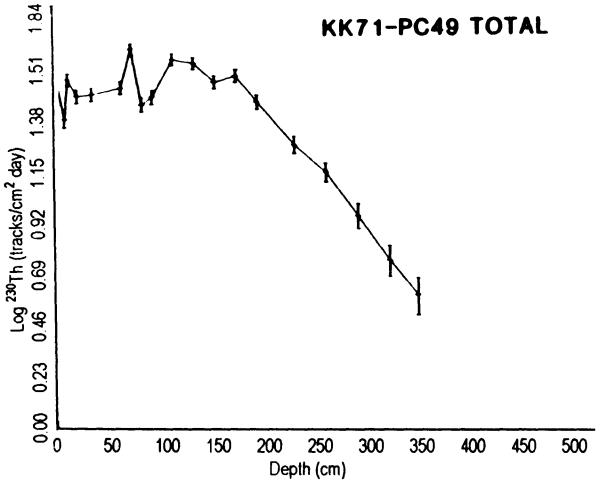

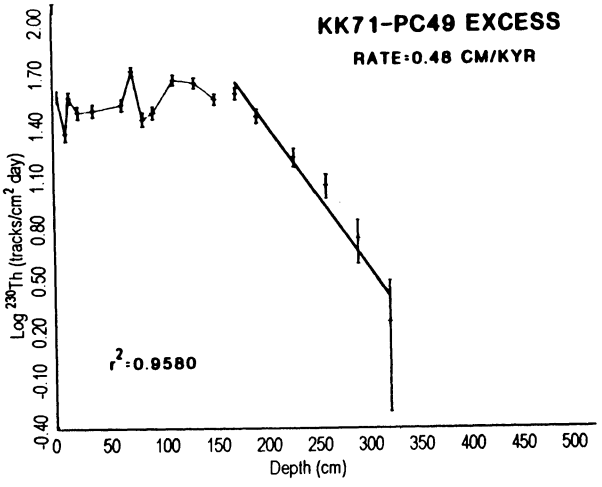

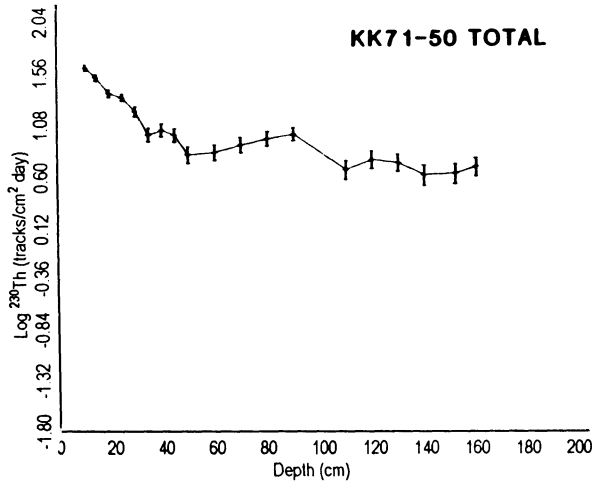

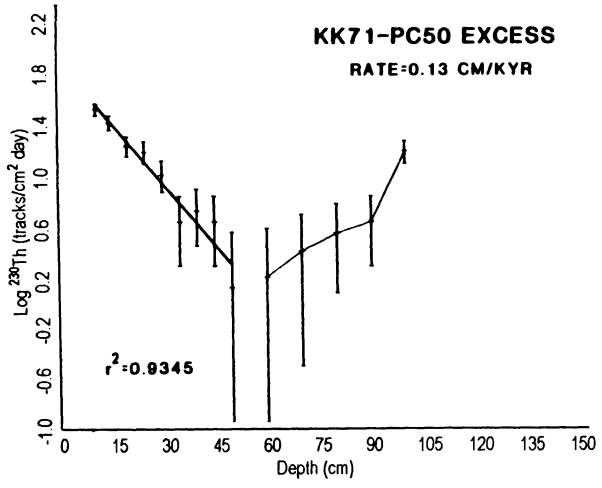

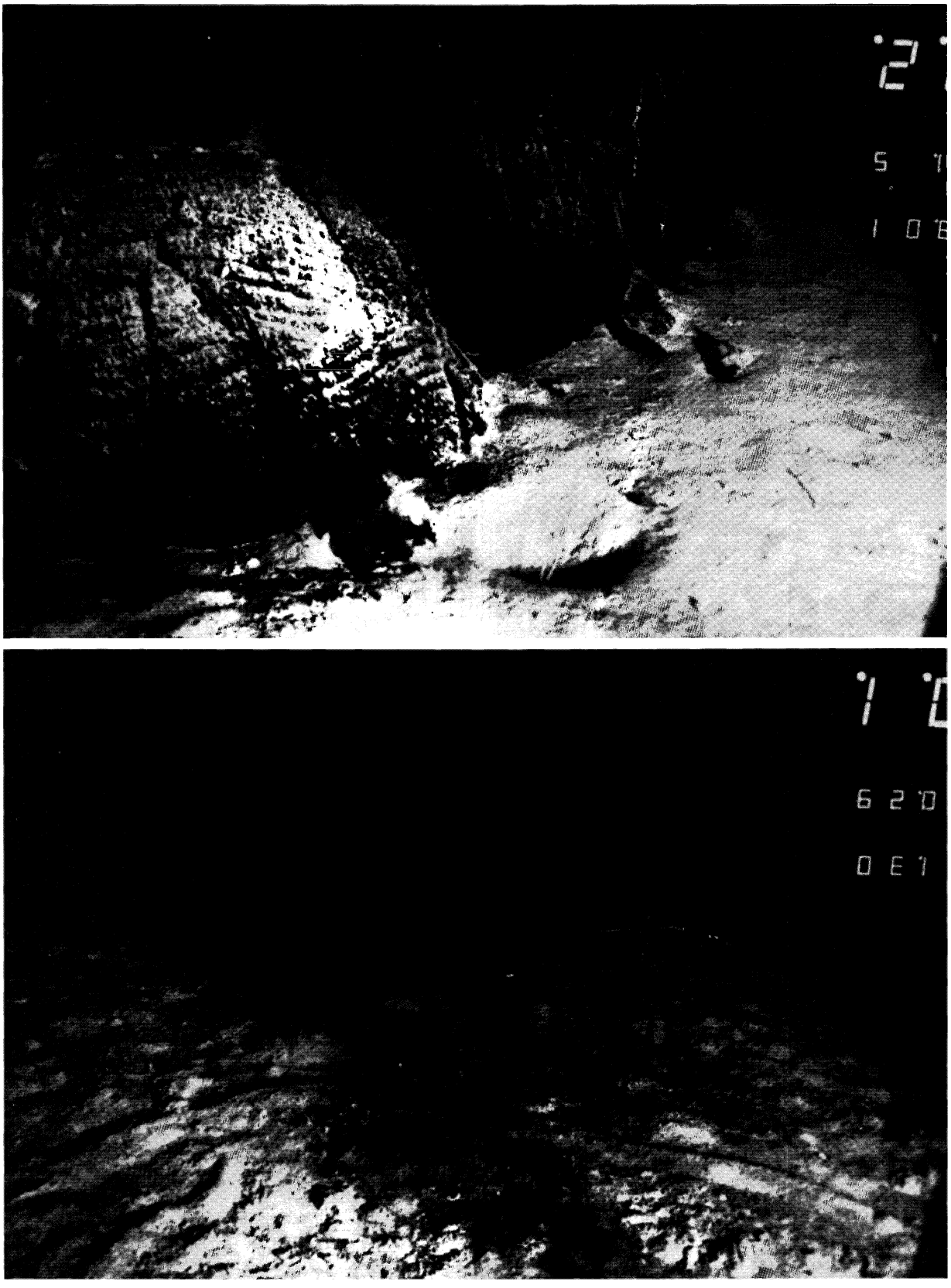

Figure 8. (top) Bottom photograph from station KK82-BC2 on the South Pandora Ridge (formerly called Hazel-Holme Fracture Zone) (Figure 2), showing fresh pillow basalts contacting pelagic sediment. Note burrow of unidentified benthic organism in foreground. (bottom) Bottom photograph from station KK82-BC1 (Figure 2) showing typical sediment cover for this region and evidence of intensive burrowing activity on the sediment surface.

Table 8. Sediment accumulation rates.

Core identification	Sedimentation rate ($cm/10^3$ yr)		Dry bulk density[1] (g/cm^3)	Accumulation rate ($g/cm^2/10^3$ yr)	
	$^{230}Th_{ex}$	Paleomagnetism[2]		$^{230}Th_{ex}$	Paleomagnetism[2]
KK82-PCOD-5	1.15 ± 0.08[3]	1.37 ± 0.06	0.64 ± 0.10 (n = 18)	0.74 ± 0.10	0.88 ± 0.11
KK82-PCOD-6	2.63 ± 0.35	>1.37	0.63 ± 0.33 (n = 20)	1.66 ± 0.80	>0.86
KK82-PCOD-7	1.26 ± 0.10	1.09 ± 0.07	0.66 ± 0.05 (n = 16)	0.83± 0.09	0.72 ± 0.06
KK82-PCOD-8	1.27 ± 0.12	>1.14	0.69 ± 0.08 (n = 17)	0.88 ± 0.12	>0.79
KK71-PC-48	1.42 ± 0.05	--	0.82 ±0.07 (n = 14)	1.16 ± 0.10	--
KK71-PC-49	0.48 ± 0.05	--	0.75 ± 0.07 (n = 8)	0.36 ± 0.03	--
KK71-PC-50	0.13 ± 0.02	--	0.80 ± 0.09 (n = 4)	0.10 ± 0.01	

[1] Average dry bulk densities calculated from measured weight/volume ratios. N = number of determinations at 50-cm intervals down core. All samples dried at 110°C for minimum of 24 hours.

[2] Rates calculated from core length and age determined from presence of Brunhes-Matuyama boundary. Rates for PCOD-6 and PCOD-8 are minimum values because Brunhes-Matuyama boundary was not encountered (Brocher et al., 1985).

[3] Sedimentation rate errors estimated from standard deviation of slope of best fit ($\pm 1\sigma$). Paleomagnetism errors estimated as ±50 cm of Brunhes-Matuyama boundary (Brocher et al., 1985).

elements) together account for 99% of the elemental variability. Scaled varimax scores for the three factors are presented in Figure 10a. Normalized factor components (Klovan, 1966) calculated from the varimax factor loadings are plotted in Figure 11. The high scores of Cr, Mg, Li, Ca, Al, Si and Fe on factor 1 (SF1) (56% of the variance) are suggestive of a smectite or its precursor material. X-ray diffraction analysis of sample PC-48, which plots closest to this factor in Figure 11, reveals that it indeed contains relatively abundant smectite in the >2-μm fraction (Figure 6a). The smectite may represent aggregates that did not separate from the >2-μm fraction during centrifugation. Smectite aggregations are known to form in metalliferous sediments (Dymond and Eklund, 1978). The high scores of K, Na, Si and Al on factor 2 (SF2) (35% of the variance) suggest a volcanic glass or ash/hyaloclastite source. Samples FFC-83 and TC-9, which plot closest to this factor in Figure 11, are very rich in volcanic glass. Except for sample PC-3, all samples in this size fraction plot along the base of the triangular diagram, showing a linear mixing trend of aggregated smectite and volcanic ash. Factor 3 (SF3) (accounting for only 8% of the elemental variation) shows high scores on the following group of elements: Mn, Zn, Pb, As, Cd, Co, Ni, Fe, Ti and Cu, in order of decreasing importance. Sample PC-3 plots closest to this factor (Figure 11). Visual inspection of core PC-3, and the mineralogy and chemistry of it reported here and elsewhere (McMurtry and Kim, unpublished data), lead us to conclude that factor 3 represents hydrothermal material.

<2-μm Fraction

Three varimax factors extracted from the data matrix of the <2-μm fraction (14 samples by 18 elements) together account for 92% of the elemental variability. Scaled varimax scores for the three factors are presented in Figure 10b. Factor 1 (CF1), accounting for 36% of the variance, is characterized by high scores on Ti, Cu, Cd, Pb, Mn, Fe, As and Co. This factor is similar to SF3, representing a hydrothermal contribution to these sediments. The high score on Ti for this factor and for SF3 is surprising, as this element and its oxide (rutile) are commonly associated with alumino-silicate detritus. However, Ti is also suggested to be incorporated within ferromanganese oxides (Aplin and Cronan, 1985). Factor 2 (CF2) (34% of the variance) displays high scores

Table 9. Element accumulation rates.

Accumulating element	Core identification TC-5	TC-6	TC-7	TC-8	PC-48	PC-49	PC-50
	rates in $mg/cm^2/10^3yr$						
$CaCO_3$	569	677	663	745	897	302	48
Non-$CaCO_3$	164	967	169	131	273	59	56
Na	2.6	20	2.2	20	3.3	0.9	1.1
K	1.3	12	1.1	0.9	2.0	0.3	0.7
Ca	6	53	5.8	5.3	11	2.1	2.4
Mg	3	25	4.2	3.5	5	1.2	1
Al	12	79	12	11	20	5	5
Si	74	434	72	56	115	26	28
Fe	15	77	17	12	35	5	3.8
Mn	2.3	4.1	2.6	1.5	1.8	0.6	0.2
	rates in $\mu g/cm^2/10^3yr$						
Ti	0.9	5.3	0.9	0.8	1.3	0.3	0.2
Cu	79	273	90	68	110	32	11
Ni	32	105	35	31	56	16	5
Zn	46	138	42	32	76	16	8
Pb	36	58	44	77	63	20	4
Co	18	74	23	19	30	9	3
Cr	12	56	15	12	32	6	3
Cd	2.1	2.8	2.2	3.4	3.2	1.0	0.2
As	4.5	8.1	4.6	2.5	3.9	1.7	0.7
Li	28	20	6.2	7	9	2.8	1

on Li, Si, Cr, Pb, Al, Ca, Zn and Fe. These elements are similar to the grouping for SF1, which is interpreted to represent a smectite or authigenic factor. Factor 3 (CF3) (22% of the variance) is characterized by high scores on Na, Mg, Al, Si, K and Ca. This factor is similar to SF2, which represents ash/hyaloclastite or detrital material.

On the basis of their similarity in elemental groupings, normalized factor components for the <2-μm fraction are plotted as overlap in Figure 11 such that factors from the <2-μm fraction (CF's) are placed on the same apex as the factors from the >2-μm fraction (SF's). By this manipulation, which neglects the order of importance of the factor scores in the respective groupings, we are able to identify endmember samples and use their chemical and mineralogical composition to help interpret the geochemical meaning of these factors in the same way as was performed above for the >2-μm fraction. Sample PC-3 and a group of samples from near the South Pandora Ridge (FFC-8, TC-5, TC-7, TC-8 and FFC-9) plot closest to CF1. The chemistry and mineralogy of the <2-μm fraction of PC-3 together with the high Mn and As accumulation rates for TC-5 and TC-7 (Table 9) reinforce the interpretation of CF1 as a hydrothermal factor. Factor 2 (CF2) is most closely represented by samples PC-49 and PC-50. Although CF2 is interpreted from its elemental scores to represent smectite or authigenic material, these samples do not display an unusually large abundance of smectite in the <2-μm fraction (Table 5). Because all <2-μm fraction samples contain significant amounts of smectite in the crystalline portion, this factor may be resolving a chemical endmember, possibly noncrystalline, that is not apparent in the clay mineralogy. Alternatively, the CF2 factor may represent smectite that is relatively free of amorphous hydrothermal and detrital (volcanic glass) material, or the abundance values reported in Table 5 may be in error. More work will be needed to resolve the geochemical significance of this factor. Factor 3 (CF3) is most closely represented by sample TC-9, which is from an ash-rich core on the Vanuatu archipelagic apron. As with SF2, this factor represents detrital or ash contributions to these sediments.

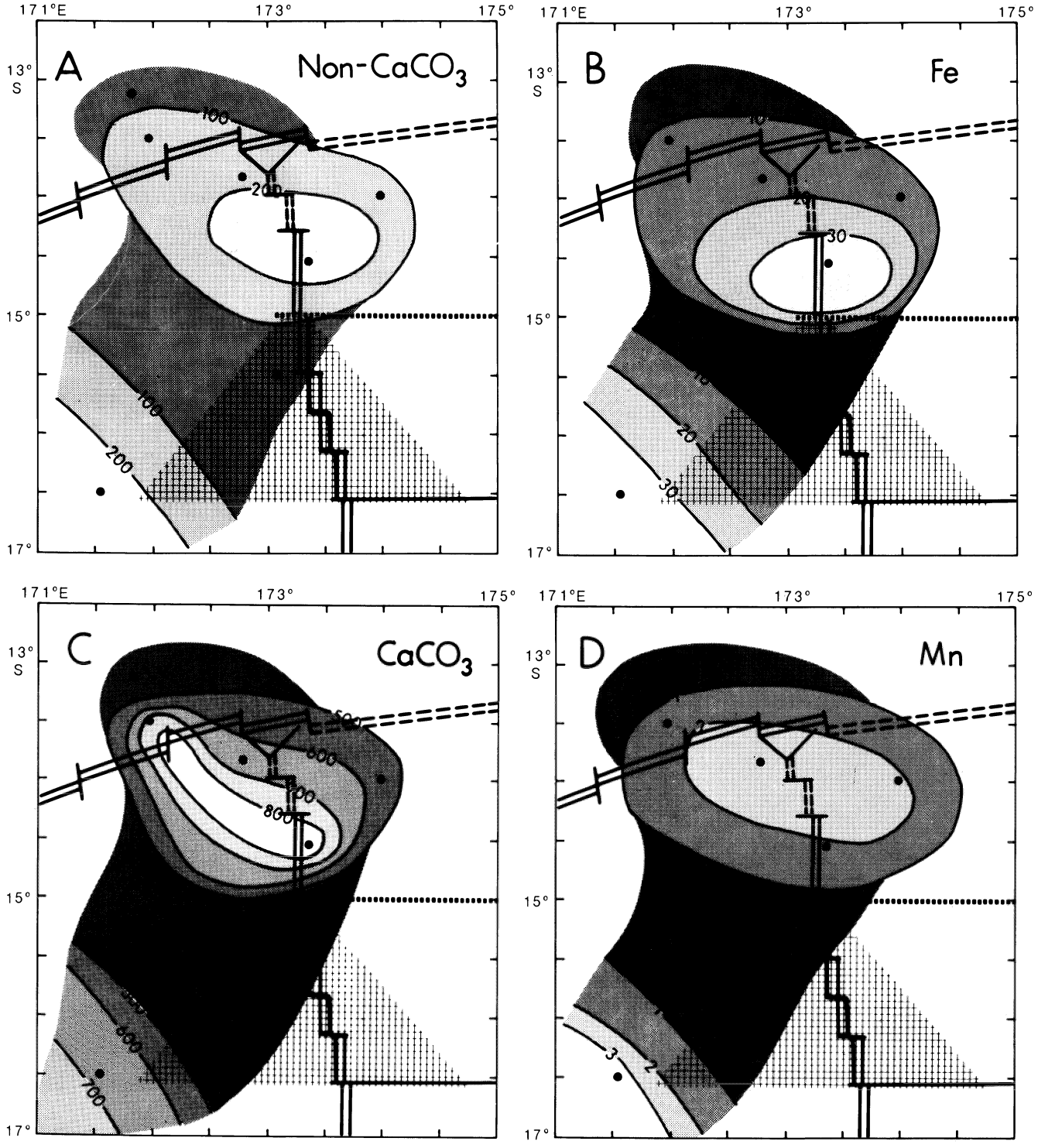

Figure 9. (a) Noncarbonate sediment accumulation rate pattern in units of mg/cm^{2}10^3 years. (b) Fe accumulation rate pattern in units of mg/cm^{2}10^3 years. Fe, Cu, Co, Cr, Ni, Ti, Zn, Mg, Al, Si, K and Ca (carbonate-free) display patterns similar to the noncarbonate sediment accumulation. (c) Carbonate accumulation rate pattern in units of mg/cm^{2}10^3 years. Cd and Pb show similar accumulation rate patterns. (d) Mn accumulation rate pattern in units of mg/cm^{2}10^3 years. Arsenic shows a similar accumulation rate pattern.

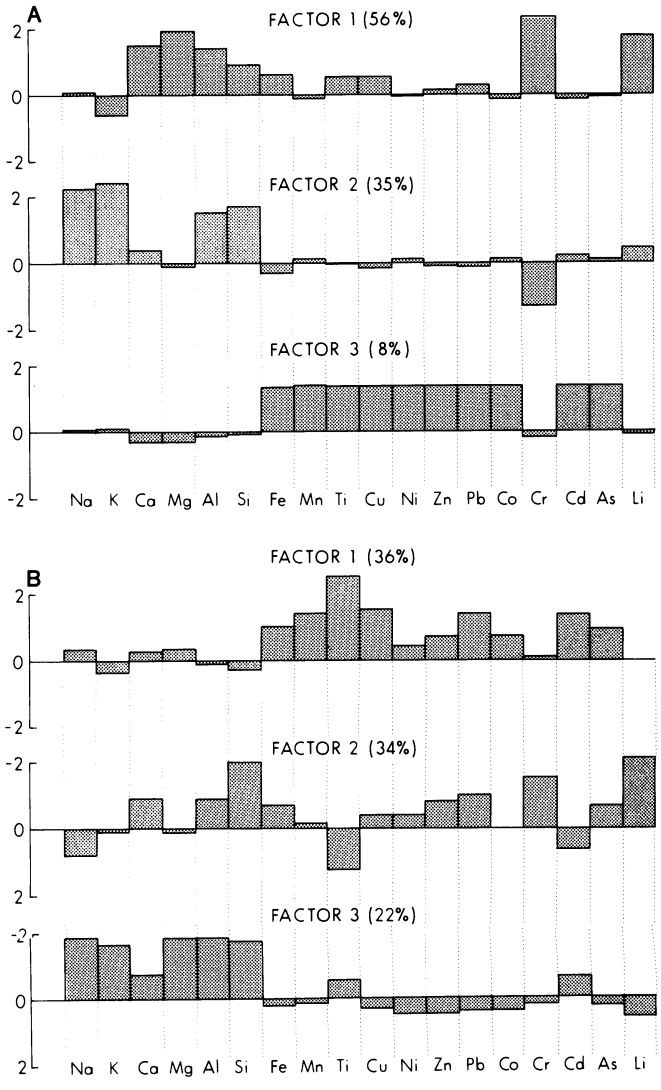

Figure 10. (a) Scaled, varimax rotated, Q-mode factor scores for North Fiji Basin sediments, >2-μm. Factor 1 (authigenic), factor 2 (detrital) and factor 3 (hydrothermal) together account for 99% of the sample variance. (b) Scaled, varimax rotated, Q-mode factor scores for North Fiji Basin sediments, <2-μm. Factor 1 (hydrothermal), factor 2 (authigenic) and factor 3 (detrital) together account for 92% of the sample variance. Note the similarity of these factor scores to those of the >2-μm fraction (a) above.

These three factors have almost the same importance in explaining the distribution of elements in the <2-μm fraction of the sediment samples. Because the <2-μm samples plot throughout the entire field of the ternary diagram and show obvious geographic groupings (Figure 11), contour plots of the hydrothermal, authigenic and detrital factor components of the samples are superimposed upon the recent tectonic configuration of the detailed survey area (Kroenke et al., this volume) in Figure 12. Three areas of significant hydrothermal contributions to these sediments are (1) a broad band associated with the South Pandora Ridge, possibly skewed to the south; (2) an area about 100 km east of the central North Fiji Basin spreading center (PC-3); and (3) an area southwest of the detailed survey area that is contributing to core TC-6 (Figure 12a). The distribution of the authigenic factor component (Figure 12b) shows two major areas of influence: (1) an area north of the South Pandora Ridge (PC-49); and (2) an area centered on PC-48 and FFC-82, FFC-83 and PC-50, which coincides with the central North Fiji Basin spreading center. The Vanuatu arc is apparently not contributing greatly as a source of authigenic material. The distribution of the detrital factor component (Figure 12c) suggests a major area of influence in the southwest corner that corresponds with the Vanuatu Archipelagic apron (TC and PCOD-6). Core TC-9, which is even closer to the arc (Figure 1), displays the highest detrital component of the <2-μm fraction (94.5%), and thus confirms this area as a major detrital source.

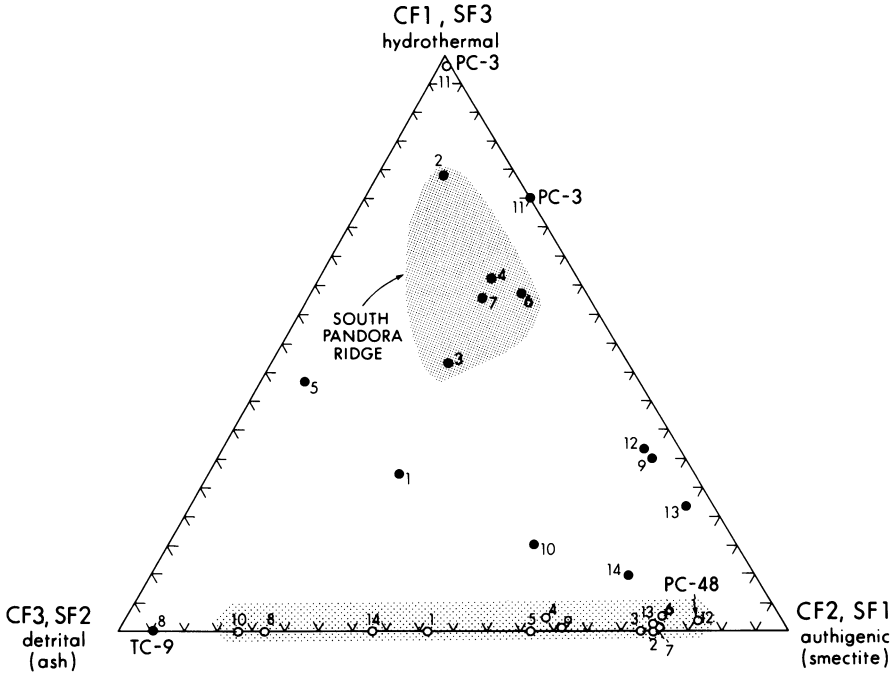

Figure 11. Plot of normalized, varimax rotated factor components for North Fiji Basin sediments, <2-μm (solid circles) and >2-μm (open circles). Small numbers indicate order of sample listing in Table 1. Note the grouping of samples near the hydrothermal factor from the vicinity of the South Pandora Ridge (shaded), and the mixing trend of the majority of >2-μm fraction sediments between the detrital and authigenic factors. PC-3, <2-μm, appears to be a mixture of nearly pure hydrothermal sediment concentrated in the >2-μm fraction and authigenic sediment.

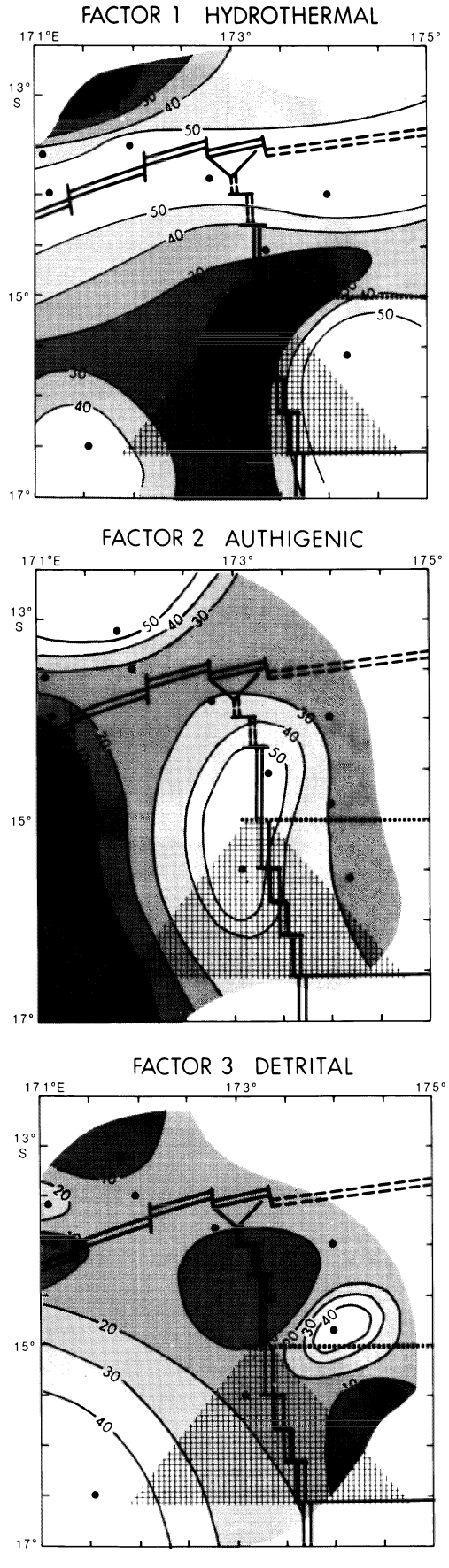

Figure 12. (a) Contour plot of factor 1 (hydrothermal) component for <2-μm sediments. Isopleths in percent. Active tectonic features are indicated (from Kroenke et al., this volume). (b) Contour plot of factor 2 (authigenic) component for <2-μm sediments. Isopleths in percent. (c) Contour plot of factor 3 (detrital) component for <2-μm sediments. Isopleths in percent.

DISCUSSION

Comparison of Chemical Data with Previous Work

Selected elemental compositions of the north central North Fiji Basin sediments are compared on a carbonate-free basis with those of sediments from other regions in the North Fiji Basin and from the southwestern and eastern Pacific in Figures 13 through 15. The sediment values are presented as >2-μm, <2-μm and bulk means ($\pm 1\,\sigma$), whereas the other sediments are reported as bulk carbonate-free values. Inspection of the Fe versus Mn plot (Figure 13) reveals that the mean of the majority of the studied sediments (excluding the PC-3 and TC-9 samples) is slightly enriched in Fe and Mn relative to the Southwest Pacific regional mean of Cronan and Thompson (1978). The >2-μm fraction of most of these sediments plots within fields for other North Fiji Basin sediments, along with both size fractions of sample TC-9. On the basis of the lithology and mineralogy of this material, the carbonate-free fractions of most of the plotted North Fiji Basin sediments, as well as those of the Southwest Pacific region, are dominated by volcanic ash-rich detritus. The <2-μm fraction of most of our sediment samples plots on an enrichment trend between the >2-μm fraction and the low-Mn metalliferous sediments of the Bauer Basin (Figure 13), suggesting that the material in this fraction is a mixture of volcanic ash and relatively pure metalliferous sedi-

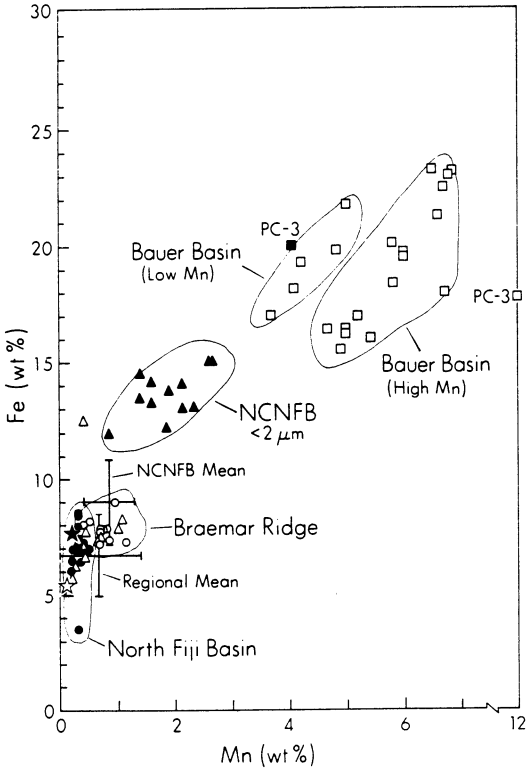

Figure 13. Plot of Fe versus Mn for north central North Fiji Basin sediments. Solid triangles, <2-μm; open triangles, >2-μm; solid star, TC-9, <2-μm; open star, TC-9, >2-μm; solid square, PC3, <2-μm; open square, PC-3, >2-μm. North Fiji Basin sediments (solid circles) from Cronan (1983). Braemar Ridge sediments (open circles) from Cronan et al. (1981). Regional mean ($\pm 1\sigma$) from Cronan and Thompson (1978). Bauer Basin sediments (open squares) from McMurtry (1979).

Table 10. Comparative metal accumulation rates.

Identification	Fe	Mn	Al	Cu	Ni	Co	Cr
	mg/cm^2 10^{3}yr			μg/cm^2 10^{3}yr			
North central North Fiji Basin (this study)[1]	3.8-77 (24)	0.2-4.1 (1.9)	5-79 (21)	11-273 (95)	5-105 (40)	3-74 (25)	3-56 (20)
Northern south Pacific sediments[2]	3.5	1.02	--	34	20	11	14
Australian dust[3]	5.8	0.05	--	20	14	4	36
East Pacific Rise, 5-20°S[4]	4-124 (28)	1-36 (8.5)	0.4-5.7 (2.1)	50-590 (190)	21-160 (75)	--	--
Bauer Basin[5]	3-25 (12)	1-6 (3.3)	0.6-7.4 (2.8)	24-180 (82)	19-140 (60)	-- --	-- --
Equatorial Pacific[6]							
Rise crest	29.3	5.4	6.7	160	80	--	--
Non-rise crest	2.5	0.6	2.0	50	15	--	--
Equatorial zone (3°N to 3°S)	4.3	1.3	4.3	110	30		
Global authigenic[7]	--	0.1-3.4 (1.3)	--	--	--	--	--

[1] Range and mean (bracketed) of the 7 cores reported in Table 9.
[2] Northern South Pacific sediment values from Windom (1970). Average accumulation rate of cores MSN 131 (8°17'S; 151°34'W) and CAP 31 (17°29'S; 158°40'W).
[3] Based on dust accumulation rates in New Zealand snow fields. The source of this material is suggested to be Australian deserts (from Windom, 1970).
[4] Range and mean (bracketed) of 17 cores along the crest of the East Pacific Rise (McMurtry et al., 1981).
[5] Range and mean (bracketed) of 10 cores from the Bauer Basin (McMurtry et al., 1981).
[6] Average accumulation rates based on 22 DSDP sites in the central equatorial Pacific (Leinen and Stakes, 1979).
[7] Range and mean (bracketed) of 38 deep-sea cores from the Atlantic, Pacific and Indian oceans (Bender et al., 1970).

ment. The <2-μm fraction of sample PC-3 plots within the field of the low-Mn metalliferous sediment, whereas the >2-μm fraction of this sample has similar Fe content but is enriched in Mn relative to high-Mn metalliferous sediment.

The plot of Cu versus Zn (Figure 14) shows similar trends to that of Fe versus Mn. The mean of most of our sampled sediments is only slightly enriched in Cu relative to the Southwest Pacific regional mean, whereas Zn shows no enrichment relative to this value. The <2-μm fraction of the majority of these north central North Fiji Basin sediments plots on an enrichment trend that approaches the mean Cu-Zn values reported for sediments from the crest of the East Pacific Rise (Figure 14). The Cu-Zn values for both size fractions of PC-3 approach and exceed those for East Pacific Rise and Bauer Basin sediments. The plot of Ni versus Pb (Figure 15) displays less significant enrichments for the studied sediments, but the trends are similar to those of Fe-Mn and Cu-Zn. The less significant enrichment of Ni and Pb in the <2-μm fraction of the sediments reflects the relative abundance of these metals in the basaltic-andesitic volcanic ash concentrated in the >2-μm fraction (Table 2). The Ni-Pb values for both size fractions of PC-3 also exceed those reported for Bauer Basin metalliferous sediments (Figure 15).

The comparative chemical compositions can by analogy give some insight into the origins of these particular metals in the sampled sediments. The ultimate origin of these metals is, however, complex and problematical. Their incorporation in metalliferous sediments results from a combination of hydrothermal, hydrogenous and detrital sources, and is probably influenced by biological and diagenetic pathways both before and after sedimentation (Dymond, 1981; McMurtry et al., 1981; Marchig et al., 1982). The use of metal accumulation rates and

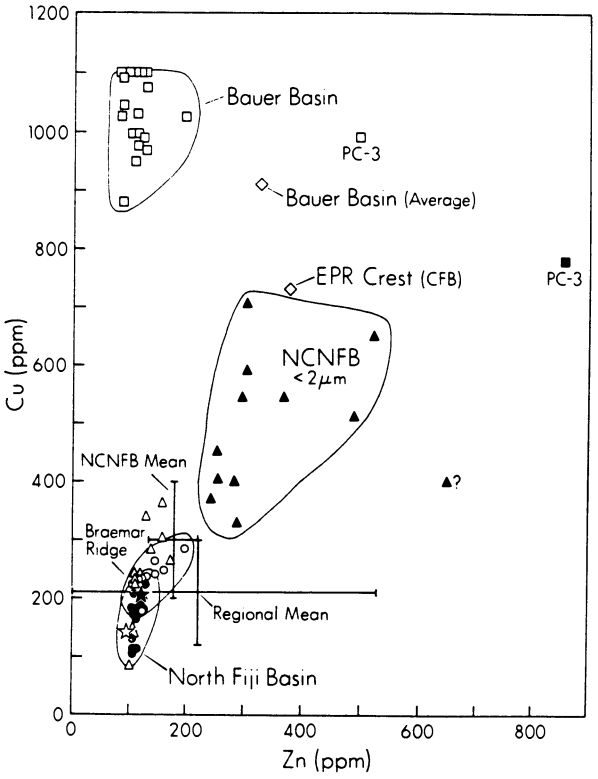

Figure 14. Plot of Cu versus Zn for North Central North Fiji Basin sediments. Symbols and sources as in Figure 13, except Bauer Basin average and East Pacific Rise (EPR) crest average, carbonate-free basis (diamonds) from Dymond et al. (1973).

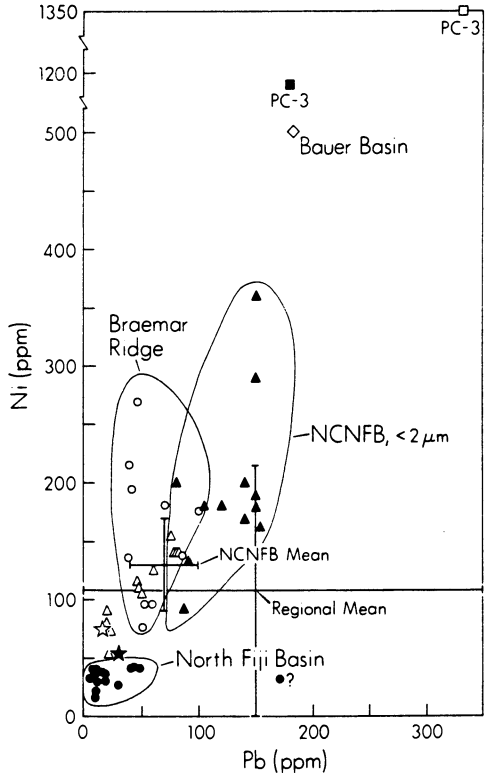

Figure 15. Plot of Ni versus Pb for north central North Fiji Basin sediments. Symbols and sources as in Figure 13, except for Bauer Basin sediment (diamond) from Dasch et al. (1971).

multivariate factor analysis has been helpful in deconvoluting some of these sources and influences in both metalliferous and normal pelagic sediments.

Comparison of Metal Accumulation Rates

Table 10 presents comparative metal accumulation rate data for North Fiji Basin sediments. Relative to South Pacific pelagic sediments report-ed by Windom (1970), North Fiji Basin sediments accumulate at rates that average six times greater for Fe, and at least double for Mn, Cu, Ni, Co and Cr. Windom (1970) also calculated the Australian dust contribution to South Pacific sediments and found that, with the exception of Mn, the above metals can be supplied from this aeolian source at rates similar to pelagic sediments receiving little detrital material (Table 10). The higher North Fiji Basin accumulation rates could therefore be a result of higher input from detritus or some other source.

The mean and range of Fe accumulation are similar to those of East Pacific Rise metalliferous sediments, whereas Mn accumulation, although slightly higher than the mean authigenic rate, is significantly lower than rates for metalliferous sediments from the East Pacific Rise and Bauer Basin (Table 10). Rates of Cu and Ni accumulation are also generally lower than for metalliferous sediments. In contrast, the Al accumulation rate for North Fiji Basin sediments is approximately ten times greater than East Pacific Rise, Bauer Basin or equatorial Pacific sediments, indicating a significant detrital contribution to the North Fiji Basin.

By using the various fluxes for Mn reported in Tables 9 and 10, we were able to demonstrate that, despite the relatively lower Mn accumulation rates for the North Fiji Basin, the hydrothermal Mn flux to these sediments is significant relative to the detrital and authigenic Mn fluxes. Of the two cores used in the calculations, one (TC-6) is receiving a large detrital contribution from the Vanuatu island arc. Futhermore, these relative flux calculations are in good general agreement with the relative source contributions to the same sediment cores independently calculated by multivariate factor analysis (see results section).

Chemical Partitioning and Multivariate Factor Analysis

The results of the chemical and size partitioning of the North Fiji Basin sediment samples generally revealed element groupings consistent with previous

work in the Eastern Pacific, with some surprises. The carbonate fraction apparently contains significant amounts of Cd and Pb, with moderate amounts of Co, Ni, Cu and Zn (Figure 3). Whether bound in the carbonate tests of the abundant foraminifera found in these sediments or in associated organic matter, a biological origin is indicated for at least this fraction of the above metals. The size partitioning of the noncarbonate material revealed an element grouping consistent with volcanic ash/hyaloclastite in the 2-μm fraction of the majority of the sediment samples (Ca, Na, K, Mg, Si, Al), and an element grouping in the <2-μm fraction consistent with smectite and amorphous ferromanganese oxides (As, Mn, Cd, Zn, Pb, Co, Cu, Fe, Cr, Ni, Li, Ti) (Figure 4a). The chemical partitioning of the <2-μm fraction further resolved this element grouping into those strongly associated with the smectite (K, Si, Al, Mg, Li, Ti, Zn, Cu, Pb), ferromanganese oxides (As, Mn, Cd) and a group of elements with intermediate associations (Fe, Cr, Co, Ni, Ca) (Figure 5).

These partitioning results are not only of intrinsic geochemical interest but also aided our interpretation of the results of the multivariate factor analysis. The Q-mode factor analysis resolved three major factors that accounted for more than 90% of the sample variance in both the >2-μm and <2-μm fractions of the noncarbonate sediment. The factor scores are similar in both size fractions, although their relative importance in each fraction is different (Figure 10). The three major factors have been interpreted on the basis of their elemental groupings as (1) detrital (ash) (Na, K, Al, Si, Ca, Mg); (2) authigenic (smectite) (Cr, Mg, Li, Ca, Al, Si, Fe, Pb, Zn); and (3) hydrothermal (ferromanganese oxides) (Mn, Zn, Pb, As, Cd, Co, Ni, Fe, Ti, Cu). The interpretation of these factors has been based on the similarity of their elemental scores to the above chemical partitioning as well as on lithologic and mineralogic information on endmembers derived by the Q-mode analysis (Figure 11). The factor analysis not only confirmed endmembers that were previously suspected on the basis of their anomalous lithology, mineralogy and chemistry (samples PC-3 and TC-9) but also revealed from the PC-48 endmember that smectite aggregations were present in the >2-μm fraction which were not recognized in the initial analysis of the sediment lithology and mineralogy.

The contour plots of the three major factor components in the <2-μm fraction were successful in revealing patterns of hydrothermal, authigenic and detrital accumulation in the north central North Fiji Basin which are generally consistent with the recent tectonic configuration of the area and the regional sedimentological framework developed by Kroenke et al. (this volume) and Eade and Gregory (this volume) (Figure 12). There is some agreement with the pattern of accumulation rates produced for this area (Figure 9), but the plots are not in exact agreement largely because they are resolving different sediment components (e.g., noncarbonate includes both authigenic and detrital material; hydrothermal includes both Mn and Fe) and, because of problems encountered with the sedimentation rate determinations for some of the cores, the coverage of accumulation rates is about half of the factor analysis coverage. There is nevertheless remarkable agreement in individual cores between the Mn flux components and those determined by factor analysis.

CONCLUSIONS

In order to characterize the sediments of the north central North Fiji Basin detailed survey area and determine recent hydrothermal contributions to these sediments and their source areas, a comprehensive geochemical survey of surface sediment samples from piston, trigger and free-fall cores was combined with detailed, down-core ^{230}Th profiles and dry bulk density determinations. Chemical and mineralogical analyses, including elemental phase and size partitioning, element accumulation rate determinations and multivariate factor analysis of the chemical data were performed. The major conclusions of this study are as follows:

(1) Simple comparisons of selected metals on a bulk, carbonate-free basis revealed slight enrichments for the sampled sediments relative to other sediments from the southwest Pacific, suggesting some metalliferous component of probable hydrothermal origin. However, phase and size partitioning revealed that (a) concentrations of the metals in the <2-μm fraction approached those for metalliferous sediments from the Eastern Pacific, and (b) the metalliferous material in the majority of these sediments is concentrated in the oxide portion of the <2-μm fraction, suggesting that dispersion from the source areas could be widespread. The chemical and size partitioning also aided the interpretation of the factor analysis results.

(2) X-ray mineralogy studies of both size fractions of the noncarbonate material determined that the >2-μm fraction is dominated by plagioclase feldspar and associated amorphous volcanic glass, with minor amounts of Fe-montmorillonite, kaolinite and quartz. The <2-μm fraction contains abundant Fe-montmorillonite, with lesser amounts of plagioclase, kaolinite and quartz. One sample (PC-3) also contains abundant vernadite ($\delta-MnO_2$) in both size fractions.

(3) Sedimentation rates were successfully determined by the excess ^{230}Th method using alpha-track autoradiography. This method, which is more rapid and less laborious and expensive than other approaches, produced detailed activity profiles that revealed coring disturbance in the topmost 1-2 m of some of the piston

cores and throughout most of the trigger and free-fall cores. The alpha-track rates are within 10% of rates determined on the same piston cores by paleomagnetic stratigraphy, which also found coring disturbance in the topmost few meters. The sedimentation rates for the sampled area range from 0.1 to 2.6 cm/10^3 years (mean = 1.2, n = 7). These rates are equivalent to those of eastern and equatorial Pacific sediments at similar levels above the carbonate compensation depth.

(4) Mean Fe accumulation rates for the area are similar to those of the East Pacific Rise metalliferous sediments. Mean Mn accumulation rates are only about twice the mean global authigenic rate, whereas Al accumulation rates are about ten times greater than East Pacific Rise, Bauer Basin and Equatorial Pacific sediments, indicating significant detrital contributions to the north central North Fiji Basin sediments. Although the Mn accumulation rates are less significant than those of the East Pacific Rise and Bauer Basin, Mn flux calculations suggest that the hydrothermal flux is significant relative to the detrital and authigenic Mn fluxes in some of the sediments.

(5) Carbonate and noncarbonate accumulation rate patterns are similar in the study area. The highest noncarbonate accumulation is displayed by a core that is receiving large amounts of detrital material from the Vanuatu island arc. The highest carbonate accumulation and second highest noncarbonate accumulation coincides with the South Pandora Ridge and the northern extension of the central North Fiji Basin spreading center. The pattern of Mn accumulation appears to be skewed toward the South Pandora Ridge, whereas Fe accumulation closely follows the noncarbonate pattern.

(6) Q-mode factor analysis of both size fractions of the noncarbonate sediment produced three major factors – hydrothermal (ferromanganese oxides), authigenic (smectite) and detrital (ash) – that accounted for more than 90% of the sample variance in each fraction. The characterization of these factors was based on interpretation of elemental scores aided by the chemical partitioning results, and by the lithology, mineralogy and chemistry of endmembers produced by the Q-mode analysis. The relative importance of these factors in each fraction generally reflected their chemistry and mineralogy; authigenic and detrital factors dominated in the >2-μm fraction, whereas hydrothermal, authigenic and detrital factors were more equally represented in the <2-μm fraction.

(7) Contour plots of the three major factor components in the <2-μm fraction reveal a major hydrothermal source area associated with the South Pandora Ridge spreading center, and two other source areas in the southeast and southwest corners of the detailed survey area. The plots of the authigenic and detrital factors show high concentrations associated with the central North Fiji Basin spreading center and the Vanuatu archipelagic apron, respectively, in good agreement with the accumulation rate patterns. The lack of a clear hydrothermal signal associated with the northern extension of the central North Fiji Basin spreading center may reflect the relative youth of this feature, as suggested by other work in this area (Kroenke et al., this volume). On the other hand, the additional hydrothermal areas which do not clearly associate with any known tectonic features suggest that the backarc rifting in this portion of the North Fiji Basin may also follow the complex model of Weissel (1981), thereby producing scattered, localized hydrothermal systems that are not easily detected with current technology. This conclusion is corroborated and extended by the distribution of heat flow measurements elsewhere in the North Fiji Basin (Halunen, 1979).

ACKNOWLEDGMENTS

We gratefully acknowledge C. Fraley, V. Greenberg, and S. Wickramaratne for analytical assistance. L.W. Kroenke and A. Malahoff provided unpublished information and helpful discussions of the tectonic history. F. Theyer and C. Mato, formerly of the HIG Core Laboratory, provided samples and lithologic information. The HIG Core Lab is supported by NSF grant OCE82-01962 to F. Theyer. This study was funded in part by the Office of Naval Research. SOEST contribution no. 1757.

REFERENCES

Andersen, M.E., and J.D. Macdougall, 1977, Accumulation rates of manganese nodules and sediments: an alpha track method: Geophysical Research Letters, v. 4, p. 351–353.

Aplin, A.C., and D.S. Cronan, 1985, Ferromanganese oxide deposits from the Central Pacific Ocean. I: Encrustations from the Line Island Archipelago: Geochimica et Cosmochimica Acta, v. 49, p. 427-436.

Ballard, R.D., and J. Francheteau, 1983, Geological processes of the midocean ridge and their relationship to sulfide deposition, in P.A. Rona, K. Bostrom, L. Laubier and K.L. Smith, Jr., eds., Hydrothermal Processes at Seafloor Spreading Centers: Plenum Press, New York and London, 796 p.

Ballard, R.D., R.T. Holcomb, and T.H. van Andel, 1979, The Galapagos Rift at 86°W, 3, Sheet flows, collapse pits, and lava lakes of the rift valley: Journal of Geophysical Research, v. 84, p. 5407-5422.

Ballard, R.D., T.H. van Andel, and R. T. Holcomb, 1982, The Galapagos Rift at 86°W; 5, variations in volcanism, structure and hydrothermal activity along a 30-km segment of the rift valley: Journal Geophysical Research, v. 87, p. 1149-1161.

Bender, M.L., T.-L. Ku, and W.S. Broecker, 1970, Accumulation rates of manganese in pelagic sediments and nodules: Earth and Planetary Science Letters, v. 8, p. 143-148.

Bernas, B., 1968, A new method for decomposition and comprehensive analysis of silicates by atomic absorption spectrometry: Analytical Chemistry, v. 40, p. 1682-1686.

Bertine, K.K., and J.B. Keene, 1975, Submarine barite-opal rocks of hydrothermal origin: Science, v. 188, p. 150–152.

Bonatti, E. and D. Joensuu, 1966, Deep-sea iron deposit from the South Pacific: Science, v. 154, p. 643-645.

Bostrom, K. and M.N.A. Peterson, 1966, Precipitates from hydrothermal exhalations on the East Pacific Rise: Economic Geology, v. 61, p. 1258-1265.

Bostrom, K. and M.N.A. Peterson, 1969, The origin of aluminum-poor ferromanganoan sediments in areas of high heat flow on the East Pacific Rise: Marine Geology, v. 7, p. 427-447.

Boylan, D.B., S. Rutgers, H. Zeitlin, and J.E. Andrews, 1980, A comparative study of copper, nickel, and cobalt trace metal species in plankton, sediment, and manganese nodules from the equatorial North Pacific: Marine Mining, v. 2, p. 171-189.

Brocher, T.M., S. Wirasantosa, F. Theyer, and C. Mato, 1985, Economic consequences of regional sedimentation patterns along the Northern Melanesian Borderland, in T.M. Brocher, ed., Geological Investigations of the Northern Melanesian Borderland, Earth Science Series, v. 3: Houston, Texas, Circum-Pacific Council for Energy and Mineral Resources, p. 77-102.

Chase, C.G., 1971, Tectonic history of the Fiji Plateau: GSA Bulletin, v. 82, p. 3087-3110.

Chase, R.L., J.R. DeLaney, J.L. Karsten, H.P. Johnson, S.K. Juniper, J.E. Lupton, S.D. Scott, V. Tunnicliffe, S.R. Hammond, and R.E. McDuff, 1985, Hydrothermal vents on an axis seamount of the Juan de Fuca ridge: Nature, v. 313, p. 212-214.

Cook, H.E., P.D. Johnson, J.C. Matti, and I. Zemells, 1975, Methods of Sample Preparation and X-ray Diffraction Data Analysis, X-ray Mineralogy Laboratory: Initial Reports of the Deep Sea Drilling Project, v. 28, p. 999-1007.

Corliss, J.B., J. Dymond, L.I. Gordon, J.M. Edmond, R.P. von Herzen, R.D. Ballard, K. Green, D. Williams, A. Bainbridge, K. Crane, and T.H. van Andel, 1979, Submarine thermal springs on the Galapagos Rift: Science, v. 203, p. 1973-1983.

Cox, M.E., 1980, Areal distribution of marine sediment mercury in the region around Fiji, South Pacific Marine Geology Notes, 1, 111-122.

Crane, K. and W.R. Normark, 1977, Hydrothermal activity and crustal structure of the East Pacific Rise at 21°N, Journal of Geophysical Research, 82, 5336-5348.

Cronan, D.S., 1983, Metalliferous sediments in the CCOP/SOPAC region of the Southwest Pacific, with particular reference to geochemical exploration for the deposits, CCOP/SOPAC Technical Bulletin, No. 4, ESCAP, United Nations, 55 p.

Cronan, D.S. and B. Thompson, 1978, Regional geochemical reconnaissance survey for submarine metalliferous sediments in the southwestern Pacific Ocean--a preliminary note, Applied Earth Sciences, 87, B87-B89.

Cronan, D.S., G.P. Glasby, J. Halunen, J.D. Collen, K.E. Knedler, J.H. Johnston, J. Cooper, C.W. Landmesser, and R.T. Wingfield, 1981, Sediments from the Braemar Ridge and Yasawa Trough, northwest of Fiji, South Pacific Marine Geology Notes, 2, 25-35.

Cronan, D.S., G.P. Glasby, S.A. Moorby, J. Thomson, K.E. Knedler, and J.C. McDougall, 1982, A submarine hydrothermal manganese deposit from the southwest Pacific island arc, Nature, 298, 456-458.

Dasch, E.J., J.R. Dymond, and G.R. Heath, 1971, Isotopic analysis of metalliferous sediment from the East Pacific Rise, Earth and Planetary Science Letters, 13, 175-180.

De Carlo, E.H., G.M. McMurtry, and H.-W. Yeh, 1983, Geochemistry of hydrothermal deposits from Loihi submarine volcano, Hawaii, Earth and Planetary Science Letters, v. 66, p. 438-449.

Degens, E.T. and D.A. Ross, eds., 1969, Hot Brines and Recent Heavy Metal Deposits in the Red Sea, Springer-Verlag, New York, 600 p.

Dymond, J., 1981, Geochemistry of Nazca plate surface sediments: an evaluation of hydrothermal, biogenic, detrital, and hydrogenous sources, in L.D. Kulm, J. Dymond, E.J. Dasch, and D.M. Hussong, eds., Nazca Plate: Crustal Formation and Andean Convergence, GSA Memoirs 54, 824 p.

Dymond, J. and W. Eklund, 1978, A microprobe study of metalliferous sediment components, Earth Planet. Sci. Lett., 40, 243-251.

Dymond, J., J.B. Corliss, G.R. Heath, C.W. Field, E.J. Dasch, and H.H. Veeh, 1973, Origin of metalliferous sediments from the Pacific Ocean, GSA Bulletin, 84, 3355-3372.

Eade, J.V. and M. Gregory, Sediments of the North Fiji Basin: this volume.

Feely, R.A., G.J. Massoth, , H.C. Curl, Jr., M.L. Boudreau, and G.M. McMurtry, 1984, Composition of white and black smoker particulates from active vents on the Juan de Fuca and Endeavour Ridges, (abstract) Eos, Transactions of the American Geophysical Union, 65, 1112.

Fisher, D.E., 1977a, Fission/alpha analysis of the ^{238}U, ^{230}Th families, Nature, v. 265, p. 227-229.

Fisher, D.E., 1977b, f/α particle track analysis: a new geologic technique for the measurement of uranium, thorium and isotopic disequilibria, Journal of Radioanalytical Chemistry, v. 38, p. 477-490.

Flanagan, F.J., 1973, 1972 values for international geochemical reference samples: Geochimica et Cosmochimica Acta, v. 37, p. 1189-1200.

Francheteau, J. et al., 1979, Massive deep-sea sulphide ore deposits discovered on the East Pacific Rise: Nature, v. 277, p. 523-527.

Gong, H., A.W. Rose, and N.H. Suhr, 1977, The geochemistry of cadmium in some sedimentary rocks: Geochimica et Cosmochimica Acta, v. 41, p. 1687-1692.

Grassle, J.F., 1982, The biology of hydrothermal vents: a short summary of recent findings: Marine Technology Society Journal, v. 16, p. 33-38.

Halunen, A.J., Jr., 1979, Tectonic history of the Fiji Plateau: PhD dissertation, University of Hawaii, Honolulu, 127 p.

Hamburger, M.W. and B.L. Isacks, Shallow seismicity in the North Fiji Basin: this volume.

Haxby, W.F., G.D. Karner, J.L. LaBrecque, and J.K. Weissel, 1983, Digital images of combined oceanic and continental data sets and their use in tectonic studies: Transactions of the American Geophysical Union, v. 64, p. 995-1004.

Heath, G.R. and J. Dymond, 1977, Genesis and transformation of metalliferous sediments from the East Pacific Rise, Bauer Deep and Central Basin, northwest Nazca plate: GSA Bulletin, v. 80, p. 723-733.

Horibe, Y., K. Kim, and H. Craig, 1983, Off-ridge hydrothermal vents: backarc spreading centers and hotspot seamounts (abstract): Eos, Transactions of the American Geophysical Union, v. 64, p. 724.

Imbrie, J. and E.G. Purdy, 1962, Classification of modern Bahamian carbonate sediments: AAPG Memoir 1, p. 253-272.

Jackson, M.L., 1974, Soil Chemical Analysis - Advanced Course, published by the author, Department of Soils, Univerity of Wisconsin, Madison, 991 p.

Karig, D.E., 1971, Origin and Development of Marginal Basins in the Western Pacific: Journal of Geophysical Research, v. 76, p. 2542-2562.

Karl, D.M., C.O. Wirsen, and H.W. Jannasch, 1980, Deep-sea primary production at the Galapagos hydrothermal vents: Science, v. 297, p. 1345-1347.

Kim, K. and H. Craig, 1983, Methane: a 'real-time' tracer for submarine hydrothermal systems (abstract): Eos, Transactions of the American Geophysical Union, v. 64, p. 724.

Klinkhammer, G., M. Bender, and R.F. Weiss, 1977, Hydrothermal manganese in the Galapagos Rift: Nature, v. 269, p. 319-320.

Klovan, J.E., 1966, The use of factor analysis in determining depositional environments from grain-size distributions: Journal of Sedimentary Petrology, v. 36, p. 115-125.

Klovan, J.E. and J. Imbrie, 1971, An algorithm and FORTRAN-IV program for large-scale Q-mode factor analysis and calculation of factor scores: Mathematical Geology, v. 3, p. 61-77.

Kroenke, L.W. and P. Rodda, 1984, Cenozoic Tectonic Development of the Southwest Pacific: CCOP/SOPAC Technical Bulletin no. 6, ESCAP, United Nations, 122 p.

Kroenke, L.W., C. Jouannic, and P. Woodward, 1983, Bathymetry of the Southwest Pacific, chart 1 of the Geophysical Atlas of the Southwest Pacific: CCOP/SOPAC, ESCAP, United Nation.

Kroenke, L.W., R. Smith, and K. Nemoto, Morphology and crustal structure of the seafloor in the northern part of the North Fiji Basin: this volume.

Leinen, M. and R.N. Anderson, 1981, Hydrothermal sediment from the Marianas Trough (abstract): Transactions of the American Geophysical Union, v. 62, p. 914.

Leinen, M. and D. Stakes, 1979, Metal accumulation rates in the central equatorial Pacific during Cenozoic time: GSA Bulletin, v. 90, p. 357-375.

Lonsdale, P., 1977a, Clustering of suspension-feeding macrobenthos near abyssal hydrothermal vents of oceanic spreading centers: Deep-Sea Research, v. 24, p. 857-863.

Lonsdale, P., 1977b, Deep-tow observations at the mounds abyssal hydrothermal field, Galapagos Rift: Earth and Planetary Science Letters, v. 36, p. 92-110.

Lonsdale, P., 1979, A deep-sea hydrothermal site on a strike-slip fault: Nature, v. 281, p. 531-534.

Lonsdale, P., R. Batiza, and T. Simkin, 1982, Metallogenesis at seamounts on the East Pacific Rise: Marine Technology Society Journal, v. 16, p. 54-61.

Lupton, J.E. and H. Craig, 1981, A major helium-3 source at 15°S on the East Pacific Rise: Science, v. 214, p. 1318.

Macdonald, G.A., H.A. Powers, and T. Katsura, 1972, Interlaboratory comparison of some chemical analyses of Hawaiian volcanic rocks: Bulletin Volcanologique, v. 3, p. 127-139.

Malahoff, A., 1982, A comparison of the massive submarine polymetallic sulfides of the Galapagos Rift with some continental deposits: Marine Technology Society Journal, v. 16, p. 39-45.

Malahoff, A., G.M. McMurtry, J.C. Wiltshire, and H.-W. Yeh, 1982a, Geology and chemistry of hydrothermal deposits from active submarine volcano Loihi, Hawaii: Nature, v. 298, p. 234-239.

Malahoff, A., R.H. Feden, and H.S. Fleming, 1982b, Magnetic anomalies and tectonic fabric of marginal basins north of New Zealand: Journal of Geophysical Research, v. 87, p. 4109-4125.

Marchig, V., H. Gundlach, P. Moller, and F. Schley, 1982, Some geochemical indicators for discrimination between diagenetic and hydrothermal metalliferous sediments: Marine Geology, v. 50, p. 241-256.

McMurtry, G.M., 1979, Rates of Sediment Accumulation and their Bearing on Metallogenesis on the Nazca Plate, Southeast Pacific: PhD Dissertation, University of Hawaii, Honolulu, 232 p.

McMurtry, G.M. and H.-W. Yeh, 1981, Hydrothermal clay mineral formation of East Pacific Rise and Bauer Basin sediments: Chemical Geology, v. 32, p. 189-205.

McMurtry, G.M., H.H. Veeh, and C. Moser, 1981, Sediment accumulation rate patterns on the northwest Nazca plate, in L.D. Kulm, J. Dymond, E.J. Dasch and D.M. Hussongeds., Nazca Plate: Crustal Formation and Andean Convergence: GSA Memoir 154, 824 p.

McMurtry, G.M., C.-H. Wang, and H.-W. Yeh, 1983, Chemical and isotopic investigations into the origin of clay minerals from the Galapagos hydrothermal mounds field: Geochimica et Cosmochimica Acta, v. 47, p. 475-489.

McMurtry, G.M., R.C. Schneider, P.L. Colin, R.W. Buddemeier, and T.H. Suchanek, 1985, Redistribution of fallout radionuclides in Enewetak Atoll lagoon sediments by callianassid bioturbation: Nature, v. 313, p. 674-677.

Mehra, O.P. and M.L. Jackson, 1960, Iron oxide removal from soils and clays by a dithionite-citrate system buffered with sodium bicarbonate: Clays and Clay Minerals, v. 7, p. 317-327.

Moberly, R., 1972, Origin of lithosphere behind island arcs, with reference to the Western Pacific: GSA Memoir 132, p. 35-55.

Moore, C. and K. Bostrom, 1978, The elemental compositions of lower marine organisms: Chemical Geology, v. 23, p. 1-9.

Patterson, C., D. Settle, B. Schaule, and M. Burnett, 1976, Transport of pollutant lead to the oceans and within ocean ecosystems, p. 23-38 in H.L. Windom and R.A. Duce, eds., Marine Pollutant Transfer: Lexington Books, D.C. Heath and Co., Lexington, Mass.

Rona, P.A., K. Bostrom, L. Laubier, and K.L. Smith, Jr., eds., 1983, Hydrothermal Processes at Seafloor Spreading Centers: Plenum Press, New York and London, 796 p.

Sclater, J.G. and H.W. Menard, 1967, Topography and heat flow of the Fiji Plateau: Nature, v. 216, p. 991-993.

Scott, R.B., P.A. Rona, B.A. McGregor, and M.R. Scott, 1974, The TAG hydrothermal field: Nature, v. 251, p. 301-302.

Spiess, F.N., et al., 1980, East Pacific Rise: hot springs and geophysical experiments: Science, v. 207, p. 1421-1433.

Stoffyn-Egli, P. and F.T. Mackenzie, 1984, Mass balance of dissolved lithium in the oceans: Geochimica et Cosmochimica Acta, v. 48, p. 859-872.

Taylor, B., 1979, Bismarck Sea: evolution of a backarc basin: Geology, v. 7, p. 171-174.

Taylor, B. and G.D. Karner, 1983, On the evolution of marginal basins: Reviews Geophysics and Space Physics, v. 21, p. 1727-1741.

Vidal, V.M., F.V. Vidal, J.D. Isaacs, and D.R. Young, 1978, Coastal submarine hydrothermal activity off northern Baja California: Journal of Geophysical Resesarch, v. 83, p. 1757-1774.

von Stackelberg, U., and shipboard scientific party, 1985, Hydrothermal sulfide deposits in backarc spreading centers in the southwest Pacific: Bundesanstalt fur Geowissenschaften und Rohstoffe Circular 2, Hanover, 14 p.

Watts, A.B., J.K. Weissel, and R.L. Larson, 1977, Sea-floor spreading in marginal seas of the western Pacific, Tectonophysics: v. 37, p. 167-181.

Weiss, R.F., P. Lonsdale, J.E. Lupton, A.E. Bainbridge, and H. Craig, 1977, Hydrothermal plumes in the Galapagos Rift: Nature, v. 267, p. 600-603.

Weissel, J.K., 1981, Magnetic lineations in marginal basins of the western Pacific: Philosopical Transactions of the Royal Society of London, A300, p. 223-247.

Windom, H.L., 1970, Contribution of atmospherically transported trace metals to South Pacific sediments: Geochimica et Cosmochimica Acta, v. 34, p. 509-514.

Winn, C.D., D.M. Karl, and G.J. Massoth, 1986, Microorganisms in deep-sea hydrothermal plumes: Nature, v. 320, p. 744.

Index